Design, Synthesis and Screening of Potential Anti-malarial Agents
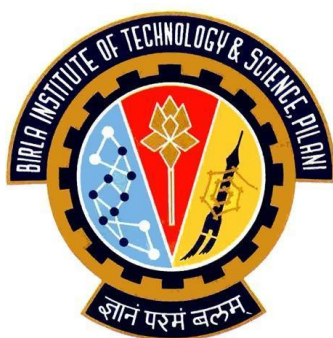
THESIS

Submitted in partial fulfilment

of the requirements for the degree of

DOCTOR OF PHILOSOPHY

by

Sourabh Mundra

Under the Supervision of

Prof. R. Mahesh

BIRLA INSTITUTE OF TECHNOLOGY & SCIENCE, PILANI

2016

This thesis is dedicated to my parents and wife

Thank you Mummy-Papa and Reshu for your

endless support and love

Contents   Page No

BIRLA INSTITUTE OF TECHNOLOGY & SCIENCE
PILANI (RAJASTHAN-333031) INDIA

CERTIFICATE

This is to certify that the thesis entitled "**Design, Synthesis and Screening of Potential Anti-malarial Agents"** and submitted by **Sourabh Mundra, ID No. 2010PHXF405P**, for the award of Ph.D. Degree of the Institute, embodies the original work done by him under my supervision.

Signature in full of the supervisor: _____

Name in capital block Letters: **Prof. R. MAHESH**

Designation: **Professor, Department of Pharmacy &**
Dean, Faculty Affairs,
Birla Institute of Technology & Science,
Pilani, Pilani Campus-333031

Date:

Palace:

Acknowledgments

I am really lucky to be placed under the guidance of **Prof. R. Mahesh,** Department of Pharmacy and Dean Faculty Affairs Division, BITS-Pilani, Pilani Campus, to carry out the present research work for PhD. It is my distinct respect and proud opportunity to acknowledge my heartiest thanks to my honoured teacher and admirable supervisor. **Prof. R. Mahesh** has been supportive and has given me the liberty to pursue my various projects without objection. I have learned from him how to grow and think like a scientist. His excellent guidance, caring and endurance provided me an excellent ambiance for doing this research work comfortably.

I am thankful to **Prof. Souvik Bhattacharyya,** Vice-Chancellor, BITS-Pilani, **Prof. V S Rao** (ex acting Vice-Chancellor, BITS-Pilani), **Prof. B. N. Jain** (ex Vice-Chancellor, BITS-Pilani) and **Prof. A. K. Sarkar,** Director, BITS-Pilani, Pilani Campus, **Prof. G. Raghurama** (ex Director, BITS-Pilani, Pilani Campus), for permitting me to carry out this research work in BITS-Pilani.

I would like to express my gratitude to **Prof. R. N. Saha**, Director, BITS-Pilani, Dubai Campus for his suggestions and impetus during my research work.

I am grateful to **Prof. S. K. Verma**, Dean, Academic Research Division and **Prof. A. K. Das** (ex Dean, ARD Division) BITS-Pilani, for their motivating words throughout my period of stay in BITS-Pilani. I owe my gratitude to **Dr. Anil Gaikwad,** Head, Department of Pharmacy for his support and guidance to persue my doctoral thesis.

I am thankful to my thesis Doctoral Advisory Committee members, **Dr. S. Murugesan**, ex Head, Department of Pharmacy and **Dr. Hemant Jadhav**, Associate Dean, Academic Research Division, for helpful discussions and suggestions during the dissertation. I would like to express my thanks to **Dr. Srikant Charde,** Asst. Prof., Department of Pharmacy BITS Pilani-Hyderabad Campus, for their constructive suggestions during my work.

I would also like to acknowledge **Dr. R P. Parekh**, **Dr. Rajeev Taliyan, Dr. Atish T. Paul** (DRC convener), **Dr. Sunil Dubey**, **Dr. Anil Jindal, Dr. Deepak Chitkara, Dr. Anupama Mittal, Dr. Priti Jain, Dr. M.M. Pandey**, **Dr. Jaipal A**, **Dr. Gautam, Dr. Aniruddha Roy**, **Mr. Mahaveer,** and **Ms. Archana**, who made my stay in Pilani, a pleasant experience.

I also owe my deepest gratitude to **Prof. R. Mahesh** collaborators **Dr. Asif Mohammed** (Research Scientist, ICGEB, New Delhi), **Dr. Lakshmi P. Kotra** (Associate Professor, Leslie Dan Faculty of Pharmacy, University of Toronto and Director, Center for Molecular Design

List of Abbreviations/Symbols

^{1}H NMR	Proton nuclear magnetic resonance
^{13}C NMR	Carbon-13 nuclear magnetic resonance
ACN	Acetonitrile
ATP	Adenosine triphosphate
ADP	Adenosine diphosphate
Å	Angstrom
AcSK	Potassium thioacetate
$Al(CH_3)_3$	Trimethylaluminium
ACP	Activators of self-compartmentalizing proteases
ACT	Artemisinin-based combination therapy
ADEP	Acyldepsipeptide
Asn	Asparagine
Ala	Alanine
BOC	*tert*-Butyl carbonate
BOP	(Benzotriazol-1-yloxy)tris(dimethylamino)phosphonium hexafluorophosphate
brs	Broad singlet
$CDCl_3$	Deuterated chloroform
CQ	Chloroquine
ClpP	Caseinolytic protease P
Cys	Cysteine
°C	Degree Celsius
CBr_4	Carbon tetrabromide
conc.	Concentration
cm	Centimeter
cm^{-1}	Centimeter inverse
DMF	*N,N*-Dimethylformamide
DIPEA	*N,N*-Diisopropylethylamine
DNA	Deoxyribonucleic acid
d	Doublet
dd	Doublet of doublet
DCM	Dichloromethane
DMSO	Dimethylsulfoxide
DCC	*N,N′*-Dicyclohexylcarbodiimide

δ	Delta
DEAD	Diethyl azodicarboxylate
dd	Doublet of doublets
d	Doublet
EtOH	Ethanol
EtOAc	Ethyl acetate
ESI	Electrospray Ionization
EDC	*N*-(3-dimethylaminopropyl)-*N'*-ethylcarbodiimide
E-64	L-transepoxysuccinyl-leucylamide-[4-guanido]-butane
E. coli	*Escherichia coli*
equiv.	Equivalent
FP-2	Falcipain-2
FT-IR	Fourier transform-Infra Red
GHP	GH polypro membrane
Gln	Glutamine
Gly	Glycine
g	Gram
H	Hydrogen
HBD	Hydrogen bond donor
HBA	Hydrogen bond acceptor
Hip	Histidine
HOBt	1-Hydroxybenzotriazole
HPLC	High Performance Liquid Chromatography
h	Hour
Hz	Hertz
HTS	High Throughput Screening
IC_{50}	Half maximal inhibitory concentration
IR	Infra red
Ile	Isoleucine
Ki	Dissociation constant of inhibitors
K_2CO_3	Potassium carbonate
Log P	Log of oil/water partition coefficient
Leu	Leucine
LCMS	Liquid chromatography–mass spectrometry
LiOH	Lithium hydroxide
m	Multiplet

mmol	Millimole
mL	Milliliter
mp	Melting point
m/z	Mass/charge
mg	Milligram
min	Minute(s)
MS	Mass spectra
MW `	Molecular weight
MWI	Microwave irradiation
M. tuberculosis	*Mycobacterium tuberculosis*
MeOH	Methanol
MIC	Minimum inhibitory concentration
μL	Microliter
μM	Micromolar
Na	Sodium
Na_2SO_4	Sodium sulfate
$NaHCO_3$	Sodium bicarbonate
nm	Nanomolar
NCEs	New chemical entities
PPh_3	Triphenylphosphine
Pd/C	Palladium on carbon
Pf	*Plasmodium falciparum*
PDB	Protein data bank
$POCl_3$	Phosphorus oxychloride
PTFE	Polytetrafluoroethylene
Phe	Phenylalanine
Phg	Phenylglycine
q	Quartet
RCSB	Research Collaboratory for Structural Bioinformatics
RNA	Ribonucleic acid
RBC	Red blood cells
RT	Retention time
RBF	Round bottom flask
RMSD	Root mean square deviation
Py	Pyridine
rt	Room temperature

SARs	Structure–activity relationships
s	Singlet
S_N2	Substitution nucleophilic bimolecular reaction
SD	Standard deviation
Ser	Serine
TLC	Thin layer chromatography
TFA	Trifluoroacetic acid
TEA	Triethylamine
t	Triplet
THF	Tetrahydrofuran
TMS	Tetramethylsilane
Trp	Tryptophan
$t_{1/2}$	Half life
UV	Ultraviolet
VT NMR	Variable temperature nuclear magnetic resonance
Val	Valine
WHO	World Health Organization
%	Percentage
=	Equal to
<	Less than
>	More than
J	Coupling constant
σ	Sigma
π	Pi
α	Alpha
β	Beta
3D	Three dimensions

List of Figures

protein (3BPF.pdb). The pink dashed line represents the possible hydrogen bond and green dashed line represents the possible hydrophobic interaction, (D): Redocked mode of E-64 (yellow) superimposed with the co-crystallized ligand (magenta)

List of Tables

Abstract

The existing armamentarium of anti-malarial drugs is not sufficient to combat malaria, primarily because of resistance developed by the parasite. The problem got further compounded due to non-enrichment of anti-malarial drug inventory. Unfortunately, an effective anti-malarial vaccine also could not be developed due to fast and constant mutations in the parasite genome. All these factors led to an urgent need for new research avenues to develop novel and more potent anti-malarial drugs.

The current research work investigates the design, synthesis and biological evaluation of *Plasmodium falciparum* proteases. This is achieved by examining the effect of inhibitor design, especially warheads, on percentage inhibition (IC_{50} values) and generation of structure activity relationships (SAR) between cysteine protease falcipain-2 **(Series I** to **IV)**, and serine protease ClpP (caseinolytic proteases) inhibitors **(Series V** and **VI)**.

Falcipain-2 protease has been a subject of intense research over the past two decades. Inhibition of *Plasmodium* falcipain-2 proteases is a strategy to develop novel drugs against malaria. As per the pharmacophoric requirements of falcipain-2 inhibitors, three different non-peptidic small molecule series namely, 2-(4-(substituted benzoyl)-1,4-diazepan-1-yl)-*N*-phenylacetamide derivatives **(Series I)**, 1-(4-(substituted)piperazin-1-yl)-2-(phenylamino)ethanone derivatives **(Series II)**, and 2-(4-(substituted benzoyl)piperazin-1-yl)-*N*-phenylacetamide derivatives **(Series III)**, were designed using ligand-based approach. The 'Lipinski's Rule of Five' was adopted while designing the molecules to attain better pharmacokinetic profile. These carboxamides were synthesized from the starting material, aniline **(Series I** and **III)**, or piperazine **(Series II)**, in a sequence of reactions, respectively.

On the other hand, peptidomimetics **(Series IV)**, were designed on the structural features of FP-2 enzyme. A two-step process was used to screen *in silico* small molecule libraries against the active site of falcipain-2 employing UNITY suite of software; (I) hits were selected containing complimentary features to the enzyme active site and (II) the hits were docked into the binding pocket using Surflex Dock™ to obtain a docking pose in the active site of falcipain-2. Overall, from this screening, one potential hit was identified **(KM-1')**, exhibiting moderate *in vitro* activity. Further, the complementary features from **K11017** and **Leupeptin** (standard ligand), were incorporated in **KM-1'** hit molecule, to design and synthesize new chemical entities based on **Scaffold I**, with appropriate chemical functionalities.

The structures of the synthesized molecules were confirmed by spectral data (IR, ¹H NMR, mass) and the purity was assessed by thin layer chromatography/elemental data/HPLC. The

inhibitory activities of synthesized compounds; **RM 1 to 20 (Series I)**, **RMS 1 to 20 (Series II)**, **RMT-1 to 20 (Series III)** and **RMQ-1** to **20 (Series IV)**, were analyzed by their ability to block the *in vitro* protease activity of recombinant falcipain-2. Compounds **RM-2, RM-7, RM-8, RM-10, RM-11 (Series I)**, **RMS-6, RMS-8, RMS-14, RMS-15 (Series II)** displayed significant inhibition. Among the peptidomimietics **(Series IV)**, two compounds **RMQ-16** and **RMQ-17,** were the most potent compounds, having IC_{50} values in nano-molar range against FP-2 enzyme. Compound **RMQ-14** was the most effective inhibitor of parasite growth, with an IC_{50} value of 0.9 ± 0.1 μM, which correlated well with the inhibition of FP-2 enzyme.

Caseinolytic proteases (ClpP) carry out "housekeeping" duty common to many eukaryotes, as well as some other tasks such as protein synthesis, folding and control of metabolic activities, highly specific to the parasite survival. Drugs targeting ClpP would have the double advantage of**:** distinguishing host and parasite by targeting prokaryote-specific functions, minimizing side-effects for humans; and potentially offering a common treatment against malaria and other antibacterial disease.

Two novel series of molecules **(V** and **VI)**, based up on pyrimidine core nucleus, namely 2-(substituted)pyrimidin-4-ylthio)-*N*'-(2-phenylacetyl)-acetohydrazide derivatives and 1,6-dihydropyrimidine-5-carboxamides derivatives were designed, synthesized and evaluated as ClpP inhibitors.

Structural features of final compounds for **Series V** and **VI** were characterized by spectral data (IR, ^{1}H & ^{13}C NMR and mass). The purity of the final compounds were preliminary assured by HPLC in a minimum of two different mobile systems.

The target compounds **(Series V and VI)** were evaluated for their *in vitro* protease activity of ClpP and showed varied inhibition values. The **Series V (RMP 1** to **15)** derivatives, exhibited moderate *in vitro* activity against *Plasmodium* ClpP protease, while from **Series VI**, seven compounds **(RMH-1**, **RMH-2**, **RMH-3**, **RMH-5**, **RMH-10**, **RMH-12**, **RMH-13)** displayed moderate activity. Compound **RMH-4**, was found to be most potent among both the series **(V** and **VI)** and it can also be utilized as a potential lead compound in the designing of new candidates.

1. INTRODUCTION

1.1. Malaria

Alphonse Laveran (1907, Nobel Prize Winner), a French army surgeon, was first to discover malaria parasites from the blood of a febrile patient (6th November 1880). After 20 years, Ronald Ross, Indian born, British medical doctor (1902, Nobel Prize Winner), described the transmission of malaria parasites from febrile patients to Anopheles mosquitoes (Zucca et al., 2013).

Malaria is a severe infectious disease that has opposed all efforts of control, and eradication programme for over a century. Malaria has tremendous economic cost, with estimation around $100 billion over the last 35 years (Go, 2003). World Health Organization malaria report 2014 indicate that, there were 198 million malaria cases leading to approximately 584,000 malaria deaths in the year 2013 (World Malaria Report, 2014). Out of reported 90% malaria casualties in Africa alone, the majority were children under age of five. Globally, 80% of deaths occur in just 14 African countries. Out of the 35 countries, that responsible for ~98% of malaria casualty in the world, 30 countries that bear most of the global malaria cases, located in Sub-Saharan Africa. The four countries, Uganda, Democratic Republic of Congo, Nigeria and Ethiopia alone account for over 40% of the estimated total of malaria death worldwide (World Malaria Report, 2012). Whereas, in South East Asia region, three countries India (55%), Myanmar (21%) and Indonesia (21%) accounting 97% of malaria cases (World Malaria Report, 2014).

1.2. *Plasmodium* species and their geographical distribution

Malaria is a fatal disease caused by the *Plasmodium* parasite, a member belongs to phylum Apicomplexan. Approximately, 156 named species of *Plasmodium* are existing, which infect various species of vertebrates (http://www.cdc.gov/dpdx/). Among them, five species (*P. falciparum*, *P. vivax*, *P. malaria*, *P. ovale* and *P. knowlesi*), that infect human beings and cause significant malarial infections.

Plasmodium falciparum (*P. falciparum*), is most likely to cause rigorous perilous form of malaria and responsible for the majority of malarial deaths in a year worldwide (World Malaria Report, 2012). *P. falciparum*, is majorly found in tropical regions, such as Sub-Saharan Africa, Melanesia, Hispaniola and Western Pacific as well as in the Southeast Asia, and in countries sharing the Amazon Basin of South America. *P. vivax* is the most prevalent species of malaria, present in Eastern Mediterranean and in most endemic countries of the

America. Whereas, *P. malariae*, is widely distributed throughout Sub-Saharan Africa and some part of Southeast Asia.

1.3. Malaria symptoms

The incubation period (period from the bitten by the mosquito until symptoms appear), for the different species typically ranges from 9 to 36 days (American Public Health Association, 2008). Symptoms may appear in a cyclic pattern, due to the life cycle of malaria parasite. Episode of symptoms (the time between episodes of fever and other symptoms), varies from 2-3 days with the parasite species. The episode of symptoms are 48 hours (every), when infection caused by *P. vivax* or *P. ovale* and 72 hours (every), if infected with *P. malariae*.

P. falciparum does not generate a regular, cyclic fever. Hence, a symptom of fever developing less than one week, as soon as possible exposure, is not malaria. *P. falciparum* causes the most severe form of malaria with irregular clinical signs and symptoms e.g., fever, headache, chills, cough, vomiting, weakness, diarrhoea, abdominal pain and organ failures (renal failure), followed by coma and death. (Bartoloni and Zammarchi, 2012).

1.4. Parasite biology and life cycle

1.4.1. Hepatocyte invasion

Malaria infection starts with the bite of an infected female Anopheles mosquito (Croft, 2000). Mosquito during sucking of human blood to nourish her eggs, inject saliva into the human host. The sporozoites rapidly travel to the liver and invade liver cells (Chaiyaroj et al., 1994) **(Figure 1)**. Over the 5-16 days (period depends upon malaria parasite species), parasite develops an infection in liver cells. Particularly, in *P. falciparum* within a time frame of ten days a single sporozoite grows, divide and generate 10,000 merozoites per liver cell.

1.4.2. Erythrocyte invasion

After maturation of the merozoites in 1-3 days, they exit from liver hepatocytes, re-enter into blood streams and invade erythrocytes **(Figure 1)**, via a receptor-mediated process (Nussenzweig and Long, 1994). During invasion to erythrocytes, a vacular membrane is generated, which contains lipids and proteins derived from both host and parasite. Once the replication cycle begins (48 hours of the period), a single merozoite produces 20 new daughter merozoites or schizonts, each have a tendency to invade a new red cell.The stage of development for schizonts starts from the ring-formation, known as trophozoite stage.

1.4.3. Sporozoite stage

Once blood meal is taken up by a mosquito from an infected person, the infected human blood cells burst and gametocytes are released. Further, development phase in mosquito's midgut accomplished by mature sex cells (male and female gametes). Fusion of gametes form diploid zygotes **(Figure 1)**. The zygotes develop into a motile form known as ookinetes, which later develops in to oocytes. Division and then replication of oocytes produce approximately 10,000 active haploids forms (sporozoites). The cycle of infection restarts when a mosquito bites to a healthy volunteer and inject the sporozoites from its saliva to human blood.
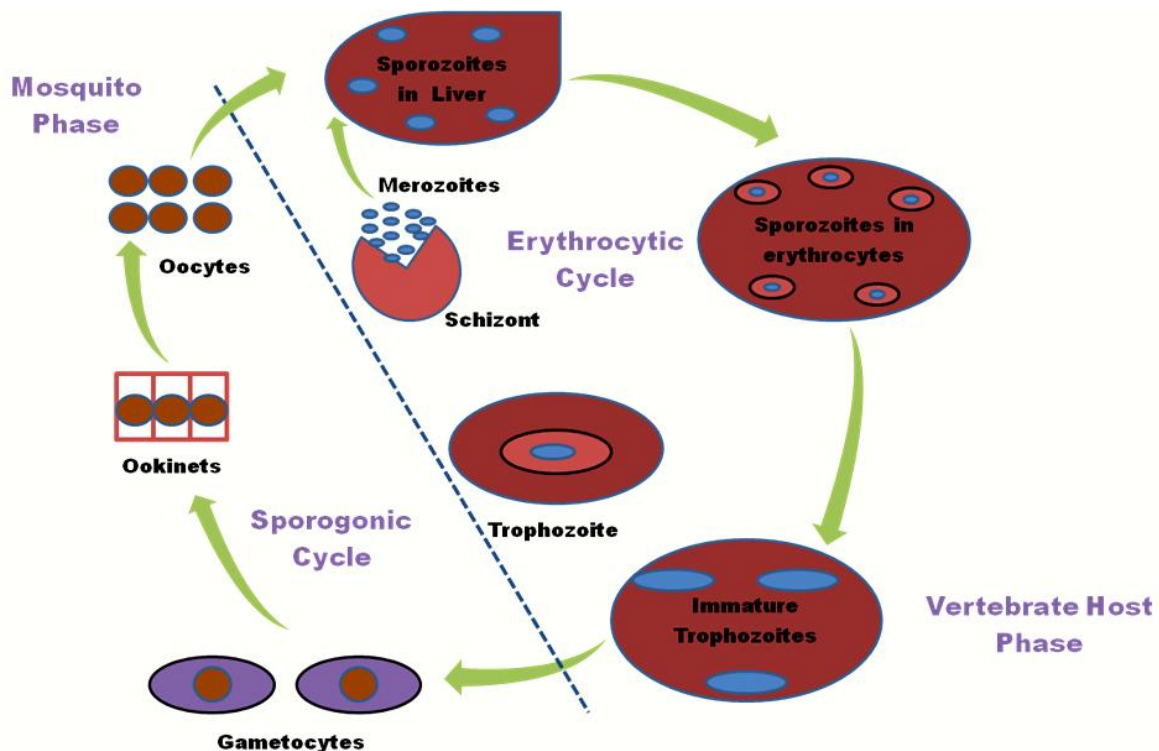
Figure 1: Malaria parasite life cycle

1.5. Evolution of classical anti-malarial drugs and present drugs for treatment of malaria

The first attempt to develop synthetic anti-malarial drugs originated from the observation that methylene blue had anti-malarial activity (Coatney, 1963). With the changes on its structure, the first synthetic anti-malarial plasmoquine called as pamaquine (**1**; PamQ), was synthesized in 1926. Later, pamaquine was found to be too toxic, and then a lesser toxic analog primaquine **(2)** was synthesized. Systematic modifications of quinine **(3)** and methylene blue, led to the generation of 6-methoxy-8-aminoquinoline based derivatives,such as pentaquine **(4)** and isopentaquine **(5)**; represented in **Figure 2**. Scientists at the Bayer

laboratories, Germany synthesized the 4-aminoquinoline resochin. In early stages, Resochin was thought to be too toxic for clinical use and ignored for a decade. Later, Resochin was found to be safe at therapeutic concentrations and was renamed chloroquine (CQ; **6**) and taken into clinical trials in 1943.

As an attempt to contribute to eradicate malaria, in the early 1960's, the World Health Organization supplied tons of chloroquine for inclusion in table salt in parts of South America, Africa and Asia. Shortly afterwards, the first cases of CQ resistance were reported from the same areas where this chloroquinized salt was distributed. To counteract CQ resistance, further modification by medicinal chemists, led to the identification of Hydroxy-Chloroquine (HCQ; **7**) and amodiaquine **(8)**.

Efforts included attempts to make more effective versions of the HCQ. Pyrimethamine **(9)**, in combination with sulfadoxine **(10)**, was introduced in the 1970s and named Fansidar. Details about the most common prophylactic and therapeutic drugs for malaria are presented in following sections.
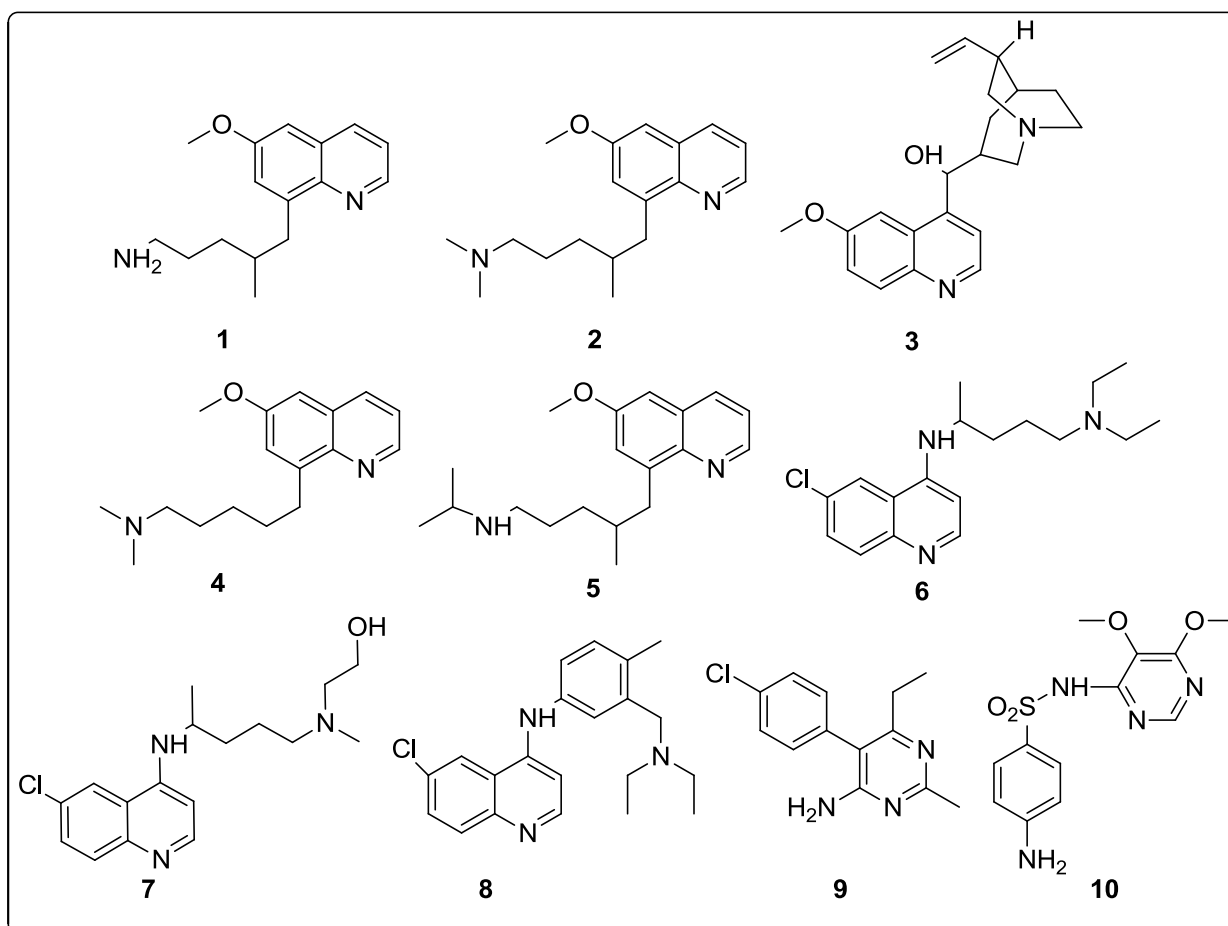
Figure 2: Classical quinoline derivatives

1.5.1. Artemisinin and first-generation derivatives

Artemisinin was isolated by Chinese scientists in 1972, is a natural component identified from the traditional Chinese plant *Artemisia annua*, possessed significant anti-malarial activity against both *P. falciparum* and *P. vivax* (Chawira et al., 1987). Structurally, Artemisinin **(11**; **Figure 3)**, is not related to any other anti-malarial drugs. Limitations associated with this drug are low solubility, short plasma half-life, poor oral bioavailability and high rates of recurrence of the disease, which prompted investigations into the discovery of its other analog with better physicochemical and pharmacokinetic profiles (Lee and Hufford, 1990; Lin and Miller, 1995).

Artemether **(12)**, Artesunate **(13)** and Dihydroartemisinin **(13A)** (Barradell and Fitton, 1995), are the fast acting modified analog of Artemisinin **(Figure 3)**, all of have rapid clearance tendency against erythrocytic forms (blood schizonts) of malaria parasite from the blood (Lin and Miller, 1995). Moreover, some recently investigated derivatives such as 12 β-allyldexoartemisinin **(14)** and trioxanes derivatives **(15**, **Figure 3)**, have been found to be effective as arteether against drug-resistant strain of *P. falciparum* (Ploypradith 2004., Maurya et al., 2012).
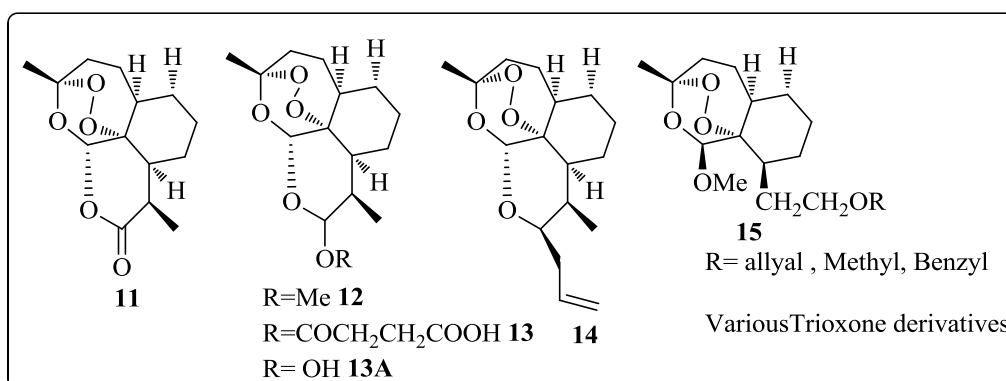
Figure 3: Artemisinin and its derivatives

1.5.2. Antimetabolites

On the basis of mode of action, the antimetabolites are divided into two categories:

Type 1: Known as sulfa drugs, the most important among them include dapsone **(16)** and sulfamethoxazole **(17)**; shown in **Figure 4**, inhibit the activity of dihydropteroate synthetase by competing with PABA (p-aminobenzoic acid).

Type 2: known as principle antifolates, e.g., pyrimethamine **(9)** and proguanil **18** (active form cycloguanil), compete with dihydrofolate to inhibit dihydrofolate reductase (Warhurst, 1986), as shown in **Figure 4**.
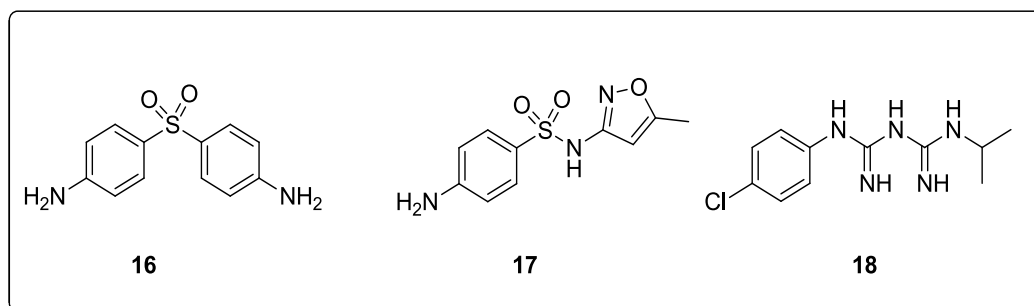
Figure 4: Type 1 and Type 2 antifolates

1.5.3. Aminoquinolines

Aminoquinolines are the derivatives of quinoline and are classified into three different categories.

(I) 4-aminoquinolines: which include chloroquine **(6)**, hydroxychloroquine **(7)** and amodiaquine **(8)**, (II) 8-aminoquinolines: include pamaquine **(1)** and primaquine **(2)**, (III) Miscellaneous analogs: include mefloquine (**19**, Cerami et al., 1992) and halofantrine (**20**, Dvorak et al., 1975), as shown in **Figure 5.**
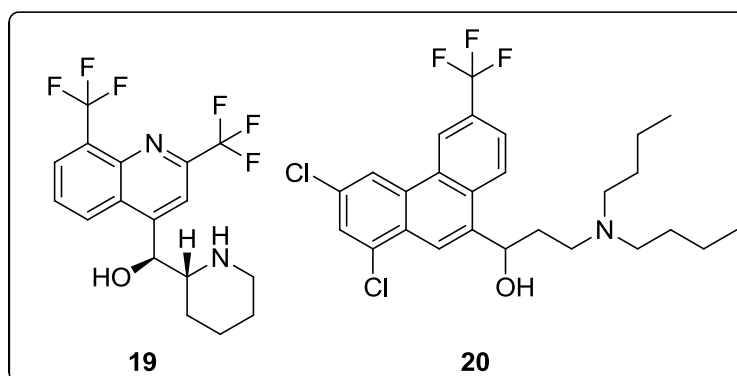
Figure 5: Structure of some aminoquinolines

1.5.4. Antibiotics

The most commonly used antibiotics in malaria treatment are doxycycline **(21A; Figure 6)**, tetracycline **(21B)** and clindamycin **(21C)**. Structurally, doxycycline is a tetracyclic compound; synthesized from oxytetracycline. The mode of action of doxycycline and tetracycline is to inhibit parasite mitochondrial protein synthesis (Kiatfuengfoo et al., 1989).
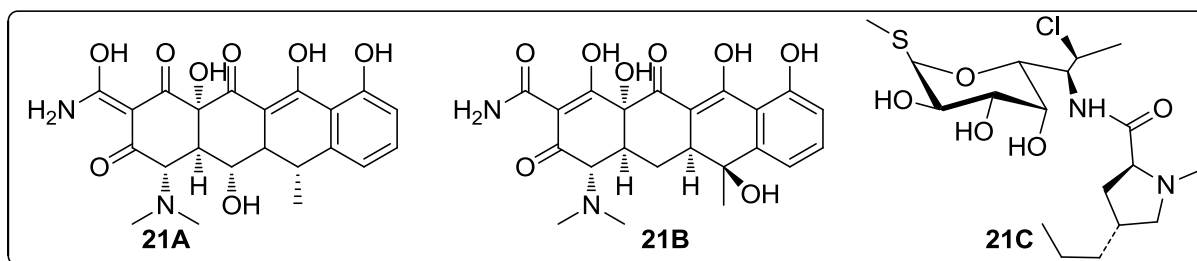
Figure 6: Structure of some antibiotics

1.5.5. Malarone

Malarone (derivative of naphthoquinone) is a new synergistic combination of atovaquone **(22**; **Figure 7)** and proguanil **(16)**, (Looareesuwan et al., 1999). Atovaquone stops the growth of malaria parasite *P. falciparum* by inhibiting electron transport chain system. However, single administration of atovaquone resulted in rapid resistance.
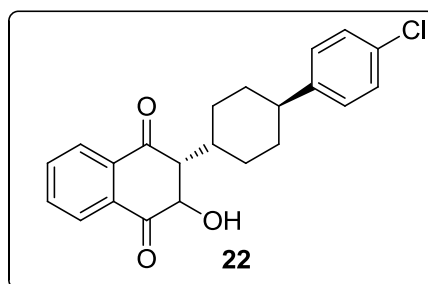
Figure 7: Structure of Atovaquone

1.5.6. β-Carboline alkaloids

β-carboline is a widespread moiety in plants and animals and considered as an important class of indole alkaloids. Structurally, it consists of a pyridine ring that is fused with indole skeleton. Investigation on this scaffold demonstrated that, harmala alkaloids **(Figure 8)**, such as harmine **(23)**, harmane **(24)** and harmaline **(25)** possess moderate *in vitro* antiplasmodial activity against three *Plasmodium falciparum* strains W2, D6 and TM91C235 (Kuo et al., 2003), whereas Manzamine alkaloid, Manzamine A **(26)** and 8-hydroxymanzamine A **(27)**, retained potent activity towards chloroquine sensitive strain D6 and W2 (Penta et al., 2013).
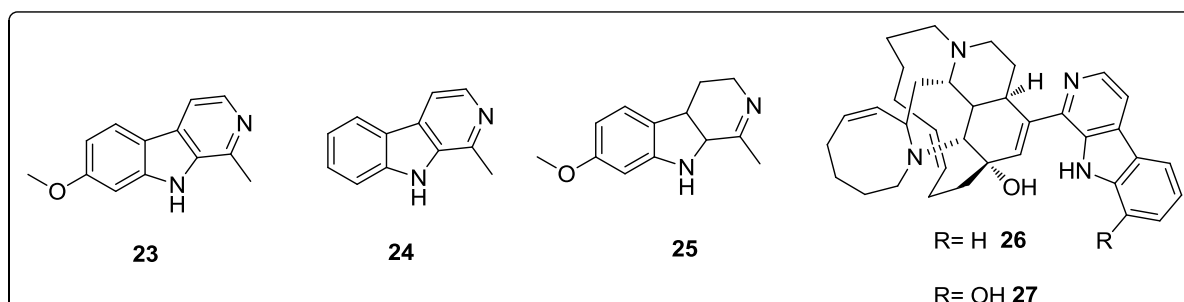
Figure 8: Structure of some β-carboline alkaloids

1.6. Potential chemotherapeutic targets in the malaria parasite

1.6.1. Digestive vacuole and proteinases

The digestive vacuole (an acidic, lysosome-like organelle) of parasite and cytoplasm of both the parasite and the host cell undertake many key processes for the survival of the parasite. Thus, both act as potential chemotherapeutic targets for malaria drug discovery and development. As soon as the digestive vacuole is formed in the parasite, it appears to be the primary site of haemoglobin hydrolysis.

To date, virtually all the haemoglobin degrading capability is ascribed to two aspartic proteinases (plasmepsin I and plasmepsin II), one cysteine proteinase (falcipain) and at least one metalloaminopeptidase (falcilysin), (Coombs et al., 2001). The Inhibition of these enzymes have been shown to block hemoglobin catabolism and kill the plasmodia parasite in culture systems (Kamchonwongpaisan et al., 1997). Therefore; these three proteinase are potential chemotherapeutic targets for anti-malarial drug discovery and development.

The transport of haemoglobin to the vacuole is initiated by vesicle bud from the cytostome (pinocytosis; **Figure 9**). Quinine and 4-aminoquinoline (chloroquine), as front-line anti-malarials, are thought to act primarily by binding to the heme (Olliaro and Yuthavong, 1999).
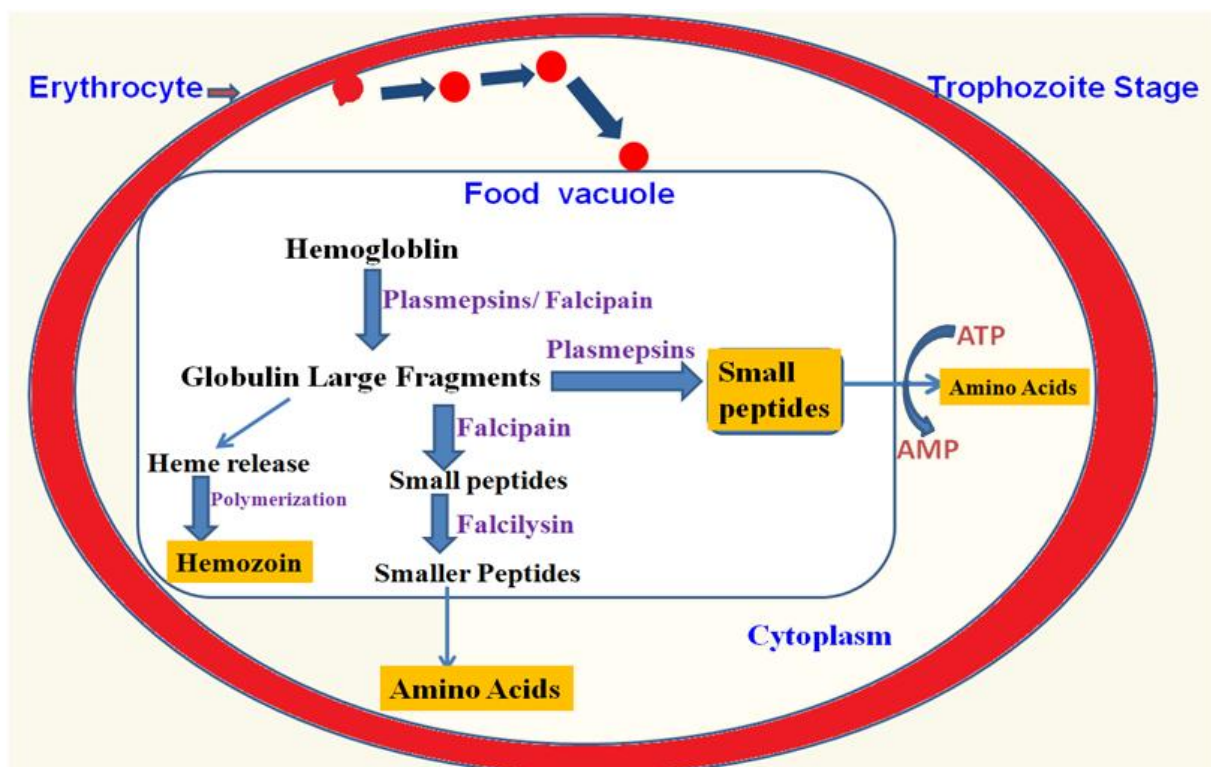
Figure 9: Hemoglobin degradation pathway in *P. falciparum*

The consequence of this binding leads to the inhibition of heme polymerization process and generation of toxicity inside the parasite. Resistance has emerged through drug extrusion mechanism at the digestive vacuole membrane level rather than by mutation at the binding site (Slater, 1993).

1.6.2. Apicoplast

The apicoplast (plastid like organelle) has been identified in most apicomplexan, including the malaria parasite (Kohler et al., 1997). The functions of apicoplast is to maintain certain particular functions including fatty acid, amino acid and heme metabolism (Roos et al., 2002). The apicoplast has a unique prokaryotic genome sequence, and this certainly demonstrates the anti-malarial action of antibacterial drugs that otherwise does not affect eukaryotes. However, most apicoplast genomes are sequenced in the nucleus and then transferred to the apicoplast organelle by a unique mechanism (Foth et al., 2003). Some of the antibacterial compounds are efficacous though slow-acting, anti-malarials (Clough and Wilson, 2001). The mode of action of these compounds, e.g., tetracyclines, chloramphenicol and clindamycin, is to inhibit the mitochondrial or/and apicoplast patways (Rosenthal, 2003).

1.6.3. Glycolysis

Glycolysis is a cytosolic pathway in which glucose is converted into pyruvate. Plasmodia parasites are solely dependent on this pathway for free energy production. Some reports have suggested that, involvement of enzyme lactate dehydrogenase in the glycolysis pathway, that can be used as a target for anti-malarial drug design (Dunn et al., 1996; Deck et al., 1998). Despite enormous efforts to generate a potential molecule by screening of thousand of compounds against this chemotherapeutic target, still there is no known lead compound at present.

1.6.4. Nucleic acid metabolism

Nucleic acids are precursors of DNA and RNA, and its metabolism in the malaria parasite appears to be same as occur in other organisms except human (Moulder, 1951).The major difference between plasmodia and the corresponding human pathways; is that plasmodia lack the ability to synthesize the nucleotides (purines and pyrimidine) through the *de novo* pathway (Sherman, 1979), whilst mammalian cells can either salvage or synthesize *de novo* pyrimidine nucleotides. Therefore, the parasite entirely depends on the purine salvage pathway, i.e., host purine precursors.

The parasite-specific enzymes involved for salvage pathway are: hypoxanthine-guanine phosphoribosyltransferase (HGPRT), and purine nucleoside phosphorylase (PNP), (Keough et al., 1999; Shi et al., 2004). Several investigations have reported that HGPRT and PNP may be essential for parasite, as revealed by the fact that, antisense nucleotides targeting HGPRT mRNA abolish parasites growth *in vitro*. (Cassera et al., 2011; Seok et al., 2011). However, It is important to mention that, humans also possess HGPRT, therefore the selection of inhibitors must be selective and specific. So far; it is unclear whether HGPRT can ever qualify for anti-malarial drug screening (Shi et al., 2004).

1.6.5. Mitochondrial electron transport

The electron transport chain of intra-erythrocytic plasmodia parasites consists of five enzymes (Nixon et al., 2013); ubiquinone oxi-reductase succinate, glycerol-3-phosphate dehydrogenase, dihydroorotate dehydrogenase (DHODH), ubiquinone oxi-reductase (complex-2) and malate quinine oxi-reductase. The exact functional information for all these enzymes are still unclear. Dihydroorotate dehydrogenase (DHODH), impart unique property with its human analog. It is present in the mitochondria and essential for uridine monophosphate formation during pyrimidine biosynthetic pathway. Various inhibitors targeting this enzyme have been designed, synthesized, and evaluated (Krungkrai, 1995), e.g., 5-Fluorooratate and its derivatives.

1.6.6. Biosynthesis

1.6.6.1. Phospholipid metabolism

Phospholipids is an important source for parasite growth and multiplication as evidenced by lipid level of the infected erythrocyte (significantly higher), compared to that of normal erythrocytes. In plasmodia, phosphatidylcholine (PC) is the main parasite phospholipid, which is produced by ethanolamine, *via* the phosphatidylethanolamine *N*-methyltransferase pathway (Vial and Ancelin, 1992).

In addition, 60-80% of PC is obtained from *de novo* pathway (also known as Kennedy route) through CDP-choline synthetic pathway. In this context, quaternary ammonium and bis-ammonium salts with one long lipophilic alkyl chain, have been designed and screened. It is worthwhile to mention that, members of these family of compounds proved effective during *in vivo* experimental studies and are being further investigated (Olliaro and Yuthavong, 1999).

1.6.6.2. Tubulin assembly

Preliminary investigation on anticancer agent taxol **(28**; **Figure 10)** and its butyloxy carbonyl-substituted derivative, e.g., taxotere **(29; Figure 10)**, have been carried out to find their role in tubulin polymerization in parasite. In addition, tubulin fluorescence has been used to correlate spindle development with the nuclear cycle and to characterize the disruption of mitotic structures in response to anti-malarial drug treatments (Gerald et al., 2011). Nevertheless, tublin synthesis in *Plasmodium* still lacks a fully reconciled picture to design novel antimalraial agents.
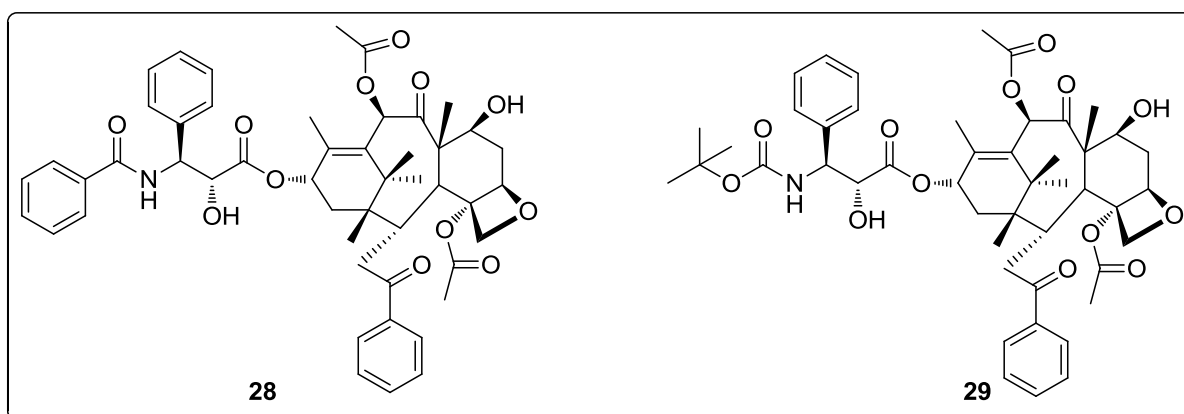
Figure 10: Structure of Taxol and Taxotere

1.6.7. Membrane processes and signaling

1.6.7.1. Trafficking

Membrane of infected erythrocytes at intra-erythrocytic phase induce profound changes that allows the parasite with increased permeability to transport nutrients from the surrounding. Theoretically, transport system to facilitate the selective entry could be utilized as a possible target (Ginsburg, 1994). Researchers have attempted to address this target from different approaches as supported by the reported literature (Linder et al., 2013; Ramya et al., 2007). However, current knowledge of trafficking pathway in *Plasmodium* is very less.

1.6.7.2. Signal transduction

Ca^{2+} signalling pathways inside *Plasmodium* has been identified as a major mechanism controlling the growth and development of parasite. Over the past few years, several studies have explored the possibilities of different signalling pathways that can be applied to *Plasmodium* (HermGotz et al., 2007; Meissner et al., 2007). However, the regulation of

signalling pathways is complicated and development of compounds with selectivity has proved as a major challange.

Overall, most of the above mentioned targets have selectivity and sensitivity as major concern. Moreover, mutation in the key enzymes or transporters of different biological targets made them resistant to current (existing) anti-malarial therapy (Alam, 2014).

Therefore, development of novel and effective chemical classes of anti-malarial drugs, especially compounds that act against novel biochemical targets could be a better approach to overcome the problem faced by clinically used drugs.

1.7. Proteases and implications for the new anti-malarial drug development approaches

1.7.1. Proteases as a valid drug target

Protozoan parasites belong to kingdom Protista, are a diverse group of unicellular organisms, that perform proteolysis. Among them, some of the proteases have developed to parasitize humans, and have had a keen impact on the history and evolution of life. This fact was showcased by Zimmer (2000), describing the relationship between the generation of different species of parasite and adaptation with respect to the humans as their primary hosts. Despite more than a century of efforts to eradicate malaria, still parasites continue to levy a tremendous medical, social and economic burden on human population, particularly in tropical and subtropical geographical foci of the world. Moreover, in protozoa parasitic, proteases carry out "housekeeping" duty common to many eukaryotes, as well as some other tasks such as protein synthesis, folding, and control of metabolic activities that are highly specific to the parasite survival. Due to the ubiquitous nature of proteases in various chemical, biological and physiological processes, these enzymes have been studied as prime targets for drug discovery. Hence, protozoan proteases belonging to the malaria parasite act as promising targets for anti-malarial drug design.

1.7.2. Proteases general classification

Based on catalytic residue, proteases are classified into four broad groups

(A) Aspartate proteases

Aspartyl proteases (APs) also known as aspartyl proteinases, or acid proteases belong to a subfamily of proteases, that use aspartate amino acid residue for peptide substrate catalysis.

Aspartyl proteases are associated in the early events of the hemoglobin hydrolysis in acidic food vacuole of *P. falciparum*. Plasmepsin I and II are the two best characterized and closely linked aspartic proteases that start the degradation of hemoglobin by hydrolysing the bond of 'α' chain of native haemoglobin, between Leu34 and Phe33 residues (Gluzman et al., 1994).

(B) Metalloproteases

Metallopeptidases are the most diverse subfamily among the four main category of proteases. These proteases use zinc metal for the further degradation of hemoglobin derived oligopeptides (Sijwali et al. 2002). PfA-M1 and Pf-LAP are the two fundamental metallopeptidases, encoded by genome sequence analysis (Dalal & Klemba, 2007).

(C) Cysteine proteases

Cysteine proteases are also known as thiol proteases, characterized by a nucleophilic cysteine thiol group in the catalytic triad active site. *P. falciparum* genome consists of 33 putative cysteine proteases (Wu et al., 2003), of which seven are papain-like cysteine proteases (major superfamily).

(D) Serine proteases

Serine proteases catalyze hydrolysis of peptide bond through reaction of the serine side chain with the substrate carbonyl. The catalytic activity of serine proteases depends on the combined action of a nucleophile, a general base and an acid. In the classic trypsin, chymotrypsin (eukaryotes), and subtilisin families (prokaryotes), serine proteases catalytic triad is composed of serine, aspartic acid and histidine residues and shows similar architecture of the active sites (Polgár, 2005).

1.8. Target selection

Among the four major classes, three proteases (aspartate, metallo and cysteine) are majorly involved in haemoglobin digestion and present in the food vacuole of parasite. Interestingly, it has been reported that, parasite can survive with a reduced growth rate, without aspartate and metalloproteases (Moura et al., 2009).

On the contrary, inhibition of cysteine proteases leads to the death of parasite, indicating its essential role in important processes in parasite life cycle. Therefore, inhibition of cysteine

proteases represents one of the most promising targets for anti-malarial drug discovery (Rosenthal et al., 2002; Liu et al., 2006).

Serine proteases especially, ATP-dependent proteases are responsible for more than 90% of the protein turnover inside the parasite apicoplast (Gottesman 2003; Rathore et al., 2010). Drugs targeting ATP-dependent protease would have the double advantage of**:** distinguishing host and parasite by targeting prokaryote-specific functions, minimizing side-effects for humans; and potentially offering a common treatment against malaria and other antibacterial diseases.

Thus, as a part of the research work, a multidisciplinary approach is taken against two different targets; cysteine protease (falcipain-2) and serine protease (ClpP), selected to develop potential drug-like lead molecules to address the persisting challenges of malaria therapy.

1.8.1. Functions of cysteine proteases

1.8.1.1. Hemoglobin hydrolysis

P. falciparum parasite is solely dependent on its host for the growth and development. Hemoglobin degradation takes place in the parasite's food vacuole escalated by the cytostome machinery. Several proteases are involved in this process, but the exact alignment of events is not well defined.

So far, there are two suggested pathways, the first pathway in which aspartyl proteases, specifically plasmepsins (Goldberg et al., 1991; Gluzman et al., 1994), have been involved to start hemoglobin degradation by hydrolysis of peptide bonds of the main chain residues (Banerjee et al., 2002), and further degradation by cysteine proteases, metalloproteases (falcilysin) and dipeptidyl aminopeptidase-1 (Liu et al., 2006). The other proposed pathway suggests that, cysteine proteases are mainly involved in the hemoglobin degradation (Rosenthal et al., 1988). Despite the conflicting sequence of events that, have been proposed during hemoglobin degradation, the involvement of cysteine proteases has been proven (Shenai et al., 2002; Wang et al., 2007).

1.8.1.2 Tissue and cell invasion

It has been concluded that, migrations from one host compartment to another, i.e., cell invasion and tissue migration is an important process in plasmodia lifecycle (Ghosh &

Edwards, 2000). Investigations on cysteine protease inhibitors have shown that, they have a pronounced effect to inhibit host cell invasion process (Rosenthal, 2004).

1.8.1.3. Protein processing and activation

The initial interaction between merozoite and erythrocyte probably involves protein-protein interactions which lead merozoite surface protein to undergo many processing and activation (Sturm et al., 2006). Cysteine protease inhibitors have shown to inhibit the functions of this protein; hence release of merozoite stops during parasite life cycle (Sajid & Mckerrow, 2002).

1.9. Cysteine proteases-falcipains (FPs)

On the basis of *P. falcipains* genomics, falcipains have been categorized into a group of four enzymes, which are: FP-1, FP-2, FP-2' and FP-3 (Rosenthal, 2004).

Falcipain-1

Falcipain-1 (FP-1) is the first discovered cysteine protease, found comparatively in very low ratio as compared to other falcipains in the parasite during erythrocytic stage. Low level of FP-1 integrates difficulties to the production of recombinant protease for high-level expression studies such as functional and structural characterization.

Falcipain-2

Falcipain-2 also called as FP-2A, is an another cysteine protease consisting of food vacuole hemoglobinase activity and is highly expressed during merozoites, trophozoites and early schizonts stages (Shenai et al. 2000). Inhibition of FP-2 blocks degradation of hemoglobin and consequently parasite growth and development (Sijwali et al. 2006; Mahesh et al., 2014; Mundra & Mahesh, 2015). This makes it a prominant target for drug development.

Falcipain-2'

Falcipain-2' (FP-2') or falcipain-2B (FP-2B) is almost similar to FP-2 and is present on chromosome 11 adjacent to falcipain-2A gene (Jeong et al., 2006). The major difference between FP-2A and FP-2B is that, FP-2B cleaved ankyrin (erythrocyte membrane) but not protein 4.1, which is important for host cell rupture (Jeong et al., 2006). So far, FP-2B has

not been fully characterized, and the functional significance of the amino acids variation remains unvalidated.

Falcipain-3

Falcipain-3 (FP-3) is predominantly expressed in early schizonts, trophozoites and later in erythrocytic stage of the parasite life cycle. Sequence analysis demonstrated that, 66% (catalytic domain only) sequence of this enzyme is identical with falcipain-2. However, the concentration of FP-3 is almost 1.8 time lesser than FP-2 and is very less affected by typical cysteine protease inhibitors (Sijwali et al. 2002).

1.9.1. Falcipain-2 protease as a drug target

Among, falcipains, FP-2 is a principal cysteine protease, that plays a major role in parasite food assimilation by its ability to degrade haemoglobin. Many *in vitro* studies have affirmed that, inhibitors of falcipain-2, prevents the growth of culture parasites (Shenai et al., 2003; Lee et al., 2003; Domínguez et al., 1997; Huang et al., 2002). Some of them were also effective against *in vivo* severe malaria (Rosenthal et al., 1993).

In addition, among the four *P. falciparum* cysteine proteases, falcipain-2 is the most intensely studied enzyme. Structural and functional data suggests that, it is an important target for therapeutic intervention (Pandey et al., 2005; Wang et al., 2006). Further, falcipain-2 shares 95% amino acid sequence homology with falcipain-2' enzyme. Therefore, this enzyme is not only involved in the degradation of hemoglobin, but also involved in the degradation of erythrocyte-membrane skeletal proteins (ankyrin and the band 4.1), leading to the fast host cell rupture and release of the mature merozoites (Rosenthal, 2011; Dasaradhi et al., 2005).

1.10. General structural features of FP-2

Three-dimensional structures of FP-2 in complex with cystatin (1YVB pdb code), (Wang et al., 2006) and free FP-2 (inactivated by iodoacetamide, pdb code 2GHU, and 3E1Z), have been investigated (Hogg et al., 2006), and deposited in the Protein Data Bank. The crystal structures of FP-2 (3BPF.pdb code) in complexation with E-64 appeared in the PDB database (Kerr et al., 2009). Study shows that, the FP-2$_{nose}$ is essential for proper folding of the protease (Ettari et al. 2010), and deletion analysis of FP2$_{nose}$ demonstrates that, it contains 17 amino acids (Sijwali et al., 2002). Whereas, FP2$_{arm}$ which comprises of 14 amino acids, is present at the distal end (residues 183–196), of the R domain.

The catalytic triad of Cys 42, Asn 173 and Hip 174 are located in the cleft between the two structurally distinct domains (Ettari et al. 2010). Overall, FP-2 enzyme has a broad active site and carries different binding pockets, as represented in **Figure 11**.

Falcipain-2 active site

FP-2 has a large active site which is divided into pockets comprised of S1-S3 and S1' corresponding to the T_3, T_1, T_2 and $T_{3'}$ position of the inhibitors (Pandey and Dixit, 2011).

The S1 sub site has a highly conserved amino acid residue of 'Glutamine' that plays a crucial role for substrate stabilization during transient state (Sabnis et al. 2003). The S2 sub site which is a major hydrophobic pocket in cysteine proteases determine ligand specificity and selectivity, characterized by a high abundance of Asp234, Ile 85 and Leu 84 amino acids (Pandey & Dixit, 2012). The S3 subsite is a Glycine affluent region, which is conserved across all homologs of cysteine proteases. The S1' sub site is mainly involved in hydrophobic interactions between protease and substrate (Sabnis et al. 2003).
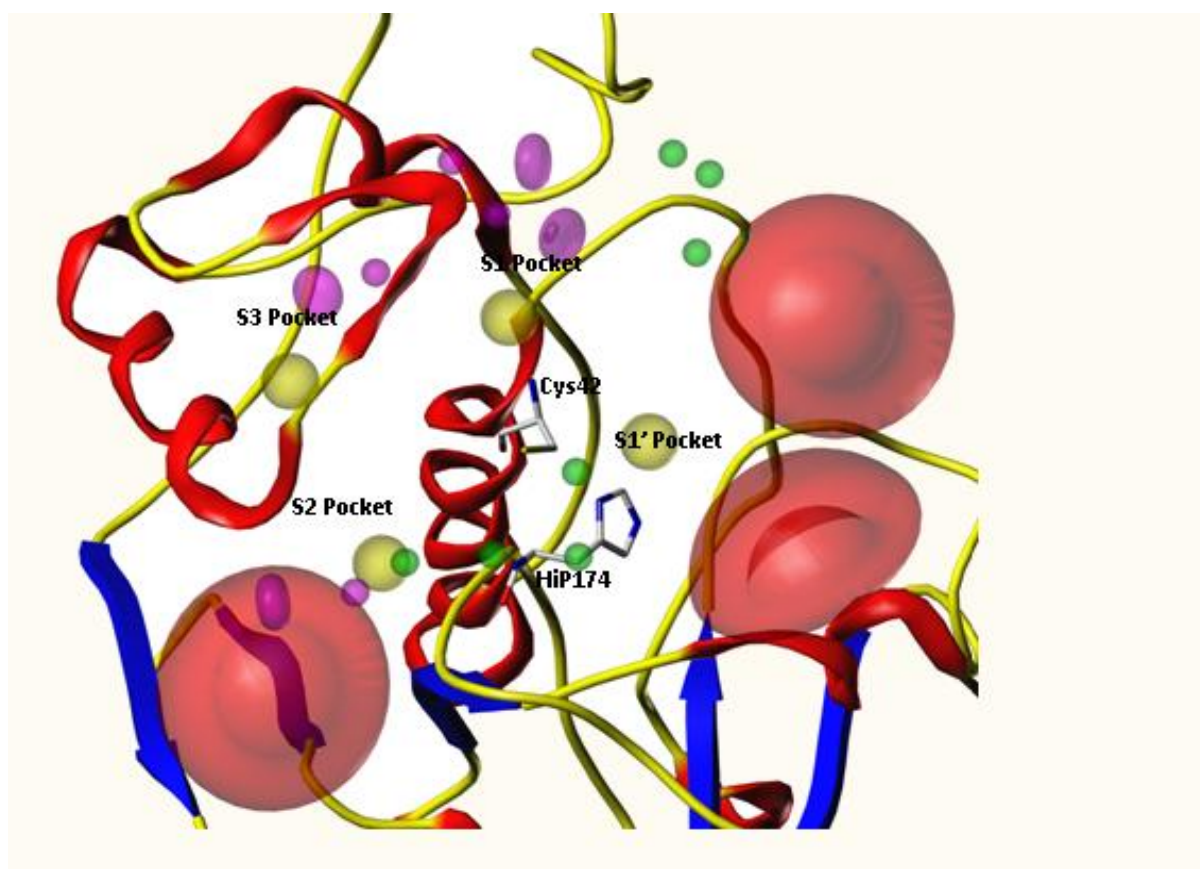
Figure 11: Falcipain-2 enzyme three-dimensional structure (PDB ID: 1YVB). Catalytic residues Cys42 and Hip174 are shown in capped-stick representation (Chakka et al., 2015)

1.11. ATP-dependent proteases

1.11.1. General introduction

In 1987, two scientists BJ Hwang and Yoko Katayama, identified Clp proteases (Hwang et al., 1987; Katayama et al., 1987) in *E. coli*. These proteins are mainly involved in the degradation of casein protein, thus called as Caseinolytic Proteases. ClpP family belongs to a broad family called 'AAA' (ATPase associated with various activities) proteins (Neuwald et al., 1999).

The ATP-dependent proteases ClpP, are highly expressed in bacteria and eukaryotes (Yu and Houry, 2007), and carries two essential components. First component (A) comprises of ATPase activity, e.g., ClpA, ClpC, ClpE or ClpX (Hwang et al., 1987) and the other component (P), is proteolytic in nature e.g. ClpP or ClpQ. The first component recognizes the target protein and second component in proteolytic chamber translocate, unfold the substrate protein and degrade the protein into 4-8 amino acid peptides.

1.11.2. Distribution of ATP-dependent proteases

1.11.2.1. Eukaryotic proteasomes

In eukaryotic mitochondria, 26S proteasome is the major energy dependent protease, involved in regulation of protein degradation (Glickman and Ciechanover, 2002). It consists of two subunits, a regulatory unit 19S and a proteolytic subunit 20S. The formation of 19S subunit requires assembling of six different 'AAA' proteins. This component recognizes the protein substrate and starts the process of translocation and unfolding, and later 20S subunit degrades the targated protein into peptide fragments (Lupas et al., 1997; Wickner et al., 1999).

1.11.2.2. *E. coli* proteases

E. coli consists various ATP-dependent proteases; ClpAP, ClpXP, ClpYQ, FtsH and Lon. They play a vital role in various cellular processes and to maintain the protein quality.

1.11.2.3. Proteases in *Bacillus subtulis*

Gram-negative bacteria *Bacillus subtulis* carry three different types of ClpP proteases (ClpXP, ClpCP and ClpEP). In the development cycle of the bacteria, the ClpP proteases not

only participate in proteolysis, but also regulate sporulation (Turgay et al., 1998, Turgay et al., 1997; Kirstein et al. 2005).

1.11.2.4. Clp proteases in parasite

In apicoplast of the genus *Plasmodium*, ClpP proteases have been identified. The specific *P. falciparum* ClpP (*Pf*ClpP) protein shows a high level of sequence homology with cyanobacteria, such as *Nodularia spumigena* (47% homology), *Isochrysis galbana* (47% homology), Nostoc sp (47% homology) and *Burkholderia multivorans* (51% homology) (prince et al., 2007; Rathore et al., 2010). While, ClpQ protease (*Pf*ClpQ) machinery is localized in the mitochondrion of malarial parasite (Rathore et al., 2010), and ClpR protease (*Pf*ClpR), inactive homologue of *Pf*ClpP is located in apicoplast (Houry and co-workers, 2013).

1.11.3 Significance of proteolysis

The survival of cell solely depends on maintaining suitable concentrations of intracellular macromolecules. Intracellular stimulants caused by cellular differentiation, proliferation, and extracellular signals produced by environmental changes, lead to a shift in protein content and gene expression in a cell.

Translational and transcription are not only processes, controlling responses to the intracellular and extracellular changing conditions. Regulation over protein expression administers control over the synthesis of a protein as well as manages the activity of a processed protein. Numerous mechanisms, e.g., proteolytic processing, changes in localization of proteins, protein turnover by interactions with proteases and covalent modification of a protein molecule have been involved to control protein activity. Unlike, ADP-ribosylation, adenylation, phosphorylation and covalent modification, proteolysis, is an irreversible way of cellular regulation.

1.11.4. Rational support for ATP-dependent protease (Clp) as a valid target for drug discovery

Protein unfolding and degradation is an important cellular process by which the cell regulates important physiological functions, such as signal transduction (Hochstrasser, 1996), cell cycle control (Hartwell and Kastan, 1994; Jenal and Hengge-Aronis, 2003), the recycling of proteins (Wickner et al. 1999), antigen development (Lindsey et al. 1998), cell processes (Ben-Shahar et al. 1997) and programmed cell death (Bota et al. 2005). Diseases

linked to improper protein degradation includes, Huntington's disease (Di Figlia et al. 1997), Alzheimer's disease (Wisniewski et al. 1997) and Prion disease (Prusiner 1997). Thus, aberrant degradation by these proteases leads to a severe diseased state.

1.11.5. The mechanisms of unfolding and degradation by ATP-dependent proteases (ClpP)

The reaction carried out by ATP-dependent proteases is a multi-step catalyzed reaction, which include unfolding and subsequent degradation of the substrate as depicted in **Figure 12**. The first step, involves the rapid formation of ATPase-Protease complexes (Singh et al. 1999), require ATP (Maurizi et al. 1998).

Protein degradation process initiated with the noncovalent interaction in-between ATPase-protease complexes with ATPase ring component of the ATP-dependent protease. The next step, which involves ATP binding and hydrolysis process, leads to the substrate engagement and unfolding within the ATPase ring. Consequently, the unfolded polypeptide translocates through a very narrow channel into the proteolytic chamber. In this chamber, the polypeptide chain interacts with the active sites (Reid et al. 2001; Kenniston et al. 2003), and degrades into small peptides and the products are released into the cytosol (Thompson et al. 1994).

In proteolysis, selectivity is extremely paramount for a targeted protein by ATP-dependent proteases. When an appropriate protein is required within the cell, the cellular machinery guards the proper synthesis of a particular regulatory protein.

Moreover, when an operative (active) protein is no longer required for physiological cellular activity, the cell has effective ways to eliminate that protein from its duties. Sometime protein also fold into an another three dimensional structure, causing a loss of normal protein functioning.

Thus, proteolytic mechanism is responsibile for the degradation of both native and misfolded proteins. Balance between generation and destruction of active proteins determine cellular activity, and imbalance between these two tasks may lead to a disruption of normal cellular function. Thus, the mechanism of compartmentalization selection, safeguards the ATP-dependent protease to degrade only inactive proteins.
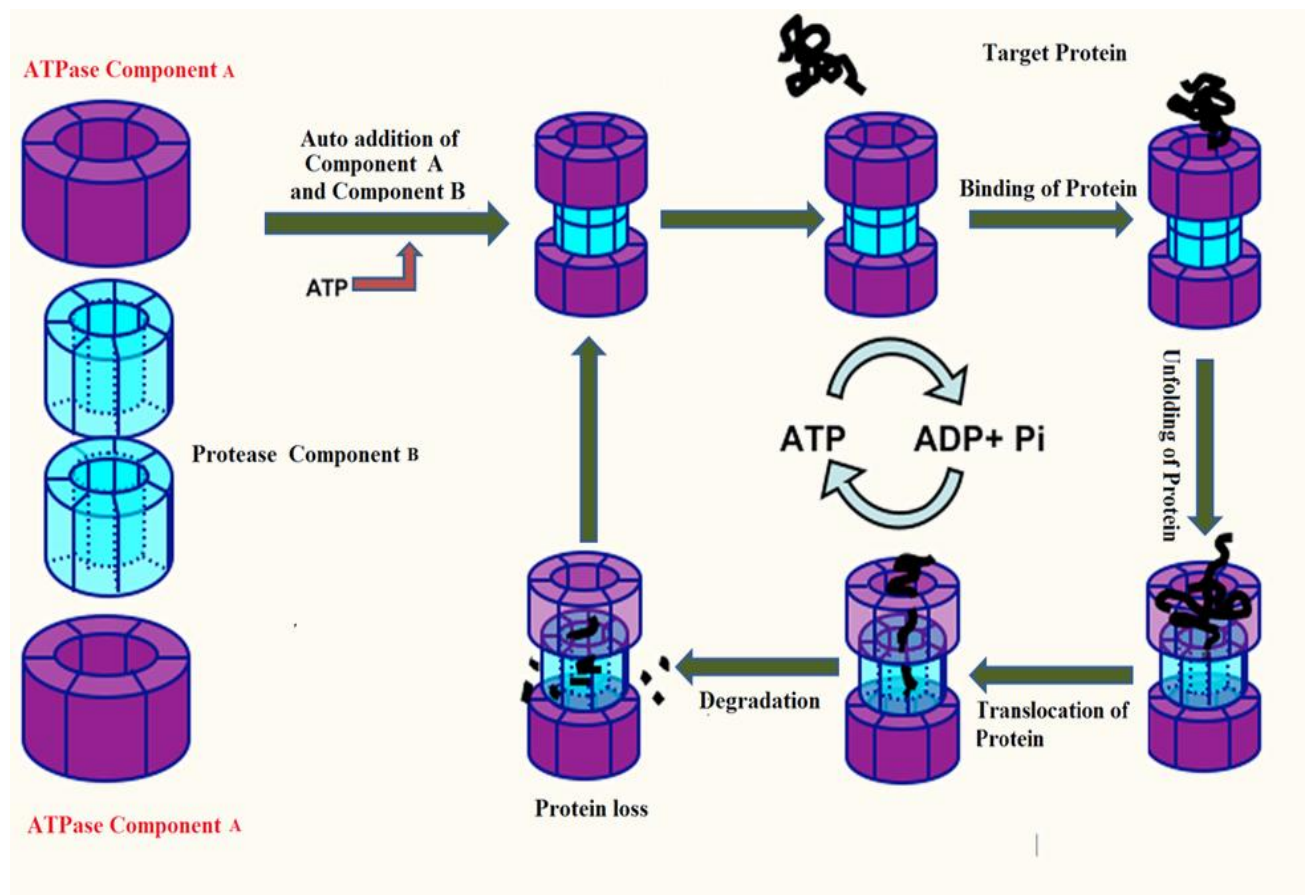
Figure 12: The mechanism of unwinding and degradation occurred by ATP-dependent proteases (Singh et al. 1999; Maurizi et al. 1998)

1.11.6. Implication of *Plasmodium falciparum* ClpP protease for the novel anti-malarial drug design

The campaign for malaria treatment, stresses the need for new anti-malarial drugs, that will be effective in treating current drug resistance in parasites (Research agenda for malaria eradication, 2011), and in accordance with this the efforts in the past years have shifted towards developing novel classes of anti-malarial drugs. Another attractive approach would be to develop drugs directed against novel targets that have not yet been fully exploited for therapeutic use.

Despite the extensive research on the various aspects of the proteases, the study envisioned on the role of ATP-dependent protease ClpP inhibitors as anti-malarial is very less. Thus, ATP-dependent protease ClpP can be considered as potential drug target.

In the malarial parasite, apicoplast is present as reduced cyanobacterial plastid and plays a vital role in the biosynthesis of fatty acids and haem (Ralph et al., 2004). Studies have shown that, nuclear-encoded proteins are mainly responsible for the proper functioning of apicoplast (Waller et al., 2000).

Thus, the selection of protease involved in protein synthesis and degradation in apicoplast could be selected as a potential target in malaria drug discovery (Waller and McFadden, 2005; Goodman et al., 2007; Schlitzer, 2007; Dahl and Rosenthal, 2008).

P. falciparum (*Pf*ClpP), which is orthologue to cyanobacterial ClpP protease, expressed during late trophozoite stages for the rupturing and invasion of new red blood cells by merozoites. Interestingly, all these events in the erythrocytic life cycle are energy dependent and completed by an abundance of proteolytic events in the cell of the parasite. Therefore, inhibition of the prokaryotic ATP-dependent protease *Pf*ClpP machineries in the malaria parasite may represent potential drug target (Rathor et al., 2010).

1.12. ClpP general structure

Various crystal structures are available on PDB database for ClpP proteases (3MT6, ITYF, 2FZS, 4EMM, 3KTG, 2ZLO, 2CE3, 4MXI, 3KTI, 1YG6, IYG8, 4JCT, 1TG6, 2F6I). The structures of ClpP from different organisms have shown two distinct structure states.

The first state observed from *E. Coli*, *Homo sapiens*, and *Helicobacter pylori* is the extended state. In this state, the catalytic triad 'Ser-Hip-Asp' is present in the active site sequestered within a very narrow proteolytic chamber.

The second state observed from *P. falciparum, S. pneumonia* and *M. tuberculosis* is the compact state, which is an inactive state. Unfortunately, *P. falciparum* ClpP does not have the crystal structure of extended state. Therefore, extended state of *E. Coli* crystal structures were used as a template to model the extended state of *P. falciparum* ClpP (homology modeling technique).

Clpp protease catalytic domain from *Plasmodium falciparum* consist of two rings of seven subunits to form a stable double ring structure (Kang et al., 2005). The crystal structure of *Pf*ClpP (PDB: 2F6I; Vedadi et al., 2007) with 2.45 A° resolution showed that, it contains 14 active site (**Figure 13**).
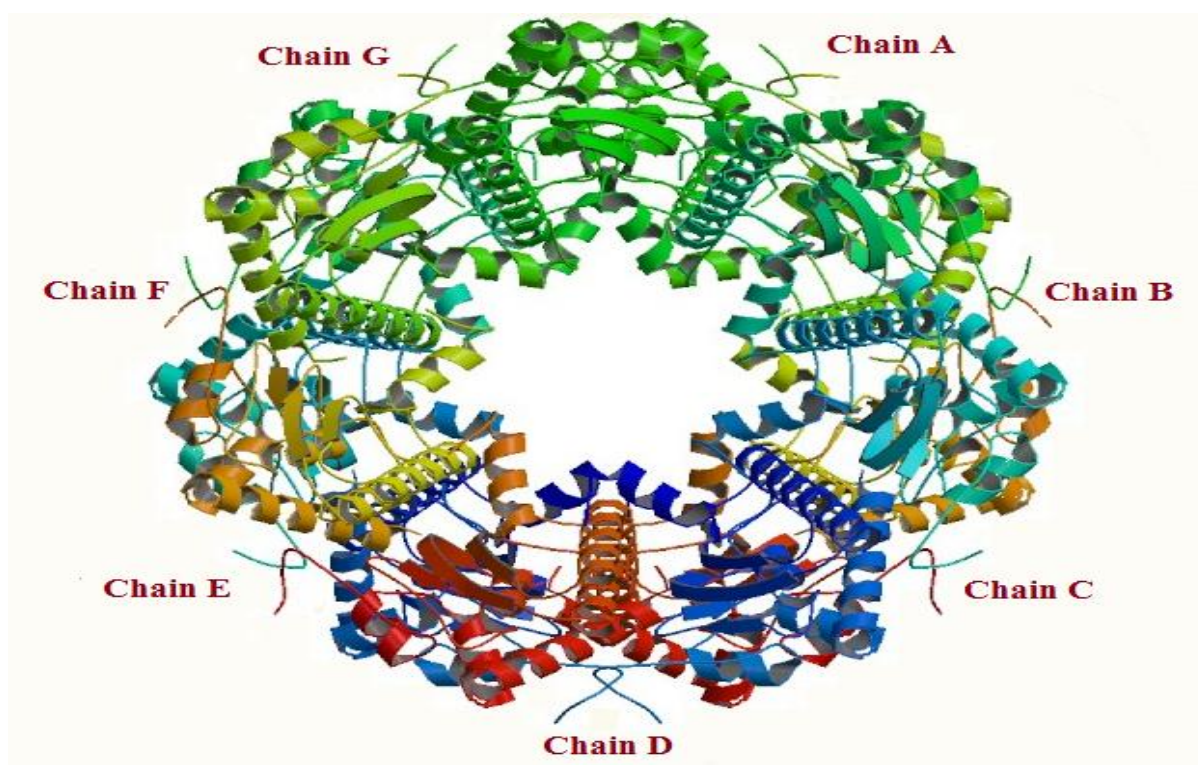
Figure 13: Crystal structure of the ClpP protease catalytic domain from *P. falciparum* (Bakkouri et al., 2010)

1.13. Gap in existing anti-malarial therapy

Emergence of drug resistance in various species of plasmodium, especially against *P. falciparum* becomes a greatest challenge to control malaria. The plasmodium parasites have become resistant to multiple drug therapies (Wirth and co-workers, 1993; Krishna and co-workers, 1999). Often within a few years, resistance has appeared to the each new drug. The rapid re-emergence of resistance to all available drugs made malaria a more acute problem, hence represents a severe limitation of effective drugs in many high-risk areas. Chloroquine continues to be a drug of choice, where it is still effective; however resistance to chloroquine is now widespread, permeating almost 90 percent of the endemic areas, leaving only few regions where it can use reliably. Artemisinin-based drugs have recently emerged as the first line of therapy in the developing world. Unfortunately, some malaria strains have been identified that are resistant to Artemisinin, and the problem is worsening day by day. Thus, drug resistance to all existing anti-malarial drugs is a cause for immediate concern. Further, adverse effects and varied efficacy profile associated with the available drugs and higher production costs limits their widespread application. Therefore, stressing the requirement for development of novel and highly effective analogs that would bind selectively to the biochemical targets in order to minimize the toxicity, adverse effects while retaining the potential for high activity and specificity.

2. LITERATURE REVIEW

2.1. Falcipain-2 inhibitors

To date, a large number of falcipain-2 inhibitors such as peptides, peptidomimetics, chalcones, thiosemicarbazones and isoquinolines have been synthesized for the treatment of malaria.

2.1.1. Peptidic falcipain-2 inhibitors

2.1.1.1. Peptidyl fluoromethyl ketones

Rosenthal et al., (1988) reported that, benzyloxycarbonyl (Z)-Phe-Arg-CH$_2$F **(1)** based peptidyl fluoromethyl ketones, exhibited potent activity (IC$_{50}$ = 0.36 nM) against FP-2. Compound **1** was screened against different strains (Itg2, FCR3, W2 and D6) of *P.falciparum*, and proved as nontoxic, as well as effective in a mid nanomolar to picomolar concentrations.

1

Rosenthal et al., (1993) replaced T$_2$ terminal of fluoromethyl ketones with morpholine group and evaluatd against FP-2 enzyme. Mu-Phe-HomoPhe- CH$_2$F **(2)** (IC$_{50}$ = 3.0 nM) and Mu-Leu-HomoPhe-CH$_2$F **(3)** (IC$_{50}$ = 0.42 nM), were found to be most effective inhibitors. Furthermore, Mu-Phe-HomoPhe-CH$_2$F **(2)**, was also tested against *P. vinckei* cysteine protease (IC$_{50}$ = 5.1 nM) and found as most potent inhibitor. Moreover, it was reported that administration of compound **2** in *P. vinckei*-infected mice (four times a day for four days), cured 80% mice by producing long-lasting immunity.

2　　　　　　　　　　　　　　**3**

24

2.1.1.2. Peptidyl vinyl sulfones

In another study, Rosenthal et al., (1996) developed a series of peptide-based vinyl sulfones and tested against FP-2. Among this series, compound **4** (Mu-Phe-HomoPhe-VS Ph), exhibited IC_{50} values of 0.08 µM and 0.1 µM, against FP-2 and *P. vinckei* protease, respectively. However, the screening results for peptide Mu-Leu-HomoPhe-VSPh **(5)**, which contained a Leucine residue at T_1 terminal, exhibited improved activity against FP-2 (IC_{50} = 0.003 µM), whereas activity against the *P. vinckei* parasite was decreased (IC_{50} = 0.2 µM). Further, morpholine group was replaced with the *N*-methyl piperazine group and the resultant compounds **6** and **7** displayed more inhibition than the parent molecule **5**. Moreover, compounds **6** and **7** strongly inhibited parasite growth and hemoglobin degradation in cultured *P. falciparum* parasites in the nanomolar range.
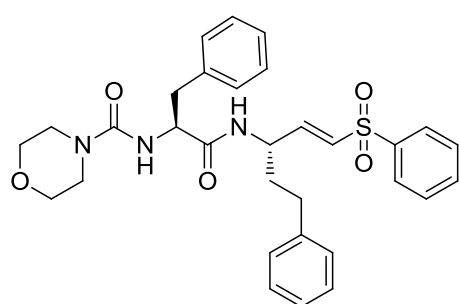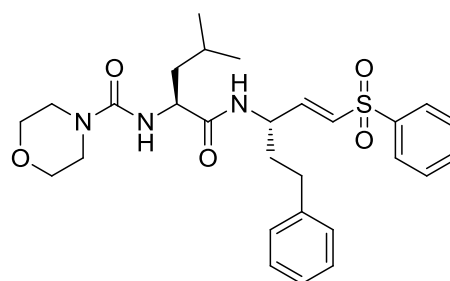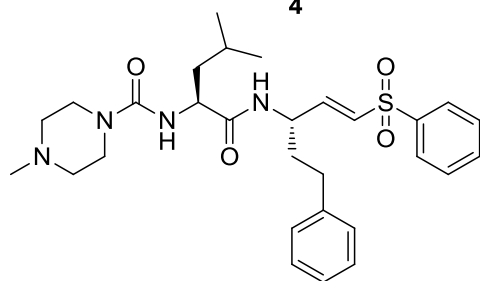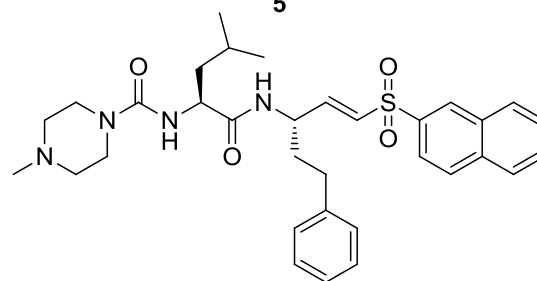
Based on the earlier studies, Shenai et al., (2003) initated efforts to develop a new series of derivatives, contained three different substituents (peptidyl vinyl sulfones, vinyl sulphonamides, and vinyl sulfonate esters) at $T_{3'}$ terminal. Screening results demonstrated that, phenyl vinyl sulfone compound **8**, with IC_{50} in the low nanomolar range was found to be most potent inhibitor. Sulfonamides **9** and sulfonates **10**, were found to be less active against the parasite, but exhibited greater activity against FP-2 enzyme.

Interstingly, vinyl sulfonate esters contained an isonipecotic ester moiety **(8f**, **9f**, and **10f)**, while other ones contained a tertiary amine group **(8c** and **9c)**, displayed the highest inhibitiory values against malarial parasite. On the contrary, prolinol substituted compounds at T_2 terminal **(8b, 9b** and **10b)**, exhibited relatively weak antiplasmodial activity. However, some usual problems appeared in peptide inhibitors due to (i) limited bioavailability and (ii) degradation by protease.

2.1.1.3. α-Ketoamide and Peptidyl aldehyde derivatives

Much effort has been made with regard to the modification of the substituents at the $T_{3'}$ terminal to generate peptidic Inhibitors. This modification has allowed Rosenthal and his colleagues (2003) to develop compounds **11** (aldehyde based) and **12** (ketoamide based), with an IC_{50} value of 1 nM. Further, these compounds were reported to possess significant activity against multiple strains of *P. falciparum*. Other representative inhibitor was Z-Leu-homoPhe-al **(13)** that exhibited an IC_{50} value of 2 nM.

11 **12** **13**

2.1.1.4A. E-64

Hanada et al., (1978) isolated the epoxysuccinyl peptide known as E-64 (N-(L-3-Trans-carboxyoxiran-2-carbonyl)-L-leucyl)-amido(4-guanido)butane), from the culture of *Aspergillus japonicas*. Structurally, E-64 consists a trans configured (2S, 3S) epoxide ring and exhibited potent activity, while Cis form did not express any inhibitory activity. E-64 is an irreversible inhibitor of cysteine proteases (clan CA, family C1), exhibited IC_{50} values of 0.015 μM and 0.075 μM, against FP-2 and FP-3, respectively (Schulz et al., 2007).

E-64

2.1.1.4B. Chymostatin

Umezawa et al., (1970), discovered chymostatin (N-{[(1S)-1-[(4S)-2-Amino-1,4,5,6-tetrahydro-4-pyrimidinyl]-2-{[(2S)-4-methyl-1-oxo-1-{[(2S)-1-oxo-3-phenyl-2-propanyl]amino}-2-pentanyl]amino}-2-oxoethyl]carbamoyl}-L-phenylalanine), through microbial culture filtrates of *Streptomyces hygroscopicus*. Basically, this microbial product contains different ratios of phenyalanine, leucine, valine and isoleucine amino acids residue. Chymostatin is a reversible proteases inhibitor, especially against serine and cysteine proteases (effective concentration 10-100 μM).

Chymostatin

2.1.1.5. Peptidyl aziridines

Power et al., (2002) and Schirmeister T et al., (2003) demonstrated that, aziridines displayed pronounced reactivity due to highly strained ring structures. Therefore, aziridine was considered as one of the key pharmacophore to generate potential falcipain-2 inhibitors. Aziridine peptides were categorized into three different classes **(Table 1)**.

Table 1: Various classes of aziridines
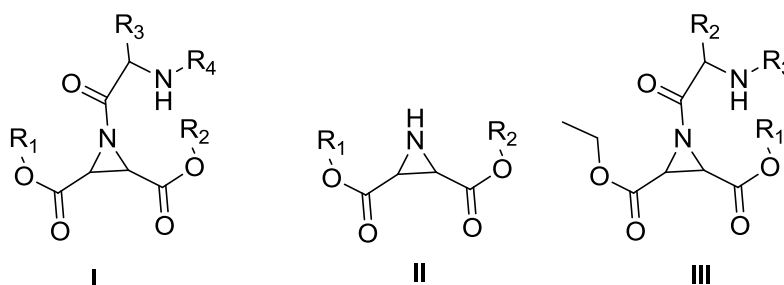
Sr. N.	Class	R_1	R_2	R_3	R_4
I	*N*-acylated aziridine scaffolds	Ethyl, Hydrogen	Ethyl, Benzyl	Amino acid side chain	Protecting group, Amino acid dipeptide
II	Epoxysuccinyl peptides analogs	Ethyl, Hydrogen	Amino acid	-	-
III	*N*-acylated aziridines	Amino acid	Amino acid, Peptide	Protecting group	-

2.1.2. Peptidomimetic FP-2 Inhibitors

2.1.2.1. 1,4-Benzodiazepine peptidomimetics

Micale et al., (2006) developed a series of derivatives based on benzodiazepine (BZD) nucleus. Structure-activity relationships was generated for this series, and it was found that, substitution at 4th position of the phenyl moiety influenced the activity. Therefore, 4-chloro derivative **14**, which contained a methyl group as electron donating substituent on 2nd position showed IC_{50} values of 8.2 µM and 11.2 µM, against FP-2A and FP-2B enzymes, respectively. However, compound **15**, which contained trifluoromethyl group as electron withdrawing substituent on 2nd position, displayed weaker potency with IC_{50} values of 8.7 µM and 25.9 µM, against FP-2A and FP-2B, respectively.

14: R= CH$_3$
15: R=CF$_3$
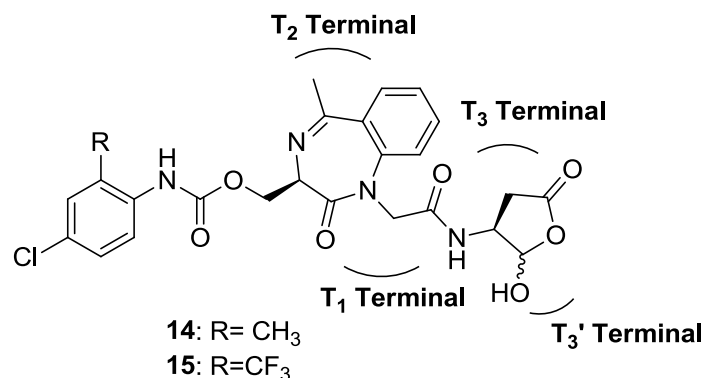
Ettari et al., (2008) developed two different kind of series containing benzodiazepine as an essential core. These series were designed to optimize compound **14**, in which aspartyl aldehyde group was replaced with different vinyl sulfones. Series one, comprised of homo-Phe residue at T$_3$ terminal, as shown by compound **16**, and in second series homo-Phe residue was changed with glycine amino acid as shown in compound **17**. Screening of compounds **16** and **17**, against the malarial parasite displayed IC$_{50}$ values of 9.1 µM and 9.2 µM, respectively.

16: R= CH$_2$CH$_2$Ph; R'= CH$_2$CH$_3$
17: R=H; R'= CH$_2$CH$_3$
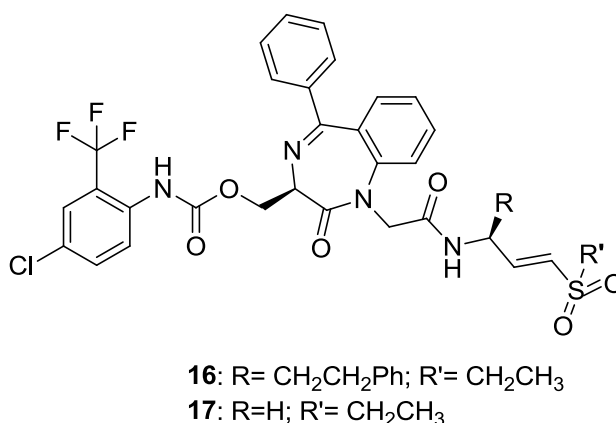
In order to further investigate the structural requirements of the aforementioned class of inhibitors, Ettari et al., (2009) envisaged the synthesis of novel peptidomimetic compounds that are derivatives of compounds **16** and **17**. This new series of analogs, comprised 1,4-benzodiazepine scaffold with a vinyl phosphonate as electron withdrawing substituent at T$_{3'}$ terminal. Unfortunately, the synthesized compounds **18** and **19**, based on vinyl phosphonate core exhibited lesser potency as compared to vinyl sulfones. Further, optimization of sulfone pharmacophore with vinyl-ketones **(20**, **23)**, amides **(21**, **24)**, esters **(22**, **25)** and nitriles **(26)** produced satisfactory results **(Table 2)**. Some compounds such as **23** (Vinyl-ketones) and **25** (ester), exhibited potent activity against the parasite as shown in **Table 2**.

18: R= CH$_2$CH$_2$Ph, R'= Me
19: R=H, R'=Et
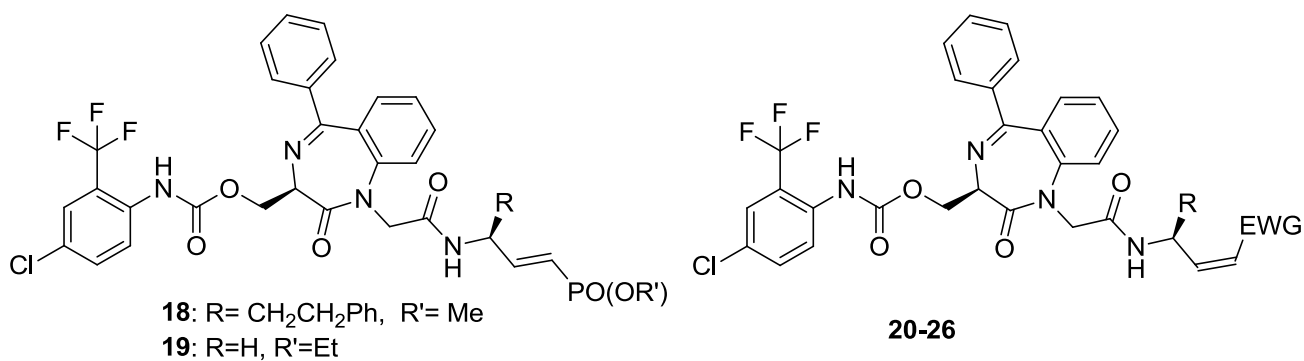
20-26

Table 2: Activity profile of 20-26 compounds

Compound	R	EWG	*P. falciparum* IC$_{50}$ (µM)
20	CH$_2$CH$_2$Ph	COMe	-
21	CH$_2$CH$_2$Ph	CONMe$_2$	-
22	CH$_2$CH$_2$Ph	COOMe	-
23	H	COMe	9.3
24	H	CONMe$_2$	> 100
25	H	COOMe	12.0
26	H	CN	36.1

2.1.2.2. Peptidomimetics based on a pyridone ring scaffold

Recently, another nonpeptidic scaffold was developed by Verissimo et al., (2008) in which pyridone as a key group was introduced in place of leucine amino acid at the T$_1$ terminal, within the inhibitor's framework. Some derivatives based on this pharmacophore, such as compound **27**, exhibited IC$_{50}$ value of 5.7 µM against parasite and compound **28**, with an IC$_{50}$ value of 10.9 µM, against falcipain-2 enzyme.

T$_1$ Terminal

27, R= CH=SO$_2$Ph
28, R= CHO
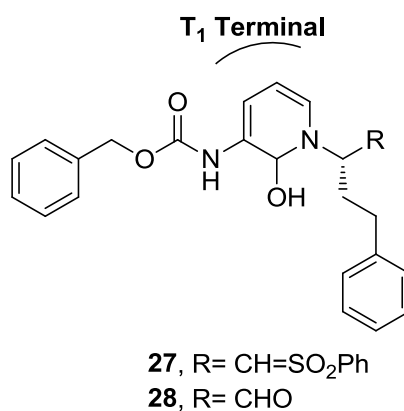
2.1.2.3. Miscellaneous

More recently, Weldon et. al., (2014) have synthesized and evaluated pseudo-prolyl-homo phenylalanyl ketones peptidomimetic for inhibition of falcipain-2 and falcipain-3 proteases. Out of twenty-two compounds screened, one peptidomimetic compound **29**, was found to be most active agent with IC_{50} values of 80 nM against FP-2, and 60 nM against FP-3 protease, respectively.

29
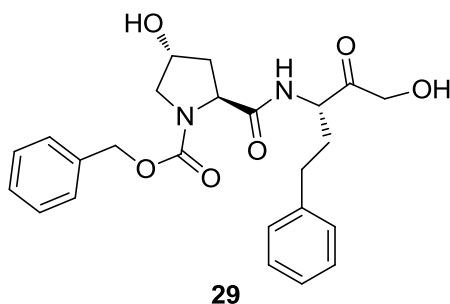
2.1.3. Non Peptidic FP-2 inhibitors

2.1.3.1. Chalcones

McKerrow and co-workers (1995) were the first investigators to develop some synthetic chalcones. Among the various derivatives, the most active chalcone was 1-(2,5-dichlorophenyl)-3(4-quinolinyl)- 2-propen-1-one **(30)** that exhibited IC_{50} value of 200 nM against both CQ-sensitive strain (D6) and CQ-resistant strain (W2) of *P. falciparum*. SAR studies demonstrated that: I) C2-C3 double bond was essential a pharmacophoric feature for exhibiting potent activity against the parasite; II) Introduction of a halogen group on ring A and electron donating moiety on ring B, improved inhibition potency; III) Presence of quinolinyl group in the ring A, increased the anti-malarial activity.

30
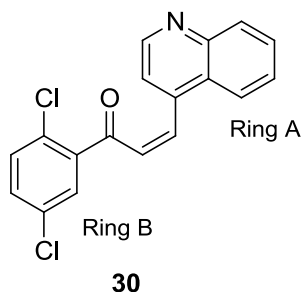
Later, Dominguez et al., (2005) demonstrated that, phenylurenyl chalcones holds excellent inhibitory activity against FP-2. Studies showed that, inhibitor 1-[4'-N- (N'-p-chlorophenylurenyl)-phenyl]-3-(3,4,5-trimethoxyphenyl)-2-propen-1-one **(31)**, was the most active molecule with an IC_{50} value of 1.8 μM, towards falcipain-2 protease.
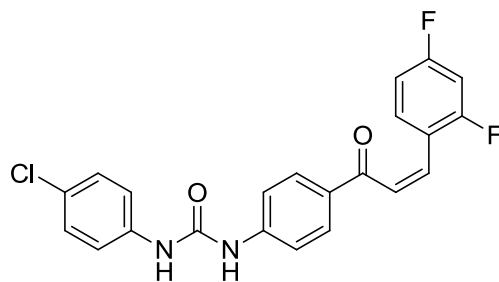
31

2.1.3.2. Isoquinolines

In absence of a crystal structure for falcipain-2 enzyme, Sabnis Y. et al., (2003) developed and validated the homology model for falcipain-2, with known vinyl sulfone inhibitors. In these studies, the interaction of 1-(4-hydroxy-phenyl) group, with Asp234 in the S2 pocket of FP-2 was considered essential (discussed in **Section 1.10**). Therefore, 1,6,7-trisubstituted dihydroisoquinolines and isoquinolines were synthesized and tested against FP-2. Interestingly, compounds **32–34**, were found to be most active and equipotent inhibitors that displayed an IC$_{50}$ value of 3.0 µM.
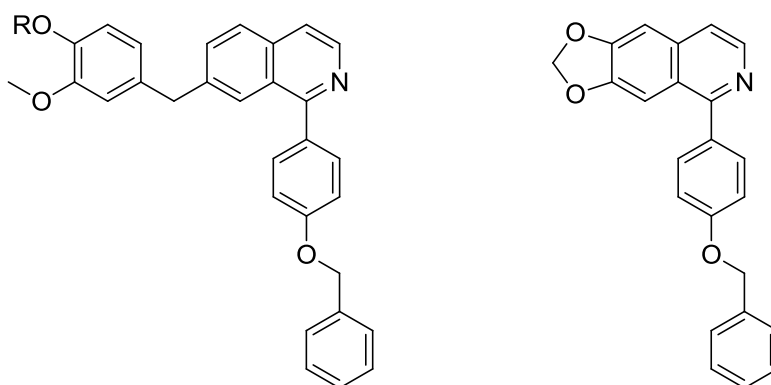
32: R= OMe
33: R= OBn

34

2.1.3.3. Thiosemicarbazones

Klayman et al., (1979) synthesized a series of thiosemicarbazone nucleus based compounds. Among the synthesized compounds, 2-acetylpyridine-4-phenyl-3-thiosemicarbazone **(35)**, was found to be potential anti-malarial agent targeted against *P. berghei*. Further, SAR studies demonstrated that: I) 2-pyridylethylidene substituent was essential to display anti-malarial activity; II) unsubstituted benzyl, phenyl, or cycloalkyl groups present at N^4 position, were important to exhibit anti-malarial activity.
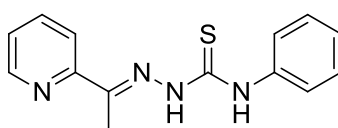
35

In another study, Chiyanzu et al., (2003) designed and synthesized a library of isatin based thiosemicarbazones FP-2 inhibitors. The most active analog from this series was compound **36**, which expressed an IC_{50} value of 4.4 µM against falcipain-2.

36
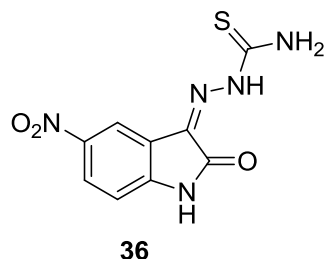
Recently, Mane UR et al., (2012) have reported a library of pyrido[1,2-a]pyrimidin-4-ones derivatives in which pharmacophoric features of α, β unsaturated chalcones and thiosemicarbazones or semicarbazones (carbamate/urea) were incorporated. The compounds were evaluated for *in vitro* activity against FP-2 protease. By the whole series, two compounds **37** and **38**, exhibited IC_{50} values of 6.0 µM and 7.0 µM, respectively; against FP-2.

37   **38**
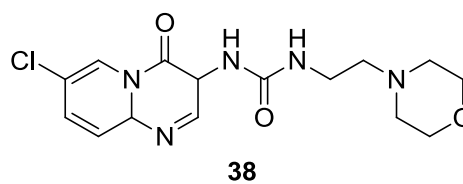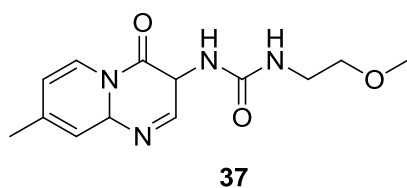
2.1.3.4. Miscellaneous

Choi et al., (2013) reported the synthesis and anti-malarial activity of a series of compounds, comprising of *N*-acetyl-L-leucyl-L-leucyl-L-norleucinal as an essential pharmacophoric element. Overall, screening results of synthesized derivatives showed that, compound *N*-methyl amide with *N*-methyl benzyl amide substituent **(40)** possessed potent anti-malarial activity as compared to other derivatives **39** and **41**.
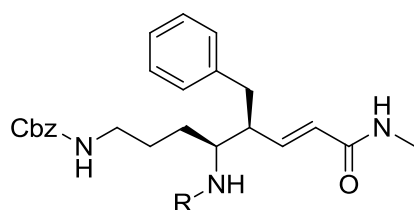
39 R=Benzyl
40 R=3,5 Dimethoxybenzy
41 R=m-Methoxybenzyl

2.2. ClpP proteases

The first ClpP inhibitors were the cyclic acyldepsipeptide antibiotics (ADEPs). The potent activity of acyldepsipeptides against many strains of bacteria, which are resistant to several antibiotics in clinical implementation, implicit a new target, known as Casenolytic proteases (ClpP).

It has been reported that, ClpP is the basic unit of a vital bacterial protease complex and essentially requires a member of the Clp-ATPases family and often some common proteins for the proper functioning of a cell (Walsh et al., 2014). Therefore, participation of ATPase component and accessory proteins with ClpP proteases are termed as "safeguard". Binding of acyldepsipeptides to ClpP, eliminates these safeguards. Therefore, in the absence of regulatory Clp-ATPases, the acyldepsipeptide operated ClpP performed proteolysis process in uncontrolled manner which leads to inhibition of bacterial cell division and eventually cell death.

Michel and Kastner (1985) synthesized a series of cyclic acyldepsipeptide known as ADEPs, contained antibiotic properties. The classical members of this series are "A54556A **(42)** and A54556B **(43)**", produced by *Streptomyces hawaiiensis* (RK-1051strain). Together, the ADEPs exhibited potent activity towards a broad range of Gram-positive bacterial organisms, e.g., *Staphylococcus aureus, Streptococcus pneumonia* and Enterococci (Brotz-Oesterhelt et al., 2005; Socha et al., 2010).
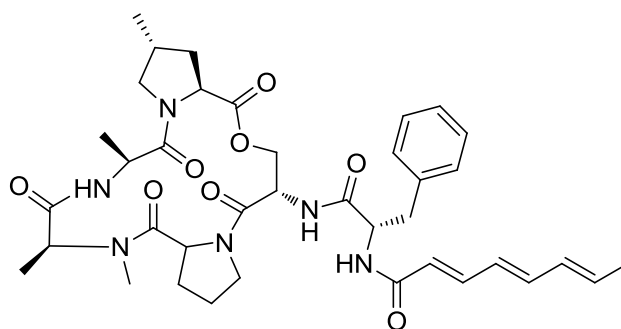
42: R= CH3
43: R= H

Hinzen et al., (2006) demonstrated that, compounds **42 & 43** possessed a poor pharmacokinetic and physicochemical profile, such as high clearance and poor aqueous solubility. In addition, it was found that these two compounds were not efficacious in severe bacterial infections. Therefore, these molecules were not considered as lead candidates for future drug discovery. Thus, a series of molecules for the parent compounds **42 & 43**, as well as some previously published ADEPs **(44-47);** Brotz-Oesterhelt et al., 2005), were

34

synthesized and screened. overall, results showed that, compound **47**, was the most potent compound throughout the series.

44   **45**   (S)

46   (R)   **47**
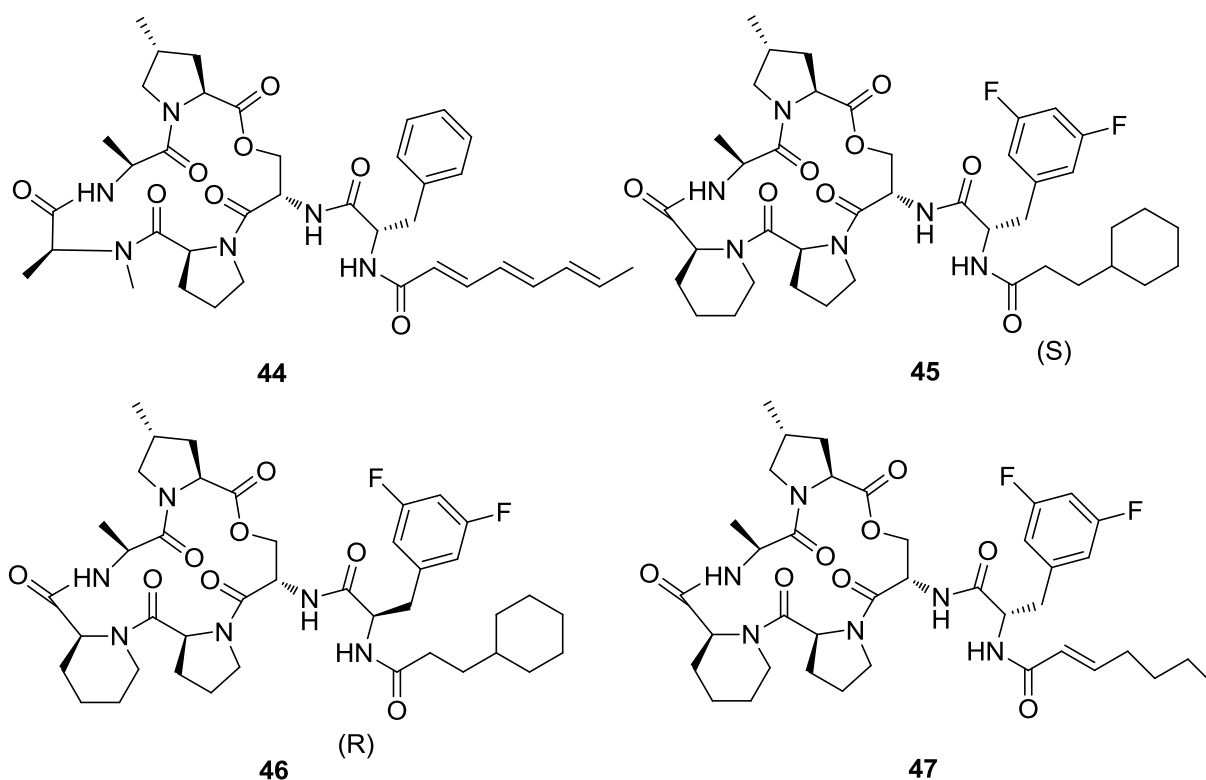
Thomas Bottcher and Stephan A. Sieber, (2008) reported that, naturally occurring β-lactones **(Figure 14)**, such as obafluorin **(48)**, valilactone **(49)**, hymeglusin **(50)**, ebelactone A **(51)** and β-lactone B **(52)** possessed potent antibiotic activity, but the exact molecular targets for these compounds remained unknown. Initially, it was found that, these molecules were highly potent in trans configuration, however later, it was reported that, β-lactones did not show a clear preference for trans configuration within the absolute stereochemistry (Tomoda et al., 1997).

48   **49**

50

51: R=CH$_3$
52: R=CH$_3$CH$_2$
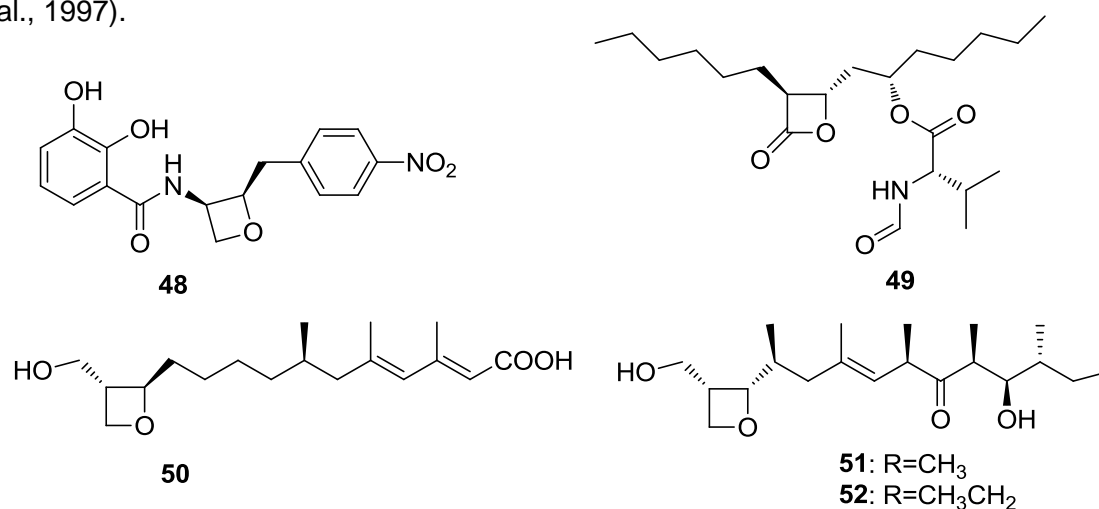
Figure 14: Structure of some biologically active, naturally occurring β-lactones

Inspired from this evidence, a small series of ten molecules containing β-lactone (2-oxetanone) as core nucleus, were synthesized. Structurally, these molecules carried various substitutions at C-3, C-4- positions including alkyne groups. This series of molecules were optically based on trans-β lactones as racemic mixtures. Screening results for these molecules against ClpP enzyme were very promising to control different fundamental roles, such as to regulate protein degradation and virulence in many pathogenic bacteria. In addition, the *in vivo* pharmacological profile showed that, compounds consists of promiscuous activity against virulence-associated ATP-dependent Clp protease (Kim et al., 2002). Four compounds **(53-57)**, were found to be potent from the library of ten compounds.

Basic Structure for ß-Lactone

53: R_1=H   **54**: R_1=CH$_3$ **55**: R_1=   **56**: R_1=   **57**: R_1=

R_2=H R_2=CH$_3$ R_2= H R_2= H R_2=H
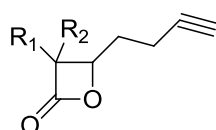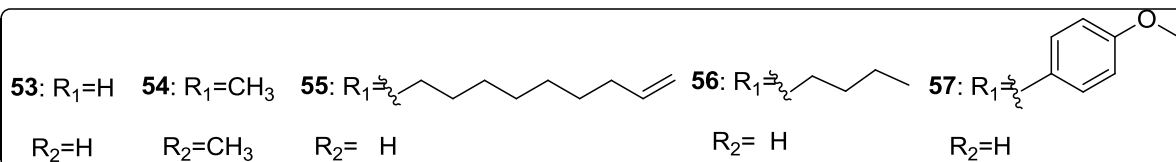
Asif and co-workers (2010) prepared a series of β-lactones, in which compound **54-57** and **59**, were synthesized by a protocol as previously applied by Bottcher et. al. (2008), except compound **58**, which was synthesized using *N,N'*-Dicyclohexylcarbodiimide (DCC) activated coupling reaction of thiophenol and 10-undecenoic acid. Screening resuls for these compounds (targeting *Pf*ClpP), are summarized in **Table 3**.

58   **59**
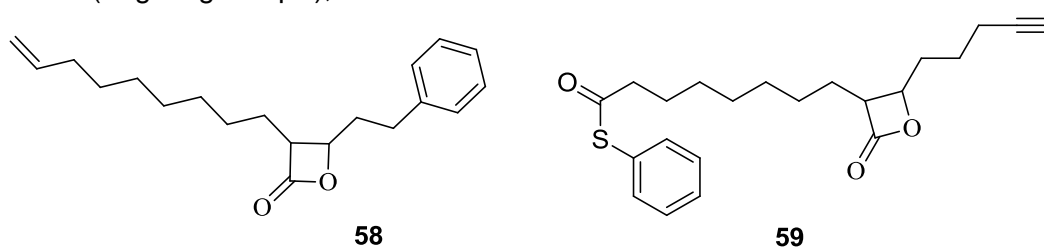
Table 3: Activity results for compounds (54-59), against *Pf*ClpP protease

Compound	IC$_{50}$ (µM)	Compound	IC$_{50}$ (µM)
54	> 50	57	> 20
55	-	58	8.38
56	> 80	59	> 20

Overall, results showed that, apicoplast is a confirmed target for *P. falciparum* ClpP protease, and ClpP plays a crucial role in *P. falciparum* parasite growth and development.

Importantly, compound **58** has no pronounced effect on mitochondria to change its morphology and segregation property, as the compound **(58)**, treated *Plasmodium* parasites were able to multiply during the second cell cycle. Thus, the study clearly demonstrated that, the *P. falciparum* ClpP present in the apicoplast was the specific (primary) target for compound **58** (Rathore et al., 2010).

Recently, Leung et al., (2011) have reported the high-throughput screening results of more than 60,000 compounds, obtained commercially from Prestwick Chemical library (1120 samples), sigma (1280 samples), Cambridge DIVERS (10,000 samples), Maybridge (50,000 samples) and Spectrum (2000 samples), targeting ClpP protease.

This chemical screening companion for diverse libraries led to the identification of five potential hits **(59-63)**, which were labelled as ACP1 to ACP5. Among them, three compounds **59**, N-1-[2-(phenyl-thio) ethyl]-2-methyl-2-{[5-(trifluoro-methyl)-2-pyridyl]sulfonyl}propanamide; **60**, 3-(tertbutoxy)-2-{[2-[(5-(tertbutoxy)-2-{[(9-H-9 fluorenylmethoxy)carbonyl]amino-5-oxopentanoyl] amino]-3 (tertbutylsulfanyl)propanoyl]amino}butanoic acid; and **61**, [4-(7-chloroquinolin-4-yl)piperazino](cyclohexyl) methanone), were from the Maybridge database. Compound **62**, ethyl 2-(2,2-dichlorovinyl)-4-hydroxy- 4-(3-nitrophenyl)-6-oxocyclohexanecarboxylate; and **63**, ethyl 4-(4-bromophenyl)-2-(2,2-dichlorovinyl)-4- hydroxy-6-oxocyclohexanecarboxylate, were obtained from the Cambridge database. Interestingly, ACP4 **(62)** and ACP5 **(63)**, were identical analogs, differing with a substituent.

59

60

61

62

63
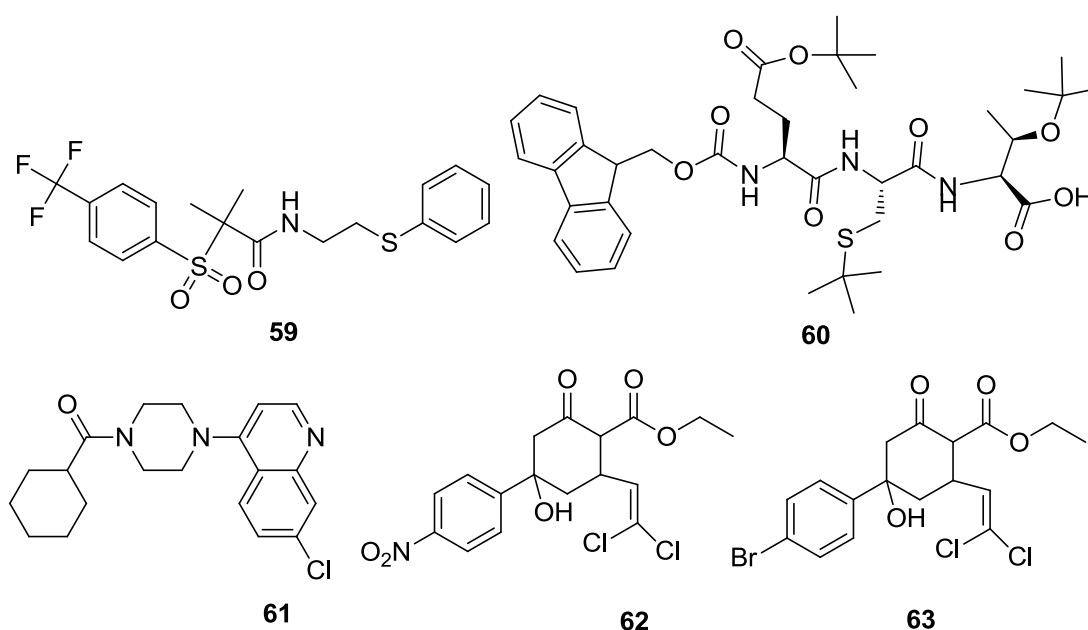
Malte Gersch et al., (2013) reported various homologus series of trans-substituted β-lactones for ClpP protease inhibition. Basic structures for these series of derivatives were represented as **64-67** pharmacophores. These structures commonly comprised of a decyl chain as R_1 substituent and various functional groups at R_2 position. it was reported that, *S,S* configured lactones, displayed less than 10% residual activity as compared to *R,R* configured lactones, as represented in **Table 4**.

64   **65**

66   **67**
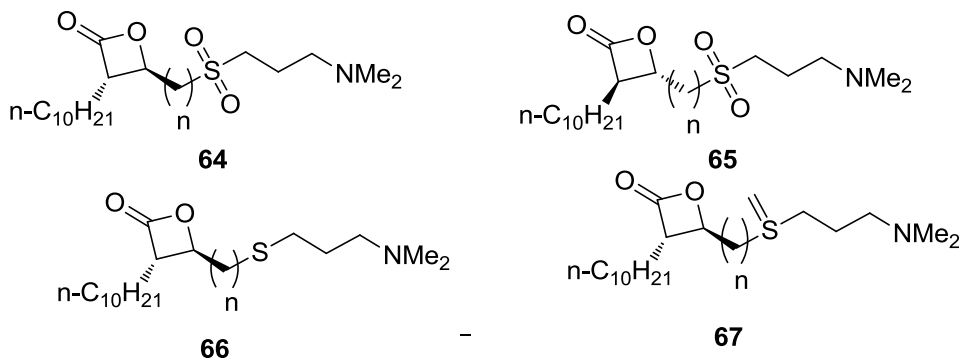
Table 4: Percentage residual activity for compounds (64-67), tested with recombinant ClpP protease (100 µM)

Code (*S,S*)	n	% Remaining Activity	Code (*R,R*)	n	% Remaining Activity
64a	2	1 ± 0	65a	2	37 ± 0
64b	3	0 ± 0	65b	3	8 ± 0
64c	4	0 ± 0	65c	4	13 ± 0
64d	5	5 ± 0	65d	5	10 ± 0
66a	2	1 ± 0	67a	2	11 ± 0
66b	3	40 ± 2	67b	3	26 ± 4
66c	4	0 ± 1	67c	4	6 ± 0
66d	5	1 ± 0	67d	5	15 ± 0

Sieber and co-workers (2014) tested commercially available libraries, comprising β-lactones, fluorophosphates, β-sultams and two novel compounds, which were synthesized in house [RKS07 **(70)** and RKS09 **(71)**]. Among them, compounds **68** (diisopropyl fluorophosphates, **DFP**), **69** (β-lactone derivative, **E2**), and **71 (RKS09, β-sultam)**, showed modification of 57%, 35% and 63% of active sites, respectively, of the ClpP proteases in *S. aureus*.

68: DFP   **69**:, E₂   **70**: R=CH₃ **(RKS07)**
                                      71: R=(CH₂)₈CHCH₂ **RKS09)**

38
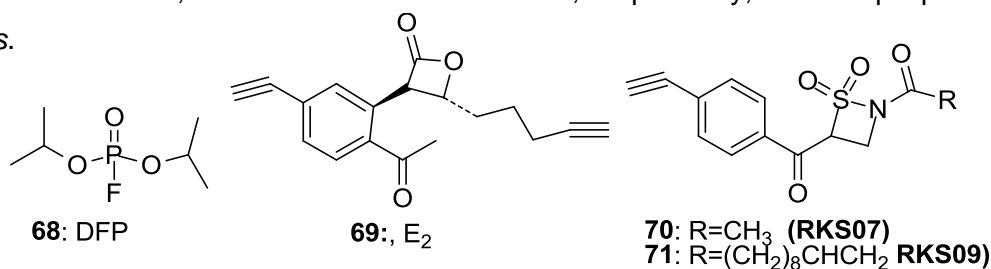
3. OBJECTIVES AND PLAN OF WORK

3.1. Objectives

The last resort and the state-of-the-art treatments for malaria are Artemisinin and related combinations (ACTs). However, in the past five years, several countries have reported Artemisinin-resistant malaria parasites in the field compromising this drug's full effectiveness and raising the stakes for the eradication of malaria. There is no fully effective malaria vaccine, despite the recent reports of a partially effective malaria vaccine completing phase III clinical trials. Further, there has been no new chemical class of anti-malarial drug introduced into the market in the past 20 years; only derivatives of existing drugs or "me-too" approaches (market share to a competitor by offering a product that is a copy of a competitor's product) have been taken. Therefore, to achieve a solution globally against this infection, the development of the safe and effective chemical classes of drugs that act against new biological target proteins is the better approach to deceive the problem faced by clinically used drugs.

Keeping all these aspects in mind; a multidisciplinary approach was taken to develop novel potential drug-like lead molecules for two targets; falcipain-2 and ClpP proteases of malaria parasite.

The following prime objectives were set for the present study.

- ➢ To design structurally novel compounds targeting falcipain-2 (FP-2) and casienolytic proteases (ClpP) of *Plasmodium falciparum*.

- ➢ To synthesize the designed new chemical entities (NCEs) using conventional and microwave assisted organic synthetic approach, and characterize them using spectral analysis.

- ➢ To evaluate synthesized molecules, for their potential falcipain-2 and casienolytic protease inhibitor activity as anti-malarial agents.

3.2. Plan of Work

3.2.1. Design of new chemical entities

Several compounds related to FP-2 inhibitors structure, as discussed in the literature review **(Section 2)**, were initially studied to determine the essential pharmacophoric features. Based on the core features, a new pharmacophore model was built **(Figure 15)**. Using this pharmacophore model, novel FP-2 inhibitors **(Series I-III)** were designed, which may be potent and plausibly with minimum side-effects. In order to attain the better pharmacokinetic profile, molecules were designed according to the 'Lipinski's Rule of Five (1997).
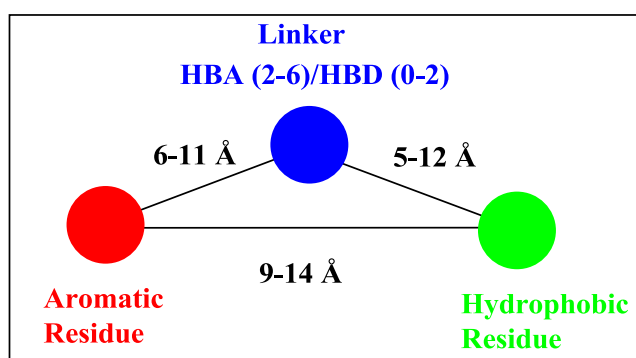
Figure 15: Proposed pharmacophore model (Green Color: Represents hydrophobic residue; an aromatic group, Red Color: Represents an aromatic residue (monocyclic/bicyclic), Blue Color: Represents the numbers of hydrogen bond donor and acceptor atoms)

The novel pharmacophore consists of key elements: a) An aromatic residue (monocyclic/bicyclic), which is attached to the hydrophobic moiety; an aromatic residue through a hydrogen bond donor and acceptor atom(s) as linker b) The hydrogen bond donor (HBD) and hydrogen bond acceptor (HBA) atom(s) are present as either in heterocyclic/alicyclic, or open chain form c) The distance between the aromatic residue and hydrophobic group was ranged from 9 to 14 Å d) The distances between the centroid of the aromatic residue to linker (HBA/HBD) and centroid of hydrophobic group to linker (HBA/HBD) were ranged from 6 to 11 Å and 5 to 12 Å, respectively and e) The numbers of hydrogen bond donor and acceptor atoms range from 0-2 and 2-6, respectively. Based on this pharmacophore model, New Chemical Entities (NCE's) were designed, synthesized and evaluated for their falcipain-2 inhibitory activity.

Keeping similar aromatic moiety, variation were made at the hydrophobic entity and linker size of the designed pharmacophore, with the intention of exploring the structure activity relationship.

'R' selected as an subtiuent containing alkyl/alkoxy group on hydrophobic residue; behaves as a electron donor due to positive inductive effect. Whereas, 'R' chosen as a halide substituent such as fluoro/chloro/trifluoromethyl group; acts as a electron withdrawing due to negative inductive effect.

In recent years, structural guided virtual screening or rational drug design approaches towards the development of peptidomimetic inhibitors have been undertaken to identify FP-2 inhibitors. FP-2 is a principal cysteine protease that plays a major role in parasite food assimilation (life cycle) by its ability to degrade haemoglobin. FP-2 also participates into destabilization of the erythrocyte invasion, erythrocyte membrane and release of merozoites through the degradation of ankyrin and band 4.1 proteins. Further, structural data suggests that, it possesses an unique long prosequence (2-3 times larger), in comparison to other parasite cysteine and mammalian proteases. Beside this, FP-2 does not require it's prodomain for acquiring a catalytically competent conformation as like other proteases. The catalytic site of this protease is composed of hydrophobic pockets in close proximity to the catalytic residues (Cys 42, Hip174 and Asn 173), as discussed in **Section 5**.

A number of attempts have been reported to generate FP-2 inhibitors as potent anti-malarial agents. However, majority of the scientific groups focused their study to identify peptide analogs as falcipain inhibitors, to interact with thiolate of the catalytic cysteine amino acid by using different electrophile, such as nitriles, vinyl sulfones, aldehydes and epoxides, as warehead. Although, peptide analogs inhibit the protease and expressed activity in nanomolar concentrations, however due to the formation of covalent bond at the active site, selectivity (druggability and toxicity) was the major concern. Therefore, it is thought worthy to investigate chemically diverse set of non peptidic/peptidomimetic FP-2 inhibitors as potential anti-malarial drugs. A series of peptidomimetics were designed, and their effects on FP-2 catalytic activity and parasite development *in vitro*, were studied. A two-step process was used to screen *in silico* small molecule libraries, against the active site of FP-2 employing UNITY suite of software; (I) hits were selected containing complimentary features to the enzyme active site and (II) the hits were docked into the binding pocket as discussed in **Section 5**. Overall, from this screening, one hit was identified **(KM-1')**, possessing moderate *in vitro* activity. The complementary features from **K11017** and Leupeptin (standard molecule), were incorporated in **KM-1'** hit molecule, to design and synthesize new chemical compounds based on **Scaffold I**, with appropriate chemical functionalities. This scaffold has four different variable groups **(Series IV)**, T_1, T_2, T_3 and T_3' correspond to R_1, R_2 and R_3 (T_3 and T_3'), substituent's as mentioned in the basic pharmacophore **(Figure 16)**.
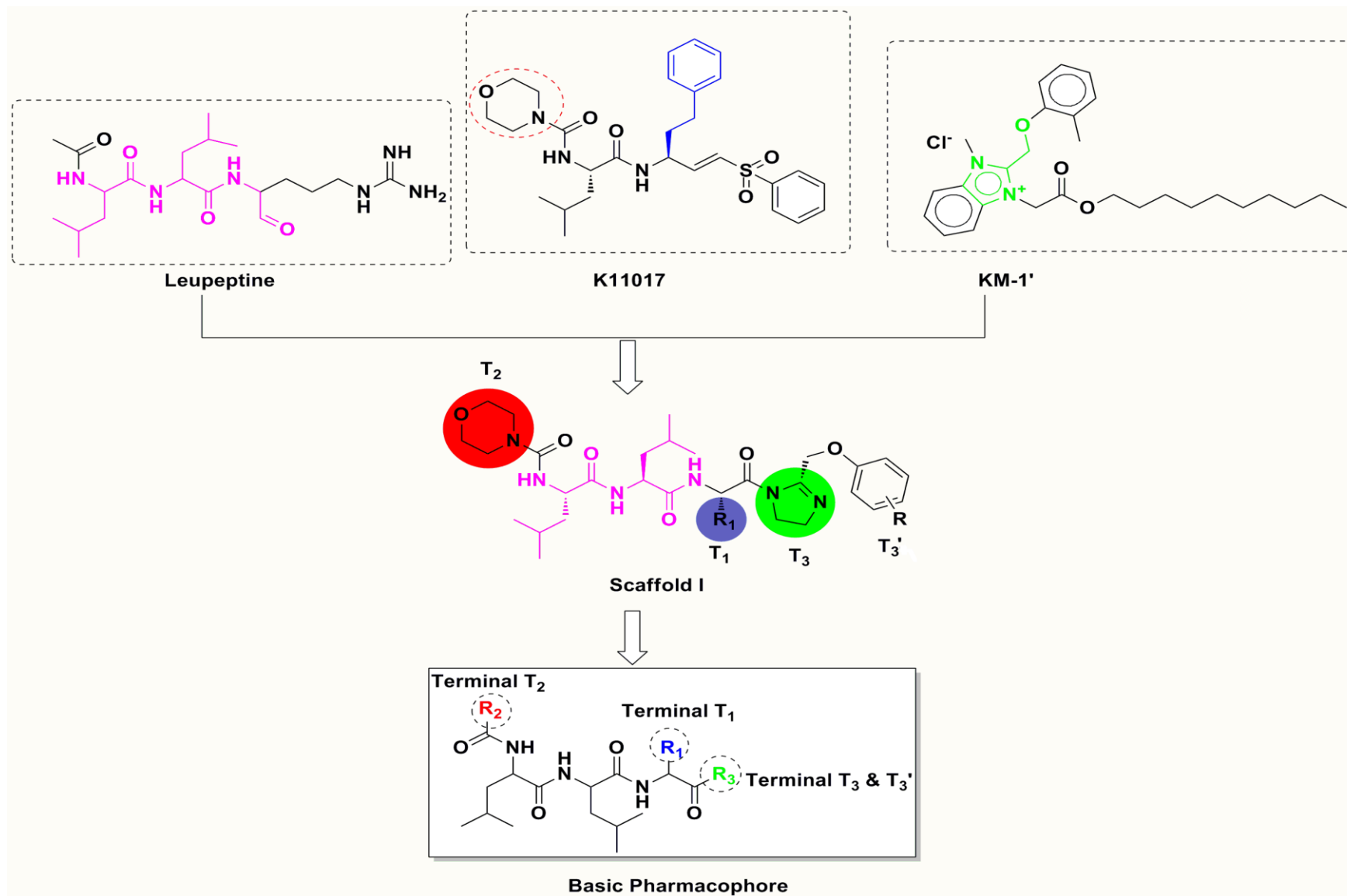
Figure 16: Representative basic structure of designed compound (Scaffold I) with structure variations (T_1, T_2, T_3 and T_3')

In context to caseinolytic protease inhibitors (ClpP) **Series V**, 2-(substituted) pyrimidin-4-ylthio)-*N'*-(2-phenylacetyl)-acetohydrazide derivatives were designed based on the framework of hit compound **KM-6 (Figure 17)**, investigated as a moderate inhibitor by Asif and co-workers, discussed in **Section 5**.
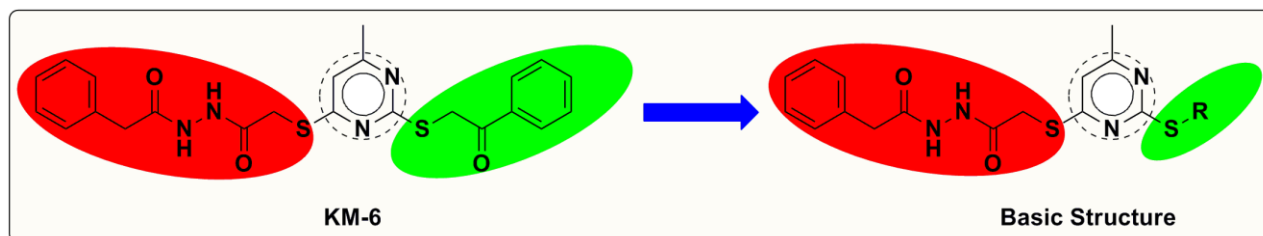
Figure 17: Basic structure of designed compound

Later on, to find out the role of substituent present at C2 position of the pyrimidine ring, compounds **KM 10-12** (discussed in **Section 5**), possessing weak to moderate *in vitro* activity, were selected to perform chemical modifications that would provide expedient and significant SAR information and improve inhibitory activity. Through this modification, a hybrid pharmacophore was generated **(Figure 18)**.

The novel pharmacophore consists of key features: a) aromatic ring (pyrimidine nucleus), b) substitution at N^3 position with variation in chain length c) variation in substituent's present at C2 position and d) fused ring **(5-isopropyl-5,7-dihydro-4H-thieno[2,3-c]pyran)** was replaced with an ester or amide linkage at 5th or 6th position of the pyrimidine ring deliberately, due to synthetic feasibility and to modulate polarity and bioavailability. Based on this pharmacophore model, **Series VI** was designed, synthesized and evaluated for their ClpP inhibitory activity.
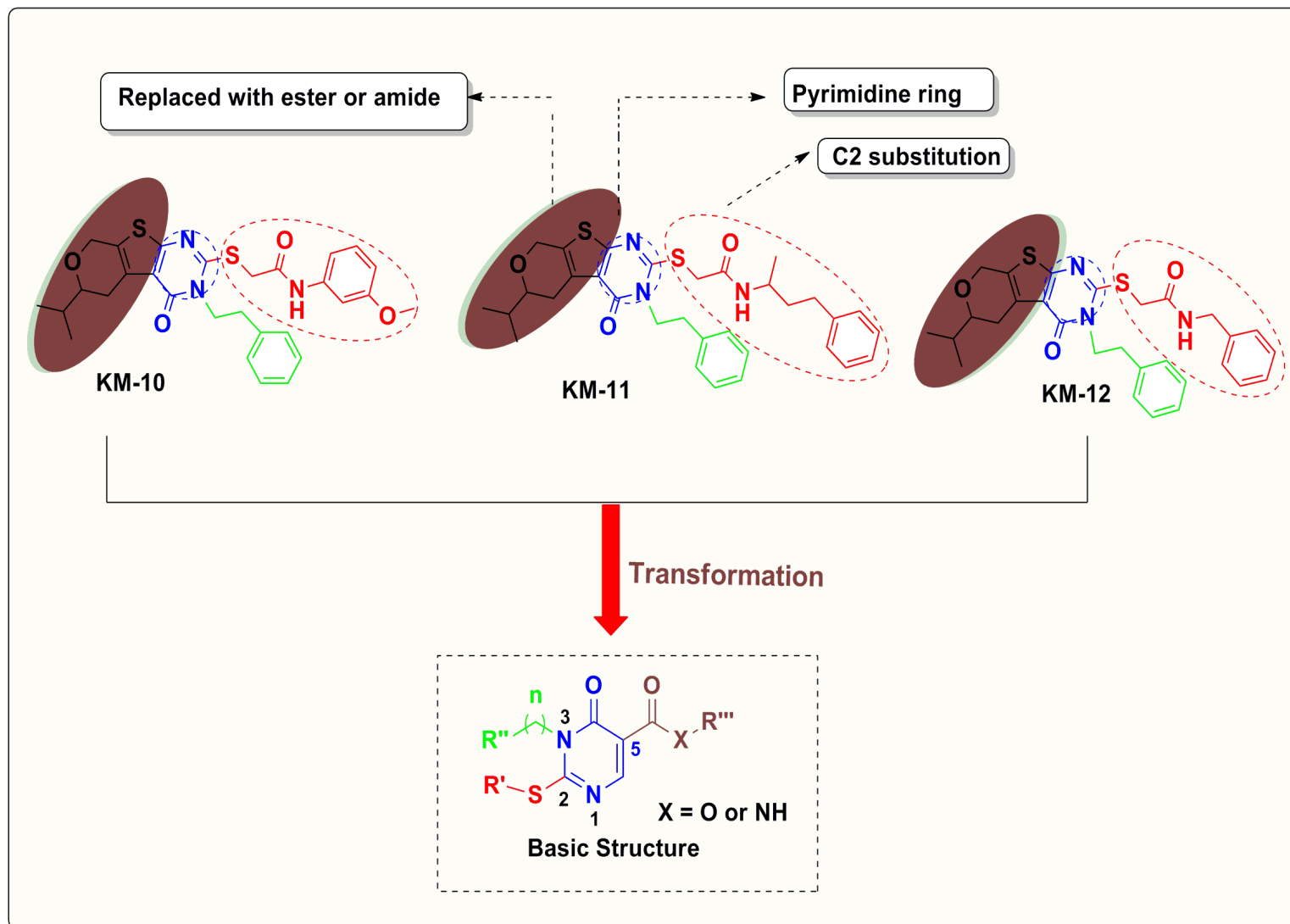
Figure 18: Rational design for synthesis of Series VI compounds

3.2.1.2. Synthesis and characterization of new chemical entities

The basic structures of the proposed molecules **(Series- I** to **VI)** are depicted below.

The synthesized compounds were characterized by physicochemical evaluation. Preliminary methods like melting point and thin layer chromatography were performed to assess the purity of the compounds. The structures of the compounds were confirmed by spectral (IR, ^{1}H & ^{13}C NMR, Mass, HPLC) and/or elemental analyses data, as required.

Series I to III: Non-peptidic small molecule inhibitors for falcipain-2 enzyme:

Series I: 2-(4-(Substituted benzoyl)-1,4-diazepan-1-yl)-*N*-phenylacetamide derivatives
Series II: 1-(4-(Substituted)piperazin-1-yl)-2-(phenylamino)ethanone derivatives
Series III: 2-(4-(Substituted benzoyl)piperazin-1-yl)-*N*-phenylacetamide derivatives
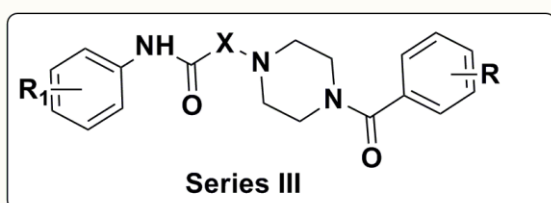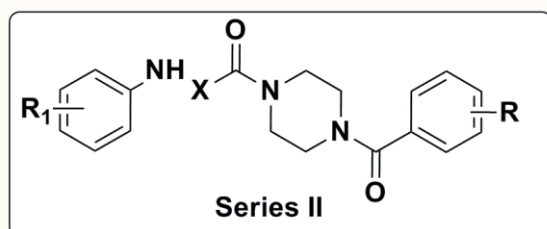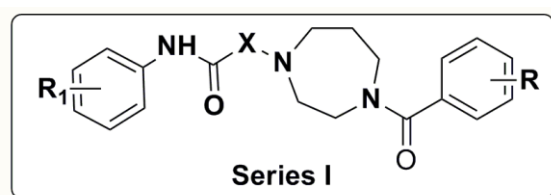
Series	X	R_1	Compounds
I	CH_2	H	RM-1 to 20
II	CH_2	H	RMS-1 to 20
III	CH_2	H	RMT-1 to 20

R = H, -CH$_3$, -CH$_2$CH$_3$, OCH$_3$,
-OCH$_2$CH$_3$, -Cl, -F, CF$_3$

Series IV: Peptidomimetic inhibitors for falcipain-2 enzyme:
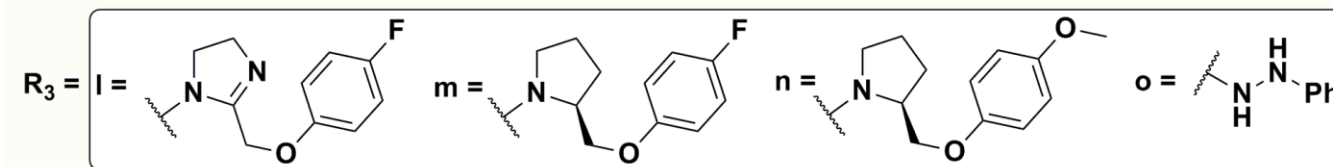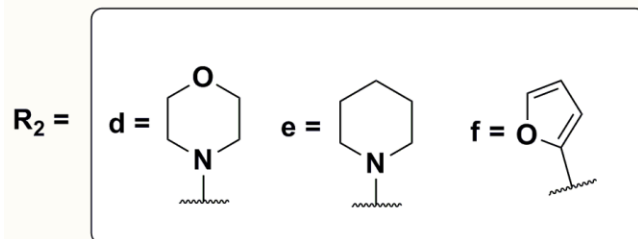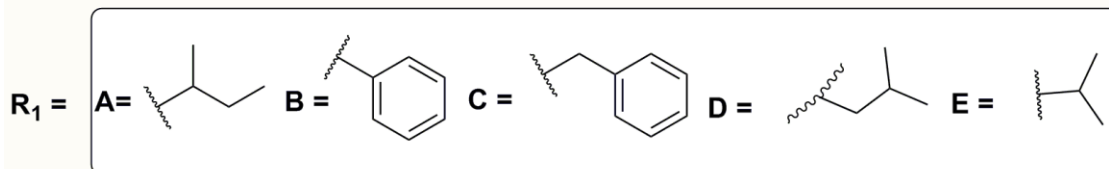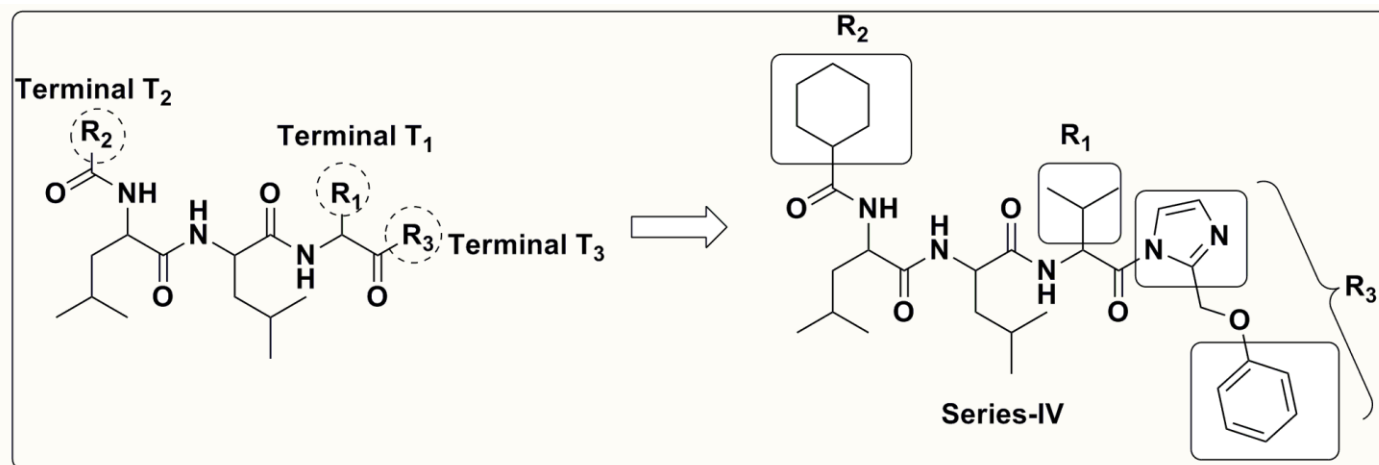
Series V: 2-(Substituted)pyrimidin-4-ylthio)-*N*-(2-phenylacetyl)-acetohydrazide derivatives as *Plasmodium falciparum* caseinolytic protease (ClpP) inhibitors:

Series V

R = A B C D E F G H I J

K L M N O
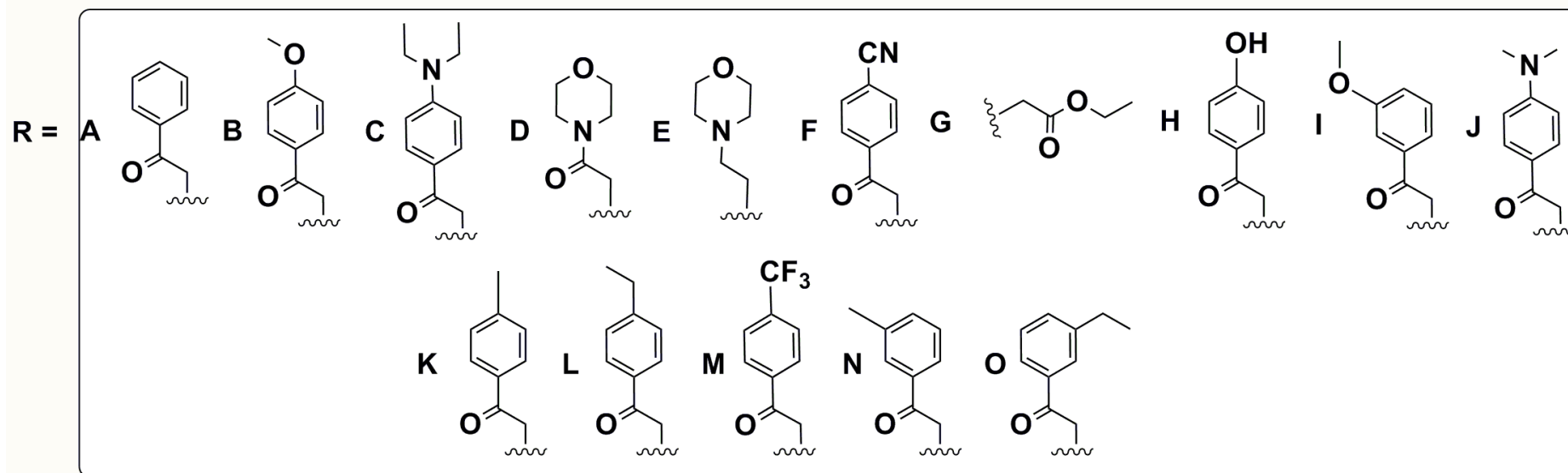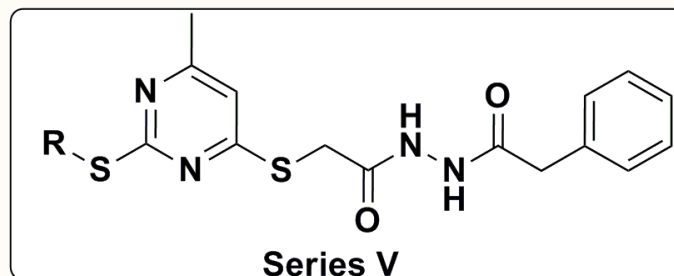
Series VI: 1,6-Dihydropyrimidine derivatives as *Plasmodium falciparum* caseinolytic protease (ClpP) inhibitors:

Series VI

R' = A, B, C, D, E, F, G, H, I

R" =

R''' =

X = O or NH
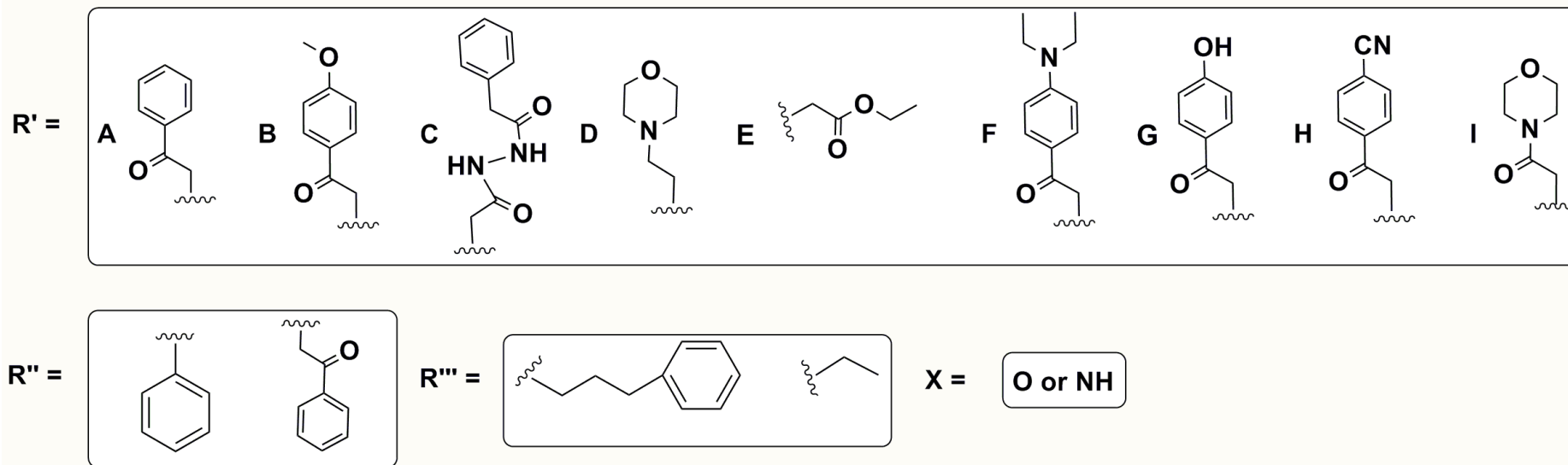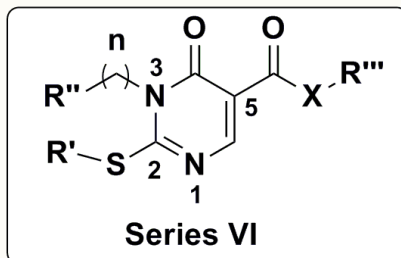
3.2.1.3. Pharmacological evaluation

The refolded protein either FP-2 or ClpP from *P. falciparum* cleaved the benzyloxycarbonyl-Phe-Arg-7-amino-4-methyl coumarin hydrochloride (ZFR-AMC) or *N*-Succinyl-Leu-Leu-Val-Tyr-AMC substrate, respectively, in a dose dependent manner. The activities of the recombinant FP-2 and ClpP enzymes were significantly inhibited by E-64 (L-transepoxysuccinyl-leucylamide-[4-guanido]-butane) or chymostatin, broad spectrum inhibitor of proteases. The effect of different synthesized compounds on enzyme activity was analyzed by pre-incubating the active enzyme with each of the compound before the addition of the substrate. The release of 7-amino-4-methylcoumarin (AMC) was monitored using an excitation wavelength 355 nm and emission at 460 nm wavelength, over 30 min at RT in Perkin Elmer Victor3 multi-label counter. Activities were compared as fluorescence released over time, in assay with or without different concentration of each compound tested. The inhibition rate (%) is calculated using the given equation:

% Inhibition = [1 - ('*F*'-test / '*F*'-standard)] × 100 ⟶ | **Equation-1** |

Where 'F'-test is the fluorescence intensity of the test compound, 'F'-standard is the fluorescence intensity of a standard compound (E64 or Chymostatin). Percentage inhibition values are represented as average of three independent determinations, and the deviations are <10 % of the average value. The IC_{50} values were calculated from Workout V 2.5 software.

3.2.1.4. *P. falciparum* growth inhibition assay

P. falciparum strain 3D7 was cultured with human erythrocytes (4% hematocrit) in RPMI media (Invitrogen) supplemented with 0.5% albumax, using a protocol described by Trager and Jensen, 2010. Cultures were synchronized by repeated sorbitol treatment following Lambros and Vanderberg (1979) protocol. Each growth inhibition assay was performed in triplicate, and the experiment was repeated twice. Each well contained 0.5 mL of complete media (RPMI (Invitrogen) with 0.5% albumax), 4% hematocrit, and parasitemia adjusted to 1%. The compound(s) was added to the parasite cultures at desired final concentrations (0–100 μM), and same amount of solvent (DMSO) was added to the control wells. The cultures were allowed to grow for 48 h. Parasite growth was assessed by DNA fluorescent dye-binding assay using SYBR green (*N*,*N*-dimethyl-*N*-[4-[(E)-(3-methyl-1,3-benzothiazol-2-ylidene)methyl]-1-phenylquinolin-1-ium-2-yl]-*N*-propylpropane-1,3-diamine; Sigma) following Smilkstein et al., 2004.

4. EXPERIMENTAL WORK

4.1. Materials and methods: chemistry

The chemicals were purchased commercially from Aldrich, Fluka, and Spectrochem. Microwave irradiations were carried out in CATA-R microwave synthesizer and Biotage Initiator equipped with a robotic arm. Reactions were monitored by Thin Layer Chromatography (TLC), which was performed with 0.2 mm Merck pre-coated silica gel 60 F_{254} aluminum sheets. Compounds were detected by UV, iodine chamber and by dipping the TLC plates in ethanolic solution of ninhydrin and heating.

Melting points (m.p.) were determined in open capillary tubes and on a Buchi 530 melting point apparatus and are uncorrected. Column chromatography was performed using silica gel, 60-120/100-200 meshes as an adsorbent and ethyl acetate/ hexane or dichloromethane/ethanol as eluent. Flash chromatography (Biotage(R)–SP4), was used for the purification of peptidomimetics using SNAP Ultra flash chromatography cartridges. IR spectra were recorded with IR prestige-21 (FT-IR, Shimadzu). ^{1}H NMR, spectra were recorded with Bruker DPX operating at 400 MHz and Varian spectrometer (600 MHz, for variable temperature experiments) in $CDCl_3$ or DMSO-d_6 solvent, with tetramethylsilane (TMS) as an internal standard. Chemical shifts were shown as *δ* values (ppm); the *J* values were expressed in Hertz (Hz). Mass spectra were recorded on a Waters™ 3100 mass detector using ESI (+ve) mode.

Purity of some final compounds were evaluated on a Waters™ LC/MS system, equipped with a photodiode array detector using an XBridge C18 5µm 4.6mm x 150mm column. All HPLC solvents were filtered through membrane filters (47 mm GHP 0.45 mm, Pall Corporation). Injection samples were filtered using Acrodisc Syringe Filters 4 mm PTFE (0.2 mm). Elemental analyser PE2400 was used to record elemental analysis of final compounds; the C, H and N analysis were repeated twice. The minimum energy conformations of the designed molecules were generated by ACDLABS-10.0/3D Viewer (CHARMM parameterization).

4.2. Synthesis

Series of synthetic schemes were designed, protocols optimized and molecules synthesized, which are briefly discussed here under

Series-I: Synthesis of 2-(4-(substituted benzoyl)-1,4-diazepan-1-yl)-*N*-phenylacetamide derivatives **(RM-1 to 20)**.

**Series-II:** Synthesis of 1-(4-(substituted)piperazin-1-yl)-2-(phenylamino)ethanone derivatives **(RMS-1 to 20)**.

Series-III: Synthesis of 2-(4-(substituted benzoyl)piperazin-1-yl)-*N*-phenylacetamide derivatives **(RMT-1 to 20)**.

Series-IV: Synthesis of peptidomimetics **(RMQ-1 to 20)**.

Series-V: Synthesis of 2-(substituted)pyrimidin-4-ylthio)-*N'*-(2-phenylacetyl)-acetohydrazide derivatives **(RMP-1 to 15)**.

Series-VI: Synthesis of 1,6-dihydropyrimidine-5-carboxamides derivatives **(RMH-1 to 14)**.

4.2.1. Series-I: Synthetic route of 2-(4-(substituted benzoyl)-1,4-diazepan-1-yl)-*N*-phenylacetamide derivatives (RM-1 to 20)

Scheme 1
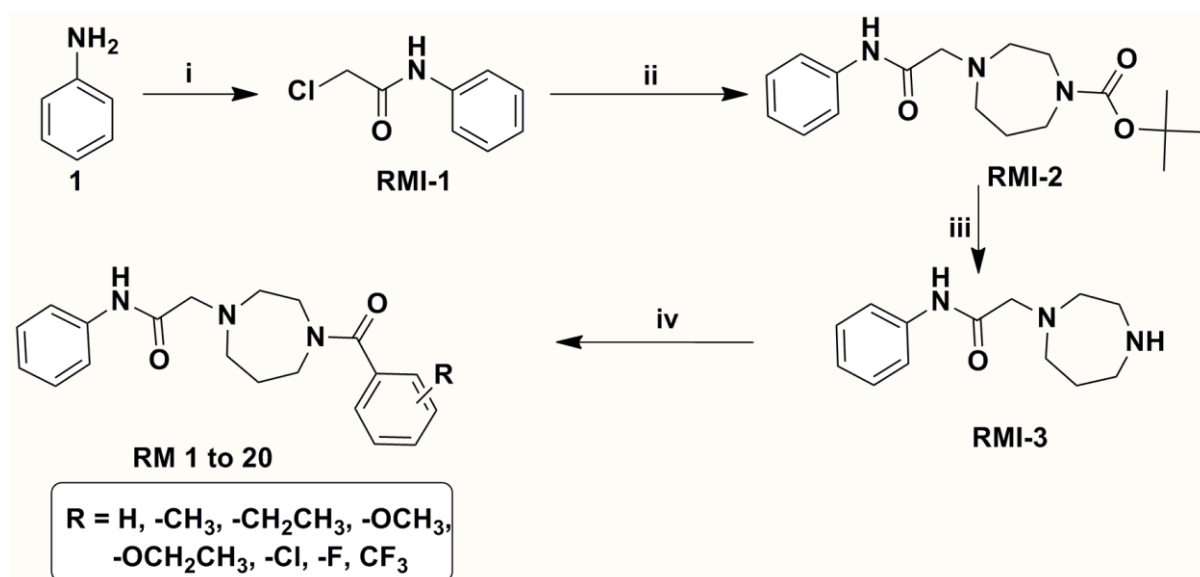
Reagents and conditions: (**i**) Chloroacetylchloride, TEA, DCM, 0°C-RT, 20 min; (**ii**) *N*-Boc-homopiperazine, K_2CO_3, CH_3CN,100°C, 5 h., (**iii**) TFA/DCM, 0°C-RT, 6 h; (**iv**) Various carboxylic acids, EDC·HCl, HOBt/DIPEA-DCM, 0°C-RT, 6 h.

4.2.2. Series-II: Synthetic route of 1-(4-(substituted)piperazin-1-yl)-2-(phenylamino)ethanone derivatives (RMS-1 to 20)

Scheme 2

R = H, -CH₃, -CH₂CH₃, -OCH₃,
-OCH₂CH₃, -Cl, -F, CF₃
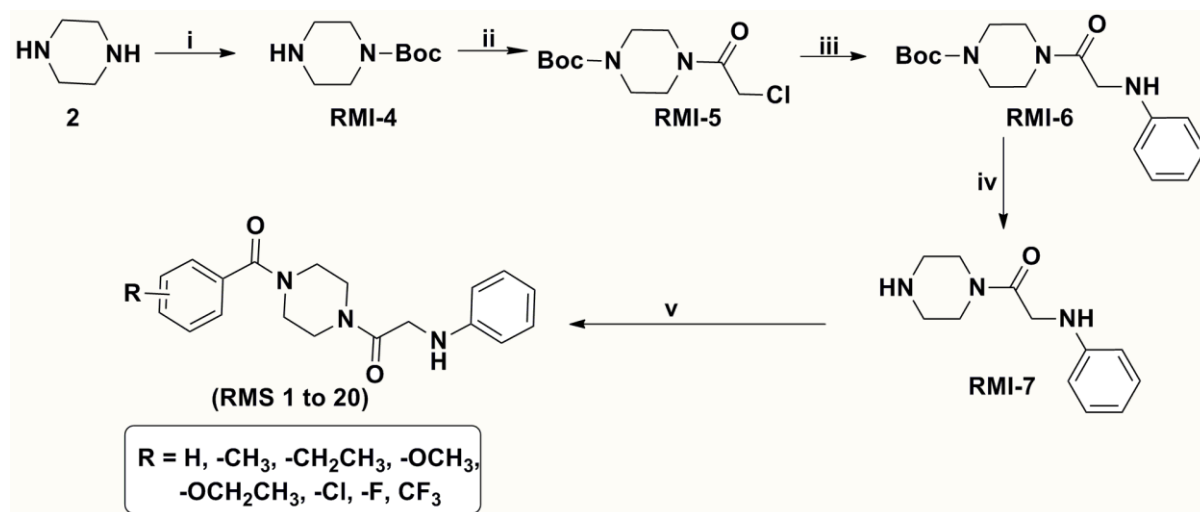
Reagents and conditions: (**i**) Boc anhydride, I_2, TFA, DCM, RT, 3 h; (**ii**) Chloroacetyl chloride, DIPEA, DCM, 0°C -RT 30 min; (**iii**) aniline, K_2CO_3, CH_3CN, 100°C, 3 h., (**iv**) TFA/DCM, 0°C-RT, 7 h; (**v**) Various carboxylic acids, EDC·HCl, HOBt/TEA-DCM, 0°C-RT, 6 h.

4.2.3. Series-III: Synthetic route of 2-(4-(substituted benzoyl)piperazin-1-yl)-*N*-phenylacetamide (RMT-1 to 20)

Scheme 3

R = H, -CH₃, -CH₂CH₃, -OCH₃,
-OCH₂CH₃, -Cl, -F, CF₃
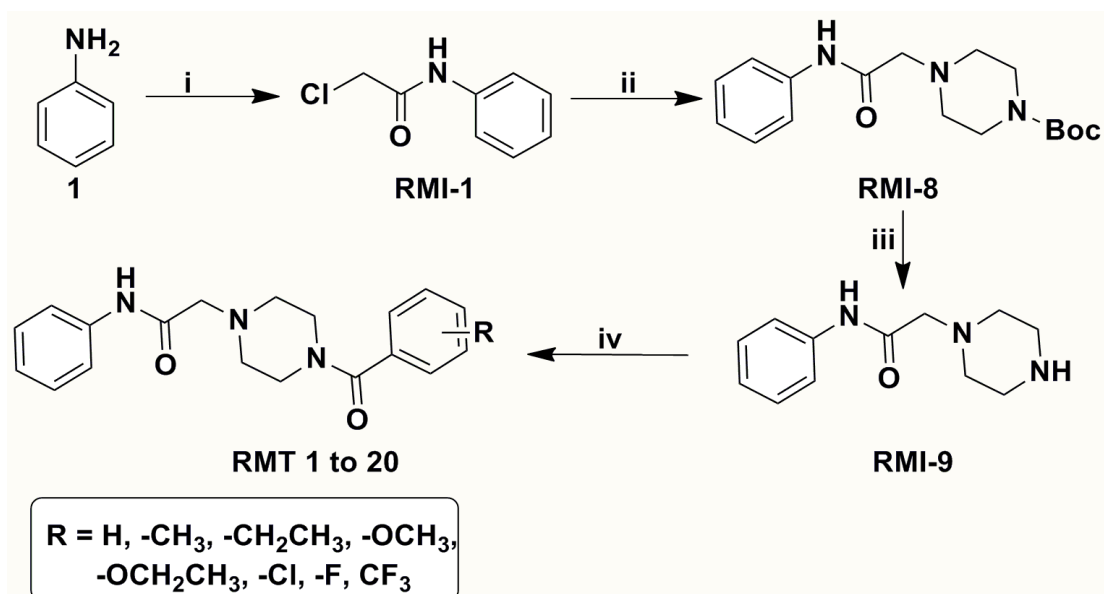
Reagents and conditions: (**i**) Chloroacetylchloride, K_2CO_3, DCM, 0°C-RT, 30 min; (**ii**) *N*-Boc-piperazine, K_2CO_3, CH_3CN, 90°C, 4 h., (**iii**) TFA/DCM, 0°C-RT, 16 h; (**iv**) Various carboxylic acids, EDC·HCl, HOBT/DIPEA-DCM, RT, 6 h.

4.2.4. Series-IV: Synthetic route of peptidomimetics (RMQ-1 to 20)

Scheme 4

N-Boc-L-Leucine (1)

2 R_1 = A, X = CH_3
3 R_1 = B, X = H
4 R_1 = C, X = CH_3
5 R_1 = D, X = CH_3
6 R_1 = E, X = CH_3

7 R_1 = A, X = CH_3
8 R_1 = B, X = H
9 R_1 = C, X = CH_3
10 R_1 = D, X = CH_3
11 R_1 = E, X = CH_3

12 R_1 = A, X = CH_3
13 R_1 = B, X = H
14 R_1 = C, X = CH_3
15 R_1 = D, X = CH_3
16 R_1 = E, X = CH_3

17 R_1 = A, X = CH_3
18 R_1 = B, X = H
19 R_1 = C, X = CH_3
20 R_1 = D, X = CH_3
21 R_1 = E, X = CH_3

22 R_1 = B, R_2 = d, X = H (RMQ-1)
23 R_1 = B, R_2 = e, X = H (RMQ-2)
24 R_1 = C, R_2 = d, X = CH_3 (RMQ-3)
25 R_1 = C, R_2 = e, X = CH_3 (RMQ-4)
26 R_1 = C, R_2 = f, X = CH_3 (RMQ-5)

24.1 R_1 = C, R_2 = d, X = CH_3
25.1 R_1 = C, R_2 = e, X = CH_3

27 R_1 = B
28 R_1 = D
29 R_1 = E

Coupling

30 R_1 = C, X = CH_3 (RMQ-6)

31 R_1 = B, R_2 = d (RMQ-7)
32 R_1 = B, R_2 = e (RMQ-8)
33 R_1 = C, R_2 = d (RMQ-9)
34 R_1 = C, R_2 = e (RMQ-10)
35 R_1 = C, R_2 = f (RMQ-11)

d =   e =   f =

53

Reagents and conditions: (**i**) BOP, L-amino ester, DIPEA, DMF, 1 h, RT; (**ii**) 20 % TFA in DCM (1 mL/0.02 mmol), anisole, 0°C-RT, 3 h; (**iii**) *Boc*-L-Leu, BOP, DIPEA, DMF, 1 h, RT; (**iv**) LiOH, THF:MeOH (3:1), RT, 16 h; (**v**) BOP, L-amino ester, DIPEA, DMF, 1 h, RT; (**vi**) R_2COCl, DIPEA, 0°C-rt, 16 h; (**vii**) chloroacetyl chloride, TEA, DCM, 0°C, 0.5 h; (**viii**) cyclic amine, KI, K_2CO_3, acetonitrile, MWI, 150°C, 15 min; (**ix**) LiOH, THF:MeOH (3:1), RT, 16 h.

Scheme 5

36 R_1 = B, R_2 = d, R_3 = l (RMQ-12)
37 R_1 = B, R_2 = e, R_3 = l (RMQ-13)
38 R_1 = B, R_2 = d, R_3 = m (RMQ-14)
39 R_1 = B, R_2 = e, R_3 = m (RMQ-15)
40 R_1 = C, R_2 = d, R_3 = m (RMQ-16)
41 R_1 = C, R_2 = e, R_3 = n (RMQ-17)
42 R_1 = C, R_2 = e, R_3 = o (RMQ-18)
43 R_1 = C, R_2 = f, R_3 = o (RMQ-19)
44 R1 =C, R2 =d, R_3 = o (RMQ-20)
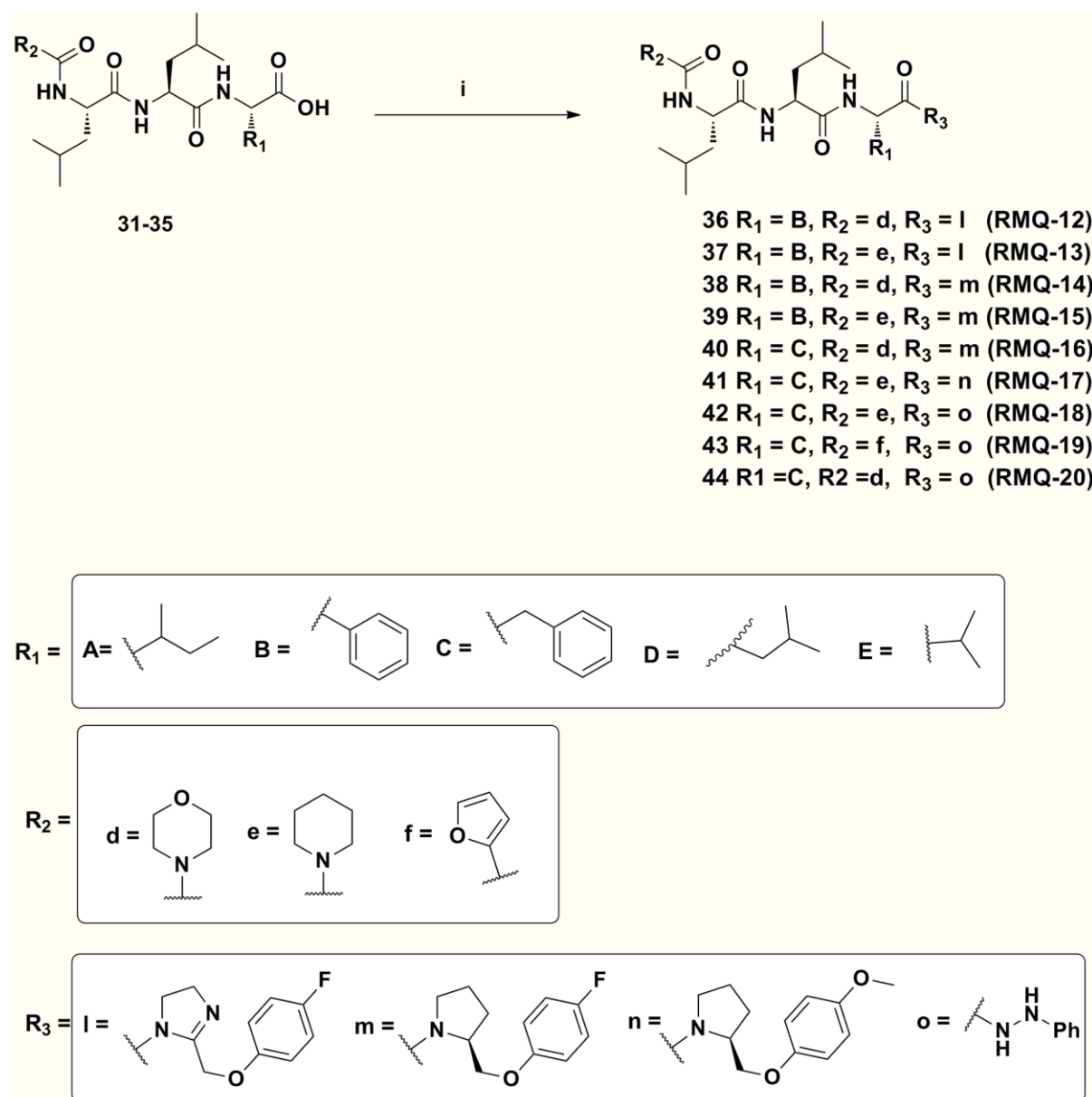
Reagents and conditions: (**i**) Compounds **47**, **51, 52** or phenyl hydrazine and BOP, DIPEA, DMF, 1.5 h, RT.

Scheme 6.

45   46   47
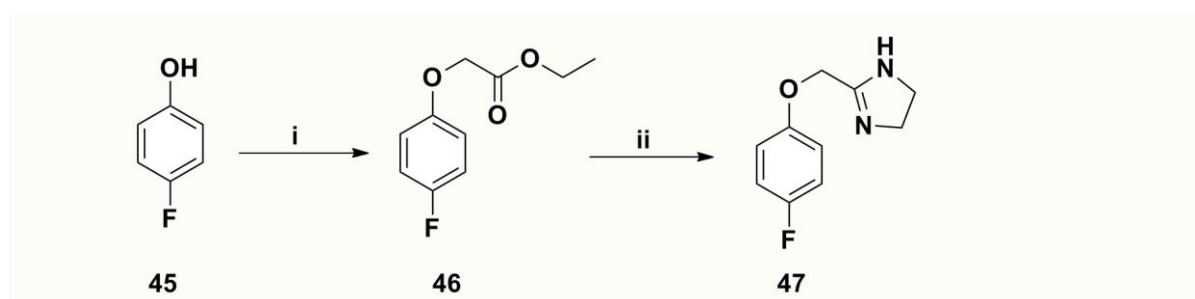
Reagents and conditions: (**i**) ethyl bromoacetate, K_2CO_3, DMF, 0°C-RT, 16 h; (**ii**) Ethylene diamine, $Al(CH_3)_3$, anhydrous toluene, 0°C-reflux, 3 h, N_2 atmosphere.

Scheme 7

48

49 R_3 = 4-fluoro phenol
50 R_3 = 4-methoxy phenol

51 R_3 = 4-fluoro phenol
52 R_3 = 4-methoxy phenol
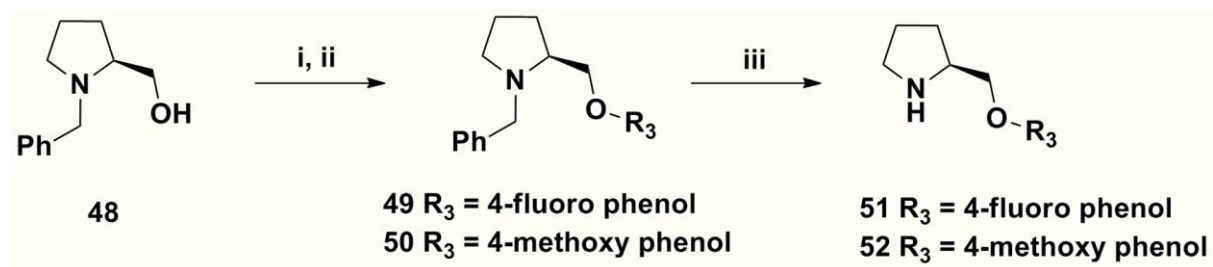
Reagents and conditions: (**i**) CBr_4, PPh_3, THF, 0°C RT, 3 h; (**ii**) 4-Fluorophenol or 4-methoxyphenol, K_2CO_3, DMF, 60°C, 6 h; (**iii**) 10 % wt. Pd/C, MeOH, H_2 (1 atm), RT, 3 h.

4.2.5. Series-V: Synthetic route of 2-(substituted)pyrimidin-4-ylthio)-*N'*-(2-phenylacetyl)-acetohydrazide derivatives (RMP-1 to 15)

Scheme 8
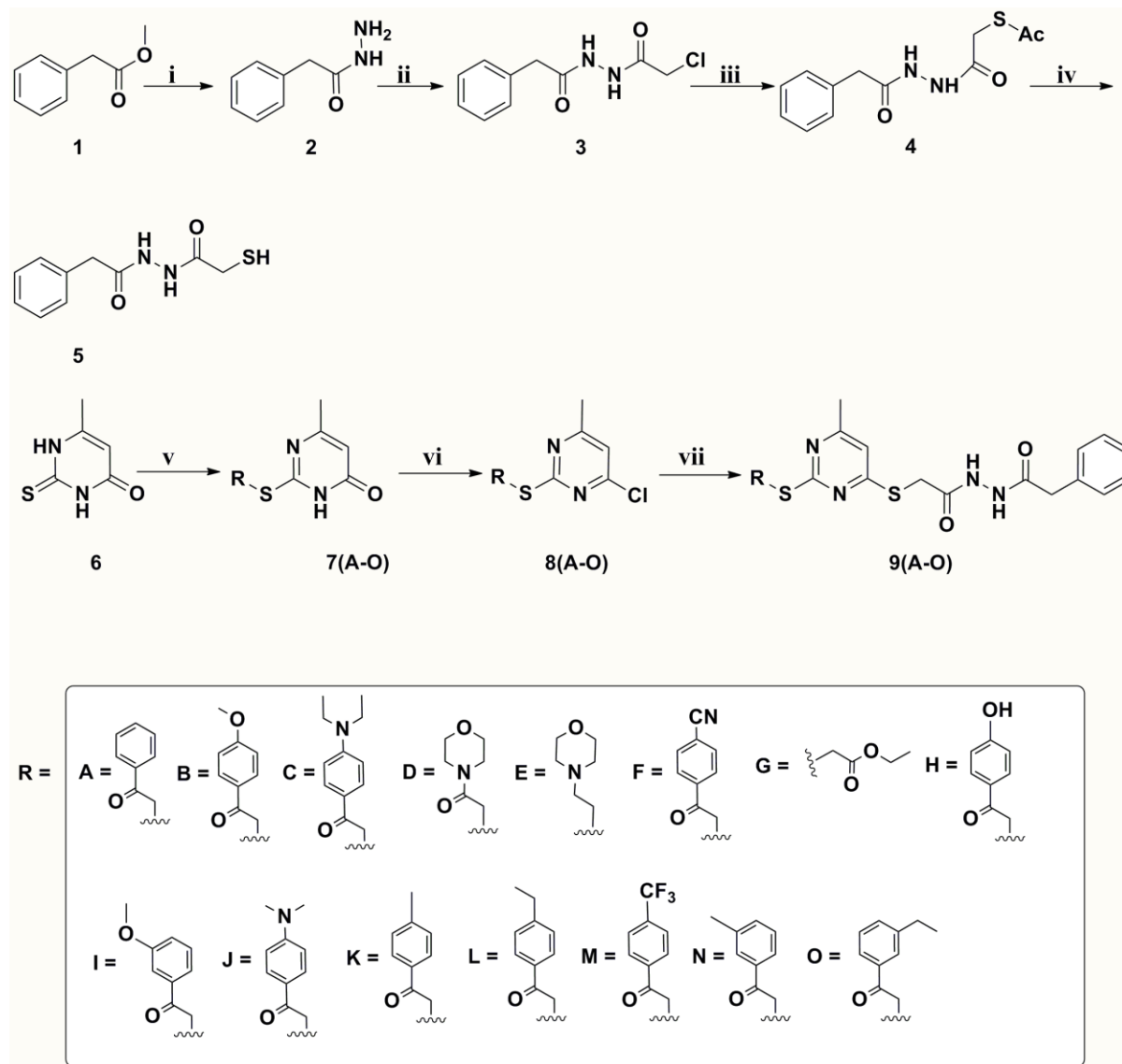
Reagents and conditions: (**i**) $NH_2.NH_2H_2O$, MeOH, 16 h, RT; (**ii**) chloroacetyl chloride, DIPEA, DCM, -10°C–RT, 05 h; (**iii**) AcSK, EtOH, RT; (**iv**) K_2CO_3, MeOH, RT, 1 h; (**v**) Reagents (**A-O**), K_2CO_3, DMF, 16 h, RT; (**vi**) $POCl_3$, 70°C, 1 h; (**vii**) 5, Et_3N, acetonitrile.

4.2.6. Series-VI: Synthetic route of 1,6-dihydropyrimidine-5-carboxamides derivatives (RMH-1 to 14)

Scheme 9
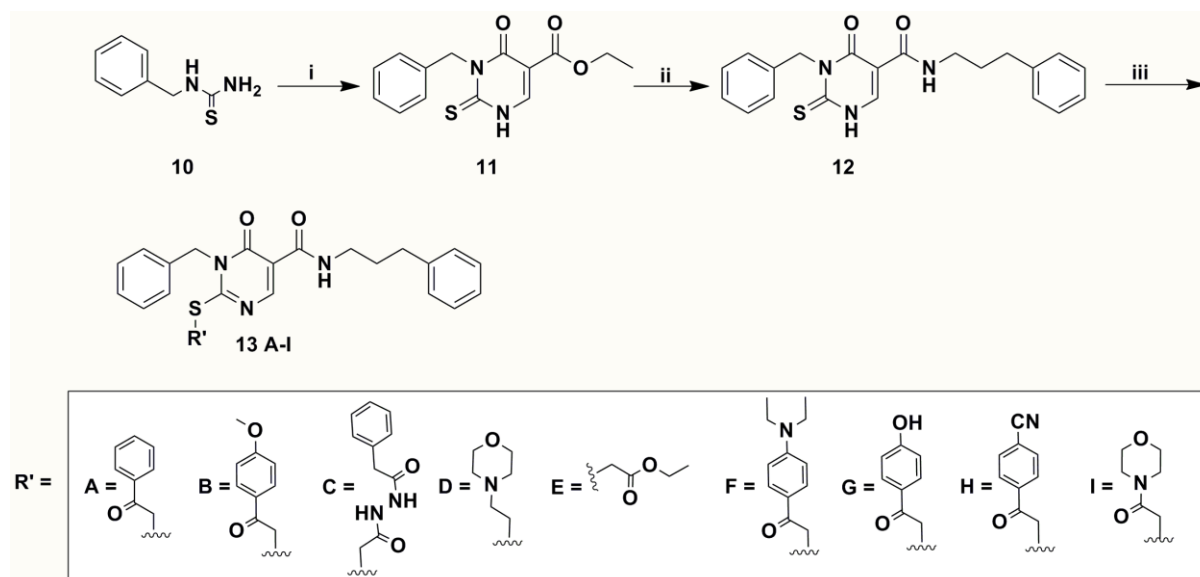
Reagents and conditions: (**i**) Diethyl (ethoxymethylene)malonate, K_2CO_3, DMF, MWI, 1 h; (**ii**) 3-Phenyl-1-propylamine, trimethyl aluminium, 16 h, 0°C- RT; (**iii**) Reagent (**A-I**), K_2CO_3, DMF, 16 h, RT.

Scheme 10
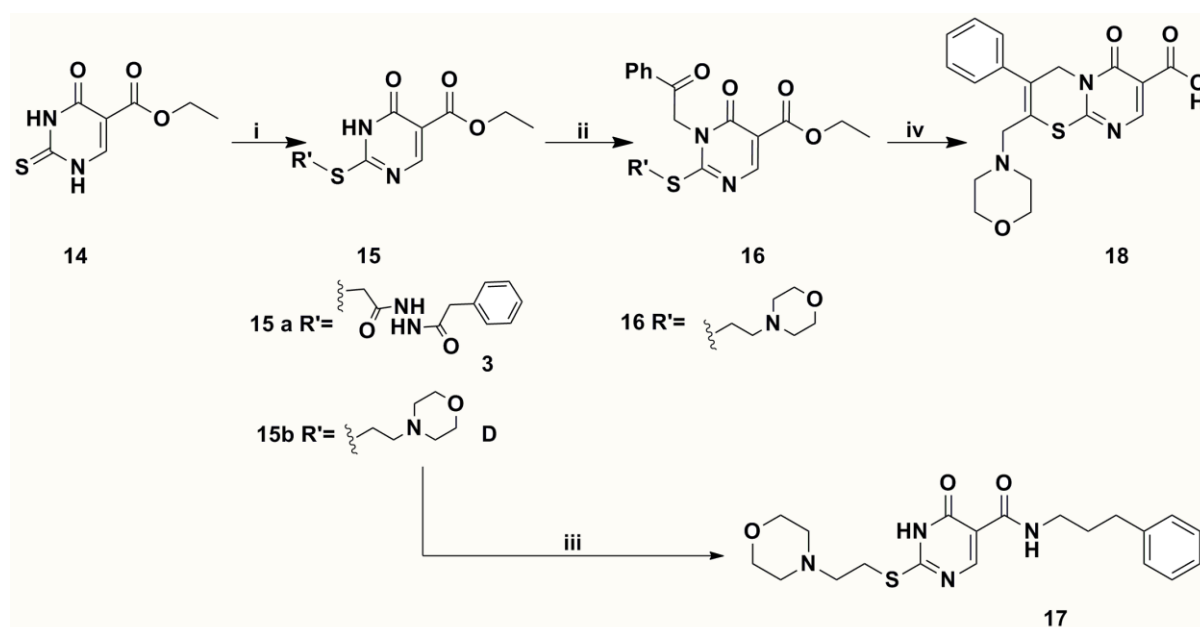
Reagents and conditions: (**i**) Reagents (**3 & D**), K_2CO_3, Acetone, 16 h, RT; (**ii**) Reagent A, K_2CO_3, Acetone, 16 h, RT (**iii**) 3-Phenyl-1-propylamine, trimethyl aluminium, 16 h, 0°C- RT; (**iv**) THF/MeOH (3/1), LiOH, 16 h, RT.

4.3. Synthetic protocol

4.3.1. Series-I: Synthesis of 2-(4-(substituted benzoyl)-1,4-diazepan-1-yl)-*N*-phenylacetamide derivatives (RM-1 to 20)

Synthesis of 2-chloro-*N*-phenylacetamide (RMI-1)

In a round bottom flask (500 mL), compound **1** (1 g, 10.7 mmol) and triethylamine (2.9 mL, 21.4 mmol) were suspended in anhydrous DCM (200 mL) and cooled to 0°C. To this, chloroacetylchloride (1.7 mL, 21.4 mmol) was added. The reaction mixture was then stirred at room temperature for 20 min; quenched with saturated sodium hydrogen carbonate (10 ml) and washed with water (2 × 10 mL). The organic extracts were evaporated under vacuum. The crude reaction mixture was purified by column chromatography using chloroform and methanol as a mobile phase to obtain a pure compound **RMI-1** as a white solid. Yield 66 %, FT-IR: (KBr, cm^{-1}) 3277 (N-H stretch), 2997 (aromatic, C-H stretch), 1674 (amide, C=O stretch), 744 (C-Cl stretch); ^{1}H NMR (400 MHz, CDCl$_3$) *δ*: 8.18 (s, 1H), 7.47 (d, *J* = 8.0 Hz, 2H), 7.28 (t, *J* = 8.0 Hz, 2H), 7.10 (t, *J* = 8.0 Hz, 1H), 4.12 (s, 2H).

Synthesis of *tert*-butyl 4-(2-oxo-2-(phenylamino)ethyl)-1,4-diazepane-1-carboxylate (RMI-2)

To a solution of compound **RMI-1** (1.0 g, 5.8 mmol), K$_2$CO$_3$ (4.0 g, 29.4 mmol), in anhydrous acetonitrile (10 mL) were stirred for 10 min at 100°C. To the above solution, *N*-Boc-homopiperazine (1.4 mL, 7.0 mmol), was added and refluxed for 5 h. After completion of the reaction, acetonitrile was removed under vacuum, the reaction crude was diluted with ethyl acetate and washed with brine (2 × 10 mL). The combined organic layers were evaporated under vacuum to get a crude mixture. The obtained crude residue was purified by column chromatography using ethylacetate and methanol as a mobile phase to obtain a pure compound **RMI-2** as a brown solid. Yield 68 %, FT-IR: (KBr, cm^{-1}) 3165 (N-H stretch), 3091 (aromatic, C-H stretch), 1716 (COO stretch), 1660 (amide, C=O stretch) 1221, 1017; ^{1}H NMR (400 MHz, CDCl$_3$) *δ*: 9.16 (s, 1H), 7.51 (d, *J* = 8.0 Hz, 2H), 7.27 (t, *J* = 8.0 Hz, 2H), 7.05 (t, *J* = 8.0 Hz, 1H), 3.52 (s, 2H), 3.50 - 3.40 (m, 2H), 3.30 – 3.20 (m, 2H), 2.81 – 2.77 (m, 4H), 1.86 – 1.82 (m, 2H),1.40 (s, 9H).

Synthesis of 2-(1,4-diazepan-1-yl)-*N*-phenylacetamide (RMI-3)

To a solution of **RMI-2** (1.0 g, 3.0 mmol) in anhydrous DCM (20 mL), in a 100 mL round bottom flask at 0°C, trifluoroacetic acid (1.1 mL, 15.0 mmol) was added. The mixture stirred

for 6 h at room temperature. Upon completion of the reaction, solvent was removed under vacuum. To the residue, saturated solution of sodium bicarbonate was added, and extracted with ethyl acetate. Ethyl acetate portion was evaporated to obtain the free amine **RMI-3** as off white solid. Yield 70 %, FT-IR: (KBr, cm^{-1}) 3212 (N-H stretch), 3198 (aromatic, C-H stretch), 1645 (amide, C=O stretch), 1155, 1086; ^{1}H NMR (400 MHz, CDCl$_3$) δ: 9.14 (s, 1H), 7.56 (dd, *J* = 8.0 Hz, 1 Hz, 1H), 7.29 – 7.21 (m, 2H), 7.06 – 7.02 (m, 2H), 3.28 (s, 2H), 3.14 – 3.10 (m, 4H), 2.91 – 2.87 (m, 2H), 2.83 - 2.79 (m, 2H), 1.94 – 1.90 (m, 2H).

General procedure for the synthesis of 2-(4-(substituted benzoyl)-1,4-diazepan-1-yl)-*N*-phenylacetamide derivatives (RM 1 to 20)

To an appropriate carboxylic acid (1g), DIPEA (2.4 equiv), EDC·HCl (1.5 equiv), and HOBt (0.8 equiv) in anhydrous DCM (10 mL) was added, and the reaction was stirred at 0°C for 5 min. To this reaction mixture, compound **RMI-3** (1.1 equiv) was added. The reaction was stirred for 6 h at room temperature and then solvents were removed under reduced pressure. The residue was dissolved in ethyl acetate (2 × 10 mL), and the organic phase was washed with 5 % aqueous sodium bicarbonate solution (2 × 10 mL). The combined organic layer dried over anhydrous sodium sulphate and evaporated under reduced pressure. The obtained residue was purified by column chromatography.

2-(4-Benzoyl-1,4-diazepan-1-yl)-*N*-phenylacetamide (RM-1)

Semi solid, hygroscopic; Yield: 62 %; FT-IR: (KBr, cm^{-1}) 3254 (N-H stretch), 3065 (aromatic, C-H stretch), 2819, 2698, 1660 (keto, C=O stretch), 1639 (amide, C=O stretch), 1507 (CH$_2$ bend), 1336, 1139, 1010; ^{1}H NMR (400 MHz, CDCl$_3$) δ: 9.10 (s, 1H), 7.62 (d, *J* = 7.9 Hz, 1H), 7.53 (d, *J* = 7.9 Hz, 1H), 7.41 (d, *J* = 7.0 Hz, 5H), 7.33 (q, *J* = 7.8 Hz, 2H), 7.12 (t, *J* = 7.0 Hz, 1H), 3.87 - 3.81 (m, 2H), 3.57 – 3.53 (m, 2H), 3.34 (s, 1H), 3.26 (s, 1H), 3.04 – 3.00 (m, 1H), 2.92 – 2.79 (m, 3H), 2.07 – 2.04 (m, 1H), 1.88 - 1.82 (m, 1H); ESI MS: m/z = 338.1 (M + 1 H)$^+$; Anal. calcd for C$_{20}$H$_{23}$N$_3$O$_2$ C, 71.19; H, 6.87; N, 12.45; found C, 71.21; H, 6.81; N, 12.41.

2-(4-(3-Fluorobenzoyl)-1,4-diazepan-1-yl)-*N*-phenylacetamide (RM-2)

White solid, Yield: 82 %; mp: 125-127°C; FT-IR: (KBr, cm^{-1}) 3324 (N-H stretch), 3062 (aromatic, C-H stretch), 2761, 1661 (keto, C=O stretch), 1640 (amide, C=O stretch), 1633, 1549 (CH$_2$ bend), 1427, 1313; ^{1}H NMR (400 MHz, CDCl$_3$) δ: 9.09 (s, 1H), 7.64 – 7.58 (m, 1H), 7.50 (d, *J* = 7.5 Hz, 1H), 7.48 - 7.44 (m, 2H), 7.38 - 7.30 (m, 3H), 7.14 – 7.10

(m, 2H), 3.85 - 3.81 (m, 2H), 3.60 - 3.54 (m, 2H), 3.44 (s, 1H), 3.16 (s, 1H), 3.14 - 3.10 (m, 1H), 3.05 – 2.97 (m, 3H), 2.14 – 2.10 (m, 1H), 1.94 – 1.90 (m, 1H); ESI MS: m/z = 356.1 (M + 1 H)$^+$; Anal. calcd for $C_{20}H_{22}FN_3O_2$ C, 67.59; H, 6.24; N, 11.82 found C, 67.61; H, 6.21; N, 11.81.

2-(4-(2-Fluorobenzoyl)-1,4-diazepan-1-yl)-*N*-phenylacetamide (RM-3)

Brown solid, Yield: 68 %; mp: 118-120°C; FT-IR: (KBr, cm^{-1}) 3270 (N-H stretch), 3058 (aromatic, C-H stretch), 2765, 1663 (keto, C=O stretch), 1630 (amide, C=O stretch), 1504 (CH$_2$ bend), 1305, 1269; ^{1}H NMR (400 MHz, CDCl$_3$) *δ*: 9.08 (s, 1H), 7.61 (dd, *J* = 8.5, 1.0 Hz, 1H), 7.55 (dd, *J* = 8.5, 1.0 Hz, 1H), 7.39 – 7.35 (m, 4H), 7.24 - 7.18 (m, 1H), 7.16 - 7.08 (m, 2H), 3.89 – 3.85 (m, 2H), 3.50 – 3.46 (m, 2H), 3.34 (s, 1H), 3.26 (s, 1H), 3.05 – 2.96 (m, 1H), 2.88 (dd, *J* = 6.2, 5.1 Hz, 1H), 2.81 (dd, *J* = 10.8, 6.7 Hz, 2H), 2.08 – 2.00 (m, 1H), 1.90 – 1.82 (m, 1H); ESI MS: m/z = 356.1 (M + 1 H)$^+$; Anal. calcd for $C_{20}H_{22}FN_3O_2$ C, 67.59; H, 6.24; N, 11.82; found C, 67.61; H, 6.21; N, 11.81.

2-(4-(3-Chlorobenzoyl)-1,4-diazepan-1-yl)-*N*-phenylacetamide (RM-4)

Semi solid, hygroscopic; Yield: 81 %; FT-IR: (KBr, cm^{-1}) 3287 (N-H stretch), 2940 (aromatic, C-H stretch), 2351, 1686 (keto, C=O stretch), 1677 (amide, C=O stretch), 1502, 1483 (CH$_2$ bend), 1433, 1301, 1282; ^{1}H NMR (400 MHz, CDCl$_3$) *δ*: 8.99 (s, 1H), 7.61 (d, *J* = 7.9 Hz, 1H), 7.53 (d, *J* = 7.9 Hz, 1H), 7.44 - 7.30 (m, 6H), 7.12 (t, *J* = 7.2 Hz, 1H), 3.86 – 3.80 (m, 2H), 3.60 -3.54 (m, 1H), 3.53 (t, *J* = 6.2 Hz, 1H) 3.37 (s, 1H), 3.28 (s, 1H), 3.06 – 3.02 (m, 1H), 2.87 – 2.83 (m, 3H), 2.08 – 2.04 (m, 1H), 1.92 – 1.86 (m, 1H); ESI MS: m/z = 371.2 (M)$^+$ and 372.2 (M + 1 H)$^+$; Anal. calcd for $C_{20}H_{22}ClN_3O_2$ C, 64.60; H, 5.96; N, 11.30; found C, 64.62; H, 5.97; N, 11.31.

2-(4-(4-Chlorobenzoyl)-1,4-diazepan-1-yl)-*N*-phenylacetamide (RM-5)

Semi solid, hygroscopic; Yield: 65 %; FT-IR: (KBr, cm^{-1}) 3286 (N-H stretch), 2939 (aromatic, C-H stretch), 2697, 1682 (keto, C=O stretch), 1677 (amide, C=O stretch), 1482 (CH$_2$ bend), 1433, 1301, 1282; ^{1}H NMR (400 MHz, CDCl$_3$) *δ*: 9.16 (s, 1H), 7.61 (d, *J* = 7.7 Hz, 1H), 7.52 (d, *J* = 7.4 Hz, 1H), 7.38 – 7.34 (m, 6H), 7.12 (t, *J* = 7.4 Hz, 1H), 3.85 – 3.81 (m, 2H), 3.56 - 3.50 (m, 2H), 3.38 (s, 1H), 3.28 (s, 1H), 3.08 – 3.02 (m, 1H), 2.89 – 2.81 (m, 3H), 2.10 – 2.02 (m, 1H), 1.90 – 1.86 (m, 1H); ESI MS: m/z = m/z 371.2 (M)$^+$ and 372.2 (M + 1 H)$^+$; Anal. calcd for $C_{20}H_{22}ClN_3O_2$ C, 64.60; H, 5.96; N, 11.30; found C, 64.62; H, 5.97; N, 11.31.

2-(4-(2-Chlorobenzoyl)-1,4-diazepan-1-yl)-*N*-phenylacetamide (RM-6)

Semi solid, hygroscopic; Yield: 62 %; FT-IR: (KBr, cm^{-1}) 3281 (N-H stretch), 2948 (aromatic, C-H stretch), 2350, 1684 (keto, C=O stretch), 1669 (amide, C=O stretch), 1433 (CH$_2$ bend), 1301, 1282; ^{1}H NMR (400 MHz, CDCl$_3$) *δ*: 9.06 (s, 1H), 7.70 (d, *J* = 8.0 Hz, 1H), 7.62 (d, *J* = 7.6 Hz, 2H), 7.50 -7.46 (m, 5H), 7.21 (t, *J* = 7.6 Hz, 1H), 3.84 – 3.76 (m, 2H), 3.60 -3.54 (m, 2H), 3.48 (s, 1H), 3.38 (s, 1H), 3.19 - 3.02 (m, 4H), 2.38 - 2.34 (m, 1H), 1.80 – 1.76 (m, 1H); ESI MS: m/z = 371.2 (M)$^+$ and 372.2 (M + 1 H)$^+$; Anal. calcd for C$_{20}$H$_{22}$ClN$_3$O$_2$ C, 64.60; H, 5.96; N, 11.30; found C, 64.62; H, 5.97; N, 11.31.

_N_-Phenyl-2-(4-(3-(trifluoromethyl) benzoyl)-1,4-diazepan-1-yl) acetamide (RM-7)

White solid, Yield: 68 %; mp: 122-124°C; FT-IR: (KBr, cm^{-1}) 3359 (N-H stretch), 3063 (aromatic, C-H stretch), 2944, 2866, 1691 (keto, C=O stretch), 1628 (amide, C=O stretch), 1442 (CH$_2$ bend), 1408, 1365, 1330; ^{1}H NMR (400 MHz, CDCl$_3$) *δ*: 9.04 (s, 1H), 7.70 (d, *J* = 5.7 Hz, 2H), 7.61 (d, *J* = 7.8 Hz, 2H), 7.54 (dd, *J* = 13.9, 7.8 Hz, 2H), 7.34 (q, *J* = 7.8 Hz, 2H), 7.15 – 7.11 (m, 1H), 3.90 – 3.82 (m, 2H), 3.60 - 3.52 (m, 1H), 3.51 (t, *J* = 6.4 Hz, 1H) 3.38 (s, 1H), 3.29 (s, 1H), 3.08 – 3.04 (m, 1H), 2.89 - 2.85 (m, 2H), 2.13 – 1.89 (m, 3H); ESI MS: m/z = 406.2 (M + 1 H)$^+$; Anal. calcd for C$_{21}$H$_{22}$F$_3$N$_3$O$_2$ C, 62.21; H, 5.47; N, 10.36; found C, 62.22; H, 5.45; N, 10.35.

_N_-Phenyl-2-(4-(4-(trifluoromethyl) benzoyl)-1,4-diazepan-1-yl) acetamide (RM-8)

Yellow solid, Yield: 61 %; mp: 156-158°C; FT-IR: (KBr, cm^{-1}) 3275 (N-H stretch), 3059 (aromatic, C-H stretch), 2939, 2357, 2336, 1670 (keto, C=O stretch), 1646 (amide, C=O stretch), 1412 (CH$_2$ bend), 1315, 1278, 1265; ^{1}H NMR (400 MHz, CDCl$_3$) *δ*: 9.04 (s, 1H), 7.69 (t, *J* = 8.1 Hz, 2H), 7.61 (d, *J* = 7.6 Hz, 1H), 7.54 (t, *J* = 8.5 Hz, 3H), 7.34 (q, *J* = 8.1 Hz, 2H), 7.13 (t, *J* = 7.6 Hz, 1H), 3.88 – 3.84 (m, 2H), 3.55 (t, *J* = 5.1 Hz, 1H), 3.50 (t, *J* = 6.2 Hz, 1H), 3.36 (s, 1H), 3.28 (s, 1H), 3.06 – 3.02 (m, 1H), 2.94 – 2.86 (m, 1H), 2.84 – 2.80 (m, 2H), 2.09 – 2.05 (m, 1H), 1.89 – 1.85 (m, 1H); ESI MS: m/z = 406.2 (M + 1 H)$^+$; Anal. calcd for C$_{21}$H$_{22}$F$_3$N$_3$O$_2$ C, 62.21; H, 5.47; N, 10.36; found C, 62.22; H, 5.45; N, 10.35.

_N_-Phenyl-2-(4-(2-(trifluoromethyl) benzoyl)-1,4-diazepan-1-yl) acetamide (RM-9)

White solid, Yield: 61 %; mp: 140-142°C; FT-IR: (KBr, cm^{-1}) 3293 (N-H stretch), 3060 (aromatic, C-H stretch), 2354, 1691 (keto, C=O stretch), 1658 (amide, C=O stretch), 1501 (CH$_2$ bend), 1444, 1415; ^{1}H NMR (400 MHz, CDCl$_3$) *δ*: 9.04 (s, 1H), 7.72 – 7.66 (m, 2H), 7.61 (d, *J* = 8.0 Hz, 1H), 7.56 – 7.52 (m, 3H), 7.36 - 7.32 (m, 2H), 7.13 (t, *J* = 8.0 Hz, 1H),

3.92 - 3.88 (m, 2H), 3.55 (d, *J* = 6.2 Hz, 1H), 3.49 (t, *J* = 6.2 Hz, 1H), 3.38 (s, 1H), 3.30 (s, 1H), 3.15 – 3.09 (m, 1H), 2.97 – 2.93 (m, 1H), 2.89 – 2.85 (m, 2H), 2.14 – 2.10 (m, 1H), 1.87 – 1.83 (m, 1H); ESI MS: m/z = 406.2 (M + 1 H)$^+$; Anal. calcd for $C_{21}H_{22}F_3N_3O_2$ C, 62.21; H, 5.47; N, 10.36; found C, 62.22; H, 5.45; N, 10.35.

2-(4-(2-Methoxybenzoyl)-1,4-diazepan-1-yl)-*N*-phenylacetamide (RM-10)

Semi solid, hygroscopic; Yield: 64 %; FT-IR: (KBr, cm^{-1}) 3301(N-H stretch), 3001 (aromatic, C-H stretch), 2771, 1690 (keto, C=O stretch), 1629 (amide, C=O stretch), 1522 (CH$_2$ bend), 1301, 1249, 1172; ^{1}H NMR (400 MHz, CDCl$_3$) *δ*: 9.16 (s, 1H), 7.63 (dd, *J* = 8.6, 1.0 Hz, 1H), 7.56 – 7.52 (m, 1H), 7.36 – 7.32 (m, 3H), 7.26 – 7.20 (m, 1H), 7.13 - 7.09 (m, 1H), 7.01 - 6.97 (m, 1H), 6.92 (dd, *J* = 8.3, 4.5 Hz, 1H), 3.97 – 3.93 (m, 1H), 3.86 – 3.82 (m, 1H), 3.81 (s, 3H), 3.47 – 3.43 (m, 1H), 3.35 (s, 2H), 3.28 – 3.24 (m, 1H), 3.01 - 2.97 (m, 1H), 2.85 – 2.77 (m, 4H), 2.06 - 2.02 (m, 1H); ESI MS: m/z = 368.2 (M + 1 H)$^+$; Anal. calcd for $C_{21}H_{25}N_3O_3$ C, 68.64; H, 6.86; N, 11.44; found C, 68.65; H, 6.87; N, 11.46.

2-(4-(3-Methoxybenzoyl)-1,4-diazepan-1-yl)-*N*-phenylacetamide (RM-11)

Semi solid, hygroscopic; Yield: 73 %; FT-IR: (KBr, cm^{-1}) 3313 (N-H stretch), 3042 (aromatic, C-H stretch), 2930, 1688 (keto, C=O stretch), 1664 (amide, C=O stretch), 1597 (CH$_2$ bend), 1329, 1273, 1236, 1141; ^{1}H NMR (400 MHz, CDCl$_3$) *δ*: 9.09 (s, 1H), 7.62 (d, *J* = 7.8 Hz, 1H), 7.53 (d, *J* = 7.8 Hz, 1H), 7.33 (dd, *J* = 14.8, 7.8 Hz, 3H), 7.12 (d, *J* = 7.0 Hz, 1H), 6.99 – 6.97 (m, 3H), 3.88 – 3.84 (m, 1H), 3.81 (s, 3H), 3.80 – 3.76 (m, 1H), 3.57 – 3.53 (m, 2H), 3.34 (s, 1H), 3.26 (s, 1H), 3.05 – 2.97 (m, 1H), 2.90 – 2.86 (m, 1H), 2.82 – 2.78 (m, 2H), 2.06 – 2.02 (m, 1H), 1.88 – 1.82 (m, 1H); ESI MS: m/z = 368.2 (M + 1 H)$^+$, Anal. calcd for $C_{21}H_{25}N_3O_3$ C, 68.64; H, 6.86; N, 11.44; found C, 68.65; H, 6.87; N, 11.46.

2-(4-(4-Methoxybenzoyl)-1,4-diazepan-1-yl)-*N*-phenylacetamide (RM-12)

Semi solid, hygroscopic; Yield: 87 %; FT-IR: (KBr, cm^{-1}) 3317 (N-H stretch), 3062 (aromatic, C-H stretch), 2945, 1677 (keto, C=O stretch), 1668 (amide, C=O stretch), 1597 (CH$_2$ bend), 1427, 1365; ^{1}H NMR (400 MHz, CDCl$_3$) *δ*: 9.11 (s, 1H), 7.60 – 7.54 (m, 2H), 7.40 (d, *J* = 8.4 Hz, 2H), 7.33 (t, *J* = 7.3 Hz, 2H), 7.11 (t, *J* = 7.3 Hz, 1H), 6.91 (d, *J* = 8.4 Hz, 2H), 3.87 – 3.84 (m, 1H), 3.82 (s, 3H), 3.81 - 3.77 (m, 1H), 3.61 – 3.57 (m, 2H), 3.30 (s, 2H), 3.03 - 2.99 (m, 1H), 2.97 – 2.93 (m, 1H), 2.84 – 2.80 (m, 2H), 2.06 – 2.02 (m, 1H), 1.89 – 1.85 (m, 1H); ESI MS: m/z = 368.2 (M + 1 H)$^+$; Anal. calcd for $C_{21}H_{25}N_3O_3$ C, 68.64; H, 6.86; N, 11.44; found C, 68.65; H, 6.87; N, 11.46.

2-(4-(3-Ethoxybenzoyl)-1,4-diazepan-1-yl)-*N*-phenylacetamide (RM-13)

Semi solid, hygroscopic; Yield: 66 %; FT-IR: (KBr, cm^{-1}) 3249 (N-H stretch), 3186 (aromatic, C-H stretch), 3068, 2843, 2358, 1691 (keto, C=O stretch), 1668 (amide, C=O stretch), 1598 (CH$_2$ bend), 1411, 1327; ^{1}H NMR (400 MHz, CDCl$_3$) *δ*: 9.17 (s, 1H), 7.69 – 7.65 (m, 2H), 7.50 (d, *J* = 8.4 Hz, 2H), 7.37 (t, *J* = 7.3 Hz, 2H), 7.21 (t, *J* = 7.3 Hz, 1H), 6.90 (d, *J* = 8.4 Hz, 2H), 4.15 (q, *J* = 8.0 Hz, 2H), 3.87 – 3.83 (m, 1H), 3.80 – 3.76 (m, 1H), 3.63 - 3.59 (m, 2H), 3.40 (s, 2H), 3.23 – 3.15 (m, 1H), 2.92 – 2.88 (m, 1H), 2.85 – 2.81 (m, 2H), 2.06 – 2.02 (m, 1H), 1.89 – 1.85 (m, 1H), 1.32 (t, *J* = 8.0 Hz, 3H); ESI MS: m/z = 382.3 (M + 1 H)$^+$; Anal. calcd for C$_{22}$H$_{27}$N$_3$O$_3$ C, 69.27; H, 7.13; N, 11.02; found C, 69.24; H, 7.11; N, 11.04.

2-(4-(2-Ethoxylbenzoyl)-1,4-diazepan-1-yl)-*N*-phenylacetamide (RM-14)

Semi solid, hygroscopic; Yield: 71 %; FT-IR: (KBr, cm^{-1}) 3201 (N-H stretch), 3184 (aromatic, C-H stretch), 2845, 2358, 1691 (keto, C=O stretch), 1636 (amide, C=O stretch), 1546, 1413 (CH$_2$ bend), 1327, 1273, 1165; ^{1}H NMR (400 MHz, CDCl$_3$) *δ*: 9.12 (s, 1H), 7.79 – 7.75 (m, 2H), 7.57 (d, *J* = 8.0 Hz, 2H), 7.37 (t, *J* = 7.3 Hz, 2H), 7.23 (t, *J* = 7.3 Hz, 1H), 6.79 (d, *J* = 8.0 Hz, 2H), 4.21 (q, *J* = 8.0 Hz, 2H), 3.90 – 3.86 (m, 1H), 3.84 – 3.80 (m, 1H), 3.73 – 3.69 (m, 2H), 3.45 (s, 2H), 3.31 – 3.27 (m, 1H), 2.92 – 2.86 (m, 1H), 2.83 – 2.79 (m, 2H), 2.16 – 2.12 (m, 1H), 1.99 – 1.95 (m, 1H), 1.30 (t, *J* = 8.0 Hz, 3H); ESI MS: m/z = 382.3 (M + 1 H)$^+$; Anal. calcd for C$_{22}$H$_{27}$N$_3$O$_3$ C, 69.27; H, 7.13; N, 11.02; found C, 69.24; H, 7.11; N, 11.04.

2-(4-(4-Ethoxybenzoyl)-1,4-diazepan-1-yl)-*N*-phenylacetamide (RM-15)

Semi solid, hygroscopic; Yield: 71 %; FT-IR: (Cm-1) 3261 (N-H stretch), 3188 (aromatic, C-H stretch), 3118, 3069, 2358, 1696 (keto, C=O stretch), 1642 (amide, C=O stretch), 1546 (CH$_2$ bend), 1327, 1273, 1165; ^{1}H NMR (400 MHz, CDCl$_3$) *δ*: 9.14 (s, 1H), 7.64 – 7.60 (m, 2H), 7.51 (t, *J* = 8.4 Hz, 2H), 7.40 – 7.34 (m, 2H), 7.21 (d, *J* = 8.4 Hz, 1H), 6.92 – 6.88 (m, 2H), 4.19 (q, *J* = 8.1 Hz, 2H), 3.83 – 3.77 (m, 2H), 3.73 – 3.69 (m, 2H), 3.34 (s, 2H), 3.31 – 3.27 (m, 1H), 2.94 – 2.90 (m, 1H), 2.81 – 2.77 (m, 2H), 2.16 – 2.12 (m, 1H), 1.86 -1.82 (m, 1H), 1.28 (t, *J* = 8.1 Hz, 3H); ESI MS: m/z = 382.3 (M + 1 H)$^+$; Anal. calcd for C$_{22}$H$_{27}$N$_3$O$_3$ C, 69.27; H, 7.13; N, 11.02; found C, 69.24; H, 7.11; N, 11.04.

2-(4-(3-Methylbenzoyl)-1,4-diazepan-1-yl)-*N*-phenylacetamide (RM-16)

Semi solid**,** hygroscopic; Yield: 66 %; FT-IR: (KBr, cm^{-1}) 3303 (N-H stretch), 2938 (aromatic, C-H stretch), 2352, 1691 (keto, C=O stretch), 1628 (amide, C=O stretch), 1414 (CH$_2$ bend), 1303, 1280; ^{1}H NMR (400 MHz, CDCl$_3$) *δ*: 9.10 (s, 1H), 7.62 (d, *J* = 7.7 Hz, 1H), 7.52 (t, *J* =

7.9 Hz, 1H), 7.43 - 7.39 (m, 4H), 7.23 – 7.19 (m, 2H), 7.08 – 7.04 (m, J = 7.3 Hz, 1H), 3.92 – 3.88 (m, 2H), 3.67 – 3.63 (m, 2H), 3.31 (s, 1H), 3.20 (s, 1H), 3.14 -3.10 (m, 1H), 2.80 – 2.76 (m, 3H), 2.33 (s, 3H), 2.07 – 2.03 (m, 1H), 1.81 – 1.77 (m, 1H); ESI MS: m/z = 352.2 (M + 1 H)$^+$; Anal. calcd for $C_{21}H_{25}N_3O_2$ C, 71.77; H, 7.17; N, 11.96; found C, 71.76; H, 7.18; N, 11.95.

2-(4-(4-Methylbenzoyl)-1,4-diazepan-1-yl)-*N*-phenylacetamide (RM-17)

Semi solid, hygroscopic; Yield: 81 %; FT-IR: (cm-1) 3330 (N-H stretch), 2955 (aromatic, C-H stretch), 2922, 2785, 1690 (keto, C=O stretch), 1630 (amide, C=O stretch), 1416 (CH$_2$ bend), 1386, 1282, 1252; ^{1}H NMR (400 MHz, CDCl$_3$) $δ$: 9.11 (s, 1H), 7.62 (d, J = 7.7 Hz, 1H), 7.52 (d, J = 7.7 Hz, 1H), 7.34 – 7.30 (m, 4H), 7.23 – 7.19 (m, 2H), 7.11 (t, J = 7.3 Hz, 1H), 3.87 – 3.79 (m, 2H), 3.55 (dd, J = 14.2, 7.9 Hz, 2H), 3.34 (s, 1H), 3.26 (s, 1H), 3.04 – 3.00 (m, 1H), 2.85 – 2.81 (m, 3H), 2.07 – 2.03 (m, 1H), 2.38 (s, 3H), 1.89 – 1.81 (m, 1H); ESI MS: m/z = 352.2 (M + 1 H)$^+$; Anal. calcd for $C_{21}H_{25}N_3O_2$ C, 71.77; H, 7.17; N, 11.96; found C, 71.76; H, 7.18; N, 11.95.

2-(4-(2-Methylbenzoyl)-1,4-diazepan-1-yl)-*N*-phenylacetamide (RM-18)

Semi solid, hygroscopic; Yield: 62 %; FT-IR: (KBr, cm^{-1}) 3272 (N-H stretch), 2936 (aromatic, C-H stretch), 2918, 2825, 1691 (keto, C=O stretch), 1631 (amide, C=O stretch), 1502 (CH$_2$ bend),1300, 1282, 1244, 1159; ^{1}H NMR (400 MHz, CDCl$_3$) $δ$: 9.10 (s, 1H), 7.64 – 7.60 (m, 1H), 7.55 – 7.51 (m, 1H), 7.34 – 7.30 (m, 3H), 7.24 – 7.16 (m, 3H), 7.14 – 7.10 (m, 1H), 3.94 - 3.90 (m, 2H), 3.39 – 3.35 (m, 4H), 3.06 (s, 1H), 2.90 – 2.84 (m, 2H), 2.75 (s, 1H), 2.34 (s, 3H), 2.09 – 2.05 (m, 1H), 1.86 – 1.82 (m, 1H); ESI MS: m/z = 352.2 (M + 1 H)$^+$; Anal. calcd for $C_{21}H_{25}N_3O_2$ C, 71.77; H, 7.17; N, 11.96; found C, 71.76; H, 7.18; N, 11.95

.
2-(4-(4-Ethylbenzoyl)-1,4-diazepan-1-yl)-*N*-phenylacetamide (RM-19)

Semi solid, hygroscopic; Yield: 70 %; FT-IR: (KBr, cm^{-1}) 3259 (N-H stretch), 3201 (aromatic, C-H stretch), 2978, 2843, 1691 (keto, C=O stretch), 1629 (amide, C=O stretch), 1420 (CH$_2$ bend), 1327, 1273, 1165, 1141; ^{1}H NMR (400 MHz, DMSO d_6) $δ$: 10.98 (s, 1H), 7.79 (s, 1H), 7.68 (d, J = 7.9 Hz, 2H), 7.40 – 7.36 (m, 2H), 7.30 – 7.26 (m, 3H), 7.11 (t, J = 7.9 Hz, 1H), 4.35 – 4.31 (m, 2H), 3.87 – 3.83 (m, 1H), 3.61 – 3.57 (m, 4H), 3.26 (s, 2H), 2.68 (q, J = 7.6 Hz, 2H), 2.60 – 2.56 (m, 2H), 2.50 – 2.46 (m, 1H), 1.25 (t, J = 7.6 Hz, 3H); ESI MS: m/z = m/z 366.2 (M + 1 H)$^+$; Anal. calcd for $C_{22}H_{27}N_3O_2$ C, 72.30; H, 7.45; N, 11.50; found C, 72.31; H, 7.42; N, 11.51.

2-(4-(3-Ethylbenzoyl)-1,4-diazepan-1-yl)-*N*-phenylacetamide (RM-20)

Semi solid, hygroscopic; Yield: 79 %; FT-IR: (KBr, cm^{-1}) 3256 (N-H stretch), 3197 (aromatic, C-H stretch), 2988, 2843, 1692 (keto, C=O stretch), 1630 (amide, C=O stretch), 1420 (CH$_2$ bend), 1327, 1273, 1165, 1141; ^{1}H NMR (400 MHz, DMSO d_6) δ: 10.78 (s, 1H), 7.80 (s, 1H), 7.66 (d, J = 7.9 Hz, 2H), 7.40 – 7.36 (m, 2H), 7.32 – 7.28 (m, 3H), 7.21 (t, J = 7.9 Hz, 1H), 4.34 - 4.26 (m, 2H), 3.77 – 3.73 (m, 1H), 3.59 – 3.55 (m, 4H), 3.46 (s, 2H), 2.66 (q, J = 7.6 Hz, 2H), 2.62 – 2.54 (m, 3H),1.95 (t, J = 7.6 Hz, 3H); ESI MS: m/z = 366.2 (M + 1 H)$^+$; Anal. calcd for C$_{22}$H$_{27}$N$_3$O$_2$ C, 72.30; H, 7.45; N, 11.50; found C, 72.31; H, 7.42; N, 11.51.

4.3.2. Series-II: Synthesis of 1-(4-(substituted)piperazin-1-yl)-2-(phenylamino)ethanone derivatives (RMS-1 to 20)

Synthesis of *N*-Boc-piperazine (RMI-4)

In a 250 ml round bottom flask, compound **2** (10g, 116.1 mmol) was dissolved in methanol (100 mL). To this, water (2 mL) and trifluoroacetic acid (8.9 mL, 116.1 mmol) diluted in methanol (15 mL) were added at 0-5°C and the reaction mixture was stirred for 30 min at room temperature. To the above solution di-tert-butyldicarbonate (58.6 mL, 116.1 mmol) was added followed by iodine (10 mol %). The reaction mixture was again stirred at room temperature for 3 h. Upon completion of the reaction, solvent was removed under vacuum. To the obtained residue, 5 % sodium thiosulphate solution (15 mL) was added and extracted with ethyl acetate (2 x 50mL), dried over magnesium sulfate and concentrated under vacuum. The obtained crude compound was purified by column chromatography and pure product obtained as a colorless liquid **RMI-4**. Yield 50%, FT-IR: (KBr, cm^{-1}) 1722 (COO stretch), 1256, 1198, 1011; ^{1}H NMR (400 MHz, DMSO-d_6) δ: 3.26 – 3.18 (m, 4H), 2.63 – 2.59 (m, 4H), 1.38 (s, 9H).

Synthesis of 2-*tert*-butyl 4-(2-chloroacetyl) piperazine-1-carboxylate (RMI-5)

To a solution of **RMI-4** (4 g, 21.4 mmol), di-isopropylethylamine (4.3 mL, 32.2 mmol) in anhydrous DCM (200 mL) were taken in a round bottom flask (500 mL) at 0°C. To this reaction mixture, chloroacetyl chloride (1.7 mL, 21.4 mmol) was added. The reaction mixture was stirred at room temperature for 30 min; quenched with saturated sodium hydrogen carbonate (10 mL) and washed with water (2 x 50mL). Solvent was concentrated under vacuum, and the resultant residue was recrystallized from ethanol to afford the desired compound **RMI-5** as a white solid. Yield 70 %, FT-IR: (KBr, cm^{-1}) 1709 (COO stretch), 1271, 1081; 751 (C-Cl stretch); ^{1}H NMR (400 MHz, DMSO d_6) δ: 4.39 (s, 2H), 3.46 – 3.42 (m, 4H), 3.32 (s, 4H), 1.40 (s, 9H).

Synthesis of *tert*-butyl 4-(2-(phenylamino)acetyl)piperazine-1-carboxylate (RMI-6)

To a solution of compound **RMI-5** (2.5 g, 9.5 mmol), in anhydrous acetonitrile (25 mL), K$_2$CO$_3$ (3.9 g, 28.6 mmol), and aniline (0.95 ml, 10.3 mmol) were added. The reaction was refluxed for 3 h at 100°C; completion of the reaction was confirmed by TLC. Solvent was removed under vacuum and organic compound was extracted with chloroform (2 x 25 mL). The combined organic extracts were dried over magnesium sulphate and evaporated to get crude compound, which was purified by column chromatography and obtained as a

colourless liquid **RMI-6**. Yield 65 %, FT-IR: (KBr, cm⁻¹) 3215 (N-H stretch), 3135 (aromatic, C-H stretch), 1728 (COO stretch), 1660 (amide, C=O stretch), 1259, 1011; ¹H NMR (400 MHz, DMSO d_6) *δ*: 7.09 – 7.05 (m, 2H), 6.59 – 6.55 (m, 2H), 6.46 (d, *J* =6 Hz, 1H), 4.12 (s, 2H), 3.67 – 3.63 (m, 4H), 3.14 – 3.10 (m, 4H), 1.42 (s, 9H).

Synthesis of 2-(phenylamino)-1-(piperazin-1-yl)ethanone (RMI-7)

To a solution of **RMI-6** (1 g, 3.5 mmol) in anhydrous DCM (20 mL) in a round bottom flask at 0°C, trifluoroacetic acid (1.94 mL, 17.7 mmol) was added and stirred the reaction for 7 h at room temperature. Completion of the reaction was confirmed by TLC. After completion of the reaction, the solvent was removed under vacuum. To the resultant crude, saturated solution of sodium bicarbonate (10 mL) was added and extracted with ethyl acetate (2 x 50 mL). Ethyl acetate portion was evaporated to obtain the free amine **RMI-7** as white solid. Yield 70 %, FT-IR: (KBr, cm⁻¹) 3342 (N-H stretch), 3253 (aromatic, C-H stretch), 1649 (amide, C=O stretch), 1178, 1056; ¹H NMR (400 MHz, DMSO d_6) *δ*: 8.53 (brs, IH), 7.09 – 7.05 (m, 2H), 6.59 – 6.55 (m, 2H), 6.46 (d, *J* =6 Hz, 1H), 5.55 (d, *J* =4.0 Hz, 1H), 3.93 (s, 2H), 3.67 – 3.63 (m, 4H), 3.14 – 3.10 (m, 4H).

General procedure for the synthesis of 1-(4-(substituted)piperazin-1-yl)-2-(phenylamino)ethanone derivatives (RMS 1 to 20)

To an appropriate quantity of carboxylic acid (1 g), TEA (2.4 equiv), EDC·HCl (1.5 equiv), and HOBt (0.8 equiv) in anhydrous DCM were stirred for 5 min at 0° C, followed by addition of compound **RMI-7** (1.1 equiv). The mixture was stirred for 6 h at room temperature, after completion of the reaction; solvents removed under reduced pressure. The crude was dissolved in dichlromethane, washed with brine solution (10 mL) and dried over anhydrous sodium sulphate, which were evaporated under reduced pressure. The desired compound was obtained after purification by column chromatography.

1-(4-Benzoylpiperazin-1-yl)-2-(phenylamino)ethanone (RMS-1)

Brown solid, Yield: 58 %; mp: 141-143°C; FT-IR: (KBr, cm⁻¹) 3328 (N-H stretch), 3082 (aromatic, C-H stretch), 1753 (keto, C=O stretch), 1658 (amide, C=O stretch), 1598 (CH₂ bend), 1438, 1323, 1300; ¹H NMR (400 MHz, CDCl₃) *δ*: 7.41 – 7.37 (m, 2H), 7.36 – 7.32 (m, 3H), 7.13 (t, *J* = 7.8 Hz, 2H), 6.67 (t, *J* = 5.2 Hz, 1H), 6.56 (d, *J* = 7.6 Hz, 2H), 3.85 (s, 2H), 3.64 (s, 4H), 3.45 – 3.37 (m, 4H); ESI MS: m/z = 324.1 (M + 1 H)⁺ ; Anal. calcd for C₁₉H₂₁N₃O₂ C, 70.57; H, 6.55; N, 12.99; found C, 70.52; H, 6.49; N, 12.95.

1-(4-(2-Fluorobenzoyl)piperazin-1-yl)-2-(phenylamino)ethanone (RMS-2)

White solid, Yield: 69 %; mp: 146-148°C; FT-IR: (KBr, cm^{-1}) 3363 (N-H stretch), 3064 (aromatic, C-H stretch), 1740 (keto, C=O stretch), 1658 (amide, C=O stretch), 1598 (CH$_2$ bend), 1205, 1093, 1033; ^{1}H NMR (400 MHz, CDCl$_3$) *δ*: 7.49 – 7.45 (m, 2H), 7.26 – 7.22 (m, 3H), 7.15 (t, *J* = 8.6 Hz, 1H), 6.80 – 6.74 (m, 1H), 6.64 – 6.60 (m, 2H), 3.98 (s, 2H), 3.92 – 3.88 (m, 4H), 3.57 – 3.53 (m, 4H); ESI MS: m/z = 342.1 (M + 1 H)$^+$; Anal. calcd for C$_{19}$H$_{20}$FN$_3$O$_2$ C, 66.85; H, 5.91; N, 12.31; found C, 66.82; H, 5.85; N, 12.35.

1-(4-(4-Fluorobenzoyl)piperazin-1-yl)-2-(phenylamino)ethanone (RMS-3)

Yellow solid, Yield: 54 %; mp: 127-129°C; FT-IR: (KBr, cm^{-1}) 3285 (N-H stretch), 2942 (aromatic, C-H stretch), 2701, 1682 (keto, C=O stretch), 1670 (amide, C=O stretch), 1483 (CH$_2$ bend), 1433, 1301, 1282; ^{1}H NMR (400 MHz, CDCl$_3$) *δ*: 7.47 – 7.41 (m, 2H), 7.22 (t, *J* = 7.8 Hz, 2H), 7.16 – 7.12 (m, 2H), 6.76 (t, *J* = 7.2 Hz, 1H), 6.65 (d, *J* = 7.8 Hz, 2H), 3.94 (s, 2H), 3.77 – 3.69 (m, 5H), 3.58 – 3.52 (m, 3H); ESI MS: m/z = 342.1 (M + 1 H)$^+$; Anal. calcd for C$_{19}$H$_{20}$FN$_3$O$_2$ C, 66.85; H, 5.91; N, 12.31; found C, 66.77; H, 5.94; N, 12.34.

1-(4-(4-Chlorobenzoyl)piperazin-1-yl)-2-(phenylamino)ethanone (RMS-4)

Brown solid, Yield: 65 %; mp: 134-136°C; FT-IR: (KBr, cm^{-1}) 3346 (N-H stretch), 3084 (aromatic, C-H stretch), 1921, 1745 (keto, C=O stretch), 1656 (amide, C=O stretch), 1598 (CH$_2$ bend), 1327, 1014; ^{1}H NMR (400 MHz, CDCl$_3$) *δ*: 7.45 – 7.41 (m, 4H), 7.23 (t, *J* = 7.4 Hz, 2H), 6.78 (t, *J* = 7.6 Hz, 1H), 6.67 (d, *J* = 4.0 Hz, 2H), 3.95 (s, 2H), 3.77 - 3.69 (m, 1H), 3.53 – 3.47 (m, 7H); ESI MS: m/z = 357.2 (M)$^+$ and 358.2 (M + 1 H)$^+$.Anal. calcd for C$_{19}$H$_{20}$ClN$_3$O$_2$ C, 63.77; H, 5.63; N, 11.74; found C, 63.78; H, 5.64; N, 11.71.

2-(Phenylamino)-1-(4-(4-(trifluoromethyl)benzoyl)piperazin-1-yl)ethanone (RMS-5)

White solid, Yield: 61 %; mp: 130-132°C; FT-IR: (KBr, cm^{-1}) 3296 (N-H stretch), 3057 (aromatic, C-H stretch), 2360, 1690 (keto, C=O stretch), 1658 (amide, C=O stretch), 1502 (CH$_2$ bend), 1444, 1415; ^{1}H NMR (400 MHz, CDCl$_3$) *δ*: 7.75 (d, *J* = 8.0 Hz, 2H), 7.59 – 7.55 (m, 2H), 7.23 (t, *J* = 8.0 Hz, 2H), 6.78 (t, *J* = 7.2 Hz, 1H), 6.70 – 6.66 (m, 2H), 3.96 (s, 2H), 3.73- 3.69 (m, 4H), 3.55 – 3.47 (m, 4H); ESI MS: m/z = 392.1 (M + 1 H)$^+$; Anal. calcd for C$_{20}$H$_{20}$F$_3$N$_3$O$_2$ C, 61.38; H, 5.15; N, 10.74; found C, 61.37; H, 5.14; N, 10.71.

1-(4-(2-Methylbenzoyl)piperazin-1-yl)-2-(phenylamino)ethanone (RMS-6)

Off white solid, Yield: 56 %; mp: 132-134°C; FT-IR: (KBr, cm^{-1}) 3381 (N-H stretch), 3122 (aromatic, C-H stretch), 3061, 1740 (keto, C=O stretch), 1656 (amide, C=O stretch), 1597 (CH$_2$ bend), 1323, 920; ^{1}H NMR (400 MHz, CDCl$_3$) *δ*: 7.27 – 7.23 (m, 1H), 7.20 – 7.14 (m, 3H), 7.13 (t, *J* = 7.8 Hz, 2H), 6.71 – 6.67 (m, 1H), 6.59 – 6.55 (m, 2H), 3.89 (s, 2H), 3.80-3.76 (m, 2H), 3.34 – 3.30 (m, 6H), 2.17 (s, 3H); ESI MS: m/z = 338.2 (M + 1 H)$^+$; Anal. calcd for C$_{20}$H$_{23}$N$_3$O$_2$ C, 71.19; H, 6.87; N, 12.45; found C, 71.15; H, 6.81; N, 12.44.

1-(4-(3-Methylbenzoyl)piperazin-1-yl)-2-(phenylamino)ethanone (RMS-7)

White solid, Yield: 76 %; mp: 118-120°C; FT-IR: (KBr, cm^{-1}) 3311(N-H stretch), 2937 (aromatic, C-H stretch), 2353, 1690 (keto, C=O stretch), 1629 (amide, C=O stretch), 1414 (CH$_2$ bend), 1303, 1280; ^{1}H NMR (400 MHz, CDCl$_3$) *δ*: 7.21 – 7.15 (m, 6H), 6.68 (t, *J* = 7.3 Hz, 1H), 6.57 (d, *J* = 7.8 Hz, 2H), 3.85 (s, 2H), 3.64 – 3.60 (m, 4H), 3.42 – 3.38 (m, 4H), 2.32 (s, 3H); ESI MS: m/z = 338.1 (M + 1 H)$^+$; Anal. calcd for C$_{20}$H$_{23}$N$_3$O$_2$ C, 71.19; H, 6.87; N, 12.45; found C, 71.15; H, 6.81; N, 12.44.

1-(4-(4-Methylbenzoyl)piperazin-1-yl)-2-(phenylamino)ethanone (RMS-8)

Brown solid, Yield: 81%; mp: 142-144°C; FT-IR: (KBr, cm^{-1}) 3346 (N-H stretch), 3061 (aromatic, C-H stretch), 1940, 1746 (keto, C=O stretch), 1651 (amide, C=O stretch), 1597 (CH$_2$ bend), 1438, 1319; ^{1}H NMR (400 MHz, CDCl$_3$) *δ*: 7.27 – 7.23 (m, 2H), 7.17 – 7.15 (m, 2H), 7.14 – 7.10 (m, 2H), 6.68 (t, *J* = 5.2 Hz, 1H), 6.57 (d, *J* = 8.0 Hz, 2H), 3.85 (s, 2H), 3.65 – 3.61 (m, 4H), 3.44 – 3.40 (m, 4H), 2.33 (s, 3H); ESI MS: m/z = 338.1 (M + 1 H)$^+$; Anal. calcd for C$_{20}$H$_{23}$N$_3$O$_2$ C, 71.19; H, 6.87; N, 12.45; found C, 71.15; H, 6.81; N, 12.44.

1-(4-(2-Methoxybenzoyl)piperazin-1-yl)-2-(phenylamino)ethanone (RMS-9)

White solid, Yield: 71 %; mp: 139-141°C; FT-IR: (KBr, cm^{-1}) 3323 (N-H stretch), 2945 (aromatic, C-H stretch), 1740 (keto, C=O stretch), 1649 (amide, C=O stretch), 1597 (CH$_2$ bend), 1249, 1028; ^{1}H NMR (400 MHz, CDCl$_3$) *δ*: 7.41 (t, *J* = 7.4 Hz, 1H), 7.25 – 7.19 (m, 3H), 7.04 (t, *J* = 7.4 Hz, 1H), 6.94 (d, *J* = 8.0 Hz, 1H), 6.76 – 6.72 (m, 1H), 6.66 – 6.62 (m, 2H), 3.97 (s, 2H), 3.86 (s, 3H), 3.66 – 3.62 (m, 4H), 3.36 – 3.32 (m, 4H); MS ESI MS: m/z = 354.1 (M + 1 H)$^+$; Anal. calcd for C$_{20}$H$_{23}$N$_3$O$_3$ C, 67.97; H, 6.56; N, 11.89; found C, 67.92; H, 6.54; N, 11.84.

1-(4-(3-Methoxybenzoyl)piperazin-1-yl)-2-(phenylamino)ethanone (RMS-10)

White solid, Yield: 62 %; mp: 122-124°C; FT-IR: (KBr, cm^{-1}) 3321 (N-H stretch), 3284 (aromatic, C-H stretch), 2833, 2376, 1740 (keto, C=O stretch), 1645 (amide, C=O stretch), 1597 (CH$_2$ bend), 1435, 1319; ^{1}H NMR (400 MHz, CDCl3) *δ*: 7.27 (t, *J* = 8.0 Hz, 1H), 7.15 – 7.11 (m, 2H), 6.90 – 6.86 (m, 3H), 6.67 (t, *J* = 7.2 Hz, 1H), 6.56 (d, *J* = 8.0 Hz, 2H), 3.85 (s, 2H), 3.76 (s, 3H), 3.72 – 3.68 (m, 4H), 3.47 – 3.43 (m, 4H); ESI MS: m/z = 354.1 (M + 1 H)$^+$; Anal. calcd for C$_{20}$H$_{23}$N$_3$O$_3$ C, 67.97; H, 6.56; N, 11.89; found C, 67.98; H, 6.54; N, 11.81.

1-(4-(4-Methoxybenzoyl)piperazin-1-yl)-2-(phenylamino)ethanone (RMS-11)

White solid, Yield: 66 %; mp: 130-132°C; FT-IR: (KBr, cm^{-1}) 3340 (N-H stretch), 3051 (aromatic, C-H stretch), 2351, 1748 (keto, C=O stretch), 1651 (amide, C=O stretch), 1597 (CH$_2$ bend), 1435, 1325, 1182; ^{1}H NMR (400 MHz, CDCl$_3$) *δ*: 7.43 (m, 2H), 7.25 – 7.21 (m, 2H), 6.99 – 6.93 (m, 2H), 6.77 (t, *J* = 7.4 Hz, 1H), 6.66 (d, *J* = 3.6 Hz, 2H), 3.95 (s, 2H), 3.87 (s, 3H), 3.75 – 3.71 (m, 4H), 3.68 - 3.64 (m, 2H), 3.57 – 3.51 (m, 2H); ESI MS: m/z = 354.2 (M + 1 H)$^+$; Anal. calcd for C$_{20}$H$_{23}$N$_3$O$_3$ C, 67.97; H, 6.56; N, 11.89; found C, 67.98; H, 6.53; N, 11.84.

1-(4-(2-Ethylbenzoyl)piperazin-1-yl)-2-(phenylamino)ethanone (RMS-12)

Yellow solid, Yield: 72 %; mp: 130-132°C; FT-IR: (KBr, cm^{-1}) 3256 (N-H stretch), 3196 (aromatic, C-H stretch), 2997, 2843, 1691 (keto, C=O stretch), 1628 (amide, C=O stretch), 1420 (CH$_2$ bend), 1327, 1273, 1165, 1141; ^{1}H NMR (400 MHz, CDCl$_3$) *δ*: 7.41 – 7.37 (m, 1H), 7.36 – 7.32 (m, 1H), 7.24 – 7.20 (m, 2H), 7.13 (d, *J* = 7.4 Hz, 1H), 6.94 (t, *J* = 8.2 Hz, 1H), 6.72 - 6.64 (m, 3H), 3.90 (s, 2H), 3.80 – 3.76 (m, 4H), 3.62 – 3.58 (m, 2H), 3.55 – 3.49 (m, 2H), 2.79 (q, *J* = 7.6 Hz, 2H), 1.24 (t, *J* = 7.6 Hz, 3H); ESI MS: m/z = 352.3 (M + 1 H)$^+$; Anal. calcd for C$_{21}$H$_{25}$N$_3$O$_2$ C, 71.77; H, 7.17; N, 11.96; found C, 71.78; H, 7.11; N, 11.91.

1-(4-(3-Ethylbenzoyl)piperazin-1-yl)-2-(phenylamino)ethanone (RMS-13)

Off white solid, Yield: 73 %; mp: 116-118°C; FT-IR: (KBr, cm^{-1}) 3255 (N-H stretch), 3195 (aromatic, C-H stretch), 2988, 2843, 1692 (keto, C=O stretch), 1628 (amide, C=O stretch), 1420 (CH$_2$ bend), 1327, 1271, 1165, 1141; ^{1}H NMR (400 MHz, CDCl$_3$) *δ*: 7.27 (t, *J* = 8.0 Hz, 1H), 7.13 (d, *J* = 7.2 Hz, 1H), 6.90 – 6.86 (m, 4H), 6.69 – 6.65 (m, 1H), 6.56 (d, *J* = 8.0 Hz, 2H), 3.84 (s, 2H), 3.70 – 3.66 (m, 4H), 3.57 – 3.53 (m, 4H), 2.78 (q, *J* = 7.6 Hz 2H), 1.28 (t, *J*

= 7.6 Hz, 3H); ESI MS: m/z = 352.3 (M + 1 H)$^+$; Anal. calcd for $C_{21}H_{25}N_3O_2$ C, 71.77; H, 7.17; N, 11.96; found C, 71.77; H, 7.20; N, 11.94.

1-(4-(4-Ethylbenzoyl)piperazin-1-yl)-2-(phenylamino)ethanone (RMS-14)

Off white solid, Yield: 75 %; mp: 144-146°C; FT-IR: (KBr, cm^{-1}) 3319 (N-H stretch), 2964 (aromatic, C-H stretch), 2362, 1740 (keto, C=O stretch), 1649 (amide, C=O stretch), 1598 (CH$_2$ bend), 1531, 1435, 1325; ^{1}H NMR (400 MHz, CDCl$_3$) δ: 7.37 (d, *J* = 7.8 Hz, 2H), 7.31 – 7.25 (m, 2H), 7.22 (t, *J* = 7.8 Hz 2H), 6.76 (t, *J* = 7.4 Hz, 1H), 6.65 (d, *J* = 7.6 Hz, 2H), 3.94 (s, 2H), 3.74 – 3.70 (m, 4H), 3.55 – 3.51 (m, 4H), 2.71 (q, *J* = 7.6 Hz 2H), 1.28 (t, *J* = 7.6 Hz, 3H); ESI MS: m/z = 352.3 (M + 1 H)$^+$; Anal. calcd for $C_{21}H_{25}N_3O_2$ C, 71.77; H, 7.17; N, 11.96; found C, 71.78; H, 7.19; N, 11.94.

1-(4-(2-Ethoxybenzoyl)piperazin-1-yl)-2-(phenylamino)ethanone (RMS-15)

Brown solid, Yield: 62 %; mp: 124-126°C; FT-IR: (Cm-1) 3261 (N-H stretch), 3187 (aromatic, C-H stretch), 2981, 1697 (keto, C=O stretch), 1640 (amide, C=O stretch), 1598, 1546, 1421 (CH$_2$ bend), 1327, 1273, 1165, 1141, 1118, 1043, 1006, 935, 794, 694; ^{1}H NMR (400 MHz, CDCl$_3$) δ: 7.41 – 7.37 (m, 1H), 7.32 – 7.28 (m, 1H), 7.26 – 7.22 (m, 2H), 7.03 (t, *J* = 7.4 Hz, 1H), 6.94 (d, *J* = 8.2 Hz, 1H), 6.81 – 6.77 (m, 1H), 6.71 – 6.63 (m, 2H), 4.10 (q, *J* = 7.4 Hz, 2H), 3.98 (s, 2H), 3.93 – 3.87 (m, 1H), 3.73 – 3.69 (m, 2H), 3.60 – 3.56 (m, 2H), 3.44 – 3.40 (m, 2H), 3.31 – 3.25 (m, 1H), 1.41 (t, *J*= 7.4 Hz, 3H); ESI MS: m/z = 368.1 (M + 1 H)$^+$; Anal. calcd for $C_{21}H_{25}N_3O_3$ C, 68.64; H, 6.86; N, 11.44; found C, 68.62; H, 6.84; N, 11.40.

1-(4-(3-Ethoxybenzoyl)piperazin-1-yl)-2-(phenylamino)ethanone (RMS-16)

Off white solid, Yield: 67 %; mp: 120-122°C; FT-IR: (KBr, cm^{-1}) 3066 (N-H stretch), 2981 (aromatic, C-H stretch), 1745 (keto, C=O stretch), 1651 (amide, C=O stretch), 1597 (CH$_2$ bend), 1519, 1444, 1323; ^{1}H NMR (400 MHz, CDCl$_3$) δ: 7.28 – 7.24 (m, 1H), 7.15 – 7.11 (m, 2H), 6.93 - 6.87 (m, 2H), 6.84 – 6.80 (m, 1H), 6.67 (t, *J* = 5.4 Hz, 1H), 6.56 (d, *J* = 8.0 Hz, 2H), 3.98 (q, *J* = 7.0 Hz, 2H), 3.85 (s, 2H), 3.64 – 3.60 (m, 2H), 3.44 – 3.38 (m, 6H), 1.36 (t, *J* = 7.0 Hz, 3H); ESI MS: m/z = 368.2 (M + 1 H)$^+$; Anal. calcd for $C_{21}H_{25}N_3O_3$ C, 68.64; H, 6.86; N, 11.44; found C, 68.61; H, 6.84; N, 11.41.

1-(4-(4-Ethoxybenzoyl)piperazin-1-yl)-2-(phenylamino)ethanone (RMS-17)

Off white solid, Yield: 58 %; mp: 122-124°C; FT-IR: (KBr, cm^{-1}) 3273 (N-H stretch), 3187 (aromatic, C-H stretch), 2835, 2358, 1690 (keto, C=O stretch), 1639 (amide, C=O stretch),

1411 (CH$_2$ bend), 1327, 1273, 1165; ^{1}H NMR (400 MHz, CDCl$_3$) δ: 7.43 – 7.39 (m, 2H), 7.25 – 7.21 (m, 2H), 6.97 – 6.93 (m, 2H), 6.78 (t, *J* = 7.4 Hz, 1H), 6.68 (d, *J* = 7.6 Hz, 2H), 4.10 (q, *J* = 6.8 Hz, 2H), 3.95 (s, 2H), 3.75 - .371 (m, 2H), 3.68 – 3.64 (m, 2H), 3.52 – 3.48 (m, 4H), 1.46 (t, *J* = 6.8 Hz, 3H); ESI MS: m/z = 368.1 (M + 1 H)$^+$; Anal. calcd for C$_{21}$H$_{25}$N$_3$O$_3$ C, 68.64; H, 6.86; N, 11.44; found C, 68.63; H, 6.84; N, 11.43.

1-(4-(2-Chlorobenzoyl)piperazin-1-yl)-2-(phenylamino)ethanone (RMS-18)

Brown solid, Yield: 61 %; mp: 124-126°C; FT-IR: (KBr, cm^{-1}) 3340 (N-H stretch), 3081 (aromatic, C-H stretch), 1917, 1745 (keto, C=O stretch), 1651 (amide, C=O stretch), 1598 (CH$_2$ bend), 1327, 1014; ^{1}H NMR (400 MHz, CDCl$_3$) δ: 7.49 – 7.43 (m, 4H), 7.21 (d, *J* = 7.4 Hz, 2H), 6.77 (d, *J* = 7.6 Hz, 1H), 6.69 – 6.65 (m, 2H), 3.84 (s, 2H), 3.73 – 3.69 (m, 1H), 3.54 – 3.50 (m, 7H); MS (ESI): m/z 357.2 (M)$^+$ and 358.2 (M + 1 H)$^+$; Anal. calcd for C$_{19}$H$_{20}$ClN$_3$O$_2$ C, 63.77; H, 5.63; N, 11.74; found C, 63.78; H, 5.64; N, 11.71.
.

1-(4-(3-Chlorobenzoyl)piperazin-1-yl)-2-(phenylamino)ethanone (RMS-19)

Brown solid, Yield: 62 %; mp: 140-142°C; IR: (KBr, cm^{-1}) 3309 (N-H stretch), 3061 (aromatic, C-H stretch), 2940, 1688 (keto, C=O stretch), 1664 (amide, C=O stretch), 1596 (CH$_2$ bend), 1329, 1273, 1236, 1141; ^{1}H NMR (400 MHz, CDCl$_3$) δ: 7.45 – 7.41 (m, 4H), 7.25 – 7.21 (m, 2H), 6.78 (t, *J* = 7.6 Hz, 1H), 6.69 – 6.65 (m, 2H), 3.94 (s, 2H), 3.81 – 3.75 (m, 4H), 3.53 – 3.49 (m, 4H); ESI MS: m/z = 357.2 (M)$^+$ and 358.2 (M +1 H)$^+$; Anal. calcd for C$_{19}$H$_{20}$ClN$_3$O$_2$ C, 63.77; H, 5.63; N, 11.74; found C, 63.78; H, 5.64; N, 11.71.

1-(4-(3-Fluorobenzoyl)piperazin-1-yl)-2-(phenylamino)ethanone (RMS-20)

Yellow solid, Yield: 62 %; mp: 148-150°C; FT-IR: (KBr, cm^{-1}) 3302 (N-H stretch), 3002 (aromatic, C-H stretch), 2768, 1690 (keto, C=O stretch), 1632 (amide, C=O stretch), 1522 (CH$_2$ bend), 1301, 1249, 1172; ^{1}H NMR (400 MHz, CDCl$_3$) δ: 7.50 – 7.46 (m, 2H), 7.21 (t, *J* = 7.8 Hz, 2H), 7.17 – 7.13 (m, 2H), 6.76 (t, *J* = 7.2 Hz, 1H), 6.68 (d, *J* = 7.8 Hz, 2H), 3.91 (s, 2H), 3.72 – 3.68 (m, 5H), 3.53 – 3.49 (m, 3H); ESI MS: m/z = 342.1 (M +1 H)$^+$; Anal. calcd for C$_{19}$H$_{20}$FN$_3$O$_2$ C, 66.85; H, 5.91; N, 12.31; found C, 66.81; H, 5.90; N, 12.30.

4.3.3. Series-III: Synthesis of 2-(4-(substituted benzoyl)piperazin-1-yl)-*N*-phenylacetamide (RMT-1 to 20)

Synthesis of *tert*-butyl 4-(2-oxo-2-(phenylamino)ethyl)piperazine-1-carboxylate (RMI-8):

To a solution of compound **RMI-1** (1.0 g, 5.8 mmol), K_2CO_3 (4.0 g, 29.4 mmol), in anhydrous acetonitrile were stirred for 10 min at 90°C. To the above solution, *N*-Boc-piperazine (1.3 g, 7.0 mmol) was added, and refluxed for 4 h. Acetonitrile was removed under vacuum, and the reaction crude was diluted with ethyl acetate. The organic layer was then washed with water, dried over anhydrous sodium sulfate (Na_2SO_4) and evaporated under vacuum to get a crude mixture which was purified by column chromatography using chloroform and methanol to afford a pure compound **RMI-8** as a brown solid. Yield 78.2 %, FT-IR: (KBr, cm^{-1}) 3205 (N-H stretch), 3089 (aromatic, C-H stretch), 1711 (COO stretch), 1652 (amide, C=O stretch) 1256, 1082; ^{1}H NMR (400 MHz, CDCl$_3$) *δ*: 8.96 (s, 1H), 7.70 (d, *J* = 8.0 Hz, 2H), 7.36 (t, *J* = 8.0 Hz, 2H), 7.21 (t, *J* = 8.0 Hz, 1H), 3.54 – 3.50 (m, 4H), 3.23 (s, 2H), 2.62 – 2.58 (m, 4H), 1.50 (s, 9H).

Synthesis of *N*-phenyl-2-(piperazin-1-yl)acetamide (RMI-9):

To a solution of **RMI-8** (1.0 g, 3.0 mmol) in anhydrous DCM (20 mL), in a round bottom flask at 0°C, trifluoroacetic acid (1.1 mL, 15.0 mmol) was added. The reaction mixture was stirred at room temperature for 16 h. Upon, completion of the reaction, solvent was removed under vacuum. To this, saturated solution of sodium bicarbonate was added (pH-7), and extracted with ethyl acetate. Ethyl acetate portion was evaporated to obtain the free amine **RMI-9** as a white solid. Yield 75 %, FT-IR: (KBr, cm^{-1}) 3235 (N-H stretch), 3159 (aromatic, C-H stretch), 1667 (amide, C=O stretch) 1215, 1048; ^{1}H NMR (400 MHz, DMSO *d*$_6$) *δ*: 9.49 (s, 1H), 7.55 (d, *J* = 7.8 Hz, 2H), 7.23 (t, *J* = 7.8 Hz, 2H), 7.01 (t, *J* = 7.4 Hz, 1H), 3.13 (s, 2H), 3.10 – 3.01 (m, 4H), 2.72 – 2.61 (m, 4H).

General procedure for the synthesis of 2-(4-(substituted benzoyl)piperazin-1-yl)-*N*-phenylacetamide derivatives RMT 1 to 20.

To an appropriate carboxylic acid (1g), DIPEA (2.4 equiv), EDC·HCl (1.5 equiv), and HOBt (0.8 equiv) in anhydrous DCM were stirred for 5 min at room temperature. Then the compound **RMI-9** (1.1 equiv) was added. The mixture was stirred for 6 h at room temperature and then solvents were removed under reduced pressure. The residue was dissolved in ethyl acetate, and the organic phase was washed with saturated sodium

bicarbonate (2 × 10 mL) and brine (10 mL). The organic layer was dried over magnesium sulfate and evaporated under reduced pressure, and the crude product was purified by column chromatography.

2-(4-Benzoylpiperazin-1-yl)-*N*-phenylacetamide (RMT-1)

Yellow solid, Yield: 58 %; mp: 122-124°C; FT-IR: (KBr, cm^{-1}) 3251 (N-H stretch), 3061 (aromatic, C-H stretch), 2819, 2698, 1664 (keto, C=O stretch), 1629 (amide, C=O stretch), 1502 (CH$_2$ bend), 1336, 1139, 1010; ^{1}H NMR (400 MHz, CDCl$_3$) *δ*: 9.75 (s, 1H), 7.62 (d, *J*= 7.6 Hz, 2H), 7.43 – 7.39 (m, 5H), 7.29 (t, *J* = 8.0 Hz, 2H), 7.15 (t, *J* = 8.0 Hz, 1H), 3.70 - 3.66 (m, 2H), 3.37 – 3.33 (m, 2H), 3.18 (s, 2H), 2.57 – 2.51 (m, 4H); ESI MS: m/z = 324.1 (M + 1 H)$^+$.

2-(4-(4-Methylbenzoyl)piperazin-1-yl)-*N*-phenylacetamide (RMT-2)

Brown solid, Yield: 56 %; mp: 142-144°C; FT-IR: (KBr, cm^{-1}) 3273 (N-H stretch), 2935 (aromatic, C-H stretch), 2918, 2825, 1691 (keto, C=O stretch), 1629 (amide, C=O stretch), 1502 (CH$_2$ bend),1300, 1282, 1244, 1159; ^{1}H NMR (400 MHz, CDCl$_3$) *δ*: 9.75 (s, 1H), 7.62 (d, *J*= 7.6 Hz, 2H), 7.29 – 7.25 (m, 6H), 7.05 (t, *J*= 7.2 Hz, 1H), 3.66 – 3.62 (m, 4H), 3.18 (s, 2H), 2.57 – 2.51 (m, 4H), 2.32 (s, 3H); ESI MS: m/z = 338.1 (M + 1 H)$^+$.

2-(4-(3-Chlorobenzoyl)piperazin-1-yl)-*N*-phenylacetamide (RMT-3)

White solid, Yield: 65 %; mp: 134-136°C; FT-IR: (KBr, cm^{-1}) 3287 (N-H stretch), 2940 (aromatic, C-H stretch), 2698, 1683 (keto, C=O stretch), 1668 (amide, C=O stretch), 1483 (CH$_2$ bend), 1433, 1301, 1282; ^{1}H NMR (400 MHz, CDCl$_3$) *δ*: 8.86 (s, 1H), 7.49 (d, *J* = 7.6 Hz, 2H), 7.36 – 7.32 (m, 2H), 7.30 – 7.26 (m, 3H), 7.24 – 7.20 (m, 1H), 7.06 (t, *J* = 7.6 Hz, 1H), 3.64 – 3.60 (m, 4H), 3.14 (s, 2H), 2.61 – 2.57 (m, 4H); ESI MS: m/z = 357.1 (M)$^+$ and m/z 358.1 (M + 1 H)$^+$.

2-(4-(2-Methylbenzoyl)piperazin-1-yl)-*N*-phenylacetamide (RMT-4)

Brown solid, Yield: 76 %; mp: 143-145°C; FT-IR: (Cm^{-1}) 3329 (N-H stretch), 2956 (aromatic, C-H stretch), 2922, 2785, 1690 (keto, C=O stretch), 1629 (amide, C=O stretch), 1414 (CH$_2$ bend), 1386, 1282, 1252; ^{1}H NMR (400 MHz, CDCl$_3$) *δ*: 8.94 (s, 1H), 7.58 - 7.54 (m, 2H), 7.33 – 7.29 (m, 3H), 7.24 – 7.20 (m, 2H), 7.16 – 7.12 (m, 2H), 3.96 – 3.88 (m, 2H), 3.37 – 3.33 (m, 2H), 3.19 (s, 2H), 2.75 – 2.71 (m, 2H), 2.56 – 2.50 (m, 2H), 2.33 (s, 3H); ESI MS: m/z = 338.1 (M + 1 H)$^+$.

2-(4-(3-Methylbenzoyl)piperazin-1-yl)-*N*-phenylacetamide (RMT-5)

Brown solid**,** Yield: 76 %; mp: 128-130°C; FT-IR: (KBr, cm^{-1}) 3301 (N-H stretch), 2939 (aromatic, C-H stretch), 2350, 1690 (keto, C=O stretch), 1629 (amide, C=O stretch), 1414 (CH$_2$ bend), 1303, 1280; ^{1}H NMR (400 MHz, CDCl$_3$) *δ*: 8.90 (s, 1H), 7.49 (d, *J* = 8.0 Hz, 2H), 7.27 – 7.23 (m, 3H), 7.19 – 7.15 (m, 2H), 7.11 – 7.05 (m, 2H), 3.65 – 3.61 (m, 4H), 3.13 (s, 2H), 2.60 – 2.56 (m, 4H), 2.31 (s, 3H); ESI MS: m/z = 338.1 (M + 1 H)$^+$.

2-(4-(4-Chlorobenzoyl)piperazin-1-yl)-*N*-phenylacetamide (RMT-6)

White solid, Yield: 65 %; mp: 136-138°C; FT-IR: (KBr, cm^{-1}) 3288 (N-H stretch), 2941 (aromatic, C-H stretch), 2350, 1685 (keto, C=O stretch), 1678 (amide, C=O stretch), 1483 (CH$_2$ bend), 1433, 1301, 1282; ^{1}H NMR (400 MHz, CDCl$_3$) *δ*: 8.92 (s, 1H), 7.55 (d, *J* = 8.0 Hz, 2H), 7.40 – 7.36 (m, 6H), 7.13 (t, *J* = 7.4 Hz, 1H), 3.72 – 3.66 (m, 4H), 3.20 (s, 2H), 2.68 – 2.64 (m, 4H); ESI MS: m/z = 357.1 (M)$^+$ and 358.1 (M + 1 H)$^+$.

2-(4-(2-Methoxybenzoyl)piperazin-1-yl)-*N*-phenylacetamide (RMT-7)

Yellow solid, Yield: 71 %; mp: 141-143°C; FT-IR: (KBr, cm^{-1}) 3307 (N-H stretch), 3061 (aromatic, C-H stretch), 2945, 1678 (keto, C=O stretch), 1664 (amide, C=O stretch), 1598 (CH$_2$ bend), 1427, 1365; ^{1}H NMR (400 MHz, CDCl$_3$) *δ*: 8.92 (s, 1H), 7.49 (d, *J* = 8.0 Hz, 2H), 7.28 – 7.24 (m, 2H), 7.18 (d, *J* = 8.0 Hz, 2H), 7.05 (t, *J* = 7.2 Hz, 1H), 6.93 (t, *J* = 8.0 Hz, 1H), 6.85 (d, *J* = 8.3 Hz, 1H), 3.85 – 3.81 (m, 2H), 3.78 (s, 3H), 3.29 – 3.25 (m, 2H), 3.11 (s, 2H), 2.66 – 2.62 (m, 2H), 2.49 – 2.45 (m, 2H); ESI MS: m/z = 354.2 (M + 1 H)$^+$.

2-(4-(3-Methoxybenzoyl)piperazin-1-yl)-*N*-phenylacetamide (RMT-8)

White solid, Yield: 62 %; mp: 132-134°C; FT-IR: (KBr, cm^{-1}) 3310 (N-H stretch), 3023 (aromatic, C-H stretch), 2939, 1690 (keto, C=O stretch), 1664 (amide, C=O stretch), 1598 (CH$_2$ bend), 1329, 1273, 1236, 1141; ^{1}H NMR (400 MHz, CDCl$_3$) *δ*: 8.96 (s, 1H), 7.58 – 7.54 (m, 2H), 7.35 – 7.31 (m, 3H), 7.13 (t, *J* = 7.4 Hz, 1H), 6.99 – 6.95 (m, 3H), 3.83 (s, 3H), 3.62 – 3.58 (m, 4H), 3.19 (s, 2H), 2.66 – 2.62 (m, 4H); ESI MS: m/z = 354.2 (M + 1 H)$^+$.

2-(4-(4-Methoxybenzoyl)piperazin-1-yl)-*N*-phenylacetamide (RMT-9)

White solid, Yield: 66 %; mp: 134-136°C; FT-IR: (KBr, cm^{-1}) 3301(N-H stretch), 3001 (aromatic, C-H stretch), 2771, 1690 (keto, C=O stretch), 1629 (amide, C=O stretch), 1522 (CH$_2$ bend), 1301, 1249, 1172; ^{1}H NMR (400 MHz, CDCl$_3$) *δ*: 8.98 (s, 1H), 7.56 (dd, *J* = 8.6,

1.2 Hz, 2H), 7.40 – 7.34 (m, 4H), 7.15 – 7.11 (m, 1H), 6.94 – 6.90 (m, 2H), 3.84 (s, 3H), 3.71 – 3.67 (m, 4H), 3.20 (s, 2H), 2.67 – 2.63 (m, 4H); ESI MS: m/z = 354.2 (M + 1 H)$^{+}$.

2-(4-(2-Fluorobenzoyl)piperazin-1-yl)-*N*-phenylacetamide (RMT-10)

Yellow solid, Yield: 69 %; mp: 144-146°C; FT-IR: (KBr, cm^{-1}) 3323 (N-H stretch), 3061 (aromatic, C-H stretch), 2760, 1660 (keto, C=O stretch), 1639 (amide, C=O stretch), 1549 (CH$_2$ bend), 1427, 1313 ^{1}H NMR (400 MHz, CDCl$_3$) *δ*: 8.89 (s, 1H), 7.49 (d, *J* = 8.0 Hz, 2H), 7.34 (t, *J* = 7.2 Hz, 2H), 7.27 (t, *J* = 8.0 Hz, 2H), 7.15 (t, *J* = 7.4 Hz, 1H), 7.05 (q, 8.0 Hz, 2H), 3.87 – 3.81 (m, 2H), 3.39 – 3.35 (m, 2H), 3.13 (s, 2H), 2.69 – 2.63 (m, 2H), 2.55 – 2.51 (m, 2H); ESI MS: m/z = 342.1 (M + 1 H)$^{+}$.

2-(4-(3-Fluorobenzoyl)piperazin-1-yl)-*N*-phenylacetamide (RMT-11)

White solid, Yield: 70 %; mp: 136-138°C; FT-IR: (KBr, cm^{-1}) 3271 (N-H stretch), 3059 (aromatic, C-H stretch), 2765, 1664 (keto, C=O stretch), 1629 (amide, C=O stretch), 1502 (CH$_2$ bend), 1305, 1269; ^{1}H NMR (400 MHz, CDCl$_3$) *δ*: 8.86 (s, 1H), 7.49 (dd, *J* = 8.5, 1.0 Hz, 2H), 7.33 – 7.29 (m, 3H), 7.12 – 7.06 (m, 4H), 3.48 – 3.44 (m, 4H), 3.14 (s, 2H), 2.61 – 2.57 (m, 4H); ESI MS: m/z = 342.1 (M + 1 H)$^{+}$.

2-(4-(2-Ethoxybenzoyl)piperazin-1-yl)-*N*-phenylacetamide (RMT-12)

White solid, Yield: 62 %; mp: 124-126°C; FT-IR: (KBr, cm^{-1}) 3251 (N-H stretch), 3188 (aromatic, C-H stretch), 3070, 2843, 2358, 1693 (keto, C=O stretch), 1668 (amide, C=O stretch), 1546 (CH$_2$ bend), 1411, 1327; ^{1}H NMR (400 MHz, CDCl$_3$) *δ*: 8.98 (s, 1H), 7.56 (d, *J* = 8.0, 2H), 7.36 – 7.32 (m, 3H), 7.26 – 7.22 (m, 1H), 7.15 – 7.09 (m, 1H), 6.99 (t, *J* = 8.3 Hz,1H), 6.90 (d, *J* = 8.3 Hz, 1H), 4.08 (q, *J* = 7.0 Hz, 2H), 3.92 – 3.88 (m, 2H), 3.38 – 3.34 (m, 2H), 3.18 (s, 2H), 2.70 (t, *J* = 5.1 Hz, 2H), 2.61 – 2.55 (m, 2H), 1.42 (t, *J* = 7.0 Hz, 3H); ESI MS: m/z = 368.2 (M + 1 H)$^{+}$.

2-(4-(3-Trifluoromethyl)piperazin-1-yl)-*N*-phenylacetamide (RMT-13)

White solid, Yield: 64 %; mp: 132-134°C; FT-IR: (KBr, cm^{-1}) 3295 (N-H stretch), 3059 (aromatic, C-H stretch), 2358, 1690 (keto, C=O stretch), 1660 (amide, C=O stretch), 1502 (CH$_2$ bend), 1444, 1415; ^{1}H NMR (400 MHz, CDCl$_3$) *δ*: 8.84 (s, 1H), 7.65 – 7.61 (m, 2H), 7.53 – 7.49 (m, 4H), 7.28 (t, *J* = 8.0 Hz, 2H), 7.07 (t, *J* = 7.4 Hz, 1H), 3.67 – 3.61 (m, 4H), 3.14 (s, 2H), 2.64 – 2.58 (m, 4H); ESI MS: m/z = 392.1 (M + 1 H)$^{+}$.

2-(4-(2-Trifluoromethyl)piperazin-1-yl)-*N*-phenylacetamide (RMT-14)

Yellow solid, Yield: 64 %; mp: 124-126°C; FT-IR: (KBr, cm^{-1}) 3277 (N-H stretch), 3061 (aromatic, C-H stretch), 2941, 2357, 2337, 1670 (keto, C=O stretch), 1645 (amide, C=O stretch), 1417 (CH$_2$ bend), 1315, 1278, 1265; ^{1}H NMR (400 MHz, CDCl$_3$) δ: ^{1}H NMR (400 MHz, CDCl$_3$) δ: 8.85 (s, 1H), 7.66 (d, *J* = 7.8 Hz, 1H), 7.55 (t, *J* = 7.2 Hz, 1H), 7.50 – 7.46 (m, 3H), 7.30 – 7.24 (m, 3H), 7.08 – 7.04 (m, 1H), 3.86 – 3.82 (m, 2H), 3.22 – 3.18 (m, 2H), 3.12 (s, 2H), 2.68 – 2.62 (m, 2H), 2.49 – 2.43 (m, 2H). ESI MS: m/z = 392.1 (M + 1 H)$^+$.

]2-(4-(4-Trifluoromethyl)piperazin-1-yl)-*N*-phenylacetamide (RMT-15)

White solid, Yield: 64 %; mp: 154-156°C; FT-IR: (KBr, cm^{-1}) 3358 (N-H stretch), 3062 (aromatic, C-H stretch), 2943, 2866, 1693 (keto, C=O stretch), 1630 (amide, C=O stretch), 1444 (CH$_2$ bend), 1408, 1365, 1330; ^{1}H NMR (400 MHz, CDCl$_3$) δ: 8.84 (s, 1H), 7.62 (d, *J* = 8.0 Hz, 2H), 7.46 (t, *J* = 8.5 Hz, 4H), 7.26 (t, *J* = 8.0 Hz, 2H), 7.05 (t, *J* = 7.4 Hz, 1H), 3.83 – 3.77 (m, 4H), 3.44 – 3.38 (m, 2H), 3.12 (s, 2H), 2.60 – 2.56 (m, 2H); ESI MS: m/z = 392.1 (M + 1 H)$^+$.

2-(4-(3-Ethoxybenzoyl)piperazin-1-yl)-*N*-phenylacetamide (RMT-16)

Yellow solid, Yield: 62 %; mp: 124-126°C; FT-IR: (KBr, cm^{-1}) 3271 (N-H stretch), 3186 (aromatic, C-H stretch), 2843, 2358, 1690 (keto, C=O stretch), 1638 (amide, C=O stretch), 1411 (CH$_2$ bend), 1327, 1273, 1165; ^{1}H NMR (400 MHz, CDCl$_3$) δ: 8.98 (s, 1H), 7.62 (d, *J* = 8.0 Hz, 2H), 7.18 – 7.12 (m, 2H), 6.94 – 6.80 (m, 3H), 6.69 – 6.65 (m, 1H), 6.56 (d, *J* = 8.0 Hz, 1H), 3.98 (q, *J* = 7.0 Hz, 2H), 3.64 – 3.60 (m, 2H), 3.43 – 3.39 (m, 4H), 3.20 (s, 2H), 2.48 – 2.44 (m, 2H),1.36 (t, *J*= 7.0 Hz, 3H); ESI MS: m/z = 368.2 (M + 1 H)$^+$.

2-(4-(4-Ethoxybenzoyl)piperazin-1-yl)-*N*-phenylacetamide (RMT-17)

White solid, Yield: 62 %; mp: 124-126°C; FT-IR: (Cm^{-1}) 3261 (N-H stretch), 3187 (aromatic, C-H stretch), 3070, 2358, 1698 (keto, C=O stretch), 1640 (amide, C=O stretch), 1546, 1421 (CH$_2$ bend), 1327, 1273, 1165; ^{1}H NMR (400 MHz, CDCl$_3$) δ: 8.98 (s, 1H), 7.59 (dd, *J* = 8.4, 1.0 Hz, 2H), 7.32 – 7.28 (m, 3H), 7.15 – 7.09 (m, 4H), 4.18 (q, *J* = 7.0 Hz, 2H), 3.95 – 3.91 (m, 2H), 3.42 – 3.38 (m, 2H), 3.21 (s, 2H), 2.76 – 2.72 (m, 2H), 2.56 – 2.52 (m, 2H), 1.40 (t, *J* = 7.0 Hz, 3H); ESI MS: m/z = 368.2 (M + 1 H)$^+$.

2-(4-(4-Fluorobenzoyl)piperazin-1-yl)-*N*-phenylacetamide (RMT-18)

White solid, Yield: 69 %; mp: 146-148°C; FT-IR: (KBr, cm^{-1}) 3271 (N-H stretch), 3059 (aromatic, C-H stretch), 2765, 1664 (keto, C=O stretch), 1629 (amide, C=O stretch), 1502 (CH$_2$ bend), 1305, 1269, 1251, 1141; ^{1}H NMR (400 MHz, CDCl$_3$) *δ*: 8.89 (s, 1H), 7.60 (d, *J* = 7.9 Hz, 2H), 7.34 (t, *J* = 7.2 Hz, 2H), 7.27 (t, *J* = 7.9 Hz, 2H), 7.17 – 7.13 (m, 1H), 7.08 - 7.02 (m, 2H), 3.86 – 3.82 (m, 4H), 3.11 (s, 2H), 2.68 – 2.64 (m, 2H), 2.55 – 2.51 (m, 2H); ESI MS: m/z = 342.1 (M + 1 H)$^+$.

2-(4-(2-Chlorobenzoyl)piperazin-1-yl)-*N*-phenylacetamide (RMT-19)

Yellow solid, Yield: 65 %; mp: 134-136°C; FT-IR: (KBr, cm^{-1}) 3281 (N-H stretch), 2948 (aromatic, C-H stretch), 2350, 1684 (keto, C=O stretch), 1669 (amide, C=O stretch), 1433 (CH$_2$ bend), 1301, 1282; ^{1}H NMR (400 MHz, CDCl$_3$) *δ*: 9.75 (s, 1H), 7.62 (d, *J* = 7.4 Hz, 2H), 7.30 – 7.24 (m, 5H), 7.05 (t, *J* = 7.2 Hz, 2H), 3.66 – 3.62 (m, 4H), 3.18 (s, 2H), 2.56 – 2.52 (m, 4H); ESI MS: m/z = 357.1 (M)$^+$ and 358.1 (M + 1H)$^+$.

2-(4-(4-Ethylbenzoyl)piperazin-1-yl)-*N*-phenylacetamide (RMT-20)

Yellow solid, Yield: 75 %; mp: 130-132°C; FT-IR: (KBr, cm^{-1}) 3257 (N-H stretch), 3198 (aromatic, C-H stretch), 2978, 2843, 1690 (keto, C=O stretch), 1628 (amide, C=O stretch), 1420 (CH$_2$ bend), 1327, 1273, 1165, 1141; ^{1}H NMR (400 MHz, CDCl$_3$) *δ*: 8.98 (s, 1H), 7.56 (dd, *J* = 8.6, 1.2 Hz, 2H), 7.39 – 7.35 (m, 4H), 7.15 – 7.11 (m, 1H), 6.94 – 6.90 (m, 2H), 3.96 – 3.90 (m, 2H), 3.42 – 3.38 (m, 4H), 3.21 (s, 2H), 2.63 – 2.57 (m, 2H), 2.54 (q, *J* = 7.0 Hz, 2H), 1.42 (t, *J* = 7.0 Hz, 3H); ESI MS: m/z = 352.1 (M + 1 H)$^+$.

4.3.4. Series-IV: Synthesis of peptidomimetics (RMQ-1 to 20)

General procedure 'A' for acid and amine coupling reaction 2-6, 12-16 and 36-44

To a solution of *N*-Boc-L-Leu (2.0 g, 8.6 mmol) in DMF (20.0 mL) was added L-amino ester (1 equiv), followed by benzotriazol-1-yloxytris(dimethylamino)-phosphonium hexafluorophosphate/ BOP (1 equiv) and DIPEA (5 equiv) at ambient temperature under an inert atmosphere. The reaction mixture was allowed to stir for one hour. Water (40 mL) was added to the reaction mixture, and the compound was extracted into ethyl acetate (2 × 50 mL). Organic layer was separated and washed with sat. $NaHCO_3$ (10 mL) and brine (10 mL). The organic layer was dried over anhydrous sodium sulfate, and the solvents were evaporated under reduced pressure to afford the pure *N*-Boc-protected dipeptide compound, which was used directly for the next step without purification.

General procedure 'B' for *N*-Boc deprotection to obtain 7-11 and 17-21

To a solution of *N*-Boc-protected di- or tri- peptide ester (2.0 g) in dichloromethane (10 mL), anisole (2 equiv) was added and allowed to cool 0°C. A solution of 20% trifluoroacetic acid in dichloromethane (1 mL/ 0.2 mmol) was added dropwise to the reaction mixture over 15 min, and allowed to stir at 0°C for 1 h followed by another hour at room temperature. On completion of the reaction, confirmed by TLC, the solvent was concentrated under reduced pressure, and water (2 x 20 mL) was added to the residue. The aqueous residue was basified to pH 8-9 using sat $NaHCO_3$ at 0°C, and the observed white precipitate was extracted with ethyl acetate (2 × 50 mL). The organic layer was separated and dried over anhydrous sodium sulfate. The solvents were evaporated under reduced pressure to afford the pure amine, which was used in the next step without further purification.

General procedure 'C' for the synthesis of compounds 22-26

To a solution of free amino ester (1.0 g) in anhydrous dichloromethane (40 mL), DIPEA (5 equiv) and morpholine or piperidine carbonyl chloride (1.2 equiv) were added at 0°C under an inert atmosphere in drop wise manner. After the addition was complete, the reaction mixture was allowed to stir at ambient temperature for 16 h. On completion of the reaction, confirmed by TLC, the reaction mixture was quenched with sat $NaHCO_3$ (10 mL). The organic layer was separated, washed with brine (1 × 10 mL) and dried over anhydrous sodium sulfate. This was followed by the removal of the solvents under reduced pressure to afford the crude residue, which was purified by column chromatography using 0-5% $MeOH/CH_2Cl_2$ as the eluent, to yield the desired compounds in moderate to good yields.

General procedure 'D' for the synthesis of compounds 30

To a solution of free amino ester (1 g) in anhydrous dichloromethane (20 mL), triethylamine (3 equiv) was added and cooled to 0°C. Chloroacetylchloride (1.1 equiv) was added dropwise under an inert atmosphere, and the stirring was continued for 0.5 h at the same temperature. The reaction mixture was quenched with saturated $NaHCO_3$ (1 × 20 mL), and the organic layer, separated, washed with brine (1 × 10 mL) and dried over anhydrous sodium sulfate. The solvent was evaporated to afford the crude compound which was then purified by column chromatography using 0-2% $MeOH/CH_2Cl_2$ as the eluent, to afford pure compounds **30**.

General procedure 'E' for the synthesis of compounds (halogen exchange reaction) 24.1-25.1

To a Biotage initiator microwave reaction vial, chloroacetyl derivative **30** (0.25 g, 0.48 mmol), potassium carbonate (3 equiv), potassium iodide (1 equiv) were added, followed by respective amines (1 equiv) in acetonitrile (3 mL) at room temperature. The vial was sealed with, and the reaction mixture was irradiated in the microwave at 150°C for 5 min. After irradiation, the reaction mixture was allowed to cool, and ethyl acetate (10 mL) was added to the reaction mixture. The mixture was washed with water (5 mL), and the organic layer extracted and dried over anhydrous sodium sulfate. After concentration of the solvent under reduced pressure, compound was degraded, confirmed by multiple spot formation on thin layer chromatography.

General procedure 'F' for hydrolysis 27-29 and 31-35

To a solution of tripeptide ester in THF/MeOH (3/1), LiOH (5 equiv) was added at room temperature and stirred for 16 h. The organic solvents were removed under reduced pressure, and water (5 mL) was added to the residue. The aqueous layer was acidified to pH 5, filtered, washed with water (10 mL) and dried under vacuum to yield the respective compound as solid.

Procedure 'G' for the synthesis of compounds 49 and 50

To a mixture of *N*-benzyl prolinol (1.0 g) and triphenyl phosphine (2 equiv) in THF (15 mL), carbon tetrabromide (2.2 equiv) was added at 0°C under inert atmosphere. The reaction mixture was stirred at 0 °C for 1 h, followed by at room temperature for an additional hour. Upon completion of the reaction, sat. $NaHCO_3$ solution was added, and the product

extracted with dichloromethane (40 mL). Combined organic layers were dried over anhydrous sodium sulfate, concentrated and purified immediately by column chromatography (Hexanes:Ethylacetate 9:1). The resulting bromide compound, at 0°C was dissolved in DMF (10 mL), followed by the addition of potassium carbonate (3 eq) and various phenol derivatives. The reaction was maintained at 60 ºC for 16 h. Upon completion of the reaction, water (20 mL) was added, and the reaction mixture separated out in ethyl acetate (20 mL). The combined organic extract was dried over anhydrous sodium sulfate, concentration of solvent, gave crude compound. The solid residue was purified by column chromatography afforded the desired compound **49** and **50**.

Procedure 'H' for the deprotection of benzyl group 51 and 52

A solution of benzyl protected tripeptide esters (**31** and **36**) in MeOH, were subjected to hydrogenolysis by reacting with H_2 over 10 % wt Pd/C. Upon completion of the reaction, the reaction mixture was filtered through on a pad of Celite™ and the filtrate was evaporated under reduced pressure to yield corresponding carboxylic acids as solids.

(2*S*,3*S*)-Ethyl 2-((*S*)-2-(*tert*-butoxycarbonylamino)-4-methylpentanamido)-3-methylpentanoate (2)

Compound **2** was synthesized using *N*-Boc-Leucine (12 g, 1 equiv) and leucine ethyl ester hydrochloride (8.36 g, 1 equiv), following the general procedure **'A'** as described above. The product was obtained as a white solid. Yield 86.3 %, FT-IR: (KBr, cm^{-1}) 3371, 3299 (N-H stretch), 1750 (ester, C=O stretch), 1649 (amide, C=O stretch), 1228 (C-O stretch), 1081, 740; ^{1}H NMR (400 MHz, CDCl$_3$) *δ*: 4.96 (s, 1H), 4.84 (d, *J* = 11.2 Hz, 2H), 4.32 – 4.19 (m, 3H), 2.79 (s, 1H), 1.76 (s, 1H), 1.64 (s, 1H), 1.50 – 1.45 (m, 9H), 1.39 – 1.36 (m, 4H), 1.29 (s, 1H), 1.22 (s, 1H), 1.13 – 0.97 (m, 12H).

(*S*)-Methyl 2-((*S*)-2-(*tert*-butoxycarbonylamino)-4-methylpentanamido)-2-phenylacetate (3)

Compound **3** was synthesized using *N*-Boc-Leucine (5 g, 1 equiv) and phenyl gycine methyl ester hydrochloride (2.41 g, 1 equiv), following the general procedure **'A'** as described above. The product was obtained as a white solid. Yield 94.6 %, FT-IR: (KBr, cm^{-1}) 3198, 3154 (N-H stretch), 2935 (aromatic, C-H stretch), 1759 (ester, C=O stretch), 1655 (amide, C=O stretch), 1288 (C-O stretch); ^{1}H NMR (400 MHz, CDCl$_3$) *δ*: 7.39 – 7.27 (m, 5H), 5.76

(s, 1H), 5.46 (s, 1H), 4.78 (s, 1H), 3.71 – 3.69 (m, 3H), 3.51 (s, 1H), 1.66 (d, *J* = 3.0 Hz, 2H), 1.60 (s, 1H), 1.41 – 1.37 (m, 9H), 1.07 – 0.99 (m, 6H).

Ethyl-(*tert*-butoxycarbonyl)-L-leucyl-L-phenylalaninate(4)

Compound **4** was synthesized using *N*-Boc-Leucine (3 g, 1 equiv) and phenyl alanine ethyl ester hydrochloride (2.6 g, 1 equiv), following the general procedure **'A'** as described above. The product was achieved as a white solid. Yield 92 %, FT-IR: (KBr, cm^{-1}) 3242, 3114 (N-H stretch), 2935 (aromatic, C-H stretch), 1764 (ester, C=O stretch), 1650 (amide, C=O stretch), 1302 (C-O stretch); ^{1}H NMR (400 MHz, CDCl$_3$) *δ*: 7.26 – 7.22 (m, 2H), 7.10 (d, *J* = 6.8 Hz, 2H), 6.53 (d, *J* = 7.6 Hz, 1H), 4.92 – 4.68 (m, 2H), 4.25 – 3.98 (m, 2H), 3.23 – 3.03 (m, 2H), 1.64 – 1.60 (m, 3H), 1.32 (s, 9H), 1.20 (t, *J* = 7.1 Hz, 3H), 0.89 (t, *J* = 5.6 Hz, 6H).

(*S*)-Ethyl 2-((*S*)-2-(*tert*-butoxycarbonylamino)-4-methylpentanamido)-4-methylpentanoate (5)

Compound **5** was synthesized using *N*-Boc-Leucine (7 g, 1 equiv) and Isoleucine ethyl ester hydrochloride (4.8 g, 1 equiv), following the general procedure **'A'** as described above. The product was obtained as a white solid. Yield 79.8 %, FT-IR: (KBr, cm^{-1}) 3331, 3125 (N-H stretch), 1752 (ester, C=O stretch), 1645 (amide, C=O stretch), 1250 (C-O stretch); ^{1}H NMR (400 MHz, CDCl$_3$) *δ*: 4.97 (s, 1H), 4.80 (s, 1H), 4.67 (s, 1H), 4.23 – 4.15 (m, 2H), 4.12 (s, 1H), 2.75 (s, 1H), 1.91 (s, 1H), 1.75 (s, 1H), 1.60 (s, 1H), 1.50 – 1.47 (m, 9H), 1.38 – 1.32 (m, 4H), 1.29 (s, 1H), 1.14 – 0.98 (m, 9H), 0.98 – 0.94 (m, 3H).

(*S*)-E thyl 2-((*S*)-2-(*tert*-butoxycarbonylamino)-4-methylpentanamido)-3-methylbutanoate (6)

Compound **6** was synthesized using *N*-Boc-Leucine (6 g, 1 equiv) and Valine ethyl ester hydrochloride (3.75 g, 1 equiv), following the general procedure **'A'** as described above. The crude product was taken for further synthesis.

[(2*S*,3*S*)-Ethyl 2-((*S*)-2-amino-4-methylpentanamido)-3-methylpentanoate)] (7)

Compound **7** was synthesized from compound **2** (2 g, 5.3 mmol), following general procedure **'B'** as described above. The crude product was taken for further synthesis.

(*S*)-Ethyl 2-((*S*)-2-amino-4-methylpentanamido)-2-phenylacetate (8)

Compound **8** was synthesized from compound **3** (2 g, 5.2 mmol), following general procedure **'B'** as described above. The crude product was taken for further synthesis.

Ethyl L-leucyl-L-phenylalaninate (9)

Compound **9** was synthesized from compound **4** (4.2 g, 10.3 mmol), following general procedure **'B'** as described above. The product was obtained as a white solid. Yield 92 %, FT-IR: (KBr, cm^{-1}) 3215, 3194 (N-H stretch), 3005 (aromatic, C-H stretch), 1778 (ester, C=O stretch), 1655 (amide, C=O stretch), 1269 (C-O stretch); ^{1}H NMR (400 MHz, CDCl$_3$) *δ*: 7.29 - 7.01 (m, 5H), 4.68 – 4.64 (m, 1H), 4.12 - 4.01 (m, 2H), 3.86 – 3.82 (m, 1H), 3.13 - 2.96 (m, 2H), 1.60 – 1.56 (m, 3H), 1.22 (t, *J* = 7.1 Hz, 3H), 0.95 – 0.73 (m, 6H).

[(*S*)-Ethyl 2-((*S*)-2-amino-4-methylpentanamido)-4-methylpentanoate] (10) and [(*S*)-ethyl 2-((*S*)-2-amino-4-methylpentanamido)-3-methylbutanoate] (11)

Compound **10** and **11** were synthesized from compound **5** (2 g, 5.3 mmol), and **6** (2 g, 5.6 mmol), respectively; following general procedure **'B'** as described above. The crude product was taken for further synthesis.

(6*S*,9*S*,12*S*)-Ethyl 12-sec-butyl-6,9-diisobutyl-2,2-dimethyl-4,7,10-trioxo-3-oxa-5,8,11-triazatridecan-13-oate (12)

Compound **12** was synthesized from compound **7** (2 g, 7.3 mmol), following general procedure **'A'** as described above. The crude product was taken for further synthesis.

Methyl (*tert*-butoxycarbonyl)-L-leucyl-L-leucyl-L-phenylglycinate (13)

Compound **13** was synthesized from compound **8** (2.0 g, 7.1 mmol), following general procedure **'A'** as described above. The product was obtained as a White solid. Yield 82 %, FT-IR: (KBr, cm^{-1}) 3381, 3288 (N-H stretch), 3055 (aromatic, C-H stretch), 1761 (ester, C=O stretch), 1660, 1649 (amide, C=O stretch), 1235 (C-O stretch); ^{1}H NMR (400 MHz, CDCl$_3$) *δ*: 7.34 – 7.32 (m, 5H), 7.17 – 7.13 (m, 1H), 6.42 (dd, *J* = 28.90, 7.28 Hz, 1H), 5.50 (q, *J* = 7.12, 4.64 Hz, 1H), 4.82 (brs, 1H), 4.52 – 4.47 (m, 1H), 4.12 – 4.02 (m, 1H), 3.71 (s, 3H), 1.72 – 1.55 (m, 6H), 1.43 (s, 9H), 0.93 – 0.82 (m, 12H).

Ethyl (*tert*-butoxycarbonyl)-L-leucyl-L-leucyl-L-phenylalaninate (14)

Compound **14** was synthesized from compound **9** (2.75 g, 9.0 mmol), following general procedure **'A'** as described above. The product was obtained as a white solid. Yield 75 %, FT-IR: (KBr, cm⁻¹) 3298, 3188 (N-H stretch), 2955 (aromatic, C-H stretch), 1751 (ester, C=O stretch), 1655, 1639 (amide, C=O stretch), 1288 (C-O stretch); ^{1}H NMR (400 MHz, CDCl$_3$) *δ*: 7.25 – 7.20 (m, 1H), 7.11 (d, *J* = 6.8 Hz, 2H), 6.49 (d, *J* = 7.8 Hz, 2H), 4.93 – 4.70 (m, 2H), 4.42 – 4.38 (m, 1H), 4.14 (q, *J* = 7.1 Hz, 2H), 3.19 – 3.03 (m, 2H), 1.63 – 1.59 (m, 6H), 1.43 (s, 9H), 1.21 (t, *J* = 7.1 Hz, 3H), 0.93 – 0.89 (m, 12H).

(6*S*,9*S*,12*S*)-Ethyl 12-sec-butyl-6,9-diisobutyl-2,2-dimethyl-4,7,10-trioxo-3-oxa-5,8,11-triazatridecan-13-oate (15)

Compound **15** was synthesized from compound **10** (2.0 g, 7.3 mmol), following general procedure **'A'** as described above. The crude product was taken for further synthesis.

(*S*)-Ethyl 2-(((*S*)-2-(((*S*)-2-amino-4-methylpentanamido)-4-methylpentanamido)-3-methylbutanoate (16)

Compound **16** was synthesized from compound **11** (2.0 g, 7.7 mmol), following general procedure **'A'** as described above. The crude product was taken for further synthesis.

(2*S*,3R)-Ethyl 2-(((*S*)-2-(((*S*)-2-amino-4-methylpentanamido)-4-methylpentanamido)-3-methylpentanoate (17)

Compound **17** was synthesized from compound **12** (5.0 g, 10.3 mmol), following general procedure **'B'** as described above. ^{1}H NMR (400 MHz, CDCl$_3$) *δ*: 4.76 (t, *J* = 6.0 Hz, 1H), 4.38 (t, *J* = 6.7 Hz, 1H), 4.31 (t, *J* = 6.7 Hz, 1H), 4.12 (q, *J* = 6.9 Hz, 2H), 1.77 - 1.51 (m, 9H), 1.18 (t, *J* = 6.0 Hz, 3H), 0.89 - 0.76 (m, 18H).

Methyl L-leucyl-L-leucyl-L-phenylglycinate (**18**)

Compound **18** was synthesized from compound **13** (1.0 g, 2.0 mmol), following general procedure **'B'** as described above. The product was obtained as a pale yellow oil. Yield 98 %, FT-IR: (KBr, cm⁻¹) 3215, 3194 (N-H stretch), 3005 (aromatic, C-H stretch), 1778 (ester, C=O stretch), 1655, 1640 (amide, C=O stretch), 1269 (C-O stretch); ^{1}H NMR (400 MHz, CDCl$_3$) *δ*: 7.34 - 7.23 (m, 5H), 5.44 – 5.40 (m, 1H), 4.42 – 4.38 (m, 1H), 3.81 – 3.77 (m, 1H), 3.68 – 3.64 (m, 3H), 1.68 - 1.42 (m, 6H), 0.96 - 0.72 (m, 12H).

Ethyl L-leucyl-L-leucyl-L-phenylalaninate (19)

Compound **19** was synthesized from compound **14** (3.0 g, 5.77 mmol), following general procedure **'B'** as described above. The product was obtained as a white solid. Yield 88 %, FT-IR: (KBr, cm^{-1}) 3256, 3184 (N-H stretch), 3107 (aromatic, C-H stretch), 1765 (ester, C=O stretch), 1659. 1648 (amide, C=O stretch), 1188 (C-O stretch); ^{1}H NMR (400 MHz, CDCl$_3$) *δ*: 7.24 - 7.19 (m, 2H), 7.18 (s, 1H), 7.11 (d, *J* = 7.2 Hz, 2H), 4.71 (t, *J* = 6.2 Hz, 1H), 4.31 (t, *J* = 6.7 Hz, 1H), 4.09 (q, *J* = 6.9 Hz, 2H), 3.90 (d, *J* = 6.9 Hz, 1H), 3.07 – 3.03 (m, 2H), 1.53 – 1.49 (m, 6H), 1.17 (t, *J* = 7.1 Hz, 3H), 0.99 - 0.72 (m, 12H).

(*S*)-Ethyl 2-(((*S*)-2-(((*S*)-2-amino-4-methylpentanamido)-4-methylpentanamido)-4-methylpentanoate (20)

Compound **20** was synthesized from compound **15** (3.0 g, 6.1 mmol), following general procedure **'B'** as described above. ^{1}H NMR (400 MHz, CDCl$_3$) *δ*: 4.53 (t, *J* = 6.1 Hz, 1H), 4.41 (t, *J* = 6.7 Hz, 1H), 4.32 (t, *J* = 6.7 Hz, 1H), 4.22 (q, *J* = 6.9 Hz, 2H), 1.82 - 1.62 (m, 9H), 1.21 (t, *J* = 6.1 Hz, 3H), 0.91 - 0.78 (m, 18H).

(*S*)-Ethyl 2-(((*S*)-2-(((*S*)-2-amino-4-methylpentanamido)-4-methylpentanamido)-3-methylbutanoate (21)

Compound **21** was synthesized from compound **16** (3.0 g, 6.3 mmol), following general procedure **'B'** as described above. ^{1}H NMR (400 MHz, CDCl$_3$) *δ*: 4.63 (t, *J* = 6.1 Hz, 1H), 4.52 (t, *J* = 6.7 Hz, 1H), 4.45 (q, *J* = 6.9 Hz, 2H), 3.32 (t, *J* = 6.7 Hz, 1H), 1.77 - 1.55 (m, 7H), 1.16 (t, *J* = 6.1 Hz, 3H), 0.90 - 0.80 (m, 18H).

(*tert*-Butoxycarbonyl)-L-leucyl-L-leucyl-L-phenylglycine (27)

Compound **27** was synthesized from compound **13** (2 g, 4.1 mmol), following general procedure **'F'** as described above. The product was obtained as a white solid. Yield 98 %, FT-IR: (KBr, cm^{-1}) 3442, 3194 (N-H stretch), 2955 (aromatic, C-H stretch), 1676, 1646 (amide, C=O stretch), 1288 (C-O stretch); ^{1}H NMR (400 MHz, CDCl$_3$) *δ*: 7.47 – 7.23 (m, 5H), 5.64 – 5.60 (m, 1H), 5.09 – 5.03 (m, 1H), 4.84 – 4.80 (m, 1H), 1.73 - 1.17 (m, 15H), 0.97 - 0.66 (m, 12H).

(6*S*,9*S*,12*S*)-6,9,12-Triisobutyl-2,2-dimethyl-4,7,10-trioxo-3-oxa-5,8,11-triazatridecan-13-oic acid (28)

Compound **28** was synthesized from compound **15** (2 g, 4.1 mmol), following general procedure **'F'** as described above. The product was obtained as a white solid. Yield 83.3 %, FT-IR: (KBr, cm^{-1}) 3338, 3215 (N-H stretch), 1662, 1651 (amide, C=O stretch), 1292 (C-O stretch); ^{1}H NMR (400 MHz, CDCl$_3$) *δ*: 7.57 – 7.23 (m, 5H), 5.54 – 5.50 (m, 1H), 5.18 – 5.14 (m, 1H), 4.84 – 4.80 (m, 1H), 1.69 - 1.17 (m, 15H), 0.96 - 0.66 (m, 12H).

(6*S*,9*S*,12*S*)-6,9-Diisobutyl-12-isopropyl-2,2-dimethyl-4,7,10-trioxo-3-oxa-5,8,11-triazatridecan-13-oic acid (29)

Compound **29** was synthesized from compound **16** (2 g, 4.2 mmol), following general procedure **'F'** as described above. The product was obtained as a white solid. Yield 98 %, FT-IR: (KBr, cm^{-1}) 3318, 3196 (N-H stretch), 1656, 1642 (amide, C=O stretch), 1289 (C-O stretch); ^{1}H NMR (400 MHz, CDCl$_3$) *δ*: 7.57 – 7.43 (m, 5H), 5.54 – 5.50 (m, 1H), 5.18 – 5.14 (m, 1H), 4.85 – 4.79 (m, 1H), 1.71 - 1.17 (m, 15H), 0.96 - 0.66 (m, 12H).

Ethyl 2-(4-fluorophenoxy)acetate (46)

To a solution of 4-fluorophenol **45** (2.0 g, 17.8 mmol), in DMF (10 mL) was added K$_2$CO$_3$ (7.4 g, 53.4 mmol), followed by 2-bromoethyl acetate (3.28 g, 19.5 mmol) at 0 °C under inert atmosphere. The reaction mixture was stirred for 3 h at the same temperature. On completion of the reaction, confirmed by TLC, water (1 x 20 mL) was added, and the compound was extracted in to ethyl acetate (2 x 20 mL). Organic layer was extracted, dried over anhydrous sodium sulphate, which were evaporated under reduced pressure to obtain desired product as a Colorless oil. Yield 72 %, FT-IR: (KBr, cm^{-1}) 3058 (aromatic, C-H stretch), 1680 (COO stretch), ^{1}H NMR (400 MHz, CDCl$_3$) *δ*: 7.02 – 6.93 (m, 2H), 6.89 – 6.81 (m, 2H), 4.58 (s, 2H), 4.26 (q, *J* = 14.60, 7.30 Hz, 2H), 1.29 (t, *J* = 7.14 Hz, 3H).

2-((4-Fluorophenoxy)methyl)-4,5-dihydro-1H-imidazole (47)

To a solution of ethylene diamine (1.36 g, 22.7 mmol) in a anhydrous toluene (10.0 mL), 2 M solution of trimethyl aluminum (1.63 g, 22.7 mmol) was added at 0°C under inert atmosphere. After 15 min, a solution of compound **46** (2.5 g, 12.6 mmol) in toluene (10.0 mL) was added in dropwise and heated to reflux for 4.0 h. On completion of the reaction, confirmed by TLC, reaction mixture was filtered off and washed with dichloromethane (20 mL). Solvent was concentrated under vacuum to afford the pure

dihydroimidazole derivative as a pale yellow solid. Yield 73 %, FT-IR: (KBr, cm^{-1}) 3384 (N-H stretch), 3099 (aromatic, C-H stretch), 1190 (C-O stretch); ^{1}H NMR (400 MHz, CDCl$_3$) *δ*: 7.02 – 6.95 (m, 2H), 6.93 – 6.85 (m, 2H), 4.68 (s, 2H), 3.67 (s, 4H).

(*S*)-1-Benzyl-2-((4-fluorophenoxy)methyl)pyrrolidine (49)

Compound **49** was synthesized from *N*-benzyl L-prolinol **48** (1.0 g, 5.2 mmol), following general procedure **'G'** as described above. The product was obtained as a colorless oil. Yield 83 %, FT-IR: (KBr, cm^{-1}) 3142 (aromatic, C-H stretch), 1210 (C-N, strech), 1190 (C-O stretch); ^{1}H NMR (400 MHz, CDCl$_3$) (NMR is reported as a mixture of rotamers) *δ*: 7.40 – 7.21 (m, 5H), 6.94 – 6.90 (m, 2H), 6.78 – 6.74 (m, 2H), 4.31 – 4.27 and 3.99 – 3.93 (m, 1H), 4.17 – 4.13 and 3.85 – 3.81 (m, 1H), 3.62 – 3.56 and 3.07 – 3.03 (m, 3H), 2.77 – 2.73 and 2.38 – 2.34 (m, 1H), 2.24 – 1.95 (m, 2H), 1.89 – 1.36 (m, 3H).

(*S*)-1-Benzyl-2-((4-methoxyphenoxy)methyl)pyrrolidine (50)

Compound **50** was synthesized from *N*-benzyl L-prolinol **48** (1.0 g, 5.2 mmol), following general procedure **'G'** as described above. The product was obtained as a colorless oil. Yield 75 %, ^{1}H NMR (400 MHz, CDCl$_3$) (NMR is reported as a mixture of rotamers) FT-IR: (KBr, cm^{-1}) 3201 (aromatic, C-H stretch), 1242 (C-N, strech), 1210, 1150 (C-O stretch); *δ*: 7.34 – 7.26 (m, 5H), 6.85 – 6.81 (m, 4H), 4.16 – 4.12 (m, 1H), 3.96 – 3.90 (m, 1H), 3.77 (s, 3H), 3.57 – 3.53 (m, 2H), 3.03 – 2.99 (m, 2H), 2.11 – 2.05 (m, 2H), 1.78 – 1.74 (m, 2H), 1.51 – 1.47 (m, 1H).

(*S*)-2-((4-Fluorophenoxy)methyl)pyrrolidine (51)

Compound **51** was synthesized from compound **49** (1.0 g, 3.5 mmol), following general procedure **'H'** as described above. The product was obtained as colorless oil. Yield 60 %, FT-IR: (KBr, cm^{-1}) 3338 (N-H stretch),3176 (aromatic, C-H stretch), 1260 (C-N, strech), 1190 (C-O stretch); ^{1}H NMR (400 MHz, CDCl$_3$) *δ*: 6.96 – 6.92 (m, 2H), 6.86 – 6.80 (m, 2H), 4.18 – 4.14 and 3.51 – 3.47 (m, 1H), 3.87 – 3.83 (m, 1H), 3.17 – 2.70 (m, 3H), 2.33 (brs, 1H), 1.98 – 1.94 (m, 1H), 1.87 – 1.65 (m, 2H), 1.60 – 1.41 (m, 1H).

(*S*)-2-((4-Methoxyphenoxy)methyl)pyrrolidine (52)

Compound **52** was synthesized from compound **50** (1.0 g, 3.4 mmol), following general procedure **'H'** as described above. The product was obtained as colorless oil. Yield 82%, FT-IR: (KBr, cm^{-1}) 3388 (N-H stretch), 3201 (aromatic, C-H stretch), 1242 (C-N,

strech),1230, 1140 (C-O stretch); ¹H NMR (400 MHz, CDCl₃) *δ*: 6.85 – 6.81 (m, 4H), 3.90 – 3.84 (m, 1H), 3.76 (s, 3H), 2.95 – 2.91 (m, 2H), 1.60 – 1.56 (m, 5H), 1.52 – 1.48 (m, 1H).

Methyl (*S*)-2- ((*S*)-4-methyl-2- ((*S*)-4-methyl-2- (morpholine-4- carboxamido) pentanamido) pentanamido)- 2-phenylacetate (22, RMQ-1)

Compound **22** was synthesized from compound **18** (3.0 g, 7.7 mmol), following general procedure **'C'** as described above. The product was obtained as a white solid. Yield 40 %, mp: 121-123°C; FT-IR: (KBr, cm⁻¹) 3278, 3254 (N-H stretch), 1657, 1639 (amide, C=O stretch), 1228 (C-O stretch); ¹H NMR (400 MHz, CDCl₃) *δ*: 7.40 – 7.31 (m, 6H), 6.72 (dd, *J* = 21.55, 8.64 Hz, 1H), 5.52 (t, *J* = 6.45 Hz, 1H), 4.92 (t, *J* = 8.71 Hz, 1H), 4.54 – 4.48 (m, 1H), 4.34 – 4.32 (m, 1H), 3.70 (s, 3H), 3.67 – 3.62 (m, 4H), 3.33 – 3.28 (m, 4H), 1.74 – 1.50 (m, 6H), 0.92 – 0.85 (m, 12H); ESI MS: m/z = 505.3 [M + 1 H]⁺.

Methyl (*S*)-2-((*S*)-4-methyl-2- ((*S*)-4-methyl-2- (piperidine-1-carboxamido) pentanamido) pentanamido)-2-phenylacetate (23, RMQ-2)

Compound **23** was synthesized from compound **18** (3.0 g, 7.7 mmol), following general procedure **'C'** as described above. The product was obtained as a white solid. Yield 65 %, mp: 141-143°C; FT-IR: (KBr, cm⁻¹) 3198, 3154 (N-H stretch), 1685, 1666, 1649 (amide, C=O stretch), 1288 (C-O stretch); ¹H NMR (400 MHz, CDCl₃) *δ*: 7.39 – 7.28 (m, 6H), 6.81 (dd, *J* = 20.13, 8.08 Hz, 1H), 5.51 (q, *J* = 7.33, 3.91 Hz, 1H), 4.77 (d, *J* = 7.08 Hz, 1H), 4.52 – 4.48 (m, 1H), 4.29 (q, *J* = 14.35, 7.79 Hz, 1H), 3.70 (s, 3H), 3.31 – 3.25 (m, 4H), 1.76 – 1.52 (m, 12 H), 0.92 – 0.84 (m, 12H); ESI MS: m/z = 503.2 [M + 1 H]⁺.

(*S*)-Ethyl 2-((*S*)- 4-methyl-2- ((*S*)-4-methyl- 2-(morpholine-4 -carboxamido) pentanamido) pentanamido)-3-phenyl propionate (24, RMQ-3)

Compound **24** was synthesized from compound **19** (3.0 g, 7.2 mmol), following general procedure **'C'** as described above. The product was obtained as a pale yellow solid. Yield 75 %, mp: 144-146°C; FT-IR: (KBr, cm⁻¹) 3242, 3114 (N-H stretch), 1659, 1652, 1642 (amide, C=O stretch), 1302 (C-O stretch); ¹H NMR (400 MHz, CDCl₃) *δ*: 7.24 (d, *J* = 6.9 Hz, 1H), 7.11 (d, *J* = 6.6 Hz, 2H), 6.62 – 6.50 (m, 2H), 4.82 – 4.78 (m, 2H), 4.43 – 4.24 (m, 2H), 4.14 (q, *J* = 7.2 Hz, 2H), 3.79 – 3.61 (m, 4H), 3.34 (dd, *J* = 7.9, 4.6 Hz, 3H), 3.10 (dd, *J* = 6.0, 3.8 Hz, 2H), 1.65 (d, *J* = 20.5 Hz, 3H), 1.58 – 1.45 (m, 3H), 1.23 – 1.19 (m, 3H), 0.98 – 0.80 (m, 12H); ESI MS: m/z = 533.2 [M + 1 H]⁺.

(*S*)-Ethyl 2-((*S*)-4-methyl-2- ((*S*)-4-methyl-2- (piperidine-1- carboxamido) pentanamido) pentanamido)-3- phenylpropanoate (25, RMQ-4)

Compound **25** was synthesized from compound **19** (3.0 g, 7.2 mmol), following general procedure **'C'** as described above. The product was obtained as a pale white solid. Yield 72 %, mp: 127-129°C; FT-IR: (KBr, cm^{-1}) 3331, 3125 (N-H stretch), 1679, 1660, 1655 (amide, C=O stretch), 1065 (C-O stretch); ^{1}H NMR (400 MHz, CDCl$_3$) *δ*: 7.23 (d, *J* = 8.1 Hz, 1H), 7.12 (t, *J* = 6.9 Hz, 2H), 6.81 – 6.77 (m, *J* = 8.1 Hz, 1H), 6.69 (d, *J* = 7.7 Hz, 1H), 4.76 (dd, *J* = 18.1, 7.4 Hz, 2H), 4.36 (s, 1H), 4.28 (s, 1H), 4.14 (q, *J* = 7.2 Hz, 2H), 3.32 (d, *J* = 5.5 Hz, 4H), 3.12 (dd, *J* = 17.7, 10.4 Hz, 3H), 1.98 – 1.56 (m, 10H), 1.25 – 1.19 (m, 3H), 0.99 – 0.80 (m, 12H); ESI MS: m/z = 531.2 [M + 1 H]$^+$.

(*S*)-Ethyl 2-((*S*)-2-((*S*)-2-(furan-2-carboxamido)-4-methylpentanamido)-4-methylpentanamido)-3-phenylpropanoate (26, RMQ-5)

Compound **26** was synthesized from compound **19** (3.0 g, 7.2 mmol), following general procedure **'C'** as described above. The product was obtained as a pale white solid Yield 75 %, mp: 171-173°C; FT-IR: (KBr, cm^{-1}) 3188, 3154 (N-H stretch), 1669, 1657, 1648 (amide, C=O stretch), 1125 (C-O stretch); ^{1}H NMR (400 MHz, CDCl$_3$) *δ*: 7.47 (s, 1H), 7.31 – 7.27 (m, 1H), 7.25 – 7.20 (m, 1H), 7.16 – 7.12 (m, 2H), 6.65 (t, *J* = 6.7 Hz, 1H), 6.51 (d, *J* = 8 Hz, 1H), 6.44 – 6.38 (m, 2H), 4.84 – 4.80 (m, 1H), 4.61 – 4.55 (m, 1H), 4.40 – 4.36 (m, 1H), 4.23 (q, *J* = 6.2 Hz, 2H), 3.13 (d, *J* = 6.1 Hz, 2H), 1.79 – 1.56 (m, 5H), 1.25 – 1.21 (m, 5H), 0.99 – 0.93 (m, 5H), 0.89 – 0.83 (m, 6H); ESI MS: m/z = 514.1 [M + 1 H]$^+$.

(S)-Ethyl 2-((S)-2-((S)-2-(2-chloroacetamido)-4-methylpentanamido)-4-methylpentanamido)-3-phenylpropanoate (30, RMQ-6)

To a solution of free amino ester **19** (1 g) in anhydrous dichloromethane (20 mL), triethylamine (3 equiv) was added, and cooled to 0°C. Chloroacetylchloride (1.1 equiv) was added dropwise under an inert atmosphere (to protect from moisture), and the stirring was continued for 0.5 h, at same temperature. Reaction mixture was quenched with saturated NaHCO$_3$ (1 × 20 mL), and the organic layer was separated, washed with brine (1 × 10 mL), and dried over anhydrous sodium sulfate. The solvent was evaporated to afford the crude compound, which was purified by column chromatography using 0-2% MeOH/CH$_2$Cl$_2$ as the eluent, to afford pure compound as a pale white solid. Yield 64 %, mp: 200-202°C; FT-IR: (KBr, cm^{-1}) 3335, 3227 (N-H stretch), 1676, 1668, 1651 (amide, C=O stretch), 1282 (C-O stretch); ^{1}H NMR (400 MHz, CDCl$_3$) *δ*: 7.24 - 7.19 (m, 5H), 4.61 (t, *J* = 6.2 Hz, 1H), 4.44 –

4.38 (m, 1H), 4.19 (q, *J* = 7.0 Hz, 2H), 3.90 (d, *J* = 6.9 Hz, 1H), 3.70 – 3.66 (m, 2H), 3.17 – 3.13 (m, 2H), 1.64 – 1.54 (m, 6H), 1.21 (t, *J* = 7.0 Hz, 3H), 0.91 - 0.82 (m, 12H). ESI MS: m/z = 496.0 [M + 1 H]$^+$.

(*S*)-2-((*S*)-4-Methyl-2-((*S*)-4-methyl-2-(morpholine-4-carboxamido)pentanamido)pentanamido)-2-phenylacetic acid (31, RMQ-7)

Compound **31** was synthesized from compound **22,** (3.0 g, 5.9 mmol), following general procedure **'F'** as described above. The product was obtained as a white solid. Yield 80 %, mp: 171-173°C; FT-IR: (KBr, cm^{-1}) 3442, 3194 (N-H stretch), 1676, 1650, 1646 (amide, C=O stretch), 1288 (C-O stretch); ^{1}H NMR (400 MHz, DMSO *d*$_6$) *δ*: 12.85 (brs, 1H), 8.44 (dd, *J* = 25.35, 7.88 Hz, 1H), 7.82 (d, *J* = 8.36 Hz, 1H), 7.37 – 7.29 (m, 5H), 6.50 (t, *J* = 7.98 Hz, 1H), 5.28 (dd, *J* = 29.97, 7.88 Hz, 1H), 4.41 – 4.37 (m, 1H), 4.16 – 4.11 (m, 1H), 3.53 – 3.51 (m, 4H), 3.33 (s, 6H), 3.29 – 3.22 (m, 5H), 1.99 – 1.39 (m, 6H), 0.89 – 0.79 (m, 12H). ESI MS: m/z = 491.3 [M + 1 H]$^+$.

(*S*)-2-((*S*)-4-Methyl-2-((*S*)-4-methyl-2-(piperidine-1-carboxamido)pentanamido)pentanamido)-2-phenylacetic acid (32, RMQ-8)

Compound **32** was synthesized from compound **23** (3.0 g, 5.9 mmol), following general procedure **'F'** as described above. The product was obtained as a white solid. Yield 64 %, mp: 114-116°C; FT-IR: (KBr, cm^{-1}) 3338, 3215 (N-H stretch), 1680, 1662, 1651 (amide, C=O stretch), 1292 (C-O stretch); ^{1}H NMR (400 MHz, DMSO *d*$_6$) *δ*: 12.88 (brs, 1H), 8.49 (dd, *J* = 29.20, 7.88 Hz, 1H), 7.75 (d, *J* = 8.96 Hz, 1H), 7.45 – 7.26 (m, 5H), 6.37 (t, *J* = 7.44 Hz, 1H), 5.29 (dd, *J* = 29.20, 7.76 Hz, 1H), 4.45 – 4.37 (m, 1H), 4.15 – 4.11 (m, 1H), 3.39 – 3.16 (m, 4H), 1.68 – 1.28 (m, 12H), 0.92 – 0.74 (m, 12H). ESI MS: m/z = 489.2 [M + 1 H]$^+$.

(*S*)-2-((*S*)-4-Methyl-2-((*S*)-4-methyl-2-(morpholine-4-carboxamido)pentanamido)pentanamido)-3-phenylpropanoic acid (33, RMQ-9)

Compound **33** was synthesized from compound **24** (3.0 g, 5.6 mmol), following general procedure **'F'** as described above. The product was obtained as a pale yellow solid. Yield 95 %, mp: 137-139°C; FT-IR: (KBr, cm^{-1}) 3192, 3104 (N-H stretch), 1671, 1662, 1655 (amide, C=O stretch), 1270 (C-O stretch); ^{1}H NMR (400 MHz, DMSO *d*$_6$) *δ*: 12.69 (s, 1H), 8.07 – 7.90 (m, 1H), 7.80 – 7.62 (m, 1H), 7.24 (s, 2H), 7.19 (s, 3H), 6.60 – 6.37 (m, 1H), 4.45 – 4.32 (m, 1H), 4.31 – 4.16 (m, 1H), 4.17 – 4.05 (m, 1H), 3.51 (s, 4H), 3.27 (s, 4H), 3.10 – 2.96

(m, 1H), 2.96 – 2.82 (m, 1H), 1.58 (s, 3H), 1.40 (s, 3H), 0.84 (d, J = 14.0 Hz, 12H); ESI MS: m/z = 505.3 [M + 1 H]$^+$.

(*S*)-2-((*S*)-4-Methyl-2-((*S*)-4-methyl-2-(piperidine-1-carboxamido)pentanamido)pentanamido)-3-phenylpropanoic acid (34, RMQ-10)

Compound **34** was synthesized from compound **25** (3.0 g, 5.6 mmol), following general procedure **'F'** as described above. The product was obtained as a pale white solid. Yield 76 %, mp: 130-132°C; FT-IR: (KBr, cm^{-1}) 3245, 3199 (N-H stretch), 1672, 1665, 1638 (amide, C=O stretch), 1262 (C-O stretch); ^{1}H NMR (400 MHz, DMSO d_6) δ: 7.97 (s, 1H), 7.67 (d, J = 8.7 Hz, 1H), 7.28 - 7.21 (m, 2H), 7.19 (d, J = 6.4 Hz, 3H), 6.38 (d, J = 8.2 Hz, 1H), 4.35 (s, 1H), 4.27 (d, J = 7.4 Hz, 1H), 4.12 (s, 1H), 3.30 – 3.16 (m, 7H), 3.03 (dd, J = 14.0, 5.4 Hz, 2H), 2.90 (dd, J = 14.2, 8.4 Hz, 1H), 1.46 – 1.12 (m, 8H), 0.93 – 0.70 (m, 12H); ESI MS: m/z = 503.2 [M + 1 H]$^+$.

(*S*)-2-((*S*)-2-((*S*)-2-(Furan-2-carboxamido)-4-methylpentanamido)-4-methylpentanamido)-3-phenylpropanoic acid (35, RMQ-11)

Compound **35** was synthesized from compound **26** (3.0 g, 5.8 mmol), following general procedure **'F'** as described above. The product was obtained as a pale white solid. Yield 82 %, mp: 96-98°C; FT-IR: (KBr, cm^{-1}) 3325, 3266 (N-H stretch), 1660, 1655, 1640 (amide, C=O stretch), 1259 (C-O stretch); ^{1}H NMR (400 MHz, DMSO d_6) δ: 8.23 (d, J = 8.6 Hz, 1H), 8.02 (d, J = 8.9 Hz, 1H), 7.86 (s, 1H), 7.84 (s, 1H), 7.27 – 7.08 (m, 6H), 6.62 (s, 1H), 4.46 (s, 1H), 4.27 (d, J = 7.5 Hz, 2H), 3.03 (s, 1H), 2.92 (d, J = 7.7 Hz, 1H), 1.59 (s, 3H), 1.39 (t, J = 14.5 Hz, 3H), 0.83 (dd, J = 22.2, 5.9 Hz, 12H); ESI MS: m/z = 486.3 [M + 1 H]$^+$.

N-((*S*)-1-(((*S*)-1-(((*S*)-2-(2-((4-Fluorophenoxy)methyl)-4,5-dihydro-1H-imidazol-1-yl)-2-oxo-1-phenylethyl)amino)-4-methyl-1-oxopentan-2-yl)amino)-4-methyl-1-oxopentan-2-yl)morpholine-4-carboxamide (36, RMQ-12)

Compound **36** was synthesized from compound **31** (3.0 g, 6.1 mmol), following general procedure **'A'** as described above. The product was obtained as a pale white solid. Yield 95 %, mp: 98-100°C; FT-IR: (KBr, cm^{-1}) 3222, 3181 (N-H stretch), 1660, 1649, 1641 (amide, C=O stretch); ^{1}H NMR (400 MHz, CDCl$_3$) δ: 7.48 – 7.30 (m, 6H), 6.98 – 6.92 (m, 4H), 6.60 (dd, J = 22.17 and 7.80 Hz, 1H), 5.58 (t, J = 6.88 Hz, 1H), 5.15 (d, J = 5.84 Hz, 2H), 4.44 – 4.40 (m, 1H), 4.31 – 4.27 (m, 1H), 4.11 – 3.79 (m, 4H), 3.72 – 3.60 (m, 4H), 3.40 – 3.23 (m, 4H), 1.78 – 1.33 (m, 6H), 1.01 – 0.78 (m, 12H); ESI MS: m/z = 685.3 [M + H$_2$O + 1 H]$^+$.

N-(((*S*)-1-(((*S*)-1-(((*S*)-2-(2-((4-Fluorophenoxy)methyl)-4,5-dihydro-1H-imidazol-1-yl)-2-oxo-1-phenylethyl)amino)-4-methyl-1-oxopentan-2-yl)amino)-4-methyl-1-oxopentan-2-yl)piperidine-1-carboxamide (37, RMQ-13)

Compound **37** was synthesized from compound **32** (1.0 g, 2.0 mmol), following general procedure **'A'** as described above. The product was obtained as a white solid. Yield 40 %, mp: 96–98°C; FT-IR: (KBr, cm^{-1}) 3398, 3174 (N-H stretch), 1671, 1660, 1640 (amide, C=O stretch); ^{1}H NMR (400 MHz, CDCl$_3$) *δ*: 7.78 and 7.54 (d, *J* = 8.08 Hz, 1H), 7.40 – 7.12 (m, 8H), 6.98 – 6.92 (m, 2H), 6.85 – 6.81 (m, 2H), 5.60 and 5.49 (d, *J* = 8.16 and 7.64 Hz, 1H), 4.98 and 4.72 (d, *J* = 6.64 and 2.96 Hz, 1H), 4.39 and 4.38 (s, 2H), 4.26 – 4.22 and 4.03 – 3.99 (m, 2H), 3.65 – 3.38 (m, 4H), 3.32 – 3.26 (m, 3H), 3.12 – 3.08 (m, 2H), 1.82 – 1.35 (m, 12H), 0.92 – 0.86 (m, 12H); ESI MS: m/z=683.4 [M + H$_2$O + 1 H]$^+$.

N-(((*S*)-1-(((*S*)-1-(((*S*)-2-((*S*)-2-((4-Fluorophenoxy)methyl)pyrrolidin-1-yl)-2-oxo-1-phenylethyl)amino)-4-methyl-1-oxopentan-2-yl)amino)-4-methyl-1-oxopentan-2-yl)morpholine-4-carboxamide (38, RMQ-14)

Compound **38** was synthesized from compound **31** (3.0 g, 6.1 mmol), following general procedure **'A'** as described above. The product was obtained as a white solid. Yield 34 %, mp: 95-97ºC; FT-IR: (KBr, cm^{-1}) 3256, 3222 (N-H stretch), 1671, 1666, 1656 (amide, C=O stretch); ^{1}H NMR (600 MHz, 100 °C, DMSO *d$_6$*) *δ*: 8.04 (s, 1H), 7.60 (t, *J* = 5.13 Hz, 1H), 7.39 – 7.23 (m, 5H), 7.09 – 7.01 (m, 2H), 6.99 – 6.77 (m, 2H), 6.16 (q, *J* = 4.22, 8.12 Hz, 1H), 5.75 – 5.69 (m, 1H), 4.38 – 4.34 (m, 1H), 4.23 – 4.17 (m, 1H), 3.71 – 3.46 (m, 6H), 3.39 – 3.17 (m, 6H), 2.05 – 1.83 (m, 3H), 1.73 – 1.44 (m, 8H), 0.94 – 0.79 (m, 12H); ESI MS: m/z = 668.3 [M + 1 H]$^+$.

N-(((*S*)-1-(((*S*)-1-(((*S*)-2-((*S*)-2-((4-Fluorophenoxy)methyl)pyrrolidin-1-yl)-2-oxo-1-phenylethyl)amino)-4-methyl-1-oxopentan-2-yl)amino)-4-methyl-1-oxopentan-2-yl)pipereridine-4-carboxamide (39, RMQ-15)

Compound **39** was synthesized from compound **32** (1.0 g, 2.0 mmol), following general procedure **'A'** as described above. The product was obtained as a white solid. Yield 23 %, mp: 80–82°C; FT-IR: (KBr, cm^{-1}) 3482, 3290 (N-H stretch), 1666, 1657, 1641 (amide, C=O stretch); ^{1}H NMR (600 MHz, 100 °C, DMSO *d$_6$*) *δ*: 8.04 (s, 1H), 7.61 – 7.55 (m, 1H), 7.38 – 7.19 (m, 4H), 7.09 – 6.74 (m, 5H), 6.03 – 5.99 (m, 1H), 5.71 – 5.67 (m, 1H), 4.38 – 4.32 (m, 1H), 4.21 – 4.15 (m, 1H), 4.01 – 3.95 (m, 1H), 3.70 – 3.46 (m, 2H), 3.44 – 3.24 (m, 2H),

2.96 – 2.92 (m, 4H), 2.06 – 1.83 (m, 2H), 1.73 – 1.35 (m, 14H), 0.96 – 0.76 (m, 12H). ESI MS: m/z = 666.2 [M + 1 H]$^+$.

N-((S)-1-(((S)-1-(((S)-1-((S)-2-((4-Fluorophenoxy)methyl)pyrrolidin-1-yl)-1-oxo-3-phenylpropan-2-yl)amino)-4-methyl-1-oxopentan-2-yl)amino)-4-methyl-1-oxopentan-2-yl)morpholine-4-carboxamide (40, RMQ-16)

Compound **40** was synthesized from compound **33** (1.0 g, 2.0 mmol), following general procedure **'A'** as described above. The product was obtained as a white solid. Yield 40 %, mp: 95–97°C; FT-IR: (KBr, cm^{-1}) 3325, 3225 (N-H stretch), 1661, 1653, 1649 (amide, C=O stretch); ^{1}H NMR (600 MHz, 100 °C, DMSO d_6) $δ$: 7.86 (d, J = 6.01 Hz, 1H), 7.63 (d, J = 6.02 Hz, 1H), 7.50 (d, J = 6.01 Hz, 1H), 7.41 – 7.35 (m, 1H), 7.30 – 7.11 (m, 5H), 7.10 – 7.03 (m, 2H), 7.01 – 6.84 (m, 2H), 6.21 – 6.17 (m, 1H), 4.87 – 4.79 (m, 1H), 4.52 – 4.46 (m, 1H), 4.19 – 4.15 (m, 1H), 3.82 – 3.78 (m, 1H), 3.65 – 3.40 (m, 5H), 3.36 – 3.27 (m, 4H), 3.24 – 3.16 (m, 1H), 2.87 – 2.83 (m, 2H), 1.99 – 1.26 (m, 10H), 0.95 – 0.76 (m, 12H); ESI MS: m/z = 682.2 [M + 1 H]$^+$.

N-((S)-1-(((S)-1-(((S)-1-((S)-2-((4-Methoxyphenoxy)methyl)pyrrolidin-1-yl)-1-oxo-3-phenylpropan-2-yl)amino)-4-methyl-1-oxopentan-2-yl)amino)-4-methyl-1-oxopentan-2-yl)piperidine-1-carboxamide (41, RMQ-17)

Compound 41 was synthesized from compound **34** (1.0 g, 2.0 mmol), following general procedure **'A'** as described above. The product was obtained as a pale white solid. Yield 40 %, mp: 90–92°C; FT-IR: (KBr, cm^{-1}) 3485, 3264 (N-H stretch), 1666, 1653, 1641 (amide, C=O stretch); ^{1}H NMR (600 MHz, 100 °C, DMSO d_6) $δ$: 7.84 (d, J = 6.01 Hz, 1H), 7.60 (d, J = 6.01 Hz, 1H), 7.44 (d, J = 6.01 Hz, 1H), 7.37 – 7.33 (m, 1H), 7.29 – 7.10 (m, 5H), 6.94 – 6.78 (m, 4H), 6.02 (t, J = 12.06 Hz, 1H), 4.93 – 4.87 (m, 1H), 4.28 – 4.24 (m, 1H), 4.16 – 4.12 (m, 1H), 3.91 – 3.87 (m, 1H), 3.72 – 3.68 (m, 3H), 3.60 – 3.54 (m, 1H), 3.34 – 3.26 (m, 4H), 3.14 – 3.10 (m, 1H), 2.96 – 2.92 (m, 1H), 2.83 – 2.79 (m, 1H), 1.97 – 1.26 (m, 16H), 0.94 – 0.77 (m, 12H); ESI MS: m/z = 692.2 [M + 1 H]$^+$.

N-((S)-4-Methyl-1-(((S)-4-methyl-1-oxo-1-(((S)-1-oxo-3-phenyl-1-(2-phenylhydrazinyl)propan-2-yl)amino)pentan-2-yl)amino)-1-oxopentan-2-yl)piperidine-1-carboxamide (42, RMQ-18)

Compound **42** was synthesized from compound **34** (1.0 g, 2.0 mmol), following general procedure **'A'** as described above. The product was obtained as a white solid. Yield 60 %,

mp: 204-206°C; FT-IR: (KBr, cm^{-1}) 3452, 3222 (N-H stretch), 1669, 1661, 1656 (amide, C=O stretch); ^{1}H NMR (400 MHz, CDCl$_3$) δ: 8.83 (brs, 1H), 7.44 (d, J = 9.33 Hz, 1H), 7.31 – 7.05 (m, 8H), 6.84 – 6.78 (m, 3H), 6.73 – 6.69 (m, 1H), 6.05 (d, J = 4.10 Hz, 1H), 4.94 – 4.88 (m, 1H), 4.23 – 4.19 (m, 1H), 4.12 – 4.08 (m, 1H), 3.52 – 3.20 (m, 5H), 3.06 – 3.00 (m, 1H), 1.76 – 1.31 (m, 12H), 1.03 - 0.66 (m, 12H); ESI MS: m/z = 593.1 [M + 1 H]$^+$.

N-((*S*)-4-Methyl-1-(((*S*)-4-methyl-1-oxo-1-(((*S*)-1-oxo-3-phenyl-1-(2-phenylhydrazinyl)propan-2-yl)amino)pentan-2-yl)amino)-1-oxopentan-2-yl)furan-2-carboxamide (43, RMQ-19)

Compound **43** was synthesized from compound **35** (1.0 g, 2.0 mmol), following general procedure **'A'** as described above. The product was obtained as a white solid. Yield 59 %, mp: 234–236°C; FT-IR: (KBr, cm^{-1}) 3258, 3182 (N-H stretch), 1671, 1666, 1651 (amide, C=O stretch); ^{1}H NMR (400 MHz, DMSO d_6) δ: 9.70 (s, 1H), 8.24 (d, J = 8.24 Hz, 1H), 8.19 (d, J = 8.19 Hz, 1H), 7.95 (d, J = 7.95 Hz, 1H), 7.91 – 7.83 (m, 1H), 7.70 – 7.66 (m, 1H), 7.30 – 7.14 (m, 6H), 7.02 (t, J = 7.68 Hz, 2H), 6.66 – 6.62 (m, 2H), 6.46 (d, J = 7.02 Hz, 1H), 4.61 – 4.55 (m, 1H), 4.49 – 4.43 (m, 1H), 4.36 – 4.32 (m, 1H), 3.02 – 2.96 (m, 1H), 2.90 – 2.86 (m, 1H), 1.69 – 1.33 (m, 6H), 0.92 – 0.77 (m, 12H); ESI MS: m/z = 576.2 [M + 1 H]$^+$.

N-((*S*)-4-Methyl-1-((*S*)-4-methyl-1-oxo-1-((*S*)-1-oxo-3-phenyl-1-(2-phenylhydrazinyl)propan-2-ylamino)pentan-2-ylamino)-1-oxopentan-2-yl)morpholine-4-carboxamide (44, RMQ-20)

Compound **44** was synthesized from compound **33** (1.0 g, 2.0 mmol), following general procedure **'A'** as described above. The product was obtained as an off white solid. Yield 40 %, mp: 218–220°C; FT-IR: (KBr, cm^{-1}) 3289, 3182 (N-H stretch), 1661, 1659, 1652 (amide, C=O stretch); ^{1}H NMR (400 MHz, CDCl$_3$) δ: 8.79 (s, 1H), 7.41 (dd, J = 95.6, 7.4 Hz, 2H), 7.24 – 6.95 (m, 5H), 6.85 (dd, J = 11.8, 6.3 Hz, 1H), 6.69 (dd, J = 27.7, 19.8 Hz, 2H), 6.09 (s, 1H), 5.00 – 4.63 (m, 2H), 4.36 – 4.01 (m, 2H), 3.78 – 3.48 (m, 4H), 3.44 – 3.02 (m, 5H), 2.54 – 1.97 (m, 2H), 1.29 – 1.21 (m, 6H), 1.03 – 0.72 (m, 12H); ESI MS: m/z = 595.1 [M + 1 H]$^+$.

4.3.5. Series-V: Synthesis of 2-(substituted)pyrimidin-4-ylthio)-*N'*-(2-phenylacetyl)-acetohydrazide derivatives (RMP-1 to 15)

2-Phenylacetohydrazide (2)

To a solution of methyl 2-phenylacetate **1** (500 mg, 3.3 mmol), in anhydrous methanol (25 ml), hydrazine hydrate (533 mg, 16.6 mmol) was added in portions over ten minutes period under nitrogen atmosphere at room temperature, and the reaction was stirred for further 16 h. After completion of the reaction (confirmed by TLC), the solvent was evaporated under reduced pressure. The crude residue was treated with diethyl ether (10 mL) to afford compound **2** as white precipitate, that was collected by filtration and dried under vacuum. Yield 80 %, FT-IR: (KBr, cm^{-1}) 3329, 3278 (N-H stretch), 3115 (aromatic, C-H stretch), 1652 (amide, C=O stretch); ^{1}H NMR (400 MHz, CDCl$_3$) $δ$: 7.36 (t, J = 4.2 Hz, 1H), 7.34 – 7.28 (m, 3H), 7.26 – 7.22 (m, 1H), 6.66 (s, 1H), 3.84 (s, 2H), 3.57 (s, 2H).

2-Chloro-*N'*-(2-phenylacetyl)acetohydrazide (3)

2-Chloroacetyl chloride (0.23 mL, 2.9 mmol) was added to a solution of compound **2** (400 mg, 2.6 mmol) and *N,N*-di-isopropyl ethylamine (0.46 mL, 2.6 mmol) in anhydrous dichloromethane (20 mL), at –15°C over 10 min period under inert atmosphere (to protect from moisture). The reaction was stirred for 30 min at 0°C, quenched with saturated sodium bicarbonate solution (10 ml); the organic phase was collected and dried over anhydrous sodium sulphate. After evaporation of the solvent, the crude mixture was purified by column chromatography (chloroform – methanol gradient) to yield compound **3** as a white solid. Yield 66.3 %, FT-IR: (KBr, cm^{-1}) 3301, 3218 (N-H stretch), 3115 (aromatic, C-H stretch), 1660, 1640 (amide, C=O stretch), 751 (C-Cl stretch); ^{1}H NMR (400 MHz, DMSO d_6) $δ$: 10.3 (s, 1H), 10.2 (s, 1H), 7.32 (d, J = 7.5 Hz, 1H), 7.30 (d, J = 3.2 Hz, 3H), 7.26 – 7.18 (m, 1H), 4.12 (s, 2H), 3.48 (s, 2H).

S-2-(2-(2-Phenylacetyl)hydrazinyl)ethyl ethanethioate (4)

To a solution of compound **3** (400 mg, 1.76 mmol) in ethanol (12 mL), potassium thioacetate (705 mg, 6.17 mmol) was added and the mixture was stirred at room temperature for 16 h. After completion of the reaction (TLC confirmed), the mixture was diluted with ethyl acetate (10 mL) and THF (10 mL), washed with water and brine, and dried over anhydrous sodium sulfate. The solvent was evaporated under reduced pressure. The crude compound was purified by column chromatography (chloroform methanol gradient), to yield compound **4** as a brown solid. Yield 68.2 %, FT-IR: (KBr, cm^{-1}) 3299, 3208 (N-H stretch), 3176 (aromatic, C-

H stretch), 1740 (C=O stretch), 1682, 1666 (amide, C=O stretch), 801 (C-S stretch); ^{1}H NMR (400 MHz, DMSO d_6) δ: 10.2 (s, 1H), 10.0 (s, 1H), 7.30 - 7.24 (m, 5H), 3.65 (s, 2H), 3.46 (s, 2H), 2.36 (s, 3H).

2-Mercapto-*N'*-(2-phenylacetyl)acetohydrazide (5)

To a solution of compound **4** (200 mg, 0.75 mmol) in methanol (5 mL), K_2CO_3 (207 mg, 1.5 mmol) was added and the mixture was stirred at room temperature for 1 h. The reaction mixture was diluted with ethyl acetate (10 mL) and THF (10 mL), washed with water and brine, and dried over anhydrous sodium sulphate. The solvent evaporated, and the crude mixture purified by column chromatography (chloroform - methanol gradient), to obtain compound **5** as a white solid. Yield 71.4 %, FT-IR: (KBr, cm^{-1}) 3317, 3188 (N-H stretch), 3128 (aromatic, C-H stretch), 1670, 1657 (amide, C=O stretch), 781 (C-S stretch); ^{1}H NMR (400 MHz, DMSO d_6) δ: 10.2 (s, 1H), 10.0 (s, 1H), 7.43 – 7.25 (m, 5H), 3.47 (s, 2H), 3.15 (s, 2H), 2.79 (t, $J = 7.9$ Hz, 1H).

6-Methyl-2-(2-oxo-2-phenylethylthio)pyrimidin-4(3H)-one (7A)

A mixture of compound **6** (100 mg, 0.70 mmol), 2-bromo-1-phenylethanone (139 mg, 0.70 mmol), and potassium carbonate (97 mg, 0.70 mmol) were stirred together in anhydrous *N,N*-dimethylformamide (3 mL) at room temperature for 16 h. Completion of the reaction was confirmed by TLC. The reaction content was poured on cold water (5 mL), and extracted with ethyl acetate (3 x 10 mL). The organic layers were combined, washed with brine (1 x 10 mL), dried over anhydrous sodium sulphate, and the solvent was evaporated to dryness. The crude mixture was purified by column chromatography (hexanes:ethyl acetate gradient), to obtain pure compound **7A** as a white solid. Yield 54.6 %, FT-IR: (KBr, cm^{-1}) 3322 (N–H stretch), 3128 (aromatic, C-H stretch), 1710, 1696 (C=O stretch), 788 (C-S stretch); ^{1}H NMR (400 MHz, DMSO d_6) δ: 12.0 (brs, 1H), 8.04 (d, $J = 7.8$ Hz, 2H), 7.69 – 7.65 (m, 1H), 7.56 (t, $J = 7.7$ Hz, 2H), 5.92 (s, 1H), 4.74 (s, 2H), 1.95 (s, 3H).

2-(2-(4-Methoxyphenyl)-2-oxoethylthio)-6-methylpyrimidin-4(3H)-one (7B)

Compound **7B** was synthesized using the method as described for compound **7A**, starting from compound **6** (300 mg, 2.1 mmol) and 2-bromo-1-(4-methoxyphenyl)ethanone (483 mg, 2.1 mmol) at room temperature for 16 h. The product was obtained as a pale yellow solid. Yield 50 %, FT-IR: (KBr, cm^{-1}) 3341 (N–H stretch), 3199 (aromatic, C-H stretch), 1718, 1672

(C=O stretch), 748 (C-S stretch); ^{1}H NMR (400 MHz, DMSO d_6) δ: 12.60 (s, 1H), 8.02 (d, J = 9.2 Hz, 2H), 7.07 (d, J = 9.2 Hz, 2H), 5.93 (s, 1H), 4.69 (s, 2H), 3.85 (s, 3H), 1.98 (brs, 3H).

2-(2-(4-(Diethylamino)phenyl)-2-oxoethylthio)-6-methylpyrimidin-4(3H)-one (7C)

Compound **7C** was synthesized using the method as described for compound **7A**, starting from compound **6** (200 mg, 1.4 mmol) and 2-bromo-1-(4-(diethylamino)phenyl)ethanone (380mg, 1.4 mmol) at room temperature for 16 h. The product was obtained as a orange solid. Yield 55 %, FT-IR: (KBr, cm^{-1}) 3319 (N–H stretch), 3164 (aromatic, C-H stretch), 1688, 1676 (C=O stretch), 756 (C-S stretch); ^{1}H NMR (400 MHz, DMSO d_6) δ: 7.84 (d, J = 8.8 Hz, 2H), 6.71 (d, J = 9.2 Hz, 2H), 5.91 (s, 1H), 4.63 (s, 2H), 3.43 (q, J = 7.2 Hz, 4H), 2.04 (brs, 3H), 1.12 (t, J = 7.0 Hz, 6H).

6-Methyl-2-(2-morpholino-2-oxoethylthio)pyrimidin-4(3H)-one (7D)

Compound **7D** was synthesized using the method as described for compound **7A**, starting from compound **6** (300 mg, 2.1 mmol) and 2-bromo-1-morpholinoethanone (345 mg, 2.1 mmol) heating at 70°C for 5 h. The product was obtained as a yellow solid. Yield 54 %, FT-IR: (KBr, cm^{-1}) 3352 (N–H stretch), 1732, 1649 (C=O stretch), 768 (C-S stretch); ^{1}H NMR (400 MHz, DMSO d_6) δ: 5.98 (s, 1H), 4.15 (s, 2H), 3.64 - 3.60 (m, 2H), 3.58 - 3.54 (m, 4H), 3.48 - 3.43 (m, 2H), 2.15 (s, 3H) .

6-Methyl-2-(2-morpholinoethylthio)pyrimidin-4(3H)-one (7E)

Compound **7E** was synthesized using the method as described for compound **7A**, starting from compound **6** (250 mg, 1.7 mmol), and 4-(2-bromoethyl)morpholine (327 mg, 1.7 mmol) heating at 70°C for 5.5 h. The product was obtained as a pale yellow solid. Yield 57 %, FT-IR: (KBr, cm^{-1}) 3345 (N–H stretch), 1688 (C=O stretch), 778 (C-S stretch); ^{1}H NMR (400 MHz, DMSO d_6) δ: 5.94 (s, 1H), 3.57 (t, J = 4.6 Hz, 4H), 3.25 (t, J = 7.0 Hz, 4H), 2.46 - 2.40 (m, 4H), 2.14 (s, 3H).

4-(2-(4-Methyl-6-oxo-1,6-dihydropyrimidin-2-ylthio)acetyl)benzonitrile (7F)

Compound **7F** was synthesized using the method as described for compound **7A**, starting from compound **6** (300 mg, 2.1 mmol), and 4-(2-bromoacetyl)benzonitrile (472 mg, 2.1 mmol) heating at 70°C for 6 h. The product was obtained as a pale yellow solid. Yield 54 %, FT-IR: (KBr, cm^{-1}) 3299 (N–H stretch), 3142 (aromatic, C-H stretch), 1730, (C=O stretch),

769 (C-S stretch); ^{1}H NMR (400 MHz, DMSO d_6) δ: 7.84 (d, J = 8.4 Hz, 2H), 7.61 (d, J = 8.4 Hz, 2H), 5.91 (s, 1H), 4.72 (s, 2H), 1.89 (brs, 3H).

Ethyl 2-(4-methyl-6-oxo-1,6-dihydropyrimidin-2-ylthio)acetate (7G)

Compound **7G** was synthesized using the method as described for compound **7A**, starting from compound **6** (300 mg, 2.1 mmol) and ethyl 2-bromoacetate (388 mg, 2.3 mmol) heating at 80°C for 5.5 h. The product was obtained as a pale yellow solid. Yield 60 %, FT-IR: (KBr, cm^{-1}) 3311 (N–H stretch), 1735 (ester, C=O stretch), 788 (C-S stretch); ^{1}H NMR (400 MHz, CDCl$_3$) δ: 12.4 (s, 1H), 6.06 (s, 1H), 4.22 (q, J = 7.2 Hz, 2H), 3.94 (s, 2H), 2.22 (s, 3H), 1.28 (t, J = 7.2 Hz, 3H) .

2-(4-Chloro-6-methylpyrimidin-2-ylthio)-1-phenylethanone (8A)

POCl$_3$ (1.0 mL, 1.645g, 10.7mmol) was added to the compound **7A** (100 mg, 0.38 mmol), and the mixture was heated at 70°C for 1 h. Completion of the reaction was confirmed by TLC. The reaction was quenched with sodium bicarbonate saturated solution (10 mL) and extracted with ethyl acetate (10 mL). The organic phase was washed with water (3 x 10 mL), and dried over anhydrous sodium sulphate. The solvent was evaporated to obtain a crude mixture which was purified by column chromatography (chloroform – methanol gradient) to yield compound **8A** as a white solid. Yield 60 %, FT-IR: (KBr, cm^{-1}) 3314 (N–H stretch), 3188 (aromatic, C-H stretch), 1696 (C=O stretch), 781 (C-S stretch); ^{1}H NMR (400 MHz, DMSO d_6) δ: 8.13 – 7.96 (m, 2H), 7.68 (t, J = 7.4 Hz, 1H), 7.57 (t, J = 7.6 Hz, 2H), 7.28 (s, 1H), 4.79 (s, 2H), 2.30 (s, 3H).

2-(4-Chloro-6-methylpyrimidin-2-ylthio)-1-(4-methoxyphenyl)ethanone (8B)

Compound **8B** was synthesized using the method as described for compound **8A**, heating at 70°C for 15 min, obtained as a yellow solid. Yield 80 %, FT-IR: (KBr, cm^{-1}) 3350 (N–H stretch), 3172 (aromatic, C-H stretch), 1718, (C=O stretch), 749 (C-S stretch); ^{1}H NMR (400 MHz, DMSO d_6) δ: 8.05 (d, J = 9.2 Hz, 2H), 6.97 (d, J = 8.8 Hz, 2H), 6.87 (s, 1H), 4.60 (s, 2H), 3.89 (s, 3H), 2.39 (s, 3H).

2-(4-Chloro-6-methylpyrimidin-2-ylthio)-1-(4-(diethylamino)phenyl)ethanone (8C)

Compound **8C** was synthesized using the method as described for compound **8A**, heating at 70°C for 20 min, obtained as a orange solid. Yield 85 %, FT-IR: (KBr, cm^{-1}) 3302 (N–H stretch), 3160 (aromatic, C-H stretch), 1688, (C=O stretch), 752 (C-S stretch); ^{1}H NMR (400

MHz, DMSO d_6) *δ* 7.95 (d, *J* = 8.8 Hz, 2H), 6.84 (s, 1H), 6.65 (d, *J* = 9.2 Hz, 2H), 4.59 (s, 2H), 3.43 (q, *J* = 7.0 Hz, 4H), 2.38 (s, 3H), 1.21 (t, *J* = 7.0 Hz, 6H).

2-(4-Chloro-6-methylpyrimidin-2-ylthio)-1-morpholinoethanone (8D)

Compound **8D** was synthesized using the method as described for compound **8A**, heating at 70°C for 10 min, obtained as a orange solid. Yield 78 %, FT-IR: (KBr, cm^{-1}) 3339 (N–H stretch), 1732, 1688 (C=O stretch), 777 (C-S stretch); ^{1}H NMR (400 MHz, DMSO d_6) *δ*: 6.88 (s, 1H), 4.06 (s, 2H), 3.75 - 3.64 (m, 8H), 2.44 (s, 3H).

4-(2-(4-Chloro-6-methylpyrimidin-2-ylthio)ethyl)morpholine (8E)

Compound **8E** was synthesized using the method as described for compound **8A**, heating at 75°C for 20 min, obtained as a pure white solid. Yield 70 %,. FT-IR: (KBr, cm^{-1}) 3311 (N–H stretch), 1701, 1679 (C=O stretch), 781 (C-S stretch); ^{1}H NMR (400 MHz, CDCl$_3$) *δ*: 6.86 (s, 1H), 3.76 – 3.70 (m, 4H), 3.32 – 3.26 (m, 2H), 2.74 - 2.68 (m, 2H), 2.59 - 2.53 (m, 4H), 2.43 (s, 3H).

4-(2-(4-Chloro-6-methylpyrimidin-2-ylthio)acetyl)benzonitrile (8F)

Compound **8F** was synthesized using the method as described for compound **8A**, heating at 70°C for 20 min, obtained as a pure pale yellow solid. Yield 75 %, FT-IR: (KBr, cm^{-1}) 3247 (N–H stretch), 3135 (aromatic, C-H stretch), 1730, (C=O stretch), 751 (C-S stretch); ^{1}H NMR (400 MHz, DMSO d_6) *δ*: 8.15 (d, *J* = 8.8 Hz, 2H), 7.81 (d, *J* = 8.8 Hz, 2H), 6.87 (s, 1H), 4.54 (s, 2H), 2.35 (s, 3H).

Ethyl 2-(4-chloro-6-methylpyrimidin-2-ylthio)acetate (8G)

Compound **8G** was synthesized using the method as described for compound **8A**, heating at 70°C for 15 min, obtained as a white solid. Yield 90 %, FT-IR: (KBr, cm^{-1}) 3319 (N–H stretch), 1722 (ester, C=O strech), 1701 (C=O stretch), 764 (C-S stretch); ^{1}H NMR (400 MHz, DMSO d_6) *δ*: 7.01 (s, 1H), 4.23 (q, *J* = 7.2, 2H), 3.97 (s, 2H), 2.55 (s, 3H), 1.29 (t, *J* = 7.2 Hz, 3H).

General procedure for the synthesis of 2-(substituted) pyrimidin-4-ylthio)-*N*-(2-phenylacetyl)acetohydrazide 9 (A-O)

To a solution of compound **5** and **8 (A-O)**, in anhydrous acetonitrile (10 mL), triethylamine was added, and the mixture was heated for 30 min to 6h. After completion of the reaction (confirmed by TLC), the mixture was poured on to cold water (5 mL, for quenching), and extracted with ethyl acetate (3 ×10 mL). The organic layers were combined, washed with brine (10 mL), dried with anhydrous sodium sulfate and evaporated under vacuum. The residue was purified by column chromatography (hexane - ethyl acetate gradient), and pure compound obtained as a solid.

2-(6-Methyl-2-(2-oxo-2-phenylethylthio)pyrimidin-4-ylthio)-*N*-(2-phenylacetyl)acetohydrazide (9A / RMP-1)

To a solution of compound **5** (50 mg, 0.22 mmol), and **8A** (58 mg, 0.22 mmol) in anhydrous acetonitrile (10 mL), triethylamine (0.034 mL, 0.24 mmol) was added, and the mixture heated at 70°C for 1 h. On completion of reaction (confirmed by TLC), the mixture was poured on to cold water (5 mL, for quenching), and extracted with ethyl acetate (3 ×10 mL). The organic layers were combined, washed with brine (10 mL), dried with anhydrous sodium sulfate and evaporated under vacuum. The residue was purified by column chromatography (hexane - ethyl acetate gradient), and pure compound obtained as a white solid. Yield 60 %, mp: 175-177°C; FT-IR: (KBr, cm^{-1}) 3327, 3284 (N-H stretch), 1720 (keto, C=O stretch), 1690, 1670 (amide, C=O stretch);^{1}H NMR (400 MHz, CDCl$_3$) *δ*: 9.31 (s, 1H), 8.04 - 8.02 (d, *J* = 8 Hz, 2H), 7.61 (t, *J* = 8 Hz, 1H), 7.49 (t, *J* = 8 Hz, 2H), 7.31 − 7.27 (m, 5H), 6.73 (s, 1H), 4.59 (s, 2H), 3.81 (s, 2H), 3.61 (s, 2H), 2.26 (s, 3H); ^{13}C NMR (DMSO *d$_6$*) *δ*: 194.16, 168.91, 168.67, 168.57, 165.83, 165.38, 136.02, 135.54, 133.32, 128.90, 128.64, 128.23, 128.12, 126.40, 112.98, 38.00, 30.61, 22.97; ESI MS: m/z = 467.1 [M + 1 H]$^+$.

2-(2-(2-(4-Methoxyphenyl)-2-oxoethylthio)-6-methylpyrimidin-4-ylthio)-*N*-(2-phenylacetyl)acetohydrazide (9B / RMP-2)

Compound **9B** was synthesized using the method as described for compound **9A**, heating at 75°C for 6 h; obtained as a grey solid compound. Yield 40 %, mp: 178-180°C; FT-IR: (KBr, cm^{-1}) 3385, 3319 (N-H stretch), 1732 (keto, C=O stretch), 1688, 1669 (amide, C=O stretch); ^{1}H NMR (400 MHz, DMSO *d$_6$*) *δ*: 10.2 (s,1H), 10.1 (s, 1H), 8.03 (d, *J* = 8.8 Hz, 2H), 7.30 - 7.23 (m, 5H), 7.06 - 7.04 (m, 3H), 4.74 (s, 2H), 3.86 (s, 2H), 3.84 (s, 3H), 3.45 (s, 2H), 2.22 (s, 3H); ^{13}C NMR (DMSO *d$_6$*) *δ*: 192.43, 169.11, 168.75, 168.51, 165.92, 165.41, 163.33,

135.60, 130.72, 128.96, 128.78, 128.18, 126.47, 113.93, 113.01, 55.53, 37.80 30.62, 23.06; ESI MS: m/z = 497.2 [M + 1 H]$^+$.

2-(2-(2-(4-(Diethylamino)phenyl)-2-oxoethylthio)-6-methylpyrimidin-4-ylthio)-*N'*-(2-phenylacetyl)acetohydrazide (9C / RMP-3)

Compound **9C** was synthesized using the method as described for compound **9A**, heating at 90°C for 4 h; obtained as a white solid compound. Yield 41 %, mp: 197-199°C; FT-IR: (KBr, cm^{-1}) 3398, 3318 (N-H stretch), 1699 (keto, C=O stretch), 1680, 1666 (amide, C=O stretch); ^{1}H NMR (400 MHz, DMSO d_6) δ: 10.2 (s, 1H), 10.1 (s,1H), 7.86 (d, *J* = 8.4 Hz, 2H), 7.27 - 7.22 (m, 5H), 7.06 (s, 1H), 6.69 (d, *J* = 8.0 Hz, 2H), 4.65 (s, 2H), 3.91 (s, 2H), 3.50 (s, 2H), 3.45 - 3.40 (m, 6H), 2.26 (s, 3H), 1.12 (t, *J* = 6.4 Hz, 4H); ^{13}C NMR (DMSO d_6) δ: 190.87, 169.41, 168.70, 168.41, 165.94, 165.36, 151.11, 135.60, 130.85, 130.85, 128.95, 128.95, 128.16, 128.16, 126.44, 122.43, 112.97, 110.14, 43.83, 37.41, 30.68, 23.11, 12.34; ESI MS: m/z = 538.2 [M + 1 H]$^+$.

2-(6-Methyl-2-(2-morpholino-2-oxoethylthio)pyrimidin-4-ylthio)-*N'*-(2-phenylacetyl)acetohydrazide (9D / RMP-4)

Compound **9D** was synthesized using the method as described for compound **9A**, heating at 70°C for 30 min; obtained as a yellow solid compound. Yield 40 %, mp: 156-158°C; FT-IR: (KBr, cm^{-1}) 3317, 3204 (N-H stretch), 1710 (keto, C=O stretch), 1666, 1656 (amide, C=O stretch); ^{1}H NMR (400 MHz, DMSO d_6) δ: 10.1 (s, 1H), 10.2 (s, 1H), 7.30 - 7.20 (m, 5H), 7.08 (s, 1H), 4.18 (s, 2H), 3.96 (s, 2H), 3.58 - 3.51 (m, 6H), 3.48 - 3.42 (m, 4H), 2.29 (s, 3H); ^{13}C NMR (DMSO d_6) δ: 169.32, 168.75, 168.21, 166.04, 166.01, 165.26, 128.88, 128.20, 128.08, 126.40, 112.97, 65.96, 65.90, 45.81, 41.89, 33.34, 30.57, 23.04; ESI MS: m/z = 476.2 [M + 1 H]$^+$.

2-(6-Methyl-2-(2-morpholinoethylthio)pyrimidin-4-ylthio)-*N'*-(2-phenylacetyl)acetohydrazide (9E / RMP-5)

Compound **9E** was synthesized using the method as described for compound **9A**, heating at 90°C for 4.5 h; obtained as a white solid compound. Yield 30 %, mp: 75-77°C; FT-IR: (KBr, cm^{-1}) 3381, 3266 (N-H stretch), 1679, 1661 (amide, C=O stretch); ^{1}H NMR (400 MHz, DMSO d_6) δ: 10.3 (s, 1H), 10.2 (s, 1H), 7.31 - 7.20 (m, 5H), 7.06 (s, 1H), 3.95 (s, 2H), 3.53 (t, *J* = 4.4 Hz, 4H), 3.46 (s, 2H), 3.23 (t, *J* = 7.2 Hz, 2H), 2.59 (t, *J* = 7.2 Hz, 2H), 2.44 - 2.37 (m, 4H), 2.29 (s, 3H); ^{13}C NMR (DMSO d_6) δ: 169.94, 168.67, 168.31, 165.91, 165.34,

135.54, 128.87, 128.11, 126.40, 112.73, 65.96, 57.16, 52.93, 40.07, 30.63, 27.04, 23.08; ESI MS: m/z = 462.2 [M + 1 H]$^+$.

2-(2-(2-(4-Cyanophenyl)-2-oxoethylthio)-6-methylpyrimidin-4-ylthio)-*N'*-(2-phenylacetyl)acetohydrazide (9F / RMP-6)

Compound **9F** was synthesized using the method as described for compound **9A**, heating at 90°C for 1.5 h; obtained as a white solid compound. Yield 40 %, mp: 170-172°C; FT-IR: (KBr, cm^{-1}) 3298, 3158 (N-H stretch), 1719 (keto, C=O stretch), 1672, 1656 (amide, C=O stretch); ^{1}H NMR (400 MHz, DMSO d_6) $δ$: 10.1 (s, 1H), 10.0 (s, 1H), 8.18 (d, *J* = 8.4 Hz, 2H), 8.01 (d, *J* = 8.0 Hz, 2H), 7.29 - 7.19 (m, 5H), 7.06 (s, 1H), 4.80 (s, 2H), 3.84 (s, 2H), 3.44 (s, 2H), 2.18 (s, 3H); ^{13}C NMR (DMSO d_6) $δ$: 203.26, 178.13, 175.25, 174.88, 148.81, 144.98, 142.09, 138.34, 138.27, 137.55, 135.84, 127.49, 124.67, 122.50, 40.06, 32.35; ESI MS: m/z = 492.2 [M + 1 H]$^+$.

Ethyl 2-(4-methyl-6-(2-oxo-2-(2-(2-phenylacetyl)hydrazinyl)ethylthio)pyrimidin-2-ylthio)acetate (9G / RMP-7)

Compound **9G** was synthesized using the method described for compound **9A**, heating at 90°C for 3.5 h; obtained as a white solid compound. Yield 42 %, mp: 158-160°C; FT-IR: (KBr, cm^{-1}) 3299, 3184 (N-H stretch), 1712 (ester, C=O stretch), 1675, 1668 (amide, C=O stretch); ^{1}H NMR (400 MHz, DMSO d_6) $δ$: 10.2 (s, 2H), 7.32 - 7.21 (m, 5H), 7.10 (s, 1H), 4.10 (q, *J* = 7.1 Hz, 2H), 3.99 (s, 2H), 3.94 (s, 2H), 3.46 (s, 2H), 2.29 (s, 3H), 1.17 (t, *J* = 7.0 Hz, 3H); ^{13}C NMR (DMSO d_6) $δ$: 168.87, 168.68, 168.60, 165.80, 165.51, 135.53, 128.89, 128.11, 126.39, 113.10, 60.87, 32.74, 30.40, 23.04, 13.95; ESI MS: m/z = 435.1 [M + 1 H]$^+$.

2-(2-(2-(4-Hydroxyphenyl)-2-oxoethylthio)-6-methylpyrimidin-4-ylthio)-*N'*-(2-phenylacetyl)acetohydrazide (9H / RMP-8)

Compound **9H** was synthesized using the method as described for compound **9A**, heating at 90°C for 1.5 h; obtained as a white solid compound. Yield 40 %, mp: 168-170°C; FT-IR: (KBr, cm^{-1}) 3380, 3256 (N-H stretch), 1718 (keto, C=O stretch), 1678, 1661 (amide, C=O stretch); ^{1}H NMR (400 MHz, DMSO d_6) $δ$: 10.1 (s, 1H), 10.0 (s, 1H), 8.81 (brs, 1H), 8.11 (d, *J* = 8.1 Hz, 2H), 7.30 - 7.19 (m, 7H), 7.12 (s, 1H), 4.77 (s, 2H), 3.88 (s, 2H), 3.41 (s, 2H), 2.20 (s, 3H); ^{13}C NMR (DMSO d_6) $δ$: 201.21, 177.23, 175.23, 171.87, 146.91, 141.88, 140.19, 137.31, 137.26, 136.55, 134.84, 124.52, 121.71, 120.51, 40.21, 31.31; ESI MS: m/z = 483.2 [M + 1 H]$^+$.

2-(2-(2-(3-Methoxyphenyl)-2-oxoethylthio)-6-methylpyrimidin-4-ylthio)-*N'*-(2-phenylacetyl)acetohydrazide (9I / RMP-9)

Compound **9I** was synthesized using the method as described for compound **9A**, heating at 75°C for 6 h; obtained as a grey solid compound. Yield 45 %, mp: 172-174°C; FT-IR: (KBr, cm^{-1}) 3298, 3159 (N-H stretch), 1731 (keto, C=O stretch), 1691, 1659 (amide, C=O stretch); ^{1}H NMR (400 MHz, DMSO d_6) δ: 10.2 (s,1H), 10.1 (s, 1H), 7.99 (t, *J* = 8.6 Hz, 3H), 7.34 - 7.31 (m, 4H), 7.21 - 7.19 (m, 3H), 4.71 (s, 2H), 3.87 (s, 2H), 3.80 (s, 3H), 3.50 (s, 2H), 2.17 (s, 3H); ^{13}C NMR (DMSO d_6) δ: 191.33, 168.21, 167.45, 166.51, 163.82, 163.61, 162.53, 133.50, 131.63, 127.91, 126.76, 125.20, 124.45, 115.91, 112.19, 51.54, 39.87 32.61, 25.12; ESI MS: m/z = 497.2 [M + 1 H]$^+$.

2-(2-(2-(4-(Dimethylamino)phenyl)-2-oxoethylthio)-6-methylpyrimidin-4-ylthio)-*N'*-(2-phenylacetyl)acetohydrazide (9J / RMP-10)

Compound **9J** was synthesized using the method as described for compound **9A**, heating at 100°C for 4 h; obtained as a white solid compound. Yield 43 %, mp: 192-194°C; FT-IR: (KBr, cm^{-1}) 3399, 3281 (N-H stretch), 1735 (keto, C=O stretch), 1676, 1669 (amide, C=O stretch); ^{1}H NMR (400 MHz, DMSO d_6) δ: 10.1 (s, 1H), 10.0 (s,1H), 7.81(d, *J* = 8.4 Hz, 2H), 7.52 (d, *J* = 8.0 Hz, 2H), 7.25 - 7.21 (m, 3H), 7.16 (s, 1H), 6.63 (t, *J* = 8.0 Hz, 2H), 4.71 (s, 2H), 3.89 (s, 2H), 3.39 (s, 2H), 2.21 (s, 3H), 1.18 (t, *J* = 6.4 Hz, 4H); ^{13}C NMR (DMSO d_6) δ: 187.82, 168.42, 167.78, 167.41, 164.93, 164.36, 152.12, 138.60, 135.85, 129.81, 127.94, 126.16, 126.04, 123.41, 117.97, 110.16, 43.85, 37.49, 31.68, 24.17; ESI MS: m/z = 510.2 [M + 1 H]$^+$.

2-((6-Methyl-2-((2-oxo-2-(p-tolyl)ethyl)thio)pyrimidin-4-yl)thio)-*N'*-(2-phenylacetyl)acetohydrazide (9K / RMP-11)

Compound **9K** was synthesized using the method as described for compound **9A**, heating at 80°C for 4.5 h; obtained as a white solid compound. Yield 45 %, mp: 160-162°C; FT-IR: (KBr, cm^{-1}) 3300, 3216 (N-H stretch), 1724 (keto, C=O stretch), 1682, 1664 (amide, C=O stretch); ^{1}H NMR (400 MHz, CDCl$_3$) δ: 10.1 (s, 1H), 9.37 (s, 1H), 8.28 (d, *J* = 8.4 Hz, 2H), 8.11 - 8.05 (m, 2H), 7.31 - 7.26 (m, 5H), 7.02 (s, 1H), 4.80 (s, 2H), 3.80 (s, 2H), 3.44 (s, 2H), 2.28 (s, 3H), 2.16 (s, 3H); ^{13}C NMR (DMSO d_6) δ: 191.26, 167.97, 167.68, 167.51, 164.73, 164.31, 135.12, 134.51, 132.02, 126.80, 125.14, 121.20, 120.10, 119.41, 112.90, 40.07, 32.42, 24.17, 20.97; ESI MS: m/z = 481.1 [M + 1 H]$^+$.

2-((2-((2-(4-Ethylphenyl)-2-oxoethyl)thio)-6-methylpyrimidin-4-yl)thio)-*N'*-(2-phenylacetyl)acetohydrazide (9L / RMP-12)

Compound **9L** was synthesized using the method as described for compound **9A**, heating at 95°C for 2.5 h; obtained as a yellow solid compound. Yield 42 %, mp: 176-178°C; FT-IR: (KBr, cm^{-1}) 3212, 3199 (N-H stretch), 1699 (keto, C=O stretch), 1680, 1667 (amide, C=O stretch); ^{1}H NMR (400 MHz, CDCl$_3$) δ: 10.1 (s, 1H), 9.68 (s, 1H), 8.53 (d, *J* = 8.8 Hz, 2H), 7.32 - 7.29 (m, 5H), 7.16 - 7.10 (m, 3H), 3.99 (s, 2H), 3.84 (s, 2H), 3.24 (s, 2H), 2.28 (s, 3H), 2.16 (s, 3H), 1.26 (s, 2H); ^{13}C NMR (DMSO d_6) δ: 189.02, 169.51, 168.12, 168.01, 166.13, 165.33, 137.91, 135.67, 132.12, 125.67, 121.20, 120.80, 118.11, 116.30, 112.78, 42.17, 37.24, 28.07, 21.09, 16.17; ESI MS: m/z = 495.1 [M + 1 H]$^{+}$.

2-((6-Methyl-2-((2-oxo-2-(4-(trifluoromethyl)phenyl)ethyl)thio)pyrimidin-4-yl)thio)-*N'*-(2-phenylacetyl)acetohydrazide (9M / RMP-13)

Compound **9M** was synthesized using the method as described for compound **9A**, heating at 75°C for 3.5 h; obtained as a white solid compound. Yield 47 %, mp: 190-192°C; FT-IR: (KBr, cm^{-1}) 3391, 3278 (N-H stretch), 1701 (keto, C=O stretch), 1684, 1671 (amide, C=O stretch); ^{1}H NMR (400 MHz, CDCl$_3$) δ: 10.1 (s, 1H), 9.81 (s, 1H), 8.18 (d, *J* = 8.4 Hz, 2H), 7.81 (d, *J* = 8.0 Hz, 2H), 7.21 - 7.16 (m, 5H), 7.02 (s, 1H), 4.28 (s, 2H), 3.84 (s, 2H), 3.54 (s, 2H), 2.18 (s, 3H); ^{13}C NMR (DMSO d_6) δ: 194.06, 171.70, 170.12, 169.11, 164.15, 161.20, 140.19, 139.47, 134.08, 129.80, 124.30, 122.08, 120.10, 119.54, 117.11, 115.21, 39.18, 31.22, 22.10; ESI MS: m/z = 535.1 [M + 1 H]$^{+}$.

2-((6-Methyl-2-((2-oxo-2-(m-tolyl)ethyl)thio)pyrimidin-4-yl)thio)-*N'*-(2-phenylacetyl)acetohydrazide (9N / RMP-14)

Compound **9N** was synthesized using the method as described for compound **9A**, heating at 90°C for 4.0 h; obtained as an off white solid compound. Yield 51 %, mp: 165-167°C; FT-IR: (KBr, cm^{-1}) 3328, 3214 (N-H stretch), 1714 (keto, C=O stretch), 1656, 1649 (amide, C=O stretch); ^{1}H NMR (400 MHz, CDCl$_3$) δ: 10.1 (s, 1H), 9.41 (s, 1H), 8.38 (d, *J* = 8.4 Hz, 2H), 8.12 - 8.09 (m, 2H), 7.41 - 7.24 (m, 5H), 7.16 (s, 1H), 4.47 (s, 2H), 3.81 (s, 2H), 3.60 (s, 2H), 2.20 (s, 3H), 2.14 (s, 3H); ^{13}C NMR (DMSO d_6) δ: 192.06, 172.17, 169.34, 167.05, 163.19, 162.02, 132.21, 130.11, 129.21, 129.09, 127.27, 123.18, 119.11, 116.19, 110.01, 38.18, 32.22, 28.17, 21.17; ESI MS: m/z = 481.1 [M + 1 H]$^{+}$.

2-((2-((2-(3-Ethylphenyl)-2-oxoethyl)thio)-6-methylpyrimidin-4-yl)thio)-*N*′-(2-phenylacetyl)acetohydrazide (9O/ RMP-15)

Compound **9O** was synthesized using the method as described for compound **9A**, heating at 80°C for 4.5 h; obtained as a white solid compound. Yield 57 %, mp: 181-183°C; FT-IR: (KBr, cm^{-1}) 3371, 3251 (N-H stretch), 1708 (keto, C=O stretch), 1668, 1652 (amide, C=O stretch); ^{1}H NMR (400 MHz, CDCl$_3$) *δ*: 10.1 (s, 1H), 10.0 (s, 1H), 8.58 (d, *J* = 8.6 Hz, 2H), 8.11 - 7.88 (m, 5H), 7.31 - 7.28 (m, 2H), 7.06 (s, 1H), 4.67 (s, 2H), 3.74 (s, 2H), 3.50 (s, 2H), 2.18 (s, 3H), 1.26 (s, 2H); ^{13}C NMR (DMSO *d$_6$*) *δ*: 191.52, 173.01, 171.69, 171.04, 169.21, 167.30, 139.91, 136.17, 131.13, 126.10, 125.28, 124.58, 120.42, 117.22, 114.27, 41.18, 39.16, 29.06, 23.08, 14.11; ESI MS: m/z = 495.1 [M + 1 H]$^+$.

4.3.6. Series-VI: Synthetic route to 1,6 dihydropyrimidine-5-carboxamides derivatives (RMH 1 to 14)

Ethyl 3-benzyl-4-oxo-2-thioxo-1,2,3,4-tetrahydropyrimidine-5-carboxylate (11)

A mixture of benzyl thiourea **10** (2.0 gm, 12.0 mmol), Diethyl (ethoxymethylene)malonate (2.6 gm, 12.0 mmol), potassium carbonate (3.2 gm, 24.0 mmol), and pyridine (0.1 ml catalytically) were stirred together in anhydrous *N,N*-dimethylformamide (20ml) under 120° C microwave heating (100W) for 1.0 hr. Completion of the reaction was confirmed by TLC. The solvent evaporated, and residue dissolved in ethyl acetate. The solution was washed with hydrochloric acid (1 N), dried over anhydrous sodium sulphate, and evaporated under reduced pressure. The crude product was purified by column chromatography (ethyl acetate: hexane 70:30), to produce pure compound **11** as a yellow solid. Yield 55 %, FT-IR: (KBr, cm^{-1}) 3313 (N-H stretch), 1716 (keto, C=O stretch), 1665 (ester, C=O stretch,); ^{1}H NMR (400 MHz, DMSO d_6) *δ*: 13.12 (s, 1H), 8.03 (s, 1H), 7.33 - 7.21(m, 5H), 4.18 (q, *J* =7.06, 2H), 1.24 (t, *J* = 7.06 Hz, 3H).

3-Benzyl-4-oxo-*N*-(3-phenylpropyl)-2-thioxo-1,2,3,4-tetrahydropyrimidine-5-carboxamide (12)

A stirred solution of trimethylaluminum (6.85 ml, 13.7 mmol, 2 M solution in toluene) in anhydrous dichloromethane (5 ml) was treated with compound **11** (1 gm, 3.4 mmol), dissolved in 20 ml of anhydrous dichloromethane at 0° C. After stirring for 30 min, amine (1.92 ml, 13.7 mmol) in anhydrous dichloromethane (5 ml) was added and the mixture was stirred overnight at room temperature. The reaction mixture was then quenched with sodium hydroxide (0.1N) at 0° C. The organic layer was separated, washed with water (15 ml), brine (15 ml) and dried over anhydrous sodium sulphate. Evaporation of the solvent and purification of the crude by column chromatography (ethyl acetate: hexane 60:40), produce pure compound **12** as a white solid. Yield 55 %, FT-IR: (KBr, cm^{-1}) 3270 (N-H stretch), 1710 (keto, C=O stretch), 1640 (amide C=O stretch); ^{1}H NMR (400 MHz, DMSO d_6) *δ*: 13.31 (s, 1H), 8.70 (t, *J* = 5.8Hz, 1H), 8.06 (s, 1H), 7.38 – 7.04 (m, 10H), 5.57 (s, 2H), 3.26 (dd, *J* = 13.2, 6.8 Hz, 2H), 2.58 (t, *J* = 7.6 Hz, 2H), 1.85 – 1.70 (m, 2H).

General procedure for the synthesis of 1-Benzyl-6-oxo-2-(substituted)-1,6-dihydropyrimidine-5-carboxamide (RMH-1-14)

To a solution of **12** and Group **(A-I)** in anhydrous acetonitrile (10 mL), triethylamine was added, and the reaction mixture was heated and completion of the reaction was confirmed

by TLC. The reaction content was poured in cold water (5 ml), and extracted with ethyl acetate (3 × 10 mL). The organic layers were collected, washed with brine (10 mL), dried, and evaporated to furnish crude compound, which was purified by column chromatography using hexane and ethyl acetate (50:50) as a mobile phase, to obtain compound **13A-I** as a white solid.

1-Benzyl-6-oxo-2-(2-oxo-2-phenylethylthio)-*N*-(3-phenylpropyl)-1,6-dihydropyrimidine-5-carboxamide (13A / RMH-1)

To a solution of **12** (30 mg, 0.079 mmol) and 2-bromo-1-phenylethanone (15 mg, 0.079 mmol) in anhydrous acetonitrile (10 mL), triethylamine (0.010 mL, 0.079 mmol) was added, and the reaction mixture was heated at 60°C for 45 min. Completion of the reaction was confirmed by TLC. The reaction content was poured on to cold water (5 ml), and extracted with ethyl acetate (3 × 10 mL). The organic layers were collected, washed with brine (10 mL), dried, and evaporated to furnish crude compound, which was purified by column chromatography using hexane and ethyl acetate (50:50) as a mobile phase, to obtain compound **13A** as a white solid. Yield 41 %, mp: 96-98°C; FT-IR: (KBr, cm^{-1}) 3250 (N-H stretch), 1693, 1689 (keto, C=O stretch), 1662 (amide, C=O stretch); ^{1}H NMR (400 MHz, DMSO d_6) *δ*: 8.90 (t, *J* = 5.6 Hz, 1H), 8.39 (s, 1H), 8.04 (d, *J* = 8.0 Hz, 2H), 7.69 (t, *J* = 8.0 Hz, 1H), 7.57 (t, *J* = 7.5 Hz, 2H), 7.42 – 7.13 (m, 9H), 5.41 (s, 2H), 4.98 (s, 2H), 3.32 - 3.24 (m, 2H), 2.59 (t, *J* = 6.0 Hz, 2H), 1.86 – 1.71 (m, 2H); ^{13}C NMR (DMSO d_6) *δ*: 192.33, 165.94, 161.01, 155.01, 141.41, 135.68, 134.23, 128.84, 128.69, 128.29, 128.26, 128.22, 112.41, 47.91, 40.15, 39.94, 38.23, 32.50, 30.68; ESI MS: m/z = 498.1 [M + 1 H]$^+$.

1-Benzyl-2-(2-(4-methoxyphenyl)-2-oxoethylthio)-6-oxo-*N*-(3-phenylpropyl)-1,6 dihydropyrimidine-5-carboxamide (13B / RMH-2)

Compound **13B** was synthesized using the method as described for compound **13A**, starting from compound **12** (30 mg, 0.079 mmol) and 4-(2-bromoacetyl)benzonitrile (18mg, 0.079 mmol) in anhydrous acetonitrile (10 mL), triethylamine (0.012 mL, 0.0805 mmol) was added. The reaction mixture was heated at 70°C for 30 min to obtain compound **13B** as a brown solid. Yield 41 %, mp: 113-115°C; FT-IR: (KBr, cm^{-1}) 3300 (N-H stretch), 1701, 1679 (keto, C=O stretch), 1660 (amide, C=O stretch); ^{1}H NMR (DMSO d_6) *δ*: 8.90 (t, *J* = 8.0 Hz ,1H), 8.41 (s, 1H), 8.02 (d, *J* = 8.0 Hz, 2H), 7.41 – 7.27 (m, 6H), 7.25 (d, *J* = 7.2 Hz, 2H), 7.09 (d, *J* = 8.8 Hz, 2H), 5.40 (s, 2H), 4.93 (s, 2H), 3.86 (s, 2H), 3.32 - 3.27 (dd, *J* = 13.2, 6.4 Hz, 2H), 2.60 (t, *J* = 7.4 Hz, 2H), 1.83 – 1.75 (m, 2H); ^{13}C NMR (DMSO d_6) *δ*: 190.52, 166.09, 163.55, 161.99, 161.02, 155.05, 141.41, 134.25, 130.73, 128.67, 128.45, 128.26, 128.21, 127.71,

126.90, 125.72, 114.06, 112.35, 55.61, 47.84, 38.22, 33.84, 32.50, 31.64, 30.67; ESI MS: m/z = 528.2 [M + 1 H]$^+$.

1-Benzyl-6-oxo-2-(2-oxo-2-(2-(2-phenylacetyl)hydrazinyl)ethylthio)-*N*-(3-phenylpropyl)-1,6-dihydropyrimidine-5-carboxamide (13C / RMH-3)

Compound **13C** was synthesized using the method as described for compound **13A**, starting from compound **12** (30 mg, 0.079 mmol) and compound **3** (17 mg, 0.079 mmol) in anhydrous acetonitrile (10 mL), triethylamine (0.012 mL, 0.087 mmol) was added. The reaction mixture was heated at 85°C for 20 min to obtain compound **13C** as a white solid compound. Yield 30 %, mp: 180-182°C; FT-IR: (KBr, cm^{-1}) 3473, 3269 (N-H stretch), 1737, 1701 (keto, C=O stretch), 1648 (amide, C=O stretch); ^{1}H NMR (400 MHz, DMSO d_6) *δ*: 10.21 (s, 1H), 8.96 (t, *J* = 6.0 Hz, 1H), 8.56 (s, 1H), 7.40 – 7.16 (m, 15H), 5.34 (s, 2H), 4.06 (s, 2H), 3.46 (s, 2H), 3.30 (dd, *J* = 13.0, 6.6 Hz, 2H), 2.61 (t, *J* = 7.6 Hz, 3H), 1.85 – 1.77 (m, 2H); ^{13}C NMR (DMSO d_6) *δ*: 169.04, 166.01, 165.29, 162.31, 161.25, 155.43, 141.54, 135.67, 134.27, 129.13, 128.85, 128.44, 128.37, 127.01, 126.66, 125.91, 112.49, 47.89, 34.38, 32.64, 30.81; ESI MS: m/z = 570.2 [M + 1 H]$^+$.

1-Benzyl-2-(2-morpholinoethylthio)-6-oxo-*N*-(3-phenylpropyl)-1,6-dihydropyrimidine-5-carboxamide (13D / RMH-4)

Compound **13D** was synthesized using the method as described for compound **13A**, starting from compound **12** (40 mg, 0.10 mmol) and 4-(2-chloroethyl)morpholine (19 mg, 0.10 mmol) in anhydrous acetonitrile (10 mL), triethylamine (0.038 mL, 0.26 mmol) was added. The reaction mixture was heated at 80°C for 60 min to obtain compound **13D** as a yellow solid. Yield 38 %, mp: 99-101°C; FT-IR: (KBr, cm^{-1}) 3300 (N-H stretch), 1732, (keto, C=O stretch), 1635 (amide, C=O stretch); ^{1}H NMR (400 MHz, MeOD) *δ*: 8.67 (s, 1H), 7.36 – 7.11 (m, 10H), 5.40 (s, 2H), 3.68 – 3.62 (m, 4H), 3.48 - 3.37 (m, 4H), 2.72 – 2.65 (m, 4H), 2.53 – 2.46 (m, 4H), 1.95 - 1.86 (m, 2H); ^{13}C NMR (MeOD) *δ*: 169.15, 165.49, 163.27, 157.14, 142.76, 135.74, 129.79, 129.48, 129.47, 129.01, 128.48, 128.47, 126.97, 113.19, 67.81, 58.02, 54.51, 39.89, 34.23, 32.21, 30.64; ESI MS: m/z = 493.2 [M + 1 H]$^+$.

Ethyl2-(1-benzyl-6-oxo-5-(3-phenylpropylcarbamoyl)-1,6-dihydropyrimidin-2-ylthio)acetate (13E / RMH-5)

Compound **13E** was synthesized using the method as described for compound **13A**, starting from compound **12** (100 mg, 0.26 mmol) and ethyl 2-bromoacetate (0.032 ml, 0.29 mmol) in

anhydrous acetonitrile (10 mL), triethylamine (0.042 mL, 0.29 mmol) was added. The reaction mixture was heated at 70°C for 20 min to obtain compound **13E** as a white solid. Yield 41 %, mp: 72-74°C; FT-IR: (KBr, cm^{-1}) 3321 (N-H stretch), 1698, 1679 (ester, C=O stretch), 1639 (amide, C=O stretch); ^{1}H NMR (400 MHz, MeOD) *δ*: 8.61 (s, 1H), 7.35 – 7.11 (m, 10H), 5.41 (s, 2H), 4.18 (q, *J* = 7.2 Hz, 2H), 4.08 (s, 2H), 3.39 (t, *J* = 7.0 Hz, 2H), 2.70 - 2.64 (m, 2H), 1.92 – 1.88 (m, 2H), 1.24 (t, *J* = 7.2Hz, 3H); ^{13}C NMR (MeOD) *δ*: 165.23, 163.02, 156.85, 142.77, 135.44, 129.81, 129.44, 129.43, 129.09, 128.47, 126.93, 113.59, 63.05, 39.89, 34.19, 32.12, 14.44; ESI MS: m/z = 466.1 [M + 1 H]$^+$.

1-Benzyl-2-(2-(4-(diethylamino)phenyl)-2-oxoethylthio)-6-oxo-*N*-(3-phenylpropyl)-1,6-dihydropyrimidine-5-carboxamide (13F / RMH-6)

Compound **13F** was synthesized using the method described for compound **13A**, starting from compound **12** (50 mg, 0.13 mmol) and 2-bromo-1-(4-(diethylamino)phenyl)ethanone (35 mg, 0.13 mmol) in anhydrous acetonitrile (10 mL), triethylamine (0.019 mL, 0.13 mmol) was added. The reaction mixture was heated at 70°C for 30 min to obtain compound **13F** as a white solid. Yield 20 %, mp: 146-148°C; FT-IR: (KBr, cm^{-1}) 3344 (N-H stretch), 1722, 1710 (keto, C=O stretch), 1648 (amide, C=O stretch); ^{1}H NMR (400 MHz, DMSO *d*$_6$) *δ*: 8.93 (t, *J* = 5.6 Hz, 1H), 8.46 (s, 1H), 7.84 (d, *J* = 8.8 Hz, 2H), 7.42 – 7.16 (m, 10H), 6.72 (d, *J* = 9.2 Hz, 2H), 5.40 (s, 2H), 4.85 (s, 2H), 3.46 - 3.40 (m, 4H), 3.28 (dd, *J* = 13.0, 6.6 Hz, 2H), 2.62 - 256 (m, 2H), 1.85 - 1.74 (m, 2H), 1.12 (t, *J* = 7.0 Hz, 6H); ^{13}C NMR (DMSO *d*$_6$) *δ*: 189.43, 167.13, 162.85, 161.75, 151.99, 142.08, 134.92, 131.52, 129.37, 128.96, 128.90, 127.54, 126.43, 122.66, 112.85, 110.90, 44.57, 33.16, 31.34, 12.98; ESI MS: m/z = 569.2 [M + 1 H]$^+$.

1-Benzyl-2-(2-(4-hydroxyphenyl)-2-oxoethylthio)-6-oxo-*N*-(3-phenylpropyl)-1,6-dihydropyrimidine-5-carboxamide (13G / RMH-7)

Compound **13G** was synthesized using the method as described for compound **13A**, starting from compound **12** (40 mg, 0.10 mmol) and 2-bromo-1-(4-hydroxyphenyl)ethanone (24 mg, 0.10 mmol) in anhydrous acetonitrile (10 mL), triethylamine (0.015 mL, 0.11 mmol) was added. The reaction mixture was heated at 60°C for 70 min to obtain **13G** as a white solid. Yield 46 %, mp: 171-173°C; FT-IR: (KBr, cm^{-1}) 3203 (N-H stretch), 1701, 1688 (keto, C=O stretch), 1636 (amide, C=O stretch); ^{1}H NMR (400 MHz, CDCl$_3$) *δ*: 9.30 (t, *J* = 5.8 Hz, 1H), 8.81 (brs, 1H), 8.67 (s, 1H), 7.97 (d, *J* = 8.8 Hz, 2H), 7.46 – 7.00 (m, 12H), 5.44 (s, 2H), 4.78 (s, 2H), 3.46 (dd, *J* = 13.2, 6.4 Hz, 2H), 2.71 (t, *J* = 7.8 Hz, 2H), 2.00 – 1.91 (m, 2H); ^{13}C NMR (CDCl$_3$) *δ*: 189.10, 165.38, 162.85, 161.54, 160.83, 155.22, 140.32, 132.51,

130.16, 127.89, 127.41, 127.39, 127.34, 126.70, 124.94, 114.87, 111.21, 47.41, 40.12, 38.19, 32.21, 29.92; ESI MS: m/z = 514.1 [M + 1 H]$^+$.

1-Benzyl-2-(2-(4-cyanophenyl)-2-oxoethylthio)-6-oxo-*N*-(3-phenylpropyl)-1,6-dihydropyrimidine-5-carboxamide (13H / RMH-8)

Compound **13H** was synthesized using the method as described for compound **13A**, starting from compound **12** (35 mg, 0.092 mmol) and 4-(2-bromoacetyl)benzonitrile (20mg, 0.092 mmol) in anhydrous acetonitrile (10 mL), triethylamine (0.01 mL, 0.10 mmol) was added. The reaction mixture was heated at 70°C for 30 min to obtain **13H** as a white solid. Yield 50 %, mp: 114-116°C; FT-IR: (KBr, cm^{-1}) 3323 (N-H stretch), 1715, 1701 (keto, C=O stretch), 1644 (amide, C=O stretch); ^{1}H NMR (400 MHz, DMSO d_6) δ: 8.87 (t, *J* = 5.8 Hz, 1H), 8.35 (s, 1H), 8.16 (d, *J* = 8.4 Hz, 2H), 8.05 (d, *J* = 8.0 Hz, 2H), 7.40 – 7.13 (m, 9H), 5.38 (s, 2H), 4.95 (s, 2H), 3.32 - 3.24 (dd, *J* = 13.2, 7.0 Hz, 2H), 2.58 (t, *J* = 7.8 Hz, 2H), 1.83 – 1.75 (m, 2H); ^{13}C NMR (DMSO d_6) δ: 192.24, 165.58, 161.85, 161.85, 160.88, 155.05, 141.33, 139.03, 134.09, 132.77, 128.79, 128.61, 128.18, 128.14, 127.67, 126.83, 126.59, 125.65, 117.98, 115.39, 112.42, 47.85, 38.16, 32.41, 30.58; ESI MS: m/z = 523.2 [M + 1 H]$^+$.

1-Benzyl-2-(2-morpholino-2-oxoethylthio)-6-oxo-*N*-(3-phenylpropyl)-1,6-dihydropyrimidine-5-carboxamide compound (13I / RMH-9)

Compound **13I** was synthesized using the method as described for compound **13A**, starting from compound **12** (40 mg, 0.010 mmol) and 2-bromo-1-morpholinoethanone (17 mg, 0.010 mmol) in anhydrous acetonitrile (10 mL), triethylamine (0.018 mL, 0.21 mmol) was added. The reaction mixture was heated at 75°C for 30 min to obtain **13I** as a white solid. Yield 40 %, mp: 37-39°C; FT-IR: (KBr, cm^{-1}) 3361 (N-H stretch), 1735, 1700 (keto, C=O stretch), 1650 (amide, C=O stretch); ^{1}H NMR (400 MHz, DMSO d_6) δ: 8.93 (t, *J* = 5.8 Hz, 1H), 8.56 (s, 1H), 7.43 – 7.10 (m, 9H), 5.36 (s, 2H), 4.35 (s, 2H), 3.65 - 3.58 (m, 2H), 3.57 - 3.50 (m, 4H), 3.46 - 3.40 (m, 2H), 3.29 (dd, *J* = 13.4, 7.4 Hz, 2H), 2.61 (t, *J* = 7.6 Hz 2H), 1.85-1.75 (m, 2H); ^{13}C NMR (DMSO d_6) δ: 166.24, 164.70, 162.03, 160.92, 141.28, 134.14, 128.58, 128.19, 128.14, 127.59, 126.78, 125.66, 112.34, 65.85, 47.69, 45.81, 42.05, 38.20, 35.86, 32.43, 30.54, 18.11; ESI MS: m/z = 507.2 [M + 1 H]$^+$.

Ethyl 6-oxo-2-(2-oxo-2-(2-(2-phenylacetyl)hydrazinyl)ethylthio)-1,6-dihydropyrimidine-5-carboxylate (15a / RMH-10)

A mixture of ethyl 4-oxo-2-thioxo-1,2,3,4-tetrahydropyrimidine-5-carboxylate **14** (100 mg, 0.50 mmol), 2-chloro-N'-(2-phenylacetyl)acetohydrazide **3** (112 mg, 0.50 mmol) and potassium carbonate (69 mg, 0.5 mmol) were stirred together in anhydrous acetone (3 mL) at room temperature for 16 h. Completion of the reaction was confirmed by TLC. Solvent was evaporated and the reaction content was poured in cold water (5 mL), led to the production of precipitate, washed with water (1 x 10 mL), diethy ether (1 x 10 mL) and then dried under reduced pressure to furnish the pure compound **15a** as a white solid. Yield 60 %, mp: 130-132°C; FT-IR: (KBr, cm^{-1}) 3184 (N-H stretch), 1701 (keto, C=O stretch), 1668 (ester, C=O stretch); ^{1}H NMR (400 MHz, DMSO d_6) $δ$: 10.23 (s, 2H), 8.39 (s, 1H), 7.27 (m, 5H), 4.19 (q, J = 7.06 Hz, 2H), 3.97 (s, 2H), 3.47 (s, 2H), 1.25 (t, J = 7.06 Hz, 3H); ^{13}C NMR (DMSO d_6) $δ$: 168.72, 167.58, 165.82, 163.95, 157.90, 135.54, 129.38, 129.03, 128.92, 128.21, 128.12, 127.94, 126.53, 126.41, 126.19, 110.94, 60.07, 32.12, 14.06; ESI MS: m/z = 391.0 [M + 1 H]$^+$.

Ethyl-2-(2-morpholinoethylthio)-6-oxo-1,6-dihydropyrimidine-5-carboxylate 15b / RMH-11)

A mixture of ethyl 4-oxo-2-thioxo-1,2,3,4-tetrahydropyrimidine-5-carboxylate **14** (100 mg, 0.50 mmol), 4-(2-bromoethyl)morpholine (111 mg, 0.60 mmol) and potassium carbonate (207 mg, 1.5 mmol), were stirred together in anhydrous *N,N*-dimethylformamide (3 mL) at room temperature for 16 h. Completion of the reaction was confirmed by TLC. The reaction content was poured on to cold water (5 mL), and extracted with ethyl acetate (3 x 10 mL). The organic layers were combined together, washed with brine (1 x 10 mL), dried over anhydrous sodium sulfate and evaporated the solvent under reduced pressure to furnish the crude compound, which was purified by column chromatography using dichloromethane and methanol (90:10) as a mobile phase to obtain compound **15b** as a white solid. Yield 60 %, mp: 89-91°C; FT-IR: (KBr, cm^{-1}) 3178 (N-H stretch), 1700 (keto, C=O stretch), 1675 (ester, C=O stretch); ^{1}H NMR (400 MHz, MeOD) $δ$: 8.48 (s, 1H), 4.30 (q, J = 7.2 Hz, 2H), 3.94 – 3.86 (m, 4H), 3.39 (t, J = 6.3 Hz, 2H), 3.09 (t, J = 6.3 Hz, 2H), 2.96 – 2.92 (m, 4H), 1.34 (t, J = 7.2 Hz, 3H); ^{13}C NMR (MeOD) $δ$: 166.17, 163.12, 156.21, 113.01, 66.47, 61.10, 59.88, 55.12, 54.16, 27.59, 14.56; ESI MS: m/z = 314.1 [M + 1 H]$^+$.

Ethyl 2-(2-morpholinoethylthio)-6-oxo-1-(2-oxo-2-phenylethyl)-1,6-dihydropyrimidine-5-carboxylate (16 / RMH-12)

A mixture of **RMH-11** (100 mg, 0.31 mmol), 2-bromo-1-phenylethanone (69 mg, 0.34 mmol) and potassium carbonate (43 mg, 0.31 mmol), were stirred together in anhydrous acetone (3 mL) at room temperature for 16 h. Completion of the reaction was confirmed by TLC. The reaction content was poured in cold water (5 mL), and extracted with ethyl acetate (3 x 10 mL). The organic layers were combined together, washed with brine (1 x 10 mL), dried over anhydrous sodium sulfate and evaporated the solvent under reduced pressure to furnish the crude compound, which was purified by column chromatography using dichloromethane and methanol (95:5) as a mobile phase to obtain compound **16** as a white solid. Yield 65 %, mp: 110-112°C; FT-IR: (KBr, cm^{-1}) 3198 (N-H stretch), 1722, 1705 (keto, C=O stretch), 1680 (ester, C=O stretch,); ^{1}H NMR (400 MHz, MeOD) δ: 8.82 (s, 1H), 8.05 (d, J = 7.2 Hz, 2H), 7.70 (t, J = 7.2 Hz, 1H), 7.57 (t, J = 7.2 Hz, 2H), 5.91 (s, 2H), 4.38 (q, J = 7.1 Hz, 2H), 3.56 – 3.52 (m, 4H), 3.09 – 3.05 (m, 2H), 2.48 – 2.44 (m, 6H), 1.39 (t, J = 7.1 Hz, 3H); ^{13}C NMR (MeOD) δ: 194.22, 176.64, 167.54, 164.56, 161.65, 135.57, 135.26, 130.15, 129.11, 108.62, 70.01, 67.60, 62.44, 58.49, 54.32, 28.77, 14.54; ESI MS: m/z = 432.1 [M + 1 H]$^+$.

2-(2-Morpholinoethylthio)-6-oxo-*N*-(3-phenylpropyl)-1,6-dihydropyrimidine-5-carboxamide (17 / RMH-13)

A stirred solution of trimethylaluminum (0.16 ml, 0.31 mmol, 2 M solution in toluene) in anhydrous dichloromethane (5 ml) was treated with compound **RMH-11** (50 mg, 0.15 mmol), dissolved in 20 ml of anhydrous dichloromethane, at 0° C. After stirring for 30 min, 3-phenylpropylamine (42 mg, 0.31 mmol) in anhydrous dichloromethane (5 ml) was added and the mixture was stirred overnight (12 h) at room temperature. The reaction mixture was then quenched with sodium hydroxide (0.1N) at 0° C. The organic layer was separated, washed with water (15 ml), brine (15 ml) and dried over anhydrous sodium sulphate. The solvent was evaporated under reduced pressure to furnish the crude compound, which was purified by column chromatography (dichloromethane and methanol gradient), to give the compound **17** as a white solid. Yield 60 %, mp: 77-79°C; FT-IR: (KBr, cm^{-1}) 3212 (N-H stretch), 1710 (keto, C=O stretch), 1640 (amide, C=O stretch); ^{1}H NMR (400 MHz, MeOD) δ: 8.54 (s, 1H), 7.26 – 7.22 (m, 4H), 7.17 – 7.13 (t, J = 7.1 Hz, 1H), 3.91 – 3.87 (m, 4H), 3.40 – 3.36 (m, 4H), 3.12 (t, J = 6.5 Hz, 2H), 2.99 – 2.95 (m, 4H), 2.73 – 2.69 (m, 2H), 1.93 – 1.89 (m, 2H); ^{13}C NMR (MeOD) δ: 170.23, 169.21, 167.02, 157.23, 142.80, 129.46, 129.45, 129.43, 126.93, 112.37, 66.40, 39.49, 34.15, 32.33, 27.62; ESI MS: m/z = 403.1 [M + 1 H]$^+$.

2-(Morpholinomethyl)-6-oxo-3-phenyl-4,6-dihydropyrimido[2,1-b][1,3]thiazine-7-carboxylic acid (18 / RMH-14)

To a solution of compound **16** (100 mg, 0.23 mmol) in THF/MeOH (3/1), LiOH (2.0 equiv) was added at room temperature and allowed to stir for 16 h (overnight). The organic solvents were removed under reduced pressure and water (5.0 mL) was added to the residue. The aqueous layer was acidified to pH 5, to afford the compound **18**, which was filtered off, washed with water (10.0 mL) and dried under vacuum to obtain as a brown solid compound. Yield 40 %, mp: 176-178°C; FT-IR: (KBr, cm^{-1}) 1725 (acid, C=O stretch), 1712 (keto, C=O stretch); ^{1}H NMR (400 MHz, MeOD) δ: 8.54 (s, 1H), 7.25 - 7.19 (m, 5H), 3.93 – 3.89 (m, 4H), 3.41 – 3.37 (m, 4H), 3.15 (t, J = 6.5 Hz, 2H), 2.72 – 2.68 (m, 2H); ^{13}C NMR (MeOD) δ: 154.77, 137.07, 135.10, 134.50, 130.43, 129.74, 110.79, 65.07, 57.47, 53.55, 25.62; ESI MS: m/z = 386.1 [M + 1 H]$^{+}$.

4.3.7. Purity data

From series IV-VII, compounds that have exhibited good activity (**Section 5** Results and Discussion) against proteases, were assessed further for purity using HPLC, as representative samples .

The HPLC elution methods used for the purity computation are as follows:

Method A: 5-95% CH_3CN-0.05% Trifluoroacetic acid (TFA) in H_2O-0.05% (TFA)

Method B: 10-95% CH_3CN-0.05%TFA in H_2O-0.05%TFA

Method C: 30-98% CH_3CN-0.05%TFA in H_2O-0.05%TFA

Method D: 20-80% MeOH-0.05%TFA in H_2O-0.05%TFA

Method E: 0-98% CH_3CN-0.05%TFA in H_2O-0.05%TFA

Method F: 10-98% CH_3CN-0.05%TFA in H_2O-0.05%TFA

Method G: 50-98% CH_3CN-0.05%TFA in H_2O-0.05%TFA

Method H: 20-80% MeOH-0.05%TFA in H_2O-0.05%TFA

Method I: 50-98% MeOH-0.05%TFA in H_2O-0.05%TFA

Method J: 0-98% MeOH-0.05%TFA in H_2O-0.05%TFA

Method K: 30-98% MeOH-0.05%TFA in H_2O-0.05%TFA

Method L: 30-60% CH_3CN-0.05%TFA in H_2O-0.05%TFA

Method M: 40-98% MeOH-0.05%TFA in H_2O-0.05%TFA

Table 5: HPLC purity data for compounds RMQ 12 to 19*

Compound	Method 1*			Method 2*		
	Protocol	**RT**	**Purity (%)**	**Protocol**	**RT**	**Purity (%)**
RMQ-12	A	6.45	97.2	C	3.30	99.0
RMQ-13	A	7.81	99.0	D	3.13	99.0
RMQ-14	A	8.44	99.9	D	3.87	99.9
RMQ-15	B	8.93	99.9	E	6.13	99.9
RMQ-16	A	8.51	99.0	D	3.92	99.0
RMQ-17	B	8.72	99.0	E	5.58	99.9
RMQ-18	B	5.14	99.9	E	9.2	99.9
RMQ-19	B	6.46	99.0	D	5.03	99.0

*Run time:10 min, Method: Gradient

Table 6: HPLC purity data for compounds RMP 1 to 15, RMH 1 to 5, RMH-10, RMH-12 and RMH-13

Sr. N.	Compound	Method 1*			Method 2*		
		Protocol	RT	Purity (%)	Protocol	RT	Purity (%)
1	RMP-1	J	7.41	98.8	K	4.63	98.9
2	RMP-2	G	3.85	96.6	L	6.45	96.3
3	RMP-3	J	7.08	95.1	E	6.61	99.0
4	RMP-4	J	8.47	97.1	K	6.09	97.3
5	RMP-5	J	7.41	98.8	K	4.63	98.9
6	RMP-6	M	9.73	99.0	J	6.93	99.0
7	RMP-7	M	3.69	97.0	K	7.59	97.2
8	RMP-8	I	5.70	97.8	J	8.75	98.2
9	RMP-9	I	6.21	97.2	J	8.35	98.1
10	RMP-10	H	4.51	99.1	E	7.81	99.0
11	RMP-11	K	8.19	98.4	J	8.95	98.6
12	RMP-12	J	6.18	97.1	I	4.34	97.7
13	RMP-13	I	6.70	97.4	J	8.15	98.2
14	RMP-14	I	6.11	96.1	J	8.25	95.4
15	RMP-15	I	6.21	99.9	J	8.35	99.0
16	RMH-1	J	8.93	97.1	I	5.90	97.6
17	RMH-2	J	8.02	96.1	I	5.93	95.4
18	RMH-3	K	8.09	98.8	J	10.23	98.6
19	RMH-4	J	6.68	97.1	I	4.34	97.7
20	RMH-5	I	5.70	97.8	J	8.75	98.2
21	RMH-10	C	3.00	99.1	F	4.60	99.0
22	RMH-12	F	4.97	99.1	C	3.58	99.0
23	RMH-13	F	4.74	99.1	C	3.32	99.0

*Run time:10 min, Method: Gradient

4.3.8. Interfeature distances measurement

Based on proposed pharmacophore model **(Figure 15)**, the distances between the centroid of the aromatic residue to a hydrophobic residue, centroid of the aromatic residue to linker (HBA/HBD) and centroid of hydrophobic group to linker (HBA/HBD) were measured. The observed distances between the pharmacophoric elements of all the designed NCE's (Series I-III) in accordance with the designed pharmacophoric model as desirerd.

Table 7: Distances between the pharmacophoric elements of RM 1 to 20*

Sr. N.	Compound	Centroid of aromatic residue–hydrophobic residue (Å)	Centroid of aromatic residue–HBA/HBD (Å)	Centroid of hydrophobic residue-HBA/HBD (Å)
1	RM-1	13.01-13.05	8.53-8.55	8.38-8.40
2	RM-2	13.14-13.15	8.28-8.30	8.14-8.15
3	RM-3	13.04-13.09	8.14-8.15	8.16-8.17
4	RM-4	13.05-13.07	8.25-8.26	8.18-8.19
5	RM-5	13.04-13.06	8.22-8.23	8.12-8.14
6	RM-6	13.18-13.19	8.16-8.18	8.01-8.07
7	RM-7	13.17-13.18	8.11-8.12	8.12-8.13
8	RM-8	12.99-13.00	8.32-8.34	8.34-8.36
9	RM-9	13.01-13.02	8.18-8.19	8.14-8.16
10	RM-10	12.98-13.00	8.03-8.04	8.11-8.12
11	RM-11	13.27-13.29	8.17-8.19	8.06-8.08
12	RM-12	13.28-13.29	8.11-8.13	8.31-8.32
13	RM-13	11.86-11.88	8.77-8.78	8.15-8.17
14	RM-14	11.90-11.91	8.62-8.63	8.18-8.21
15	RM-15	11.87-11.88	8.15-8.16	8.32-8.33
16	RM-16	12.01-12.02	8.62-8.63	8.22-8.23
17	RM-17	12.82-12.83	8.88-8.89	8.09-8.11
18	RM-18	12.97-12.99	8.91-8.93	8.32-8.34
19	RM-19	12.03-12.04	8.32-8.33	8.44-8.45
20	RM-20	12.87-12.89	8.13-8.14	8.15-8.16

*Average Distances calculated for 3D optimized structures at least for each three conformations using CHARMM Parametrization (ACDLABS-10.0/3D Viewer) and the values are represented in Å.

Table 8: Distances between the pharmacophoric elements of RMS 1 to 20*

Sr. N.	Compound	Centroid of aromatic residue–hydrophobic residue (Å)	Centroid of aromatic residue–HBA/HBD (Å)	Centroid of hydrophobic residue-HBA/HBD (Å)
1	RMS-1	13.11-13.14	8.78-8.80	8.45-8.46
2	RMS-2	13.24-13.26	8.38-8.39	8.16-8.19
3	RMS-3	13.19-13.21	8.19-8.20	8.22-8.23
4	RMS-4	13.22-13.24	8.42-8.43	8.11-8.15
5	RMS-5	13.04-13.05	8.37-8.38	8.09-8.10
6	RMS-6	13.08-13.10	8.08-8.11	8.22-8.24
7	RMS-7	12.87-12.89	8.11-8.12	8.43-8.44
8	RMS-8	12.89-12.90	8.55-8.56	8.26-8.27
9	RMS-9	13.21-13.24	8.19-8.21	8.64-8.65
10	RMS-10	13.38-13.40	8.78-8.80	8.16-8.17
11	RMS-11	13.21-13.23	8.62-8.63	8.08-8.10
12	RMS-12	13.20-13.21	8.18-8.19	8.32-8.36
13	RMS-13	12.91-12.93	8.20-8.21	8.10-8.11
14	RMS-14	11.21-11.23	8.36-8.39	8.52-8.53
15	RMS-15	11.51-11.53	8.85-8.86	8.35-8.36
16	RMS-16	12.20-12.22	8.14-8.15	8.23-8.24
17	RMS-17	12.91-12.93	8.25-8.26	8.16-8.17
18	RMS-18	12.91-12.94	8.66-8.67	8.19-8.20
19	RMS-19	12.04-12.06	8.52-8.55	8.64-8.65
20	RMS-20	12.81-12.83	8.22-8.23	8.38-8.39

*Average Distances calculated for 3D optimized structures at least for each three conformations using CHARMM Parametrization (ACDLABS-10.0/3D Viewer) and the values are represented in Å.

Table 9: Distances between the pharmacophoric elements of RMT 1 to 20*

Sr. N.	Compound	Centroid of aromatic residue–hydrophobic residue (Å)	Centroid of aromatic residue–HBA/HBD (Å)	Centroid of hydrophobic residue-HBA/HBD (Å)
1	RMT-1	13.01-13.04	8.89-8.90	8.92-8.96
2	RMT-2	11.90-11.92	8.69-8.70	8.89-8.90
3	RMT-3	11.87-11.89	8.65-8.66	8.74-8.77
4	RMT-4	12.01-12.05	8.92-8.93	8.65-8.67
5	RMT-5	13.04-13.06	8.62-8.63	8.59-8.61
6	RMT-6	13.18-13.21	8.55-8.56	8.87-8.90
7	RMT-7	13.14-13.17	8.71-8.76	8.49-8.51
8	RMT-8	13.04-13.07	8.77-8.80	8.45-8.47
9	RMT-9	13.05-13.08	8.78-8.82	8.72-8.73
10	RMT-10	12.87-12.90	8.69-8.70	8.81-8.87
11	RMT-11	13.27-13.30	8.52-8.53	8.66-8.68
12	RMT-12	13.28-13.29	8.56-8.57	8.47-8.50
13	RMT-13	11.86-11.87	8.62-8.63	8.62-8.64
14	RMT-14	12.20-12.22	8.59-8.60	8.55-8.57
15	RMT-15	12.91-12.93	8.65-8.66	8.88-8.90
16	RMT-16	12.91-12.93	8.32-8.34	8.64-8.69
17	RMT-17	12.82-12.85	8.49-8.50	8.28-8.29
18	RMT-18	12.97-13.00	8.65-8.67	8.65-8.66
19	RMT-19	12.03-12.04	8.85-8.89	8.44-8.46
20	RMT-20	12.03-12.04	8.64-8.67	8.66-8.68

*Average Distances calculated for 3D optimized structures at least for each three conformations using CHARMM Parametrization (ACDLABS-10.0/3D Viewer) and the values are represented in Å.

4.4. Pharmacology

4.4.1. Basic principle of florescence for *in vitro* assay

The most widely used fluorescence-based assay to measure proteases activity is shown in **Figure 19**, which includes (a) measuring the change in fluorescence signal of a fluorophore; chemically quenched by enzyme to the substrate, (b) measuring the change in fluorescent signal, via a resonance energy transfer (FRET) system, (c) measuring the change in fluorescent signal intensity from a fluorescent substrate, quenched by a near-by inhibitors
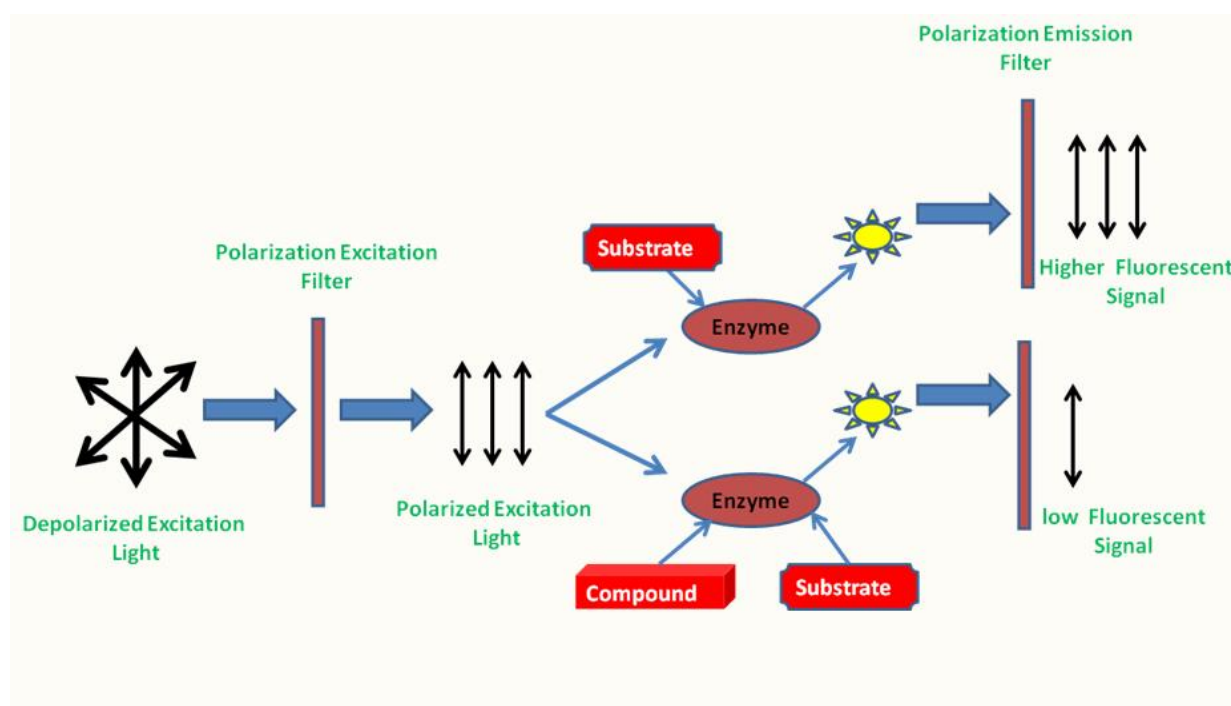
Figure 19: Binding assay using peptide displacement monitored by fluorescence polarization

4.4.1.1. Fluorometric assay for falcipain-2 inhibition:

The inhibitory potency of novel molecules were analyzed by their ability to block the activity of falcipain-2. The protocol for the purification and refolding of recombinant protein falcipain-2 as described by Shenai et al., 2000 and Korde et al., 2008, were followed. For screening of falcipain-2 inhibitors, a 96-well plate fluorometric assay was developed, following the protocol described by Kumar et al., 2004. Briefly, a mixture containing 100 mM NaOAc, 10 mM DTT, 6 µM of the enzyme and different concentrations of inhibitors, pH 5.5, 10 mM of fluorogenic substrate benzyloxycarbonyl-Phe-Arg-7-amino-4-methylcoumarin hydrochloride (ZFR-AMC), were added. The release of 7-amino-4-methylcoumarin (AMC) was monitored

using an excitation wavelength 355 nm and emission at 460 nm wavelength, over 30 min at RT in Perkin Elmer Victor3 multi-label counter. Activities were compared as fluorescence released over time, in assay with or without, different concentration of each compound, tested.

The inhibition rate (%) is calculated using the given equation:

% Inhibition = [1 - ('*F*'-test / '*F*'-standard)] × 100 $\longrightarrow$ | **Equation-1** |

Where 'F'-test is the fluorescence intensity of the test compound, 'F'-standard is the fluorescence intensity of a standard compound (E64). All values are represented as average of three independent determinations, and the deviations are <10 % of the average value. The IC_{50} values were calculated from curve fittings using Workout V 2.5 software.

4.4.1.2. Fluorometric assay for ClpP protease inhibition

The protocol for the purification and refolding of recombinant protein *Pf*ClpP as described by Houry et al., 2010, was followed. For screening of ClpP inhibitors, a 96-well plate fluorometric assay was developed, following a protocol described by Rathore et al., 2010. Briefly, in 200 µl reaction volume, containing 13 µM of the recombinant enzyme in buffer (0.1 M sodium acetate and 1.0 mM DTT at pH 7.0), with presence of different concentrations of an inhibitor, fluorogenic peptide substrate Suc-LLVY-AMC was added at 50 µM final concentrations. The release of AMC was continuously monitored as change of fluorescence using excitation wave length at 355 nm and emission wave length at 460 nm, for 3-6 h at RT in a Perkin Elmer Victor3 multi-label counter. Activities were compared as fluorescence released over time, in assay with or without, different concentration of each compound, tested. IC_{50} values were calculated by software Workout V 2.5.

4.4.1.3. *P. falciparum* growth inhibition assay

P. falciparum strain 3D7 was cultured with human erythrocytes (4% hematocrit) in RPMI media (Invitrogen) supplemented with 0.5% albumax and 4% hematocrit using a protocol described by Trager and Jensen, 2010. Cultures were synchronized by repeated sorbitol treatment following Lambros and Vanderberg (1979) protocol. Each growth inhibition assay was performed in triplicate, and the experiment was repeated twice. Each well contained 0.5 mL of complete media (RPMI (Invitrogen) with 0.5% albumax), 4% hematocrit, and parasitemia adjusted to 1%. The compound(s) was added to the parasite cultures at desired final concentrations (0–100 µM), and same amount of solvent (DMSO) was added to the

control wells. The cultures were allowed to grow for 48 h. Parasite growth was assessed by DNA fluorescent dye-binding assay using SYBR green (Sigma) following Smilkstein et al., 2004 procedure.

4.4.2. Statistical analysis

Statistical analyses were done by using Graph pad prism (version 3) software and Microsoft Office Excel (MS Office 2003). The results of falcipain-2 inhibition for **Series I to III**, are expressed as the average percentage inhibition for three independent experiments and standard deviations are <10% of the average value. The results for **Series IV to VI** are expressed in IC_{50} values as mean ± standard deviation.

4.4.3. Docking studies

To understand the structural basis for the activities of the inhibitors and to support the *in vitro* activity results, the binding models of the top active analogs as shown by **Figure 20 (A-C)**, was studied with falcipain-2 enzyme using Glide 5.9 (Schrodinger, LLC, New York, NY, 2013) running on maestro version 9.4 installed in a machine on Intel Xenon W 3565 processor and Cent OS Linux Enterprise version 6.3 as the operating system (Friesner et al., 2004; Halgren et al., 2004).

The crystal structure of falcipain-2 (PDB entry 3BPF) from *P. falciparum* was retrieved from the Protein Database Bank with a resolution of 2.9 Å. The downloaded FP-2 protein carries four chains named A, B, C, and D; complexed with epoxysuccinate E64 (Wang et al., 2000). The catalytic triad of Cys 42, Asn 173 and Hip 174 is located in the cleft between the two structurally distinct domains (Wang et al., 2014). Protein preparation module of Schrodinger suite was used for protein preparation. Proteins were pre-processed separately by deleting the substrate co-factor as well as the observed water molecules were removed from the coordinate set, followed by optimization of hydrogen bonds. Charge and protonation state was assigned and energy was minimized with Root Mean Square Deviation (RMSD) value of 0.3 Å using Optimized Potentials for Liquid Simulations-2005 (OPLS-2005) force field (Jorgensen et al., 1996). Potential of non-polar parts of receptors was softened by scaling van der Walls radii of ligand atoms by 1.00 Å to generate the grid. Analogs and standard drug E-64 structures were drawn using ChemSketch and converted to 3D structure with the help of 3D optimization tool. LigPrep module was used to optimize the geometry of the drawn ligands. The prepared ligands were docked with proteins using extra precision mode (XP). The best docked pose obtained from Glide was analyzed.

Validation of docking protocol was done to govern the reproducibility and reliability of the docking parameters used for the study. In the present study, validation of the docking was done by removing co-crystallized ligand E-64 from the active site and subjecting it again to dock into the binding pocket in the conformation found in the crystal structure **(Figure 20 D)**. Furthermore, a set of studies were performed to compute the RMSD value between the pose of co-crystallized inhibitor present in the enzyme and its best ranked pose, in the protein. As a result, the RMSD value calculated for co-crystallized ligand, E-64 was 1.68 Å against the target enzyme. The best scoring pose of the reference drug inside the FP-2 showed that interactions, are in resemblance with the reported X-ray pose interactions. These results suggested that, our docking procedure and software protocol could be relied on to predict the experimental binding mode of the designed analogs.
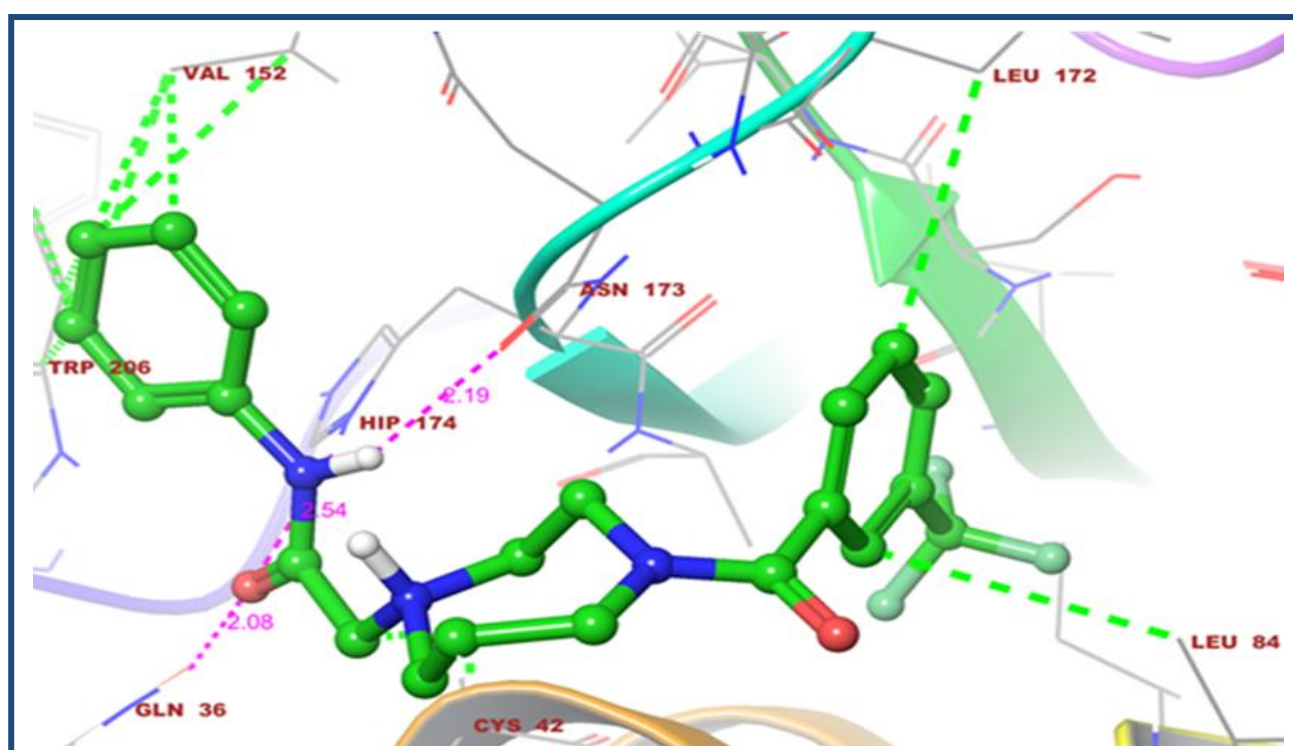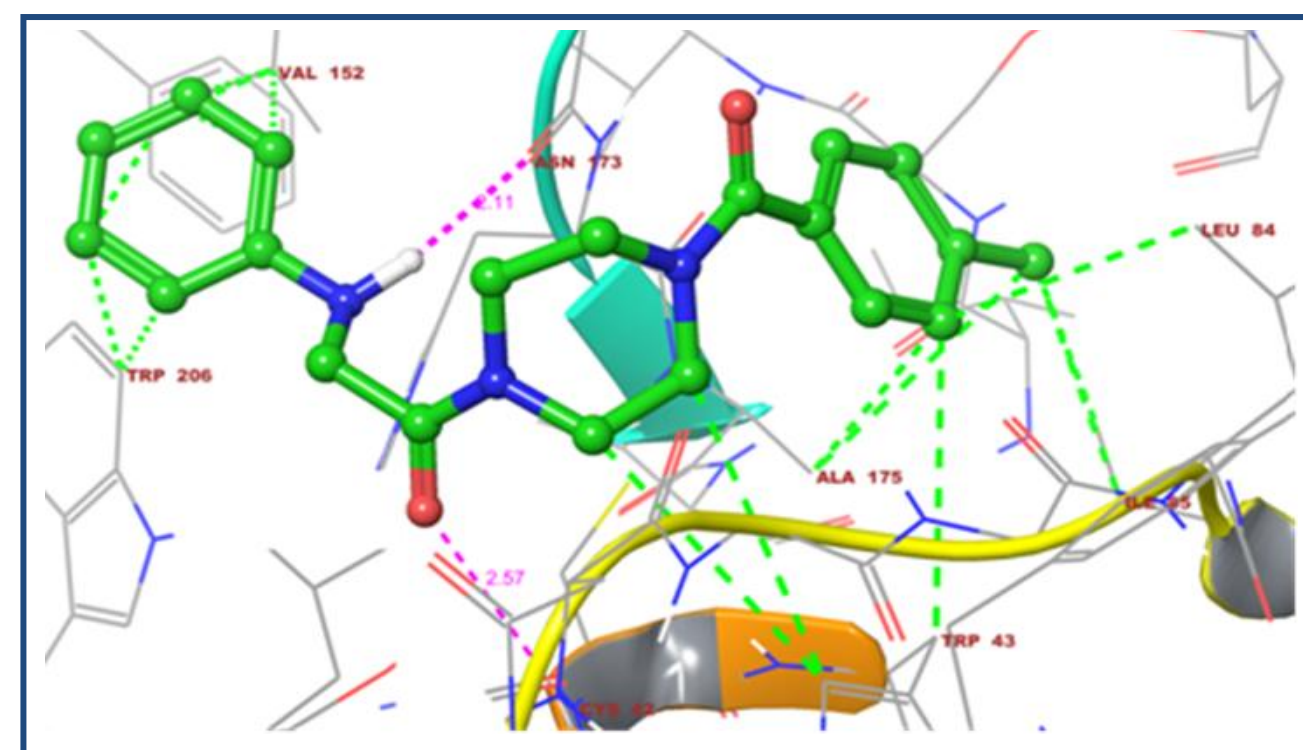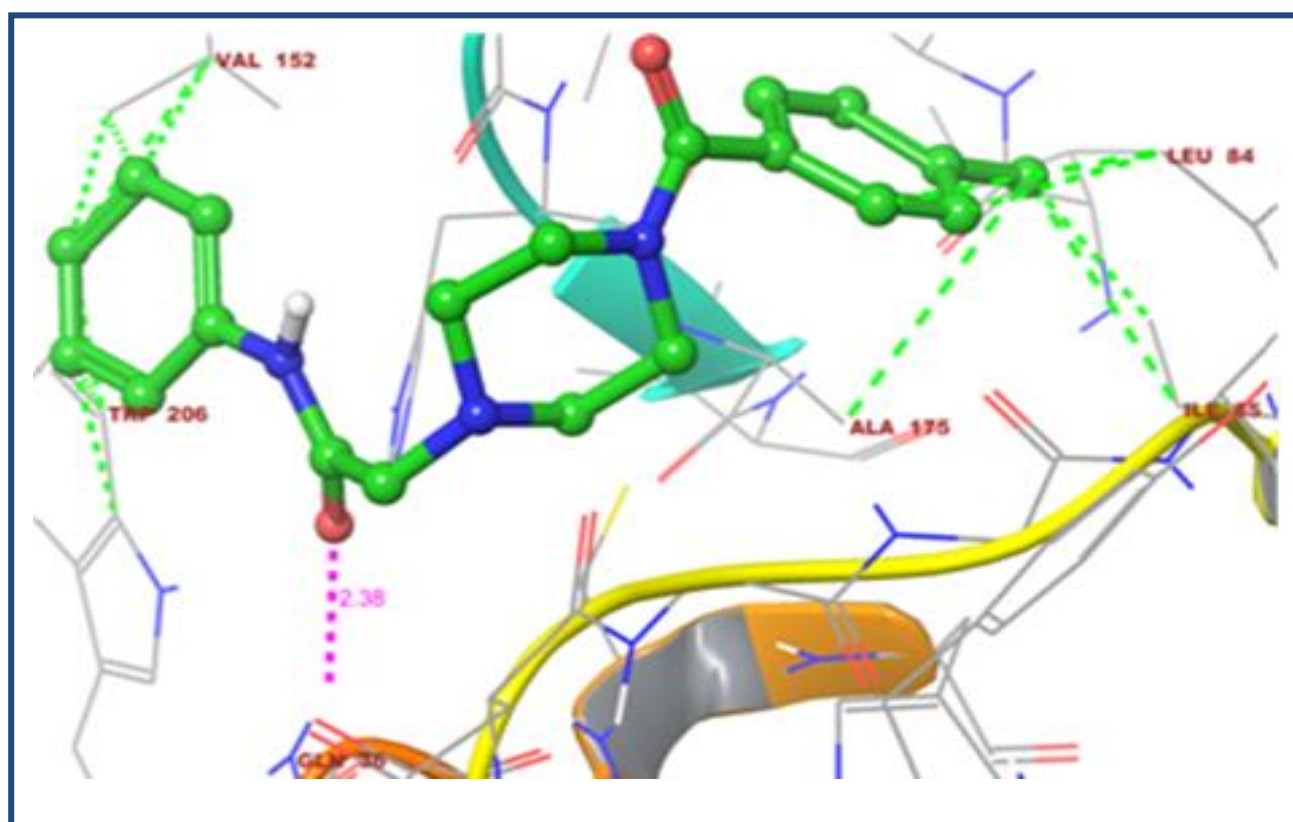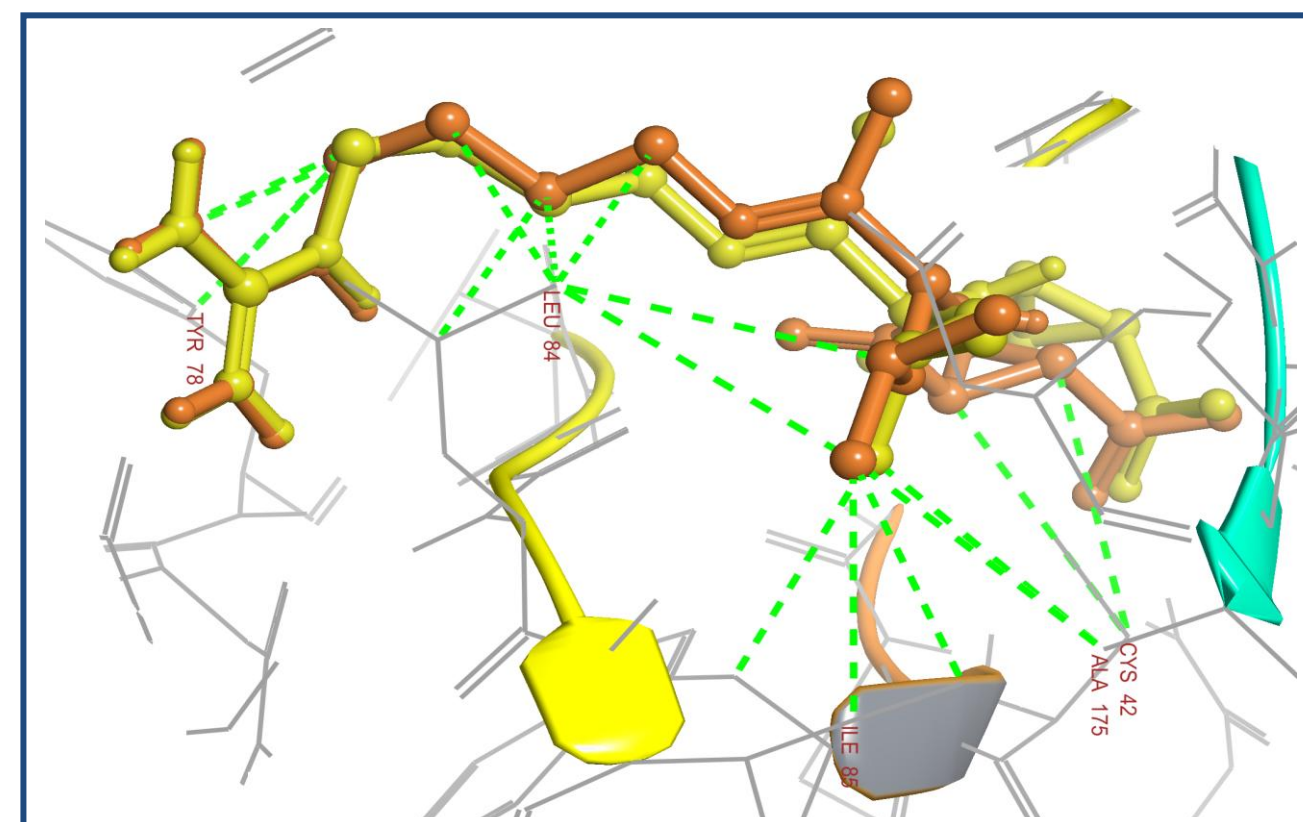
Figure 20 (A-C): Docking pose of compounds RM-7 (*N*-Phenyl-2-(4-(3-(trifluoromethyl) benzoyl)-1,4-diazepan-1-yl) acetamide), RMS-8 (1-(4-(4-Methylbenzoyl)piperazin-1-yl)-2-(phenylamino)ethanone), and RMT-2 (2-(4-(4-methylbenzoyl)piperazin-1-yl)-*N*-phenylacetamide), respectively docked to chain A of falcipain-2 protein (3BPF.pdb). The pink dashed line represents the possible hydrogen bond and green dashed line represents the possible hydrophobic interaction, **(D):** Redocked mode of E-64 (yellow) superimposed with the co-crystallized ligand (magenta)

5. RESULTS AND DISCUSSION

5.1. Pharmacophore and chemistry

5.1.1. Series I-III

Existing falcipain-2 inhibitors (Desai et al., 2004; Li et al., 2009; Desai et al., 2006), which hold moderate to potent activities **(A-H)** as represented in **Figure 21**, were used as a template for designing a pharmacophore model for falcipain-2 inhibitors.

The most common features present in the aforementioned falcipain-2 inhibitors are, an aromatic residue (monocyclic/bicyclic), which is attached to the hydrophobic moiety; an aromatic residue through a hydrogen bond donor and acceptor atom(s) as linker.

The distance between the aromatic residue to a hydrophobic group, centroid of the aromatic residue to linker (HBA/HBD) and centroid of hydrophobic group to linker (HBA/HBD) were ranged from 9 to 14 Å, 6 to 11 Å and 5 to 12 Å, respectively. The hydrogen bond donor (HBD) and hydrogen bond acceptor (HBA) atom(s) are present as either in heterocyclic/alicyclic, or open chain form. The numbers of hydrogen bond donor and acceptor atoms range from 0-2 and 2-6, respectively. The reported molecules are basic in nature due to 2° or 3° amino moiety.

By considering these characteristic features as pharmacophore for falcipain-2 inhibitors, a novel pharmacophore model was built **(Figure 15)**. Based on this model, three series **(RM-1 to 20**, **RMS-1 to 20**, **RMT-1 to 20)** of compounds were designed and the corresponding basic structure for each series is represented in synthetic **schemes 1 to 3**, respectively (Experimental Section **4**).

The least energy conformation (three minimum energy conformations for each compound) for each designed compound was generated using ACDLABS-12.0 product version 12.01/3D viewer (CHARMM parameterizations), and the pharmacophoric distances were measured from the centroid of an aromatic residue to a hydrophobic residue. The observed distances between the pharmacophoric elements of all the designed compounds are in agreement with our proposed pharmacophore model, and results are summarized in **Tables 7-9**.

To achieve better pharmacokinetic profile, the Lipinski's Rule of Five (Lipinski et al., 1997) i.e., hydrogen bond donor atoms not more than 5, hydrogen bond acceptor atoms not more than 10, molecular weight less than 500, and log P value less than 5, was adopted for the designed molecules. Lipophilicity is an important parameter to be considered while designing ligand to manifest drug-like behavior.
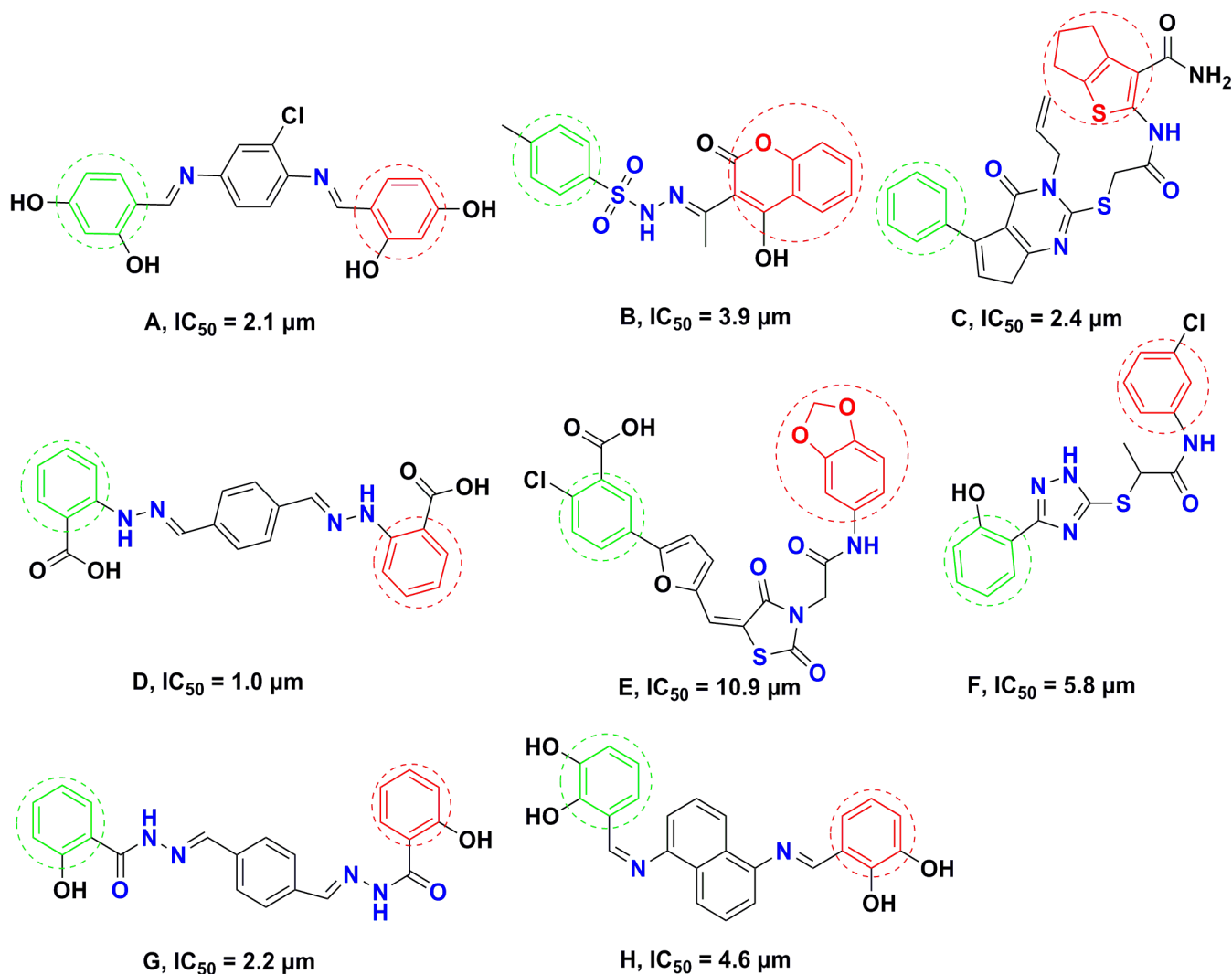
Figure 21: Chemical structures of some existing falcipain-2 Inhibitors. (Green Color: represents hydrophobic moiety; an aromatic group, Red Color: represents an aromatic residue (monocyclic/bicyclic), Blue Color: represents the numbers of hydrogen bond donor and acceptor atoms)

5.1.2. Series IV

Structure based drug design is a powerful tool for identification of chemically-diverse set of compounds as novel lead molecules in drug discovery programme. Over the years, many research groups have investigated falcipain-2 inhibitors using *in silico* screening of chemical libraries. Recently, vinyl esters were designed using molecular modeling and their binding to falcipain-2 was evaluated. These inhibitors exhibited antiplasmodial activities (IC$_{50}$) in the low micromolar range, carry a vinyl ester core capable of trapping the active site **"Cys"** through a covalent bond and function as a Michael acceptor. The poor selectivity for parasitic cysteine proteases over the human cysteine proteases remains a noteworthy concern. Rizzi et. al., 2011, designed peptidomimetics, based on the interactions of cystatin (family of cysteine protease inhibitors) with the active site of falcipain-2. These compounds showed specific inhibition of falcipain-2 activity as well as inhibition of parasite growth at low micromolar range with reduced toxicity and higher selectivity. Structure based drug design for series **IV** was carried out in collaboration with Dr. Lakshmi Kotra (University Health Network, Toronto-Canada).

5.1.2.1. Identification of initial hit

Three-dimensional structures of falcipain-2 (RCSB codes: 1YVB, 3BPF) were investigated to understand the similarities and differences between these three proteases. The catalytic site of this class of cysteine proteases is composed of hydrophobic pockets in close proximity to the catalytic residues (Cys42 and Hip174). Then, using the three-dimensional structure of falcipain-2 from *P. falciparum* (RCSB code: 1YVB) as a template, pharmacophore features for *in silico* screening of commercial chemical compounds libraries were selected. A library of more than 250,000 commercially available compounds, were screened against the active site of falcipain-2 employing UNITY module. A set of 2084 initial hits were obtained following from this screening, which were then subjected to Surflex-Dock™ based docking in the active site of falcipain-2 to generate docked poses. These poses were scored using the empirical scoring function in Surflex-Dock, and the top 200 hit molecules with the corresponding pose based on the best-fit score were selected. The molecules were then inspected individually within the binding pocket of falcipain-2 for their chemical nature, reactive structural elements, and synthetic feasibility.

Overall, one compound **(KM-1')** was identified and acquired from commercial vendors. This compound was evaluated for their efficacy to inhibit *in vitro* activity of falcipain-2. **KM-1' (Figure 22)** exhibited moderate inhibition of falcipain-2 with a IC_{50} value of 36.06 ± 0.61 µM. Furthermore, this compound inhibited *P. falciparum* growth *in vitro* with an IC_{50} of 2.5 ± 0.2 µM.
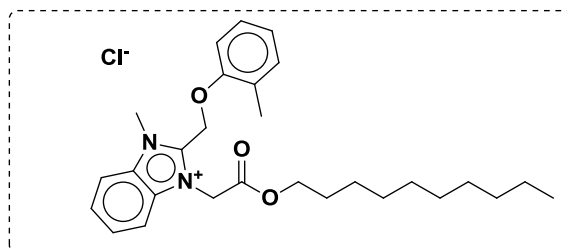
Figure 22: Structure of hit compound (KM-1')

Although **KM-1'** exhibited reasonable inhibition of falcipain-2 activity, overall chemical structure required additional modifications. Thus, this hit molecule **(KM-1')**, along with two known falcipain-2 inhibitors, leupeptin and **K11017** (compound **5;** discussed in literature review Section **2**) were docked into the binding pocket of falcipain-2 **(Figure 23B)**. Then complementary groups from the three molecules (green portions in **Figure 23A**), and their corresponding interactions with the binding site were carefully considered to finally derive the library of molecules represented in **Figure 23C**, with a new structural element, pharmacophore/scaffold.

This scaffold has four different variable groups T_1, T_2, T_3 and T_3' correspond to R_1, R_2 and R_3 (T_3 and T_3'), substituents as mentioned in the basic structure of **Series IV (Section 3)**. Leu-Leu moiety was retained from the leupeptin structure, as this group provided appropriate binding interactions. One of these Leu moieties is also a substructure in **K11017**.

Other portions of the scaffold included the imidazolyl moiety from **KM-1'**, and various heterocycles at T_2 position, essentially occupying S3 pocket of the target. Benzyl substitutions on the imidazole are designed to occupy S1' subsite (hydrophobic in nature) and T_1 position, occupying S2 pocket of the target. Based on these substitution patterns, synthetic strategies were designed, and the target compounds are featuring scaffold I, were synthesized.
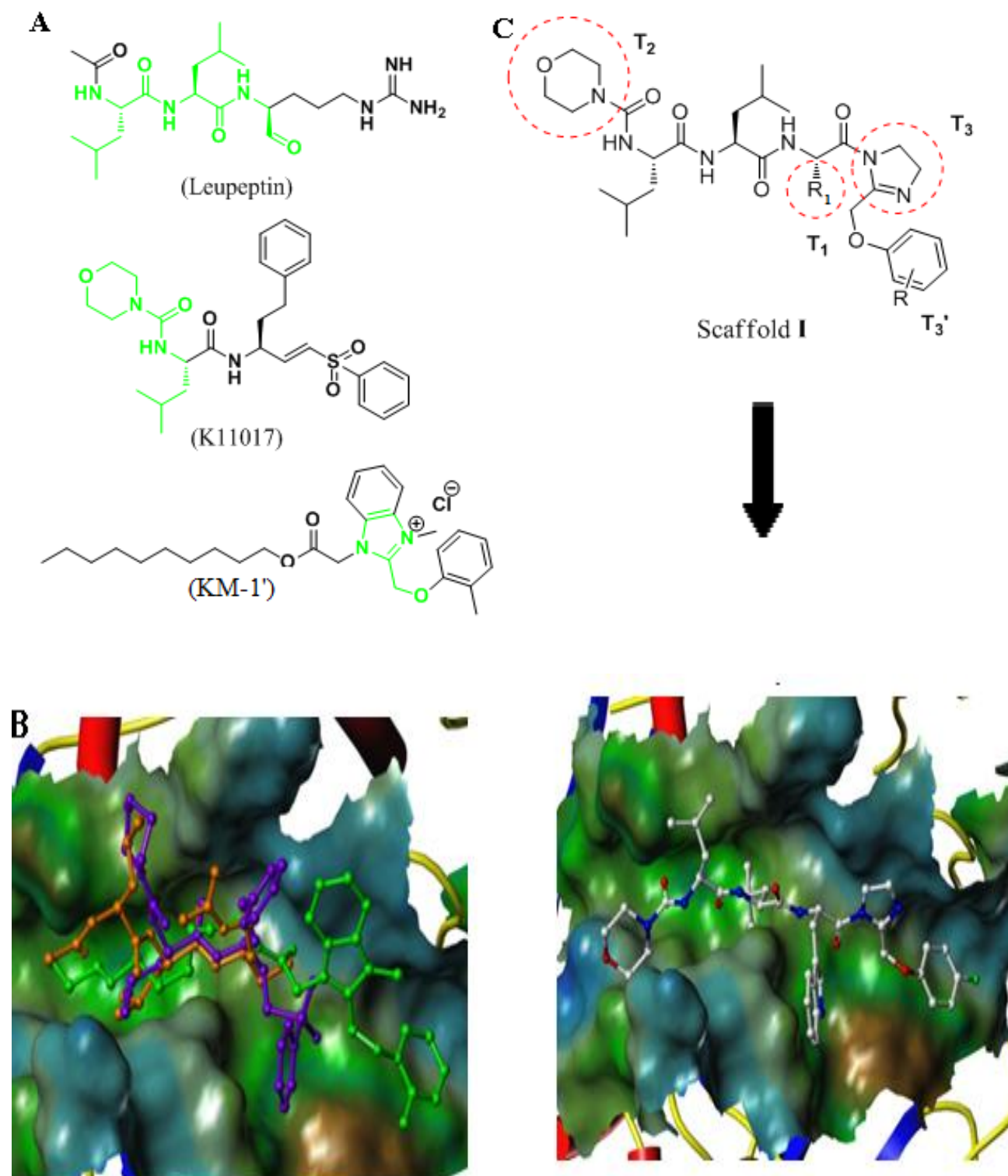
Figure 23 (A): Structures of the compounds, leupeptin, K11017 and the active hit (KM-1')
from *in silico* screening, **(B):** Binding site of falcipain-2 with docked molecules Leupeptin
(orange), K11017 (purple) and KM-1' (green), **(C):** Representative structure of designed
compound (scaffold I) with structure variations (T_1, T_2, T_3 and T_3')

5.1.3. Series V-VI

5.1.3.1. Identification of initial hits

Asif and co-workers (collaborators, ICGEB), had previously investigated (unpublished data), some novel compounds targeting ClpP **(KM-1** to **13; Figure 24)**. Among them, two compounds **KM-6** and **KM-11** with IC_{50} values 26.0 ± 1.6 µM and 23.0 ± 1.8 µM, respectively were identified as moderate inhibitors that served as a solid starting point for the future drug discovery programme. Hence, initially various derivatives **(RMP 1** to **15)** of potential hit **KM-6**, were synthesized to generate an excellent SAR. However, screening results of these compounds were almost similar to the hit compound. Hence, chemical structure required additional modifications to improve the inhibition value.

Compound **KM-11**, which was another hit compound, possessed ~ 23 µM *in vitro* inhibition value, it was therefore planned to synthesize **KM-11**, and its derivatives, having substitution at C2 position of the pyrimidine ring. However, complex synthetic route for the synthesis of **KM-11**, prompted us to modify our strategy from straight forward synthesis of hit compound towards designing of a new pharmacophore model.

Interestingly, **KM-10** and **KM-12,** were least potent (> 100 µM) against *Pf*ClpP protease which differed from **KM-11** with respect to one pharmacophoric feature, i.e., chain length of substituents present at C2 position **(Figure 25)**. Prompted from this fact, these compounds were selected to develop a scaffold that allows for expedient chemical manipulation and subsequent, detailed, SAR studies. Through these modifications, a hybrid pharmacophore was generated **(Figure 25A)**. The novel pharmacophore consists of key features: a) aromatic ring (pyrimidine nucleus), b) substitution at N^3 position with variation in chain length c) variation in substituent's present at C2 position and d) fused ring **(5-isopropyl-5,7-dihydro-4*H*-thieno[2,3-*c*]pyran)** which was replaced deliberately with an ester/amide linkage at 5th or 6th position of the pyrimidine ring, to afford synthetic feasibility and to modulate polarity and bioavailability (Meanwell, 2011).

Based on this pharmacophore, a series of compounds **(RMH 1** to **14)** were designed and synthesized. **Figure 25B** represents the formation of basic compound **RMH-1** from the designed pharmacophore.
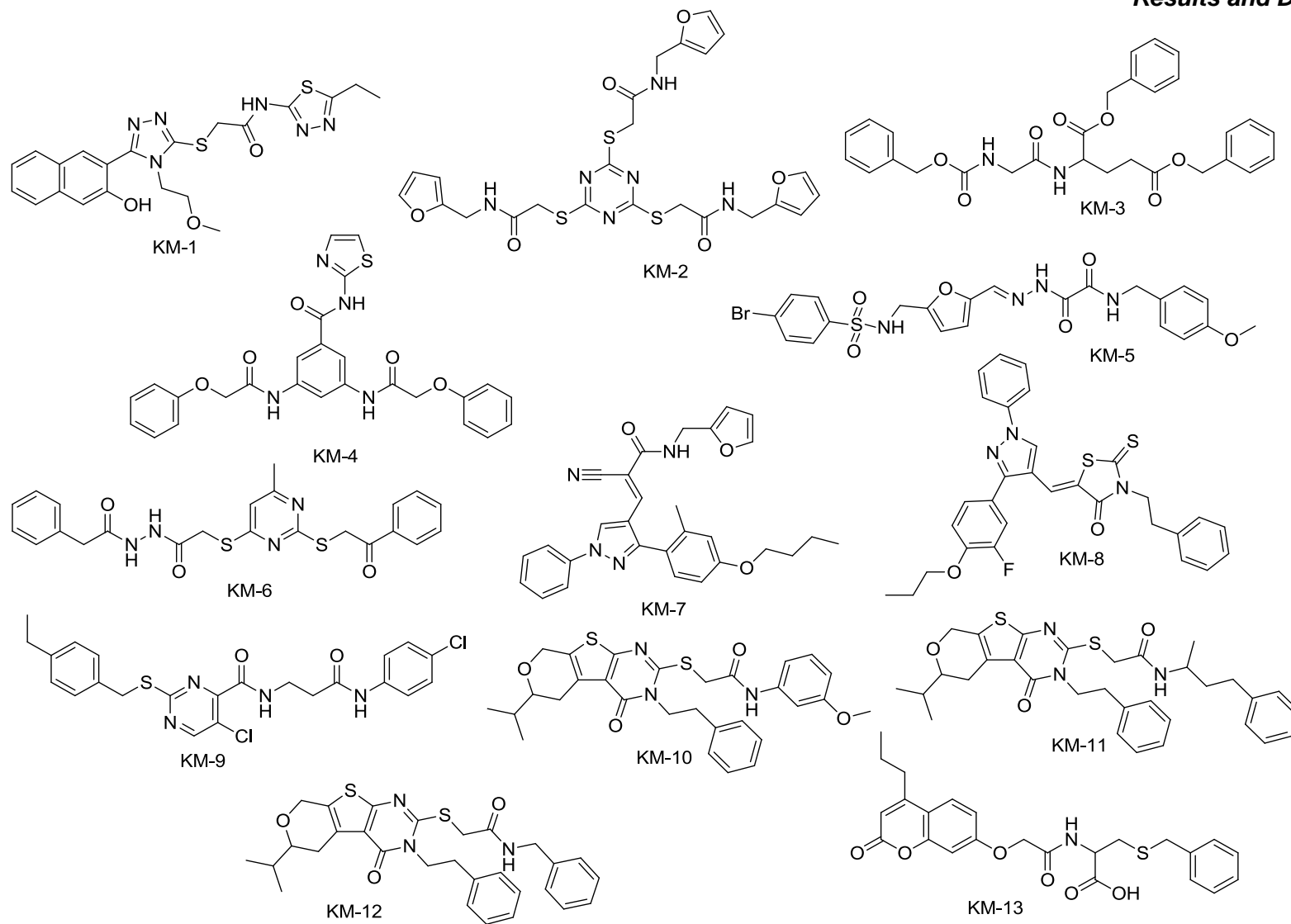
Figure 24: Structures of the some ClpP Inhibitors
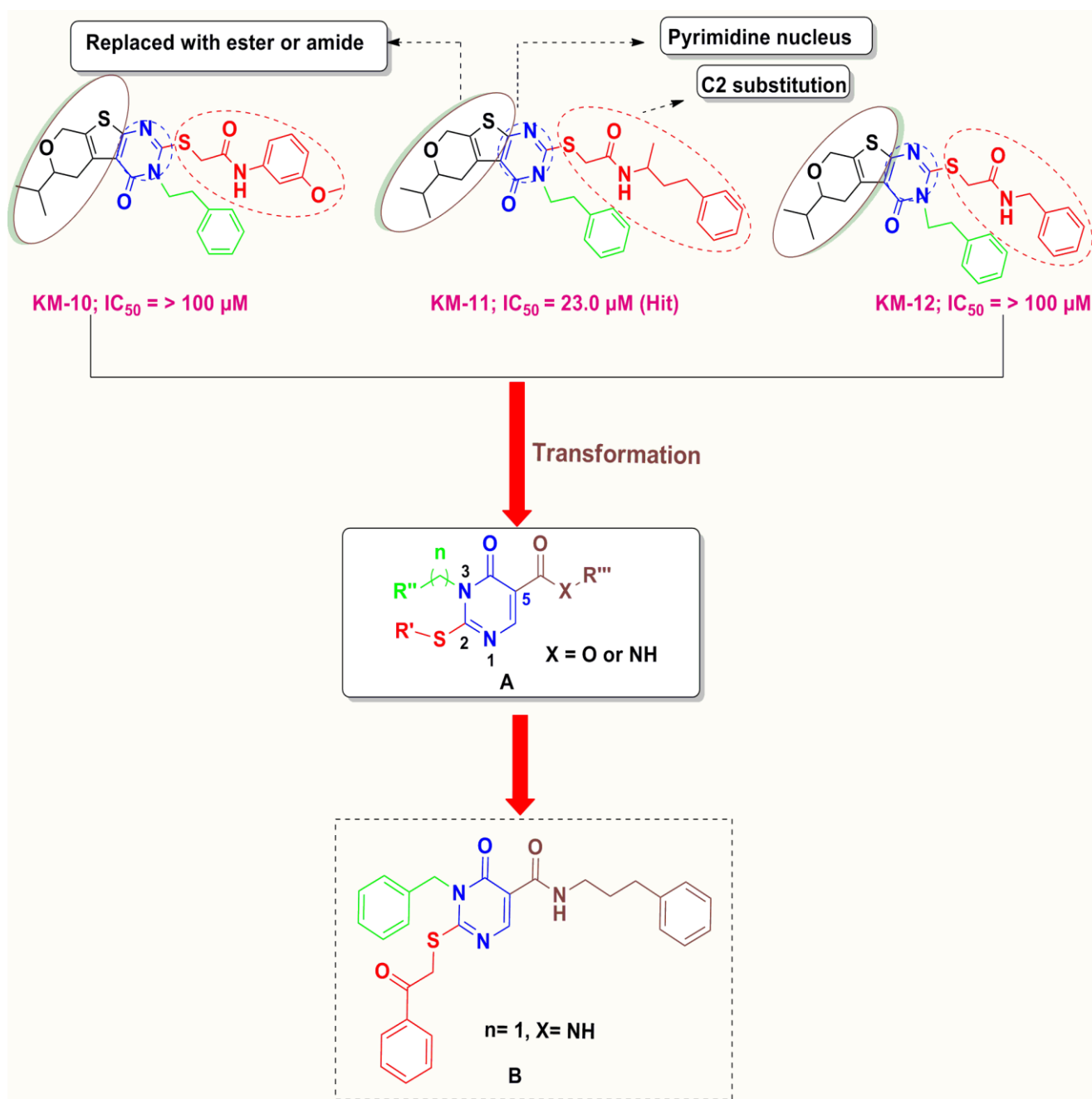
Figure 25 (A): Optimized pharmacophoric model **(B):** Structure of basic compound

5.2. Chemistry

5.2.1. Chemistry of 2-(4-(substituted benzoyl)-1,4-diazepan-1-yl)-*N*-phenylacetamide (Series-I)

In brief, the synthesis of the designed inhibitors for Series I, was accomplished by the generation of key intermediate **RMI-3**, in multi-gram scale from the starting material aniline in a sequence of reactions as outlined in **Scheme 1**.

First, chloroacetyl chloride was subjected to nucleophilic substitution reaction with aniline, which afforded compound **RMI-1**. Due to the electrophilicity differences between acyl carbon, and $-CH_2Cl$ carbon of the 2-chloroacetyl chloride, the nucleophile (nitrogen atom in aniline) selectively attacks on acyl carbon of 2-chloroacetyl chloride as compared to carbon in $-CH_2Cl$. In addition, the steric hindrance also influences the selectivity of acyl carbon atom in α-chloroacetyl chloride. Structurally, there are two electron withdrawing groups on carbonyl carbon the -Cl atom and the doubly bonded oxygen atom. While, $-CH_2Cl$ moiety of the other carbon possesses only chloro group as electron-withdrawing group (-Cl). The possible mechanism of this intermediate formation is depicted in **Figure 26**.

The intermediate **RMI-1** was reacted with *N*-Boc protected homopiperazine, to obtain compound **RMI-2**. This step involves the attack of lone pair electron of a *N*-Boc piperazine nitrogen atom on the intermediate **RMI-2**, as represented in **Figure 27**.

Subsequently, deprotection of the Boc group with trifluoroacetic acid furnished the intermediate 2-(1,4-diazepan-1-yl)-*N*-phenylacetamide **(RMI-3)**. The synthesis of this intermediate **(Figure 28)** was accomplished by the following three important steps.

➢ First step, *tert*-butyl carbamate become protonated.
➢ Release of a *tert*-butyl cation as by product.
➢ Formation of carbamic acid and decarboxylation leads to the generation of free amine.

Further, this key intermediate **(RMI-3)**, was coupled with appropriate carboxylic acids in the presence of coupling agents *N*-(3-dimethylaminopropyl)-*N'*-ethylcarbodiimide hydrochloride (EDC·HCl) and 1-hydroxybenzotriazole (HOBt), under nitrogen atmosphere to afford target compounds **RM 1** to **20**. The carboxylic acid group of the compound on activation using EDC·HCl and HOBt in a nitrogen atmosphere, afforded the active ester compound. This on aminolysis with appropriate primary and secondary amines provided the desired compounds. **Figure 29** schematically represents the mechanism of the carboxamide

formation (Montalbetti and Falque, 2005); imide nitrogen of EDC·HCl abstracts the proton from the carboxylic acid proton. The generated carboxylate anion attacks the electrophilic centre of imide carbon, which results in the formation of *O*-acylisourea **(Figure 29)**. The acyl carbon on nucleophilic attack by 1-hydroxybenzotriazole leads to the formation of active ester, and this reaction was driven by the formation of water soluble urea. The formed active ester readily undergoes nucleophilic substitution in S$_N$2 manner with appropriate primary and secondary amines to generate the corresponding secondary and tertiary carboxamides, respectively.

Synthesized molecules were isolated as pure and characterized by IR, ^{1}H NMR, mass spectroscopy and elemental analyses. The analytical data of the compounds were found to comply with the structures. IR spectra of the final compounds showed absorption bands at 1675-1700 cm^{-1} and 1625-1679 cm^{-1} indicating the presence of keto-carbonyl, and amide carbonyl groups, respectively. An absorption band at 3200-3400 cm^{-1} displayed the presence of -NH group. Two protons at *δ* 3.16-3.48 either as two separate peaks or appeared as a single peak confirmed the presence of methylene group. Mass spectra (ESI) of most of the compounds exhibited molecular ion as (M + 1H)$^+$.
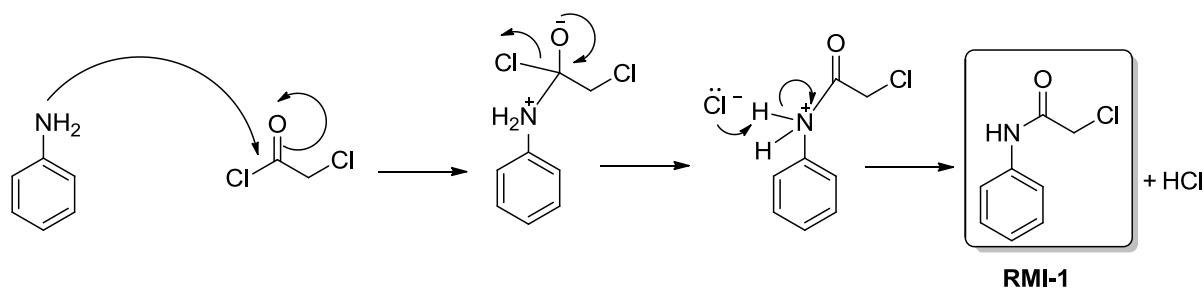
Figure 26: Mechanism of 2-chloro-*N*-phenylacetamide (RMI-1) formation
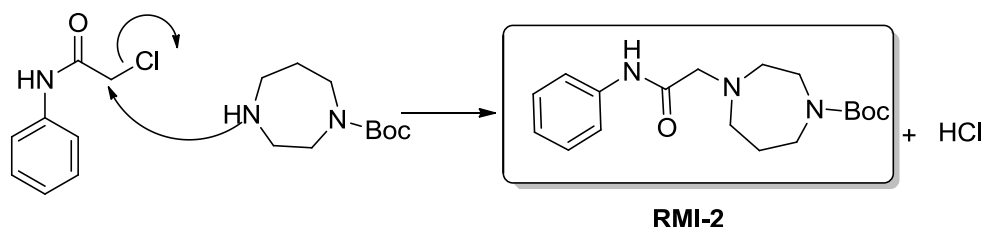
Figure 27: Mechanism of *tert*-butyl 4-(2-oxo-2-(phenylamino)ethyl)-1,4-diazepane-1-carboxylate (RMI-2) formation
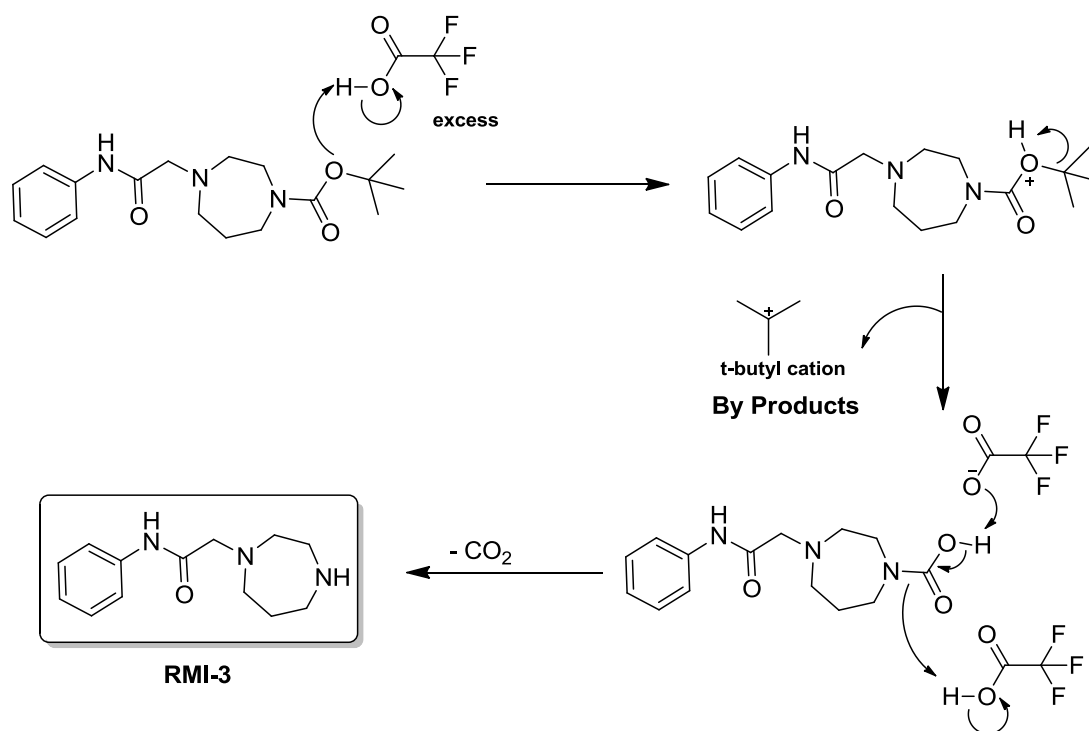
Figure 28: Mechanism for 2-(1,4-diazepan-1-yl)-*N*-phenylacetamide (RMI-3) formation
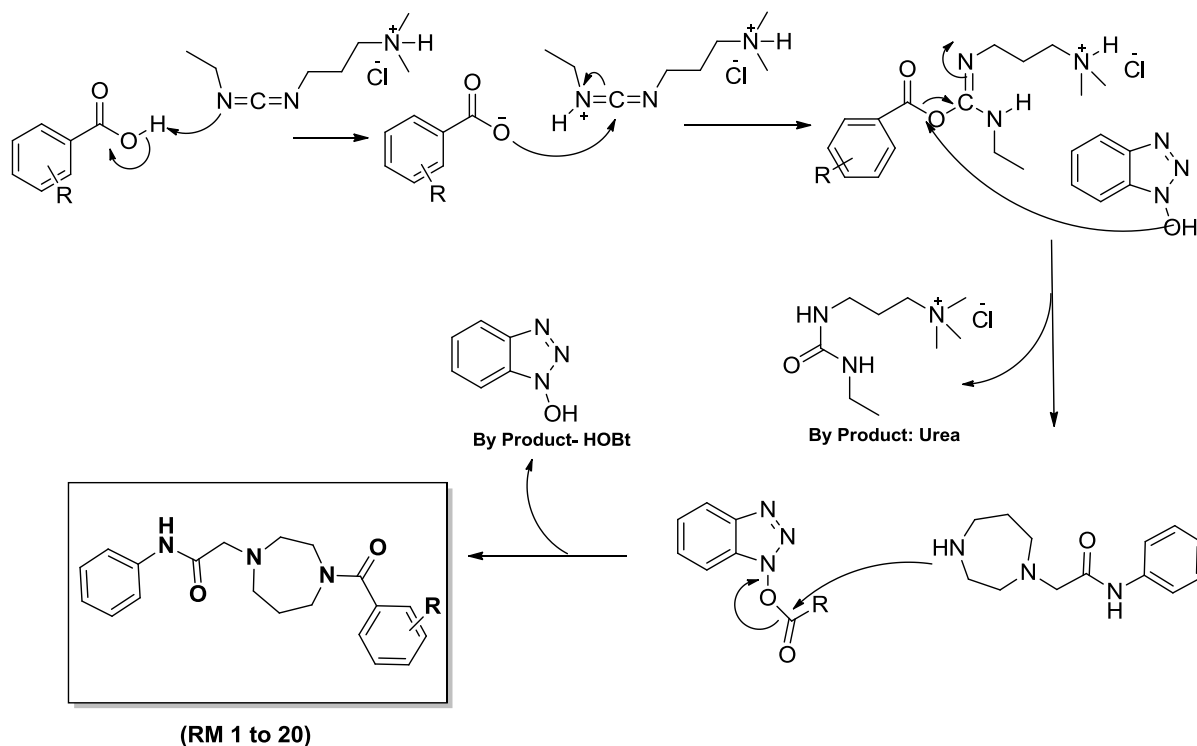
Figure 29: Plausible mechanism for the synthesis of 2-(4-(substituted benzoyl)-1,4-diazepan-1-yl)-*N*-phenylacetamide derivatives (RM 1 to 20)

5.2.2. Chemistry of 1-(4-(substituted)piperazin-1-yl)-2-(phenylamino)ethanone derivatives (Series-II)

The aforementioned target derivatives were synthesized from the starting material piperazine **(2)**, as depicted in **Scheme 2** (Experimental Section **4**). Initially, *N*-Boc piperazine **(RMI-4)**, was prepared by reacting piperazine with di-*tert*-butyldicarbonate. This reaction involves (a) activation of both carbonyl oxygen atoms of Boc anhydride by iodine, (b) making the carbonyl group more susceptible to attack by nitrogen atom of piperazine and (c) extrusion of carbon dioxide and *tert*-butanol as by product, afforded the compound **RMI-4** as shown in **Figure 30**.

Chloroacetyl chloride was subjected to nucleophilic substitution reaction with intermediate **RMI-4**, furnished the compound **RMI-5**. This intermediate was reacted with aniline, which afforded compound **RMI-6**. On subsequent, deprotection of intermediate **RMI-6** with trifluoroacetic acid, the key intermediate, 2-(phenylamino)-1-(piperazin-1-yl)ethanone **(RMI-7)** was obtained. Some key points followed for the synthesis of **RMI-7** in good yield.

➢ There was a need for a suitable trapping agent to quench the *tert*-butyl cation.
➢ The reaction had to be run in an open system, i.e.; the carbon di-oxide gas was generated during the reaction which was permitted to escape.

The final compounds **(RMI 1 to 20)** were synthesized from intermediate **RMI-7**, by coupling with appropriate carboxylic acids in the presence of EDC·HCl and HOBt under nitrogen atmosphere. The structures of the synthesized compounds were confirmed by spectral data (IR, ^{1}H NMR, mass spectroscopy) and elemental analyses. The appearance of keto carbonyl and amide carbonyl stretching absorption bands at 1645-1755 cm^{-1} and 1625-1665 cm^{-1}, respectively in IR spectra indicated the formation of desired products. Appearance of methylene two protons signal (^{1}H NMR spectra) at δ 3.85-3.98 confirmed the formation of required product. Most of the compounds exhibited molecular ion peak as (M + 1H)$^+$ in mass spectra (ESI).
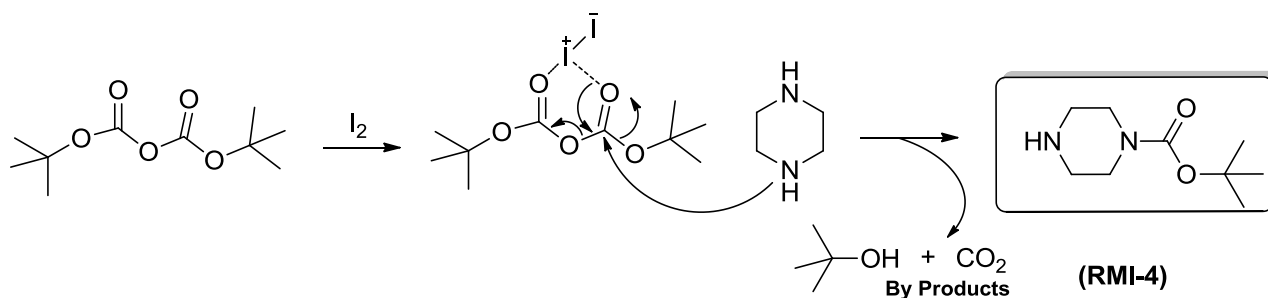
Figure 30: Mechanism *N*-Boc-piperazine (RMI-4) formation

5.2.3. Chemistry of 2-(4-(substituted benzoyl)piperazin-1-yl)-*N*-phenylacetamide (Series III)

The designed 2-(4-(substituted benzoyl)piperazin-1-yl)-*N*-phenylacetamide **RMT-1** to **20** analogs were synthesized from the key intermediate *N*-phenyl-2-(piperazin-1-yl)acetamide **(RMI-9)**. This intermediate compound was synthesized in large scale from the starting material aniline in a sequence of reactions, depicted in the **Scheme 3** (Experimental Section **4**).

Firstly, chloroacetylchloride was subjected to nucleophilic substitution reaction with aniline to mask the chloro functionality, which afforded compound **(RMI-1)**. This Intermediate was reacted with *N*-Boc protected piperazine to achieve compound **RMI-8**.

Subsequent deprotection of intermediate 3 **(RMI-8)**, with trifluoroacetic acid, furnished the intermediate *N*-phenyl-2-(piperazin-1-yl)acetamide **RMI-9**. The resultant compound was coupled with appropriate carboxylic acid in the presence of coupling agents EDC·HCl and HOBt under nitrogen atmosphere afforded the final compounds **RMT 1** to **20**.

In the coupling reaction the different substituted carboxylic acids were amidated with intermediate **RMI-9**, via formation of an active ester with the aid of HOBt and EDC·HCl to afford the desired product in good to excellent yields.

Structural features of target compounds were characterized by spectral data such as IR, ^{1}H NMR, and mass analyses. The spectral data of the compounds are found in compliance with the structure of the synthesized compounds.

IR spectra of the compounds showed absorption bands at 1660-1700 cm^{-1} and 1625-1679 cm^{-1}, respectively, which corresponds to the keto carbonyl and amide carbonyl groups, respectively. In ^{1}H NMR, two protons at δ 3.11-3.21 confirmed the presence of methylene group. Mass spectra (ESI) of the most of the derivatives exhibited molecular ion as (M + 1H)$^+$.

5.2.4. Chemistry of peptidomimetics (Series IV)

Synthesis of the designed inhibitors was accomplished by first obtaining the appropriate dipeptide precursors, which are common structural components for all compounds based on **Scaffold I**. Dipeptide *N*-Boc-L-Leu **(1)**, was coupled with different L-amino esters using (benzotriazol-1-yloxy)tris(dimethylamino)phosphonium hexafluorophosphate (BOP) as a coupling reagent and *N,N*-diisopropylethylamine (DIPEA) as a base in DMF to yield compounds **2-6**, respectively; **(Scheme 4)**. The general mechanism of coupling which involves BOP as a reagent is presented by **Figure 31**. The following steps were followed. (I) extraction of proton of the amino acid to generate the carboxylate anion **(A)**, (II) activation of the carboxy function with onium reagent **(B)**, (III) formation of stabilized hydrogen bonded precursor **(C)**, (IV) nucleophilic attack of amino component at activated carboxylic group to form amide bond **(D)** and (V) Removel of by product **E**.

The carbamate moiety **2-6** were deprotected with trifluoroacetic acid, and the products **7-11** were coupled with *N-Boc*-L-Leu to obtain the tripeptide intermediates **12-16**. Decarbamylation of compounds **12-16** under acidic conditions provided **17-21**, respectively; which then were reacted with morpholine, furoyl and piperidine carbonyl chlorides resulting in compounds **22-26 (RMQ-1** to **5)**, respectively; in moderate to good yields. Compounds **19** was reacted with chloroacetyl chloride at 0°C to obtain compounds **30 (RMQ-6)**, which was further subjected to nucleophilic substitution with a variety of cyclic amines utilizing the halogen exchange protocol with potassium iodide, potassium carbonate in acetonitrile at 150 °C for 10 min in a microwave reactor to obtain compounds **24.1-25.1**. Unfortunately, under these reaction conditions, multiple spots were observed and the desired product was not isolated. Therefore, esters **22-26** were hydrolyzed under basic conditions at room temperature to obtain the carboxylates **31-35 (RMQ 7** to **11)**, respectively, in good yields.

Parallel *via* another route, attempt was made to synthesize carboxylic acids precursours, thus tripeptide esters **13, 15** and **16** were first hydrolyzed under basic conditions to generate compounds **27, 28** and **29**, respectively. The general mechanism **(Figure 32)** of base catalysed ester hydrolysis involves (I) attack of hydroxide nucleophiles at the ester C=O, **(F)** (II) generation of tetrahedral intermediate **G**, (III) loss of leaving group to generate intermediate **H**, and (IV) attack of alkoxide anion to generate desired product.

Compounds **27-29** were subjected for coupling reaction, to generate amide derivatives. Unfortunately, coupling reaction did not work (Experimental Section **4**, **Scheme 4**). Further, a variety of side chains were chosen and synthesized to couple **31-35** to the appropriate T_3 moiety (**47, 51, 52** or phenyl hydrazine), to afford the target compounds **36-44 (RMQ 36** to

44). In this regard, compounds **47, 51** and **52** were prepared separately **(Schemes 6 and 7)**. Thus, for the preparation of **47**, ethyl bromoacetate was first coupled to 4-fluorophenol under basic conditions, followed by cyclization with ethylenediamine to yield the dihydroimidazole derivative **47** in decent yields **(Scheme 6)**.

To synthesize pyrrolidine side chains **(51** and **52)**, *N*-benzyl prolinol was converted into its bromide using CBr_4 and triphenyl phosphene. The resultant bromide intermediate was instantly reacted with 4-fluorophenol and 4-methoxyphenol under basic conditions in DMF at 60°C for 3h; gave the intermediates **49** and **50**. These intermediates were subjected to hydrogenolysis for the debenzylation using 10% wt. Pd/C in methanol to yield **51** and **52** in good yields. Interestingly, these pyrrolidine side chains showed multiple conformations, that were later confirmed to be rotamers by variable temperature NMR (VT-NMR) and LCMS analysis.

The synthesis of compounds **51** and **52** was also attempted using Mitsunobu reaction. In this reaction, attacks of triphenyl phosphine **(K)** upon diethyl azodicarboxylate **(J)** generated a betaine intermediate **L (Figure 33)**. The deprotonation of carboxylic acid **(M)** and alcohol **(O)** afforded ion pair **(N)** and a key oxyphosphonium ion **Q** intermediates respectively. Though, many intermediates are possible in the course of formation of desired product, but as a productive pathway the attacks of the carboxylate anion upon intermediate **Q** generated desired product and triphenylphosphine oxide **(R)** as side product.

The side chains **51** and **52** were coupled to the tripeptide intermediates **31-35** using BOP/ DIPEA to yield the final compounds **36-44 (Scheme 5)**. For the synthesis of compound **41**, which carried a pyrrolidine moiety at T_3, first pyrrolidine moiety was substituted with 4-methoxyphenol by replacing the 4-fluorophenol **(Scheme 7)**; yielding the intermediate **52**. Compound **52** was coupled to tripeptide carboxylate **34 (RMQ-10)** to obtain the target compound **41 (Scheme 4)**.

Compounds contained pyrrolidine moiety **(RMQ-17)** were exhibiting complex NMR and HPLC spectra. It is well known, that compounds containing pyrrolidine moieties and proline residues exhibit rotational isomerism (Sandvoss et al., 2003; Deupi et al., 2004; Zhang et al., 2009). VT-NMR experiments are very useful in delineate diastereomers vs. rotamers, thus we subjected the compounds holding the pyrrolidine moiety at the terminal T_3 position to VT-NMR experiments.

First, a complete ^{1}H NMR spectrum was acquired at 24°C for each compound. The sample was heated to 100°C to record the second ^{1}H NMR spectrum. At higher temperatures,

rotamers, if present, will merge into a single compound, overcoming the rotational barriers that were present at lower temperatures and presented a simplified nuclear magnetic resonance spectrum. One-dimensional ^{1}H NMR spectrum at 24°C appears to have more than one molecule, although the compound is pure otherwise. This profile was resolved into a spectrum representing a single conformer, when the ^{1}H NMR spectrum was recorded at 100°C. All other compounds carrying the pyrrolidine moiety were subjected to VT NMR spectral analysis and were confirmed to exhibit rotamer effects.
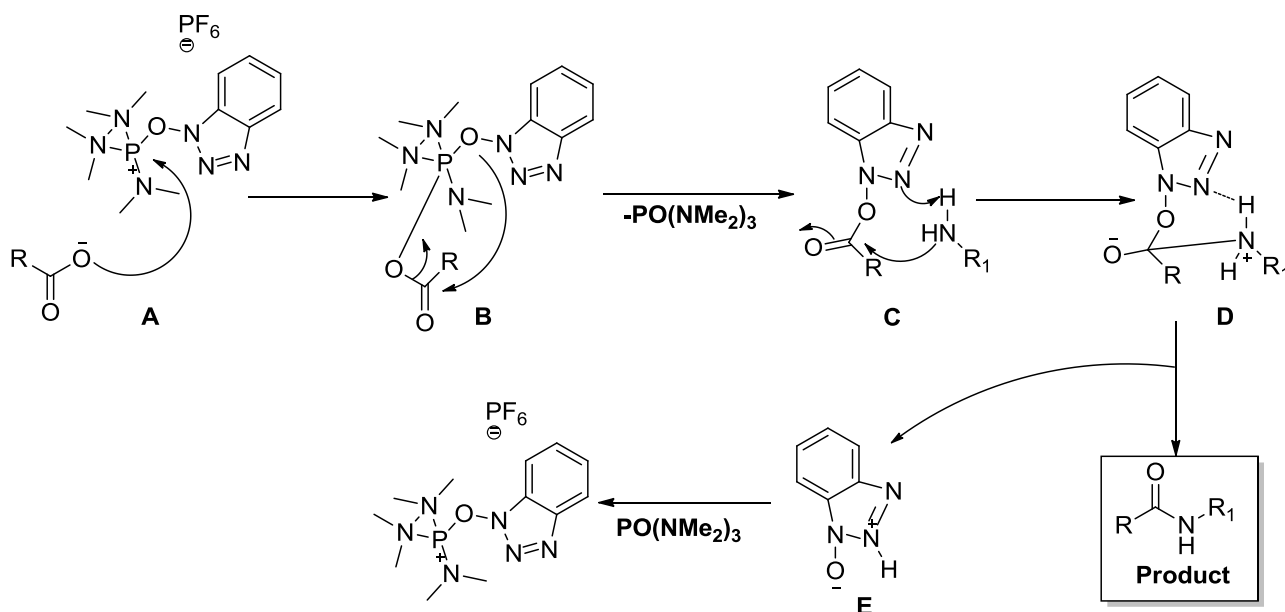
Figure 31: General mechanism of coupling reactions with BOP
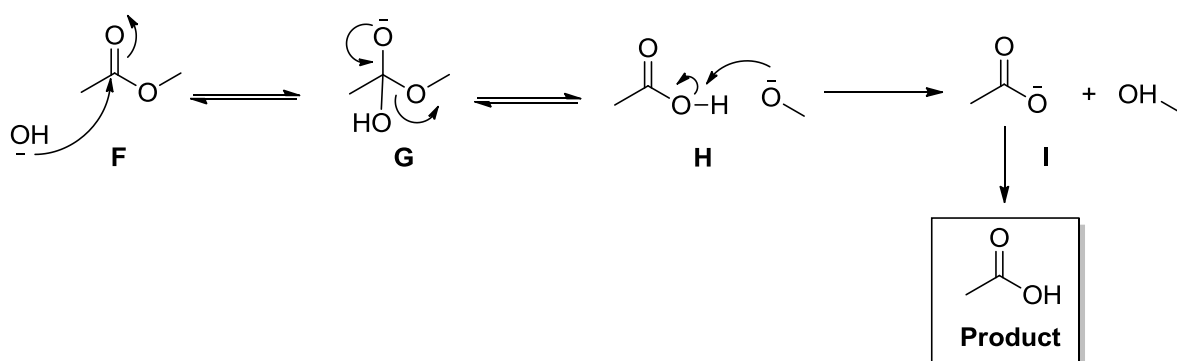
Figure 32: General mechanism of base catalysed hydrolysis
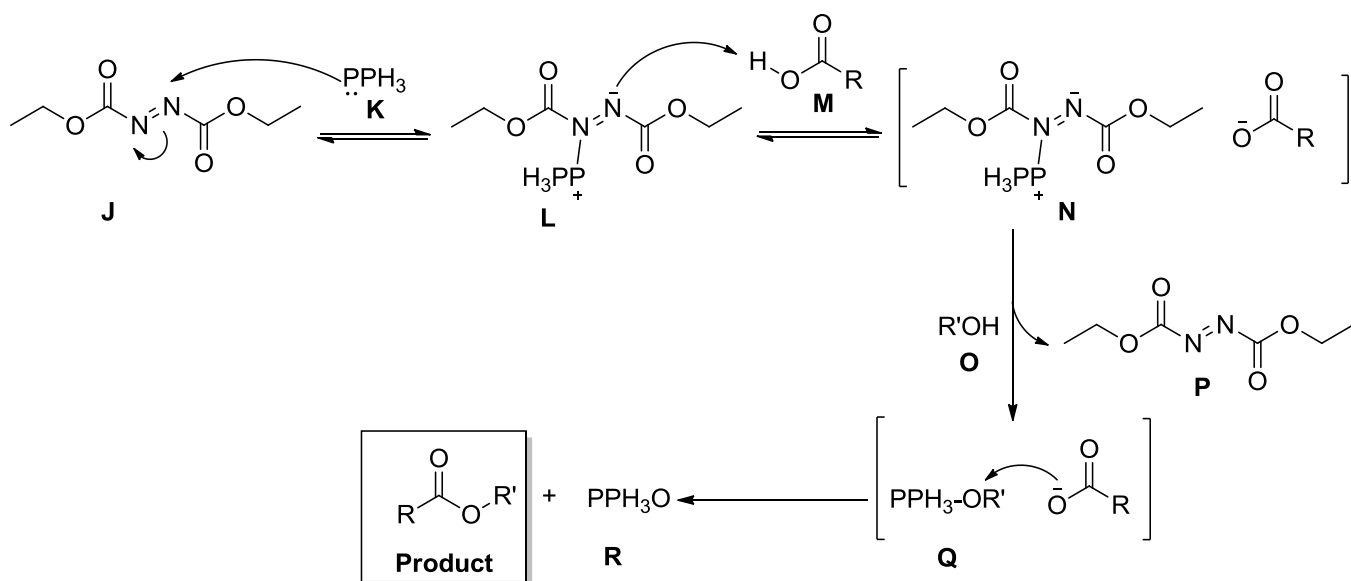
Figure 33: Mechanism of Mitsunobu reaction to generate side chains (51 and 52)

5.2.5. Chemistry of Series V-VI

Various derivatives of potential hit **KM-6**, were synthesized to generate an excellent structural activity relationships. Synthesis of these analogs was accomplished by generating the appropriate key precursors **(5)** and **8 (A-O)**. The key intermediate **5**, was generated from starting material methyl 2-phenylacetate **1**, in a sequence of reactions as depicted in **Scheme 8**. First step involved the reaction between compound **1**, with excess of hydrazine hydrate produced acylated hydrazine intermediate **2**. The selective attacks of nitrogen atom of the primary amine (intermediate **2**) on acyl carbon chloroacetyl chloride afforded compound **3**. Resultant compound reacted with potassium thioacetate, furnished the intermediate S-2-oxo-2-(2-(2-phenylacetyl)hydrazinyl)ethyl ethanethioate **(4)**. On subsequent deacetylation of intermediate **4**, in the presence of K_2CO_3/MeOH afforded mercaptoacetamide **(5)** and disulfide (produced as a byproduct) confirmed by ^{1}H NMR and mass analysis.

On the other hand, the synthesis of intermediate **8 (A-O**), was initiated with starting material 6-methyl thiouracil **(6)**, via a sequence of reactions as depicted in **Scheme 8**. Initially, compound **6** was subjected to nucleophilic substitution reaction with 2-Bromo-1-(substituted)ethanone derivatives **(A-O)**, to mask the bromo functionality, afforded **7 (A-O)** derivatives. Chlorination of **7 (A-O)** derivatives with phosphorous oxychloride in the presence of dimethylformamide as catalyst generated the 4-substituted chloro pyrimidine precursors **8 (A-O)** in quantitative yield. The disappearance of -NH proton in ^{1}H NMR, as well as mass analysis, indicated the formation of chloro compounds. The resultant derivatives **8 (A-O)** were subjected to react with mercaptoacetamide intermediate **5**, led to the synthesis of final derivatives **RMP 1** to **15.** In final products, ^{1}H NMR spectra contains two singlet signal corresponding to two proton in the range of δ 9.31-10.2 indicated the presence of two -NH proton in compound. The two methylene linkage in the target compounds were observed in their expected region at δ 3.95-4.80 (correspondiong to second position of pyrimidine ring) and δ 3.61-3.23 (correspondiong to fourth position of pyrimidine ring), respectively.

In context to **Series VI**, The first step for the synthesis of designed analogs involved the pydridine catalysed microwave assisted cyclic condensation of benzyl thioureas **(10)** with diethyl ethoxymalonate, as depicted in **Scheme 9**, which afforded the ethyl 3-benzyl-4-oxo-2-thioxo-1,2,3,4-tetrahydropyrimidine-5-carboxylate intermediate **11**. ^{1}H NMR signals for ester linkage in compound **11** observed in the expected region at δ 4.18 (CH_2 protons) and δ 1.24 (CH_3 protons), respectively. Pyrimidine moiety contain one aromatic proton (6th position), appeared in the region δ 8.05.

Interestingly, synthesis of this intermediate by this method is novel and not previously reported elsewhere. Further, pyridine in combination with potassium carbonate made this protocol simple, convergent and attractive for the construction of tetrahydropyrimidines and notably similar molecules. The schematic representation of mechanism of ethyl 3-benzyl-4-oxo-2-thioxo-1,2,3,4-tetrahydropyrimidine-5-carboxylate formation is depicted in **Figure 34**.

The reaction between intermediate **11**, with primary amine in the presence of tri-methylaluminium afforded amide intermediate **12**. Finally, compound **12** was subjected to nucleophilic substitution reaction with 2-Bromo-1-(substituted)ethanone derivatives **(A-I)**, to generate final derivatives **13 (A-I)**. ^{1}H NMR spectra for the two protons at δ 5.34-5.44 region confimed the presence of benzylic CH_2 protons (N^3 position) in final derivatives, while another two proton at δ 4.35-4.98 region are corresponding to methylene group present at second position of pyrimidine ring.

Considering the importance of scaffold **11**, an attempt of selective *N*-alkylation (3rd position) was made to synthesize key intermediate **11**, the commercial available starting material **14** was reacted with benzyl chloride using DMF as the solvent and potassium carbonate as a base. Unfortunately, under this reaction conditions formation of multi-spots possibly *S*-alkylated product (2nd position alkylated derivative) and/or simultaneously *S*- and *N*-dialkylated products (2nd and 3rd positions alkylated derivatives; Mundra & Mahesh 2016) were observed via TLC. When the same reaction was attempted by switching the reaction solvent from ethanol to a DMF/ethanol mixture (1:1), no significant conversion was noticed upon heating at 100°C for 10 h. Interestingly, by changing the reaction time, temperature and variety of bases, no fruitful results were obtained.

Additionally, a new approach was attempted to alkylate at 2nd position selectively (due to high reactivity of sulphur atom as compared to nitrogen), followed by alkylation at N^3 position on pyrimidine ring. Reaction between compound **14**, with 2-chloro-*N*-(2-phenylacetyl)acetohydrazide and 4-(2-chloroethyl)morpholine using potassium carbonate as a base at room temperature respectively, affirmed new spot formation with good intensity (confirmed by TLC). The crude mixture was subjected to column chromatography and afforded the desired products **15a (RMH-10)** and **15b (RMH-11)**. Subsequently, when these compounds (**15a** and **15b**) were reacted with benzyl chloride to carry out selective alkylation at N^3 position, reaction didn't work well (Mundra & Mahesh 2016).

On the contrary, compound **15b** was reacted with trimethyl aluminium to obtain compound **17 (RMH-13)**. Disappearance of ester proton signal (NMR spectra) at δ 4.30 (CH_2 protons), δ 1.34 (CH_3 protons) and appearance of three methylene peaks corresponding to propylene

linkage in the amide bond confirmed the formation of desired compound. Later, when this compound was reacted with benzyl chloride to carry out selective alkylation at N^3 position, reaction did not move forward and no product formation was observed (Mundra & Mahesh 2016).

Parallel via another route, compound **15b** was reacted with bromo acetophenone to afford compound **16 (RMH-12)**. The hydrolysis of this compound using weak base LiOH afforded a cyclized compound **18 (RMH-14)** confirmed by mass and ^{1}H NMR analysis.

Additionaly, several improved new procedures were attempted with compound **18**, for the synthesis of 1,6-dihydropyrimidine-5-carboxamides derivatives in our laboratory but associated with limitations, such as long reaction time, harsh conditions and expensive reagents, thereby limiting their application in sustainable ("green") chemistry.
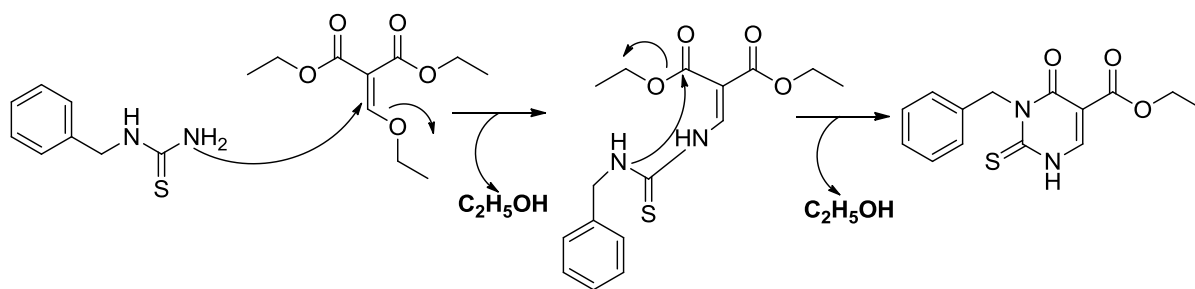
Figure 34: Mechanism of ethyl 3-benzyl-4-oxo-2-thioxo-1,2,3,4-tetrahydropyrimidine-5-carboxylate formation

Table 10: Falcipain-2 inhibitor activity profile of 2-(4-(substituted benzoyl)-1,4-diazepan-1-yl)-*N*-phenylacetamide derivatives against falcipain-2 enzyme[C)] (Series I)
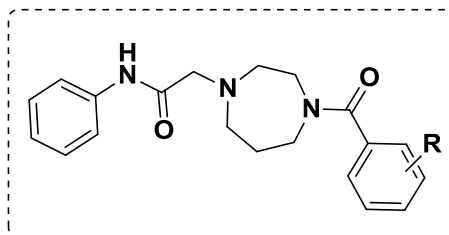
Compound	R	Inhibition value[c)] at 10 μM (%)	Compound	R	Inhibition value[c)] at 10 μM (%)
RM-1	-H	49 ± 0.3	RM-11	*m*-OCH$_3$	64 ± 0.2
RM-2	*m*-F	61 ± 0.1	RM-12	*p*-OCH$_3$	55 ± 0.2
RM-3	*o*-F	60 ± 1.1	RM-13	*m*-OCH$_2$CH$_3$	32 ± 0.8
RM-4	*m*-Cl	47 ± 1.8	RM-14	*o*-OCH$_2$CH$_3$	36 ± 0.9
RM-5	*p*-Cl	47 ± 2.1	RM-15	*p*-OCH$_2$CH$_3$	30 ± 1.1
RM-6	*o*-Cl	36 ± 0.6	RM-16	*m*-CH$_3$	49 ± 1.3
RM-7	*m*-CF$_3$	72 ± 0.8	RM-17	*p*-CH$_3$	47 ± 1.7
RM-8	*p*-CF$_3$	68 ± 1.1	RM-18	*o*-CH$_3$	48 ± 1.1
RM-9	*o*-CF$_3$	50 ± 1.8	RM-19	*p*-CH$_2$CH$_3$	30 ± 1.0
RM-10	*o*-OCH$_3$	70 ± 0.5	RM-20	*m*-CH$_2$CH$_3$	24 ± 0.7
E-64		97.4 ± 0.3			

[c)] Data are average of three independent experiments shown with their standard deviations

Table 11: Falcipain-2 inhibitor activity of 1-(4-(substituted)piperazin-1-yl)-2-(phenylamino)ethanone derivatives against falcipain-2 enzyme[c) (Series II)
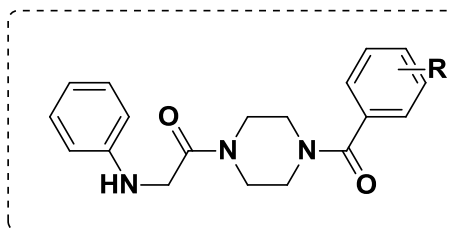
Compound	R	Inhibition value[c) at 10 µM (%)	Compound	R	Inhibition value[c) at 10 µM (%)
RMS-1	-H	25 ± 0.3	RMS-11	*p*-OCH$_3$	30 ± 0.6
RMS-2	*o*-F	15 ± 1.0	RMS-12	*o*-CH$_2$CH$_3$	24 ± 1.1
RMS-3	*p*-F	NI	RMS-13	*m*-CH$_2$CH$_3$	20 ± 0.8
RMS-4	*p*-Cl	NI	RMS-14	*p*-CH$_2$CH$_3$	43 ± 0.8
RMS-5	*p*-CF$_3$	NI	RMS-15	*o*-OCH$_2$CH$_3$	42 ± 1.3
RMS-6	*o*-CH$_3$	40 ± 0.7	RMS-16	*m*-OCH$_2$CH$_3$	20 ± 1.0
RMS-7	*m*-CH$_3$	38 ± 0.4	RMS-17	*p*-OCH$_2$CH$_3$	20 ± 0.8
RMS-8	*p*-CH$_3$	50 ± 1.3	RMS-18	*o*-Cl	NI
RMS-9	*o*-OCH$_3$	36 ± 0.7	RMS-19	*m*-Cl	NI
RMS-10	*m*- OCH$_3$	32 ± 1.4	RMS-20	*m*-F	NI
E-64		97.4 ± 0.3			

[c) Data are average of three independent experiments shown with their standard deviations

NI-No inhibition

Table 12: Percentage inhibition values of 2-(4-(substituted benzoyl)piperazin-1-yl)-*N*-phenylacetamide derivatives against falcipain-2 enzyme[c] (Series III)
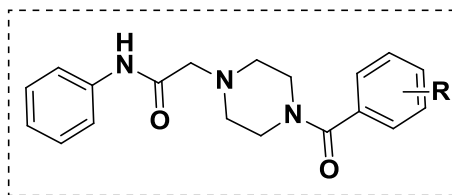
Compound	R	Inhibition value*[c] at 25 µM (%)	Compound	R	Inhibition value*[c] at 25 µM (%)
RMT-1	-H	7 ± 0.1	RMT-11	*m*-F	NI
RMT-2	*p*-CH$_3$	21 ± 0.8	RMT-12	*o*-OCH$_2$CH$_3$	5 ± 0.1
RMT-3	*m*-Cl	NI	RMT-13	*m*-CF$_3$	NI
RMT-4	*o*-CH$_3$	10 ± 0.8	RMT-14	*o*-CF$_3$	NI
RMT-5	*m*-CH$_3$	11 ± 0.5	RMT-15	*p*-CF$_3$	10 ± 0.2
RMT-6	*p*-Cl	NI	RMT-16	*m*-OCH$_2$CH$_3$	4 ± 0.1
RMT-7	*o*-OCH$_3$	11 ± 0.1	RMT-17	*p*-OCH$_2$CH$_3$	6 ± 0.3
RMT-8	*m*-OCH$_3$	10 ± 0.2	RMT-18	*p*-F	NI
RMT-9	*p*-OCH$_3$	11 ± 0.1	RMT-19	*o*-Cl	NI
RMT-10	*o*-F	NI	RMT-20	*p*-CH$_2$CH$_3$	19 ± 2.1
E-64		97.4 ± 0.3 (at 10 µm)			

[c] Data are average of three independent experiments shown with their standard deviations
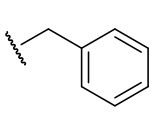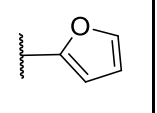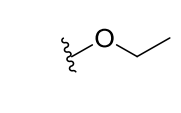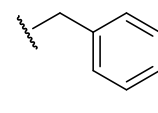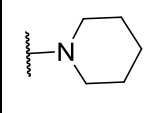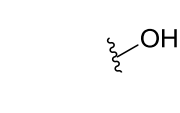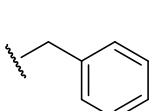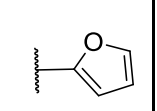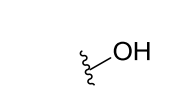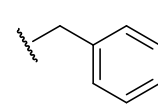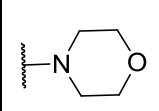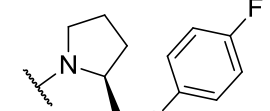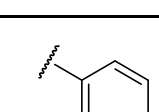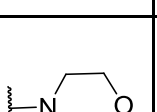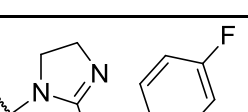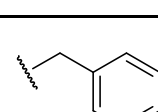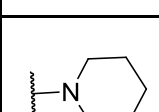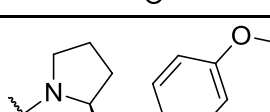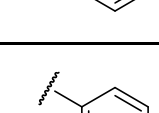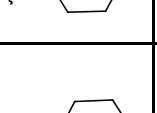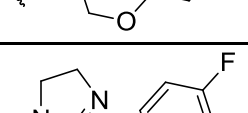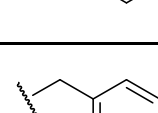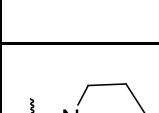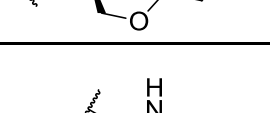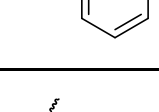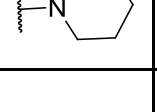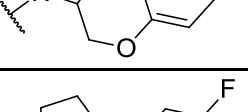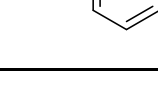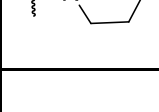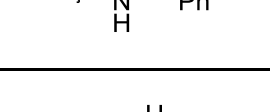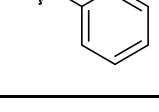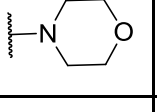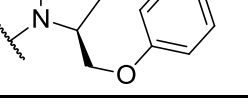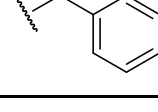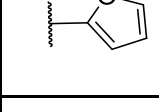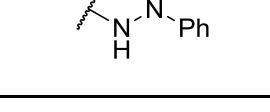
 NI-No inhibition

* Poor inhibition or no inhibition at 10 µM concentrations

Table 13: *In vitro* inhibition value of peptidomimetics against falcipain-2 enzyme[C] (Series IV)

Comp.	R$_1$	R$_2$	R$_3$	IC$_{50}$ ± SD[C] (µM)	Comp.	R$_1$	R$_2$	R$_3$	IC$_{50}$ ± SD[C] (µM)
RMQ-1	phenyl	morpholine-N	methoxy	> 25.0	RMQ-6	benzyl	CH$_2$Cl	O-ethyl	> 25.0
RMQ-2	phenyl	piperidine-N	methoxy	> 25.0	RMQ-7	phenyl	morpholine-N	OH	NI
RMQ-3	benzyl	morpholine-N	O-ethyl	> 25.0	RMQ-8	phenyl	piperidine-N	OH	NI
RMQ-4	benzyl	piperidine-N	O-ethyl	> 25.0	RMQ-9	benzyl	morpholine-N	OH	NI
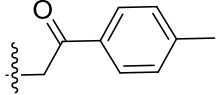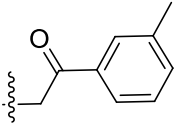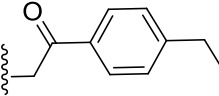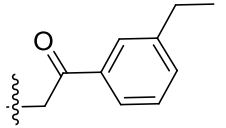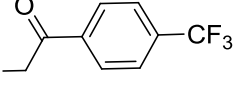
Comp.	R_1	R_2	R_3	IC$_{50}$ ± SD[c] (μM)	Comp.	R_1	R_2	R_3	IC$_{50}$ ± SD[c] (μM)
RMQ-5				> 25.0	RMQ-10				NI
RMQ-11				NI	RMQ-16				0.44 ± 0.04
RMQ-12				11.6 ± 0.8	RMQ-17				0.41 ± 0.08
RMQ-13				3.0 ± 0.5	RMQ-18				1.03 ± 0.3
RMQ-14				1.9 ± 0.8	RMQ-19				0.75 ± 0.09
RMQ-15				4.8 ± 1.1	RMQ-20				NI
E-64				0.015 ± 0.001					

[c] Data are means of three independent experiments and the values are represented as mean ± SD, NI-No inhibition

Table 14: *In vitro* inhibition value of 2-(substituted)pyrimidin-4-ylthio)-*N'*-(2-phenylacetyl)-acetohydrazide derivative against *Pf*ClpP enzyme[C)] (Series V)
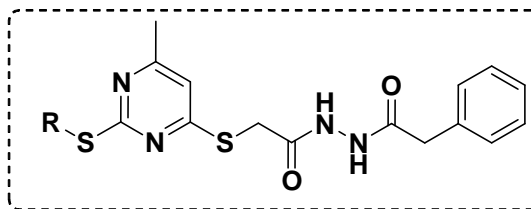
Compound	R	IC$_{50}$ ± SD[C)] (µM)	Compound	R	IC$_{50}$ ± SD[C)] (µM)
RMP-1		26.0 ± 1.6	RMP-6		26.4 ± 0.1
RMP-2		26.7 ± 0.5	RMP-7		26.6 ± 0.2
RMP-3		26.3 ± 1.1	RMP-8		26.4 ± 0.2
RMP-4		26.8 ± 1.3	RMP-9		26.2 ± 0.8
RMP-5		26.2 ± 0.1	RMP-10		26.0 ± 0.7

Compound	R	$IC_{50} \pm SD^{C)}$ (μM)	Compound	R	$IC_{50} \pm SD^{C)}$ (μM)
RMP-11		26.1 ± 0.4	RMP-14		26.2 ± 0.8
RMP-12		26.4 ± 0.2	RMP-15		26.2 ± 0.9
RMP-13		26.4 ± 1.2	Chymostatin		10.0 ± 0.32

[c)] Data are means of three independent experiments and the values are represented as mean ± SD

Table 15: *In vitro* inhibition value of 1,6-dihydropyrimidine-5-carboxamides derivatives against *Pf*ClpP protease[C)] (Series VI)
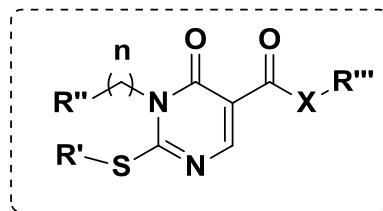
Compound	n	X	R'	R''	R'''	IC$_{50}$ ± SD (µM)[c)]
RMH-1	1	NH				24.2 ± 0.8
RMH-2	1	NH				44.6 ± 1.1
RMH-3	1	NH				72.6 ± 0.4
RMH-4	1	NH				10.5 ± 0.2
RMH-5	1	NH				58.2 ± 0.3
RMH-6	1	NH				> 100
RMH-7	1	NH				> 100
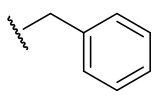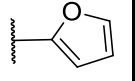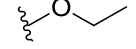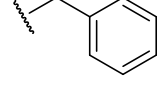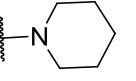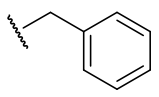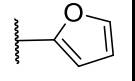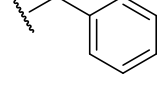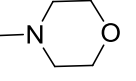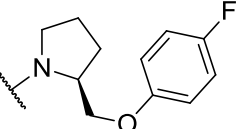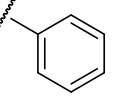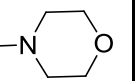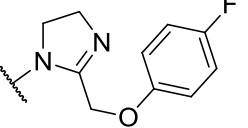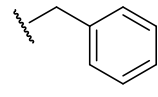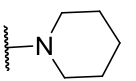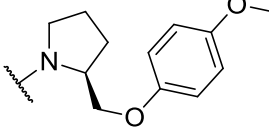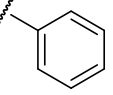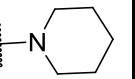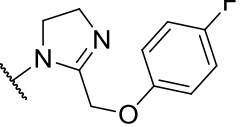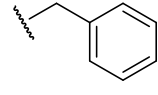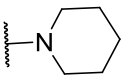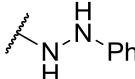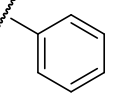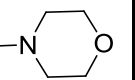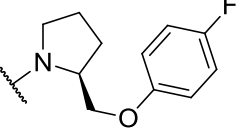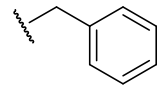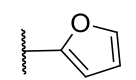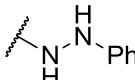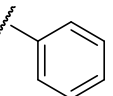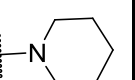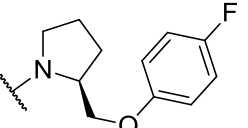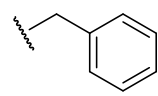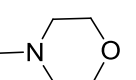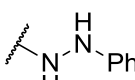
Compound	n	X	R'	R''	R'''	IC$_{50}$ ± SD (µM)[c]
RMH-8	1	NH				> 100
RMH-9	1	NH				46.0 ± 0.7
RMH-10	0	O		-H		42.4 ± 0.4
RMH-11	0	O		-H		> 100
RMH-12	1	O				39.7 ± 0.7
RMH-13	0	O		-H		44.1 ± 1.1
RMH-14						> 100
Chymostatin						10 ± 0.32

[c] Data are means of three independent experiments and the values are represented as mean ± SD

152

Table 16: *In vitro* inhibition value of peptidomimetics against *P. falciparum* 3D7 strain[C)] (Series IV)

Comp.	R₁	R₂	R₃	IC₅₀ ± SD[C)] (µM)	Comp.	R₁	R₂	R₃	IC₅₀ ± SD[C)] (µM)
RMQ-1	phenyl	N-morpholine	O-methyl	> 50.0	RMQ-6	benzyl	CH₂Cl	O-ethyl	> 25.0
RMQ-2	phenyl	N-piperidine	O-methyl	> 25.0	RMQ-7	phenyl	N-morpholine	OH	ND
RMQ-3	benzyl	N-morpholine	O-ethyl	> 50.0	RMQ-8	phenyl	N-piperidine	OH	ND
RMQ-4	benzyl	N-piperidine	O-ethyl	> 50.0	RMQ-9	benzyl	N-morpholine	OH	ND

Comp.	R₁	R₂	R₃	$IC_{50} \pm SD^{C)}$ (µM)	Comp.	R₁	R₂	R₃	$IC_{50} \pm SD^{C)}$ (µM)
RMQ-5	benzyl	furan-2-yl	ethoxy	> 25.0	RMQ-10	benzyl	piperidin-1-yl	OH	ND
RMQ-11	benzyl	furan-2-yl	OH	ND	RMQ-16	benzyl	morpholino	(4-fluorophenoxy)methyl pyrrolidine	10.3 ± 0.04
RMQ-12	phenyl	morpholino	2-((4-fluorophenoxy)methyl)imidazoline	> 10.0	RMQ-17	benzyl	piperidin-1-yl	(4-methoxyphenoxy)methyl pyrrolidine	35.7 ± 0.08
RMQ-13	phenyl	piperidin-1-yl	2-((4-fluorophenoxy)methyl)imidazoline	5.2 ± 0.47	RMQ-18	benzyl	piperidin-1-yl	N'-phenylhydrazino	14.2 ± 0.3
RMQ-14	phenyl	morpholino	(4-fluorophenoxy)methyl pyrrolidine	0.9 ± 0.1	RMQ-19	benzyl	furan-2-yl	N'-phenylhydrazino	27.9 ± 0.09
RMQ-15	phenyl	piperidin-1-yl	(4-fluorophenoxy)methyl pyrrolidine	> 10.0	RMQ-20	benzyl	morpholino	N'-phenylhydrazino	ND
Artemisinin*				0.026 ± 0.001	E-64				3.4 ± 0.2

[c)] Data are means of three independent experiments and the values are represented as mean ± SD, ND-Not done, * Positive test control

Table 17: *In vitro* inhibition value of 2-(substituted)pyrimidin-4-ylthio)-*N'*-(2-phenylacetyl)-acetohydrazide derivatives against *P. falciparum* 3D7 strain[c] (Series V)
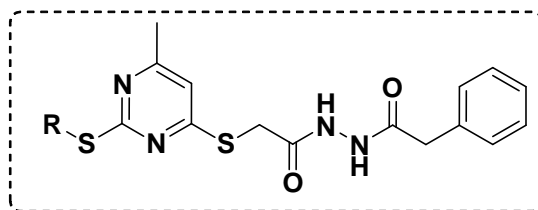
Compound	R	$IC_{50} \pm SD^{C)}$ (μM)	Compound	R	$IC_{50} \pm SD^{C)}$ (μM)
RMP-1		75.0 ± 1.4	RMP-9		11.3 ± 0.04
RMP-2		11.8 ± 0.8	RMP-10		12.8 ± 0.8
RMP-3		12.1 ± 1.1	RMP-11		11.1 ± 1.1
RMP-4		17.3 ± 0.1	RMP-12		12.3 ± 0.1
RMP-5		14.4 ± 0.04	RMP-13		12.4 ± 0.04
RMP-6		12.3 ± 0.03	RMP-14		13.3 ± 0.03
RMP-7		11.3 ± 0.04	RMP-15		12.3 ± 0.04
RMP-8		12.3 ± 0.04	Chymostatin		0.1± 0.01
Artemisinin*		0.026± 0.001			

[c] Data are means of three independent experiments and the values are represented as mean ± SD

 * Positive test control

Table 18: *In vitro* inhibition value of 1,6-dihydropyrimidine-5-carboxamides derivatives against *P. falciparum* 3D7 strain[C)] (Series VI)
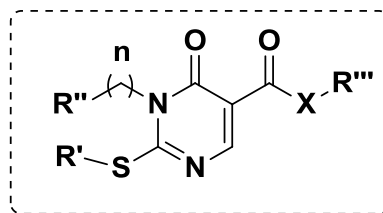
Compound	n	X	R'	R''	R'''	IC$_{50}$ ± SD (μM)[c)]
RMH-1	1	NH				20.0 ± 1.1
RMH-2	1	NH				2.0 ± 0.8
RMH-3	1	NH				> 100
RMH-4	1	NH				9.0 ± 0.2
RMH-5	1	NH				> 100
RMH-6	1	NH				ND
RMH-7	1	NH				ND

156

Compound	n	X	R'	R''	R'''	IC$_{50}$ ± SD (µM)[c]
RMH-8	1	NH				ND
RMH-9	1	NH				ND
RMH-10	0	O		-H		82.5 ± 0.5
RMH-11	0	O		-H		> 50.0
RMH-12	1	O				19.0 ± 0.4
RMH-13	0	O		-H		22.0 ± 0.5
RMH-14						ND
Artemisinin*						0.026± 0.001
Chymostatin						0.1± 0.01

[c] Data are means of three independent experiments and the values are represented as mean ± SD, ND-Not done,* Positive test control

5.3. Biological activities/pharmacology

Biological experiments were conducted in collaboration with Dr. Asif (ICGEB, New Delhi).

5.3.1. Biological activities/pharmacology for Series I

All synthesized derivatives were evaluated for their *in vitro* falcipain-2 inhibitor activity. Several compounds showed significant inhibitory activity (> 60%), against falcipain-2 at 10 µM concentrations, presented in **Table 10**. E-64 (L-transepoxysuccinyl-leucylamide-[4-guanido]-butane) was used as a reference drug in the assay.
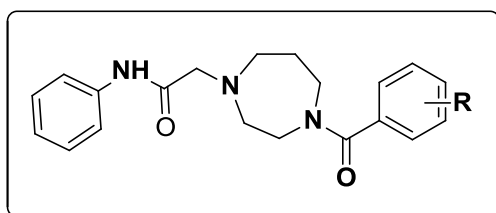
Retaining the common 2-(4-(substituted benzoyl)-1,4-diazepan-1-yl)-*N*-phenylacetamide framework, compounds **RM-1**, **RM-2** were screened, initially. Fortunately, these two compounds exhibited inhibitory activity against falcipain-2 enzyme at 10 µm concentrations with inhibition values of 49% and 61%, respectively.

With a view to explore the effects of different substituents on the aromatic moiety and generate a SAR, a couple of analogs with electron withdrawing as well as electron donating groups attached at diverse positions in the phenyl ring, were synthesized and their falcipain-2 inhibitory potential examined **(Figure 35)**.

The effect of fluorine group, an electron withdrawing substituent, was investigated at positions 2nd on the phenyl moiety (compound **RM-3**). This modification did not result in any improved potency, and compound exhibited 60% enzyme inhibition close to compound **RM-2**. Incorporation of an another electron withdrawing substituent such as chloro group at dissimilar positions in the aromatic ring gave compound **RM-4, RM-5** and **RM-6** with diminished falcipain-2 inhibitor activity (47% inhibition by **RM-4, RM-5**, and 36% by **RM-6**) as compared to compound **RM-2**.

When a strong electron withdrawing group trifluoromethyl was introduced at the 3rd position to get the compound **RM-7** (72% inhibition) and in position 4th to get the compound **RM-8** (68% inhibition), both compounds showed higher potency than the compound **RM-2**. However, investigation of trifluoromethyl group at the 2nd position of the phenyl ring showed lesser potency (50% inhibition) as compared to compound **RM-2**.

Consequently, a methoxy group, an electron releasing substituent was introduced at 2nd and 3rd positions of the phenyl ring, resulted in compounds with improved inhibition potency (70% and 64%), greater than the compound **RM-2** from this series. Attachment of a methoxy

158

group in the 4th position of the phenyl ring gave rise to compound **RM-12**, with inhibition potency (55%), which was lesser than that of **RM-2**. Compounds **RM 13** to **15** were achieved by replacement of the methoxy group to ethoxy group and leads to markedly loss in potency (32%, 36% and 30%).

Replacement of a methoxy group in phenyl ring with another weaker electron releasing group such as methylene at 2nd , 3rd and 4th positions **(RM 16 to 18)**, and ethylene group at 3rd and 4th positions **(RM-19** and **RM-20)**, lead to decrease in the potency. Overall, five compounds **RM-2**, **RM-7**, **RM-8**, **RM-10** and **RM-11** showed good inhibitory activity (> 60%), against falcipain-2 enzyme at 10 µM concentration, and fifteen compounds showed weak to moderate inhibitory activity. It is worthwhile to mention that the sceening results of this series of compounds were not in the expected range (> 75-80 %) against falcipain-2 enzyme at 10 µM concentrations. Thus, compounds were not tested on further dilutions and therefore IC$_{50}$ values were not computed.
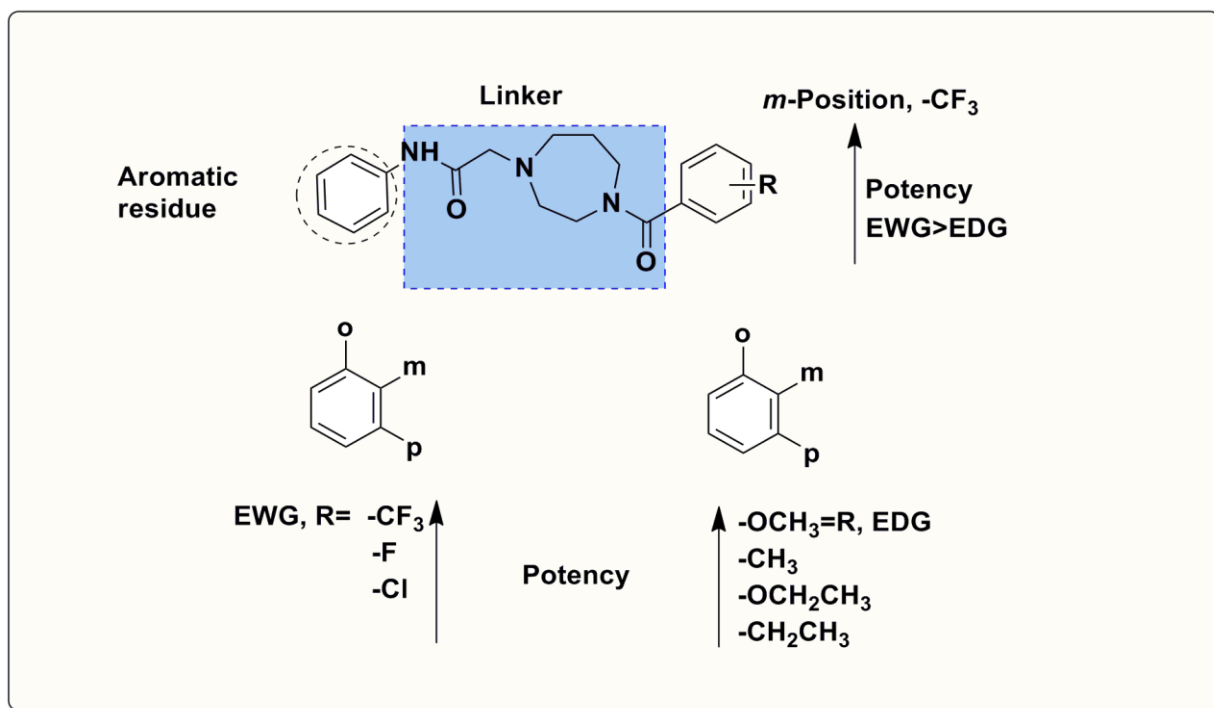
Figure 35: SAR of falcipain-2 inhibition of 2-(4-(substituted benzoyl)-1,4-diazepan-1-yl)-*N*-phenylacetamide derivatives (RM 1 to 20; Series I)

5.3.2. Docking studies

Molecular modeling studies are required to generate molecular models that assimilate all experimental evidences reported. Considering the well retrieved *in vitro* results, it was thought worthy to perform *in silico* studies for the hit molecules. Glide v5.9 (Schrodinger, Inc.) maestro version 9.4, was used to investigate the binding mode of the molecules. The crystal structure of FP-2 was obtained from the Protein Data Bank (PDB entry: 3BPF) with a resolution of 2.9 Å. The conserved catalytic site residues of Cys 42, Asn 173 and Hip 174 is located in a junction between the structurally distinct domains. Gln 36, Ser 41 and Asn 81 are conserved amino acids participate in the formation of additional hydrogen bond with substrate. In the current study, the prepared sets of ligands were docked to the receptive processed target protein and generated various possible poses on the basis of positioning. These simulations were carried out by allowing positional adaptability and torsion flexibility in ligands with the use of XP (extra precision) mode, offering full range of accuracy. Model energy function known as Glide score (G-score) is the selection parameter to filter best docked ligands among all sets of ligands. In order to analyze the ligand-receptor interactions (Hydrogen bond, Hydrophobic and electrostatic etc), Glide XP visualizer module was used.

Comparison of interacting residues of hit analogs **(RM-7** and **RM-10)** showed that, the amino acids Cys 42, Trp 206, Val 152, Asn173, Hip 174, Leu 84 and Gln 36 of FP-2 protein are most commonly involved as shown in **Figure 36 (A & B)**, respectively. Among these, the residue Asn 173 was the hydrogen bonding common interacting residue of FP-2 with ligands **(RM-7** and **RM-10)**. Compound **RM-7** showed fIve hydrophobic interactions, Leu 172, Cys 42, Trp 206, Val 152, Leu 84 ; three hydrogen bonds, Gln 36 (2.08 Å), Asn 173 (2.19 Å) and Hip 174 (2.54 Å). Compound **RM-10** showed six hydrophobic interactions, Ala 175, Leu 84, Trp 43, Trp 206, Val 152; Ile 85; two hydrogen bonds, Asn 173 (2.09 Å) and Hip 174 (2.15 Å). On the other hand, compound **RM-20**, which is a less active analogue, showed six hydrophobic interactions with Ala 175, Leu 84, Trp 43, Trp 206, Val 152; Ile 85; one hydrogen bonds, Gln 36 (2.15 Å) as shown in **Figure 36 (C)**. Further, it was found that Hip 174 involved in π-π stacking interactions and Ser 205, Ser 41, Ser 153 amino acids involved in electrostatic interactions. Overall, the present 2-(4-(substituted benzoyl)-1,4-diazepan-1-yl)-*N*-phenylacetamide analogs displayed better interactions with enzyme exhibiting their inhibitory activity. The overlay docked view (standard precision mode) of all these three compounds as shown by **Figure 36 (G)**, indicates that the pharmacophoric elements like the central homopiperazine ring with a keto group (hydrogen bond acceptor) and amide linkage (hydrogen bond donor), the aromatic moiety and diverse substituted phenyl ring plays substantial roles in forming various interactions with the active site.
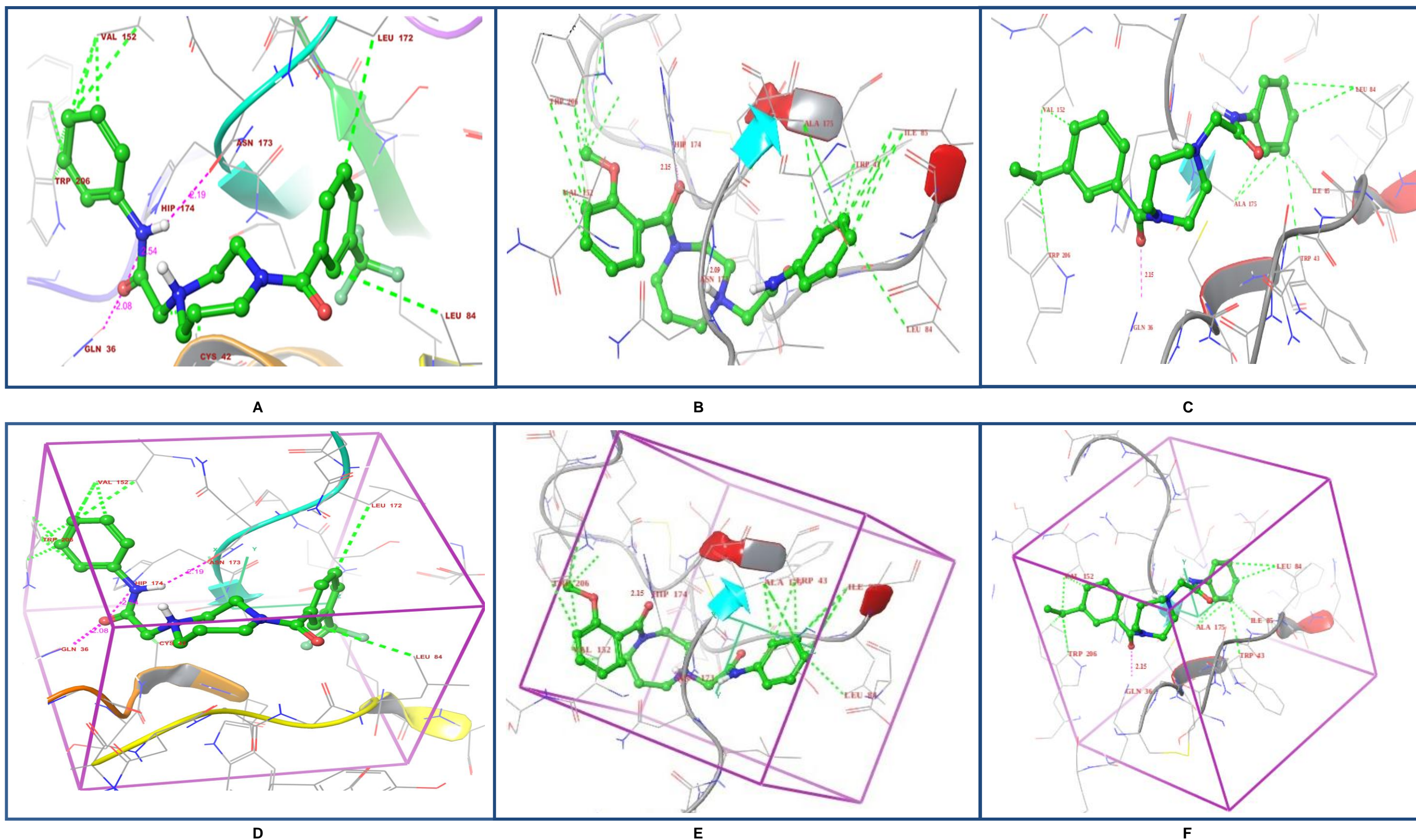
Figure 36 (A-C): Best binding poses of ligands RM-7; *N*-phenyl-2-(4-(3-(trifluoromethyl) benzoyl)-1,4-diazepan-1-yl) acetamide, RM-10; *N*-phenyl-2-(4-(4-(trifluoromethyl) benzoyl)-1,4-diazepan-1-yl) acetamide, RM-20; 2-(4-(3-Ethylbenzoyl)-1,4-diazepan-1-yl)-*N*-phenylacetamide, respectively; docked to chain A of falcipain-2 protein (3BPF.pdb). **(D-F):** Binding poses of ligands RM-7, RM-10 and RM-20; respectively; docked to chain A of falcipain-2 protein (3BPF.pdb), confined to the cubic box size 5 Å, supplied X, Y and Z coordinates with -54, -4 and -16 Å. The pink dashed line represents the possible hydrogen bond and green dashed line represents the possible hydrophobic interaction
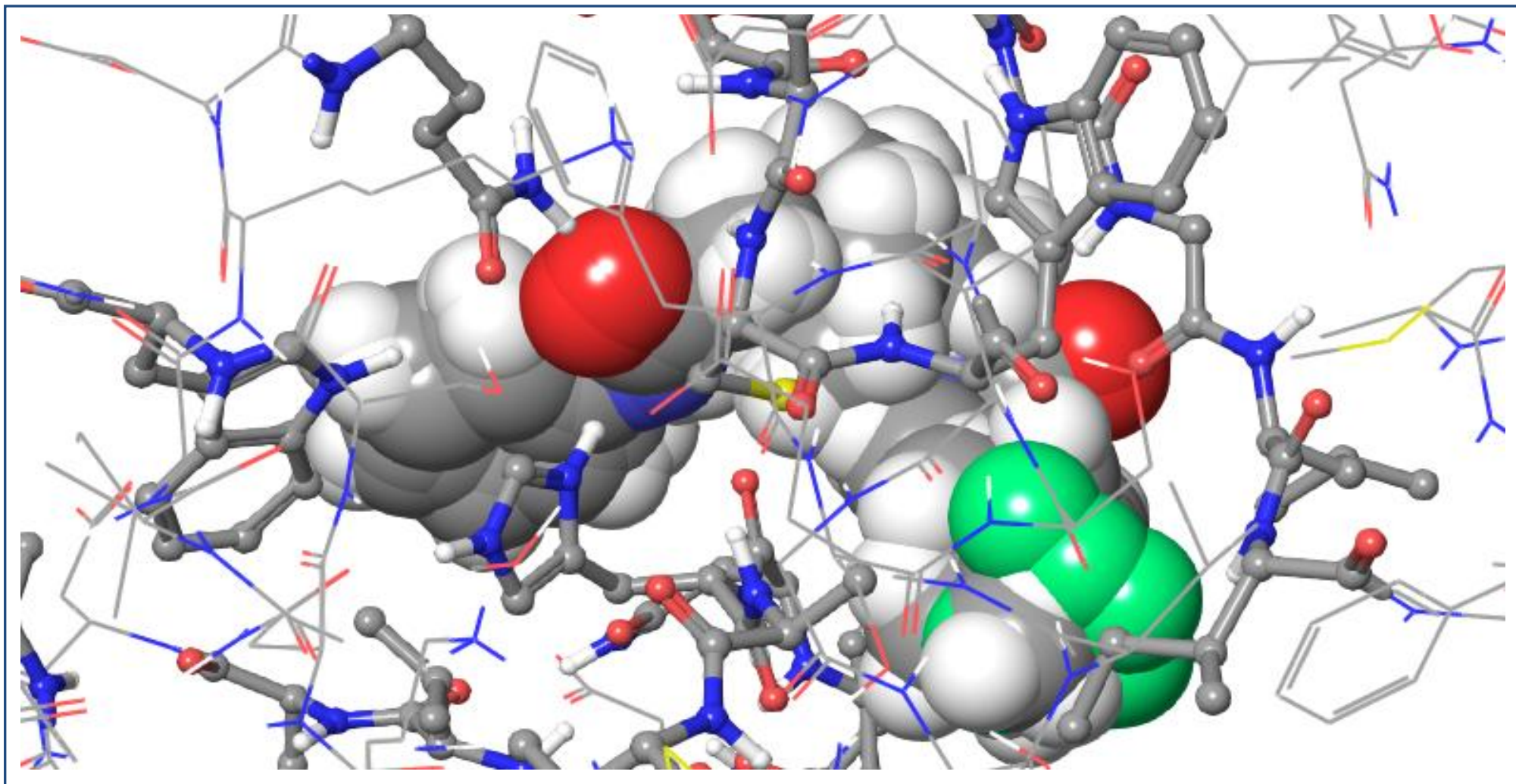
Figure 36 (G): The superimposed docking confirmation (space-filling model) of RM-7; *N*-phenyl-2-(4-(3-(trifluoromethyl) benzoyl)-1,4-diazepan-1-yl) acetamide, RM-10; *N*-phenyl-2-(4-(4-(trifluoromethyl) benzoyl)-1,4-diazepan-1-yl) acetamide, RM-20; 2-(4-(3-Ethylbenzoyl)-1,4-diazepan--yl)-*N*-phenylacetamide in chain A of falcipain-2 protein (3BPF.pdb)

To understand the participation of FP-2 enzyme amino acids as H-bond donor or acceptor, the docked pose of prototype compound **(RM-7)** was compared with co-crystallized ligand E-64 as represented in **Figure 36 (H)**. Among the various interacting amino acids of FP-2 enzyme with E-64 molecule, possesed seven hydrogen bonds with Gln 36 (2.78 Å), Cys 42 (2.12 Å), Asn 173 (2.09 Å), Gly 83 (2.19 Å), Hip 174 (2.81 Å), Asn 77 (2.29 Å), Asn 87 (2.18 Å) and seven hydrophobic interactions with Leu 172, Leu 84, Ile 85, Ala 175, Cys 42, Ala 175, Tyr 78. Comparison of interacting residues of hit analog (RM-7) with standard drug (E-64) shows that, the amino acids Gln 36, Asn 173, Hip 174 are the hydrogen bonding common interacting residues and Leu 84, Leu 172, Cys 42 are involved as common amino acids to develop hydrophobic interactions. Thus, the participation of additional amino acids such as Cys 42, Gly 83, Asn 77 and Asn 87 in hydrogen bonds and Ile 85, Ala 175, Ala 175 and Tyr 78 in the formation of hydrophobic interactions may conductively increase the activity of the standard ligand as compared to hit compound.
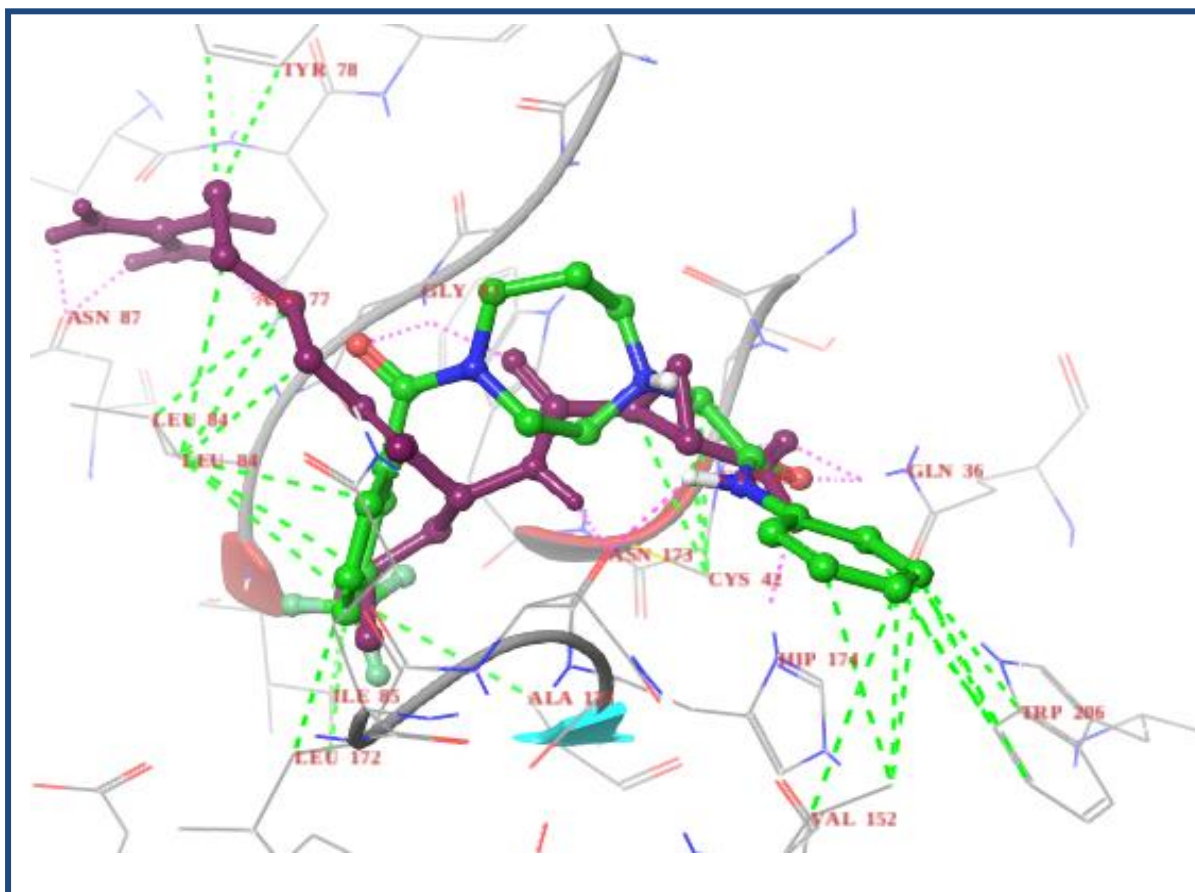
Figure 36 (H): Overlap pose of co-crystallized ligand (E-64, red color) with compound RM-7, (green color). Pink dashed line represents the possible hydrogen bond and green dashed line represents the possible hydrophobic interaction

5.3.3. Biological activities/pharmacology for Series II

All newly synthesized compounds **RMS 1** to **20** were evaluated for their *in vitro* inhibitory activities against falcipain-2 enzyme (FP-2) using the fluorometric assay, and the results are summarized in **Table 11**. Initial screening of two compounds **RMS-1** and **RMS-2** showed 25% and 15% inhibition value, respectively; at 10 µM concentrations.
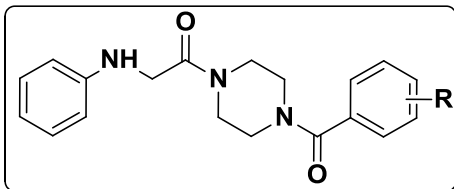
In a bid, to see the effect of different substituent on the phenyl ring and generate structure activity relationships **(Figure 37)**, a series of compounds with electron withdrawing as well as electron donating groups were introduced at different positions in the phenyl ring, synthesized and screened.

The effect of fluorine group, an electron withdrawing substituent was investigated at 3rd and 4th positions of the phenyl ring (compounds, **RMS-20** and **RMS-3**), the generated compound showed no inhibition. A similar response was observed after replacement of an electron withdrawing group with chloro at 2nd **(RMS-18)**, 3rd **(RMS-19)**, 4th **(RMS-4)** positions and trifluoromethyl substituent at 4th position of the aromatic ring (compounds **RMS-5**).

Subsequently, methyl group, a weaker electron releasing group was introduced at 2nd , 3rd and 4th positions of the phenyl ring, the resultant compounds **(RMS 6 to 8)** showed more inhibition than the hit compound **RMS-1**. It is noteworthy that, the inhibitory activity of compound **RMS-8** increased ~2 times than that of compound **RMS-1** (inhibition value increases from 25 % to 50 % **Table 11**).

Incorporation of another electron releasing methoxy group at different positions of the phenyl ring, resulted in compounds **(RMS 9** to **11)** that exhibited moderately improved inhibition than the compound **RMS-1**. Further, replacement of the methoxy group with its higher homologue, i.e., ethoxy group at position 2nd to get the compound **RMS-15** (inhibition value 42%) showed higher potency than the hit compound **RMS-1**. However, investigation of an ethoxy group at 3rd and 4th positions to get compounds **RMS-16** and **RMS-17** of the phenyl ring showed lesser potency as compared to the hit compound.

Compound **RMS-12** (ethyl at position 2nd and compound **RMS-13** (ethyl at position 3rd had the same electron releasing ethyl group at different positions (2nd and 3rd in the phenyl ring, but compound **RMS-12** (24 %) and **RMS-13** (20 %) showed lesser falcipain-2 inhibition potency than compound **RMS-1**. However, attachment of ethyl group at 4th position (compound **RMS-14**) of the phenyl ring was observed to improve the inhibitory activity as compared to its regioisomeric compounds namely, **RMS-12** and **RMS-13**. Overall, four compounds **RMS-6**, **RMS-8**, **RMS-14** and **RMS-15** showed good inhibitory activity against falcipain-2 enzyme at 10 µM concentration.
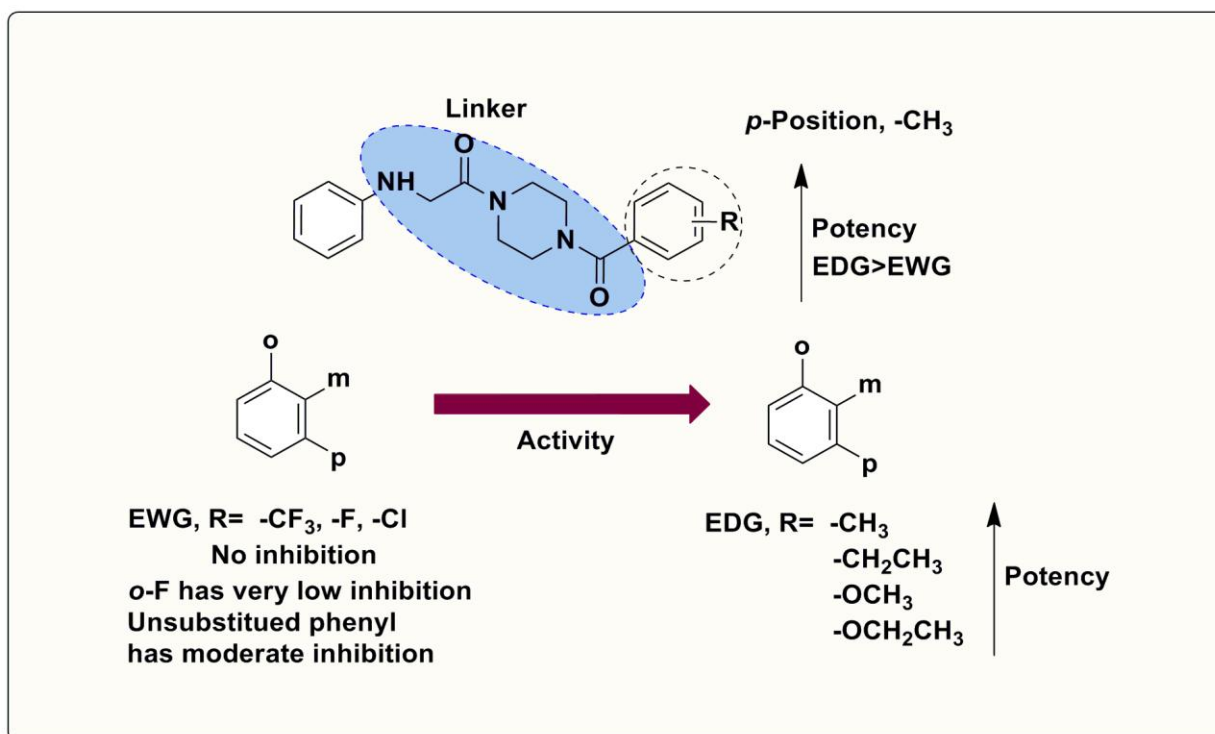
Figure 37: SAR of falcipain-2 inhibition of 1-(4-(substituted)piperazin-1-yl)-2-(phenylamino)ethanone derivatives (RMS 1 to 20; Series II)

5.3.4. Docking studies

To estimate the binding mode interactions of the designed analogs at the active site of the FP-2 with respect to the co-crystallized ligand E-64, *in-silico* docking simulation study was carried out. *In silico* studies revealed that, all the synthesized molecules showed glide score (a model energy function) toward the target protein ranging from −5.89 to −3.82 kcal/mol and compounds **RMS-8** and **RMS-14** showed minimum binding energies.

In order to gain depth information of relative binding affinities and molecular level interactions together with the most common interacting amino acids of falcipain-2 enzyme responsible for stabilizing the complex, the top compounds were investigated for detailed interpretation. On comparison of interacting residues of these active analogs **(RMS-8** and **RMS-14)**, it was observed that amino acids such as Trp 206, Ile 85, Leu 84, Val 152 were most commonly involved in hydrophobic interactions while Asn 173, Cys 42 amino acids were involved in hydrogen bonding as shown in **Figure 38 (A & B)**, respectively.

The most potent compound **RMS-8** showed six hydrophobic interactions Trp 206, Ile 85, Leu 84, Val 152, Ala 175, Trp 43; two hydrogen bonds, Asn 173 (2.11 Å), Cys 42 (2.57 Å). Compound **RMS-14** showed five hydrophobic interactions, Trp 206, Ile 85, Leu 84, Val 152, Ala 175; two hydrogen bonds, Asn 173 (2.26 Å), Cys 42 (2.62 Å). In addition, it was found that Hip 174 involved in π-π stacking interactions and Ser 149, Ser 86, Ser 4, Ser 41 amino acids involved in electrostatic interactions to stabilize the enzyme substrate complex more strongly. On the other hand, compound **RMS-4**, which is a inactive analogue, showed only two hydrophobic interactions with Leu 84 and Trp 206 as shown in **Figure 38 (C)**. The overlay docked view of all these three compounds, is depicted in **Figure 38 (G)**.

Overall, docking analysis revealed that, hydrogen bond (HB) formation and hydrophobic interactions, conductive to increase the binding efficiency and lead to effectively span and occupy the enzyme pockets with respect to the substrate sites.

A

B

C

D

E

F
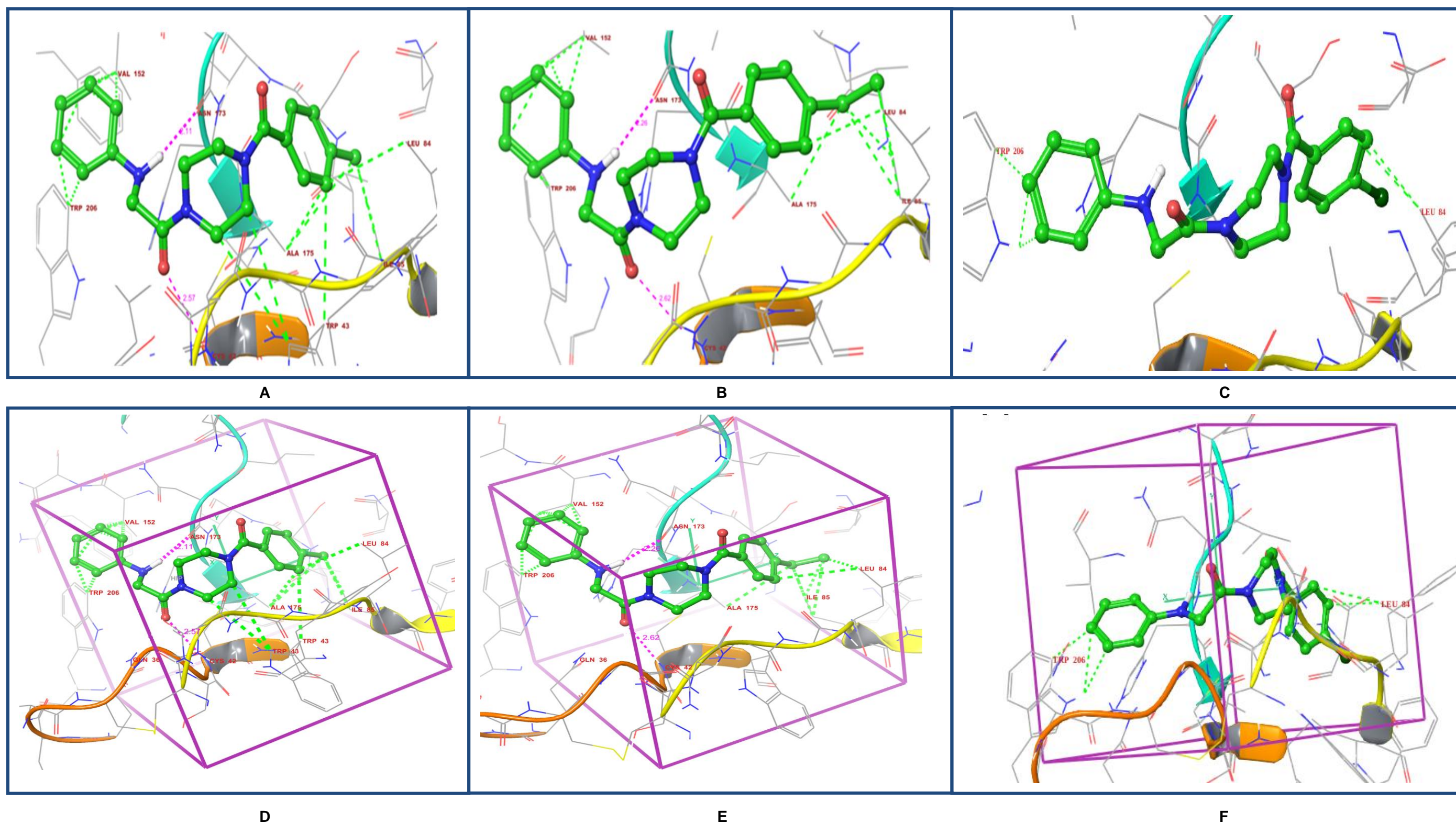
Figure 38 (A-C): Best binding poses of ligands RMS-8; (1-(4-(4-methylbenzoyl)piperazin-1-yl)-2-(phenylamino)ethanone), RMS-14; (1-(4-(4-ethylbenzoyl)piperazin-1-yl)-2-(phenylamino)ethanone), and RMS-4; 1- (4-(4-chlorobenzoyl)piperazin-1-yl)-2-(phenylamino)ethanone, respectively; docked to chain A of falcipain-2 protein (3BPF.pdb). **(D-F):** Binding poses of docked ligands RMS-8, RMS-14 and RMS-4, respectively; docked to chain A of falcipain-2 protein (3BPF.pdb), confined to the cubic box size 5 Å, supplied X, Y and Z coordinates with -54, -4 and -16 Å. The pink dashed line represents the possible hydrogen bond and green dashed line represents the possible hydrophobic interaction

167
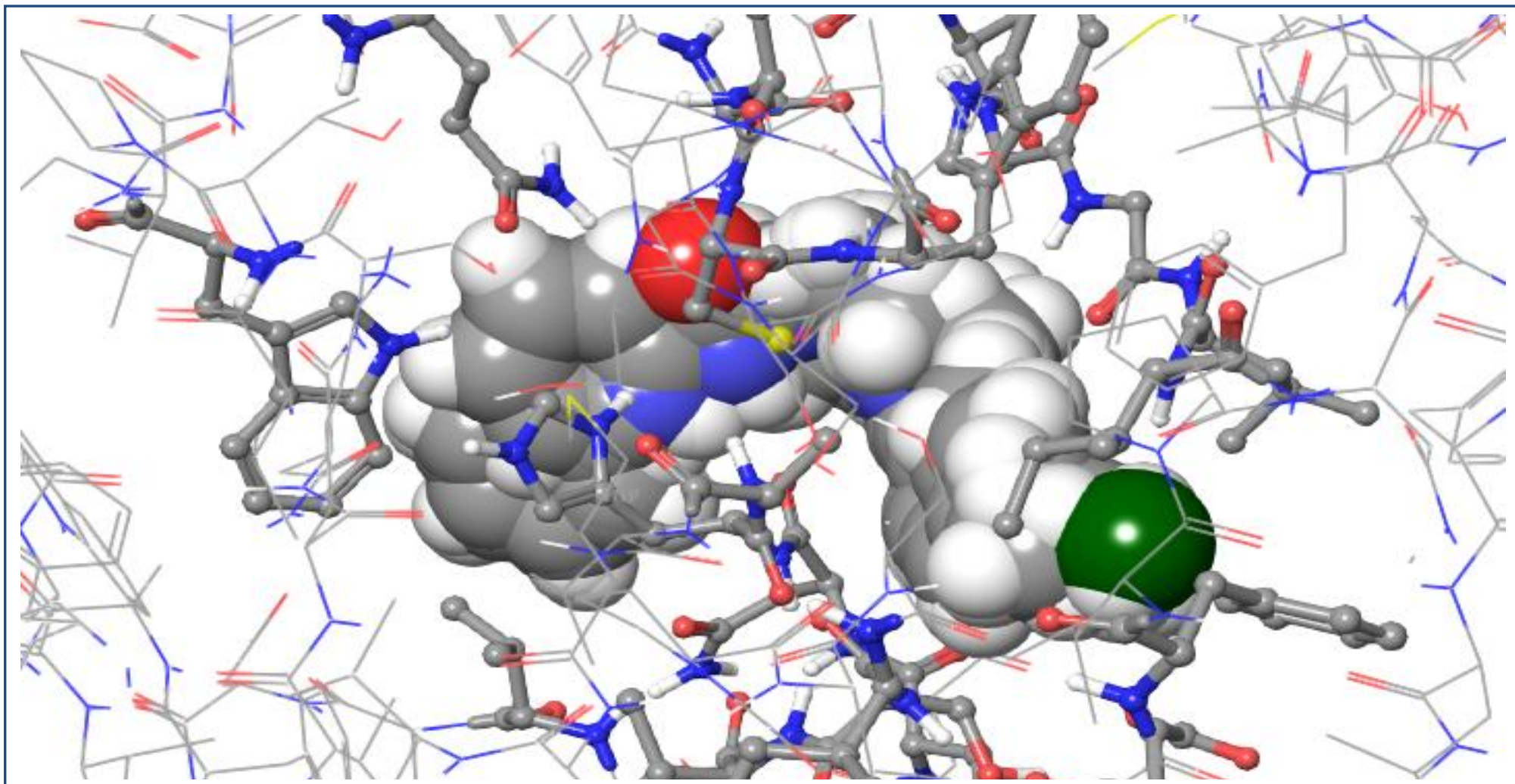
Figure 38 (G): The Superimposed docking confirmation (space-filling model) of RMS-8; (1-(4-(4-methylbenzoyl)piperazin-1-yl)-2-(phenylamino)ethanone), RMS-14; (1-(4-(4-ethylbenzoyl)piperazin-1-yl)-2-(phenylamino)ethanone), and RMS-4; 1- (4-(4-chlorobenzoyl)piperazin-1-yl)-2-(phenylamino)ethanone in chain A of falcipain-2 protein (3BPF.pdb)

5.3.5. Biological activities/pharmacology for Series III

All synthesized molecules were evaluated for their *in vitro* falcipain-2 inhibitory activity and inhibition data are represented in **Table 12**. It is worthy to mention that, initial screening at 10 μM concentrations showed poor or no inhibition. Therefore, all the compounds were subjected to evaluate at 25 μM concentrations. In order to understand the importance of
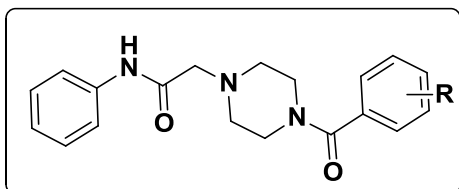
aromatic residue in the designed structure and generate structure activity relationships **(Figure 39)**, various electron withdrawing as well as electron donating substituents appended at different positions on the phenyl ring.

The results indicated that, the unsubstituted phenyl group as in compound **RMT-1** displayed very weak inhibitory activity whereas **RMT-2** was moderately favoured and showed 21% inhibition value. Compound **RMT-4, RMT-5**, **RMT-7, RMT-8**, **RMT-9,** and **RMT-15,** exhibited very less to moderate inhibitory activity. Whereas, compounds **RMT-12**, **RMT-16** and **RMT-17** displayed a very weak inhibition value for falcipain-2 enzyme. Compound **RMT-20** had almost equal potency as compared to **RMT-2**. Overall, two compounds **RMT-2**, and **RMT-20** showed moderate inhibitory activity against falcipain-2 enzyme at 25 μM concentration, and remaining compounds showed weak inhibitor activity.
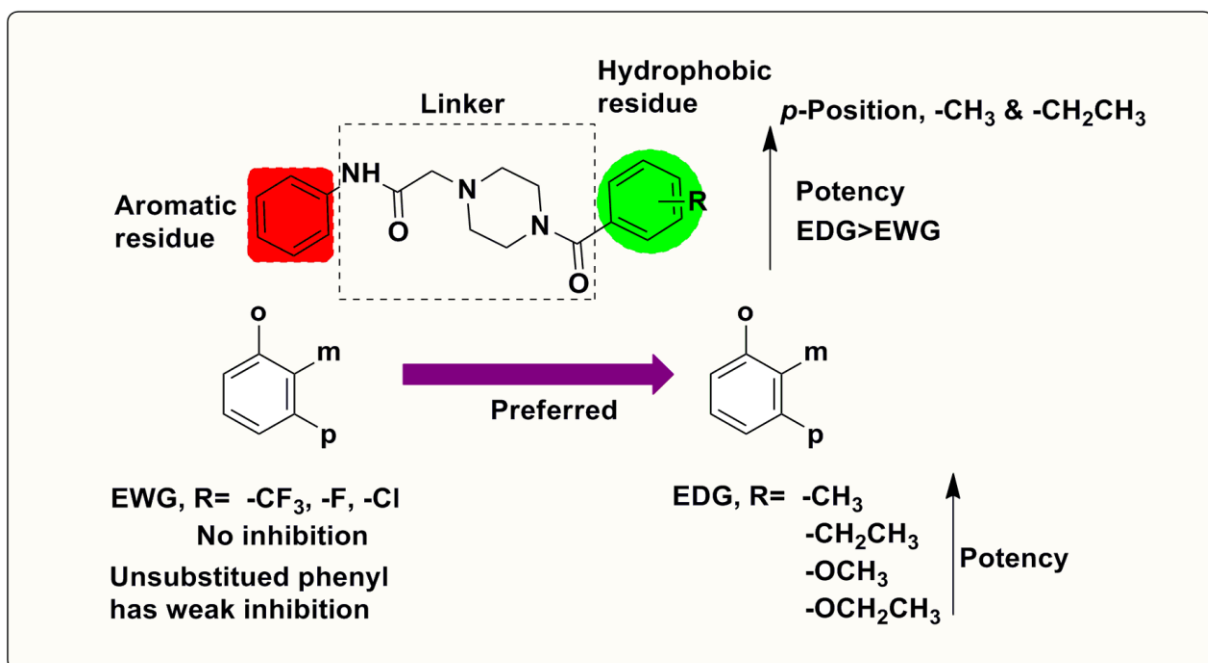
Figure 39: SAR of falcipain-2 inhibition of 2-(4-(substituted benzoyl)piperazin-1-yl)-*N*-phenylacetamide derivatives (RMT 1 to 20; Series III)

5.3.6. Docking studies

Docking studies were performed for the representatives of this new series compounds to predict their relative binding affinities and binding modes in the active site of the falcipain-2 enzyme. Molecular docking studies of two top analogs **(RMT-2 and RMT-20)** revealed that, they interacted with Ile 85, Leu 84, Val 152, Ala 175 residues of 3BPF protein, via hydrophobic interactions **Figure 40 (A & B)**, respectively. The interactions of compound **RMT-2** with the active site of enzyme was found to be contributed by five hydrophobic interactions, Ile 85, Leu 84, Val 152, Ala 175, Trp 206 and one hydrogen bonds, Gln 36 (2.38 Å), whereas the interaction of compound **RMT-20** showed six hydrophobic interactions, Ile 85, Leu 84, Val 152, Ala 175, Cys 42, Trp 206 and no hydrogen bonds. On the other hand, compound **RMT-19**, which is a inactive analogue, showed only three hydrophobic interactions with Leu 84 Trp 206 and Ala 175 and as shown in **Figure 40 (C)**. Further, it was found that these compounds did not exhibit any π-π stacking interactions and electrostatic interactions. The superimposition docked view of all these three compounds, is shown in **Figure 40 (G)**. Overall, the present 2-(4-(substituted benzoyl)-1,4-diazepan-1-yl)-*N*-phenylacetamide analogs displayed weak interactions with enzyme exhibiting their inhibitory activity.

A

B

C

D

E

F
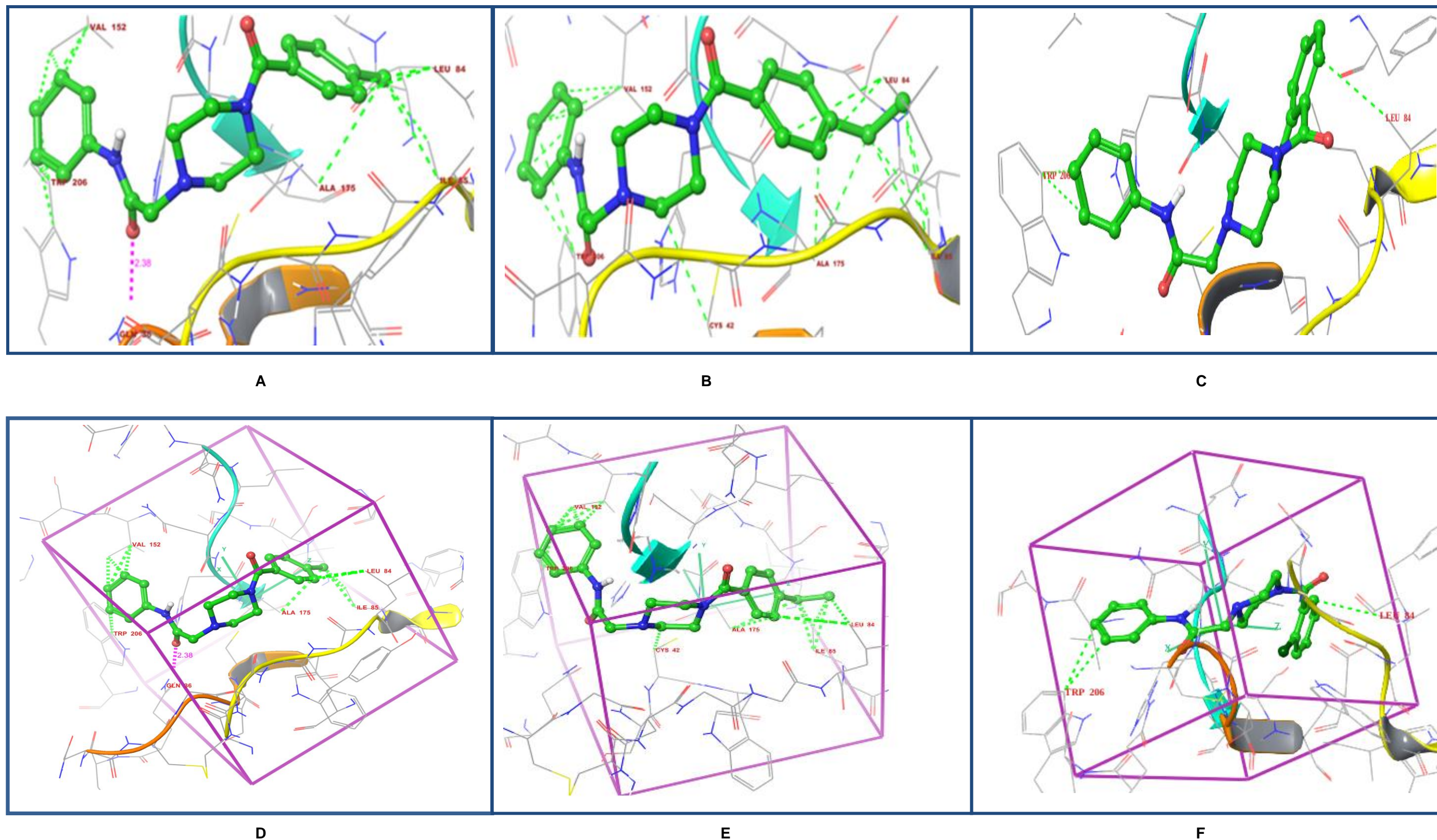
Figure 40 (A-C): Best binding poses of ligands RMT-2; (2-(4-(4-methylbenzoyl)piperazin-1-yl)-*N*-phenylacetamide), RMT-20; (2-(4-(4-ethylbenzoyl)piperazin-1-yl)-*N*-phenylacetamide) and RMT-19; 2-(4-(2-chlorobenzoyl)piperazin-1-yl)-*N*-phenylacetamide, respectively; docked to chain A of falcipain-2 protein (3BPF.pdb). **(D-F):** Binding poses of docked ligands RMT-2, RMT-20 and RMT-19, respectively; docked to chain A of falcipain-2 protein (3BPF.pdb), confined to the cubic box size 5 Å, supplied X, Y and Z coordinates with -54, -4 and -16 Å. The pink dashed line represents the possible hydrogen bond and green dashed line represents the possible hydrophobic interaction

171
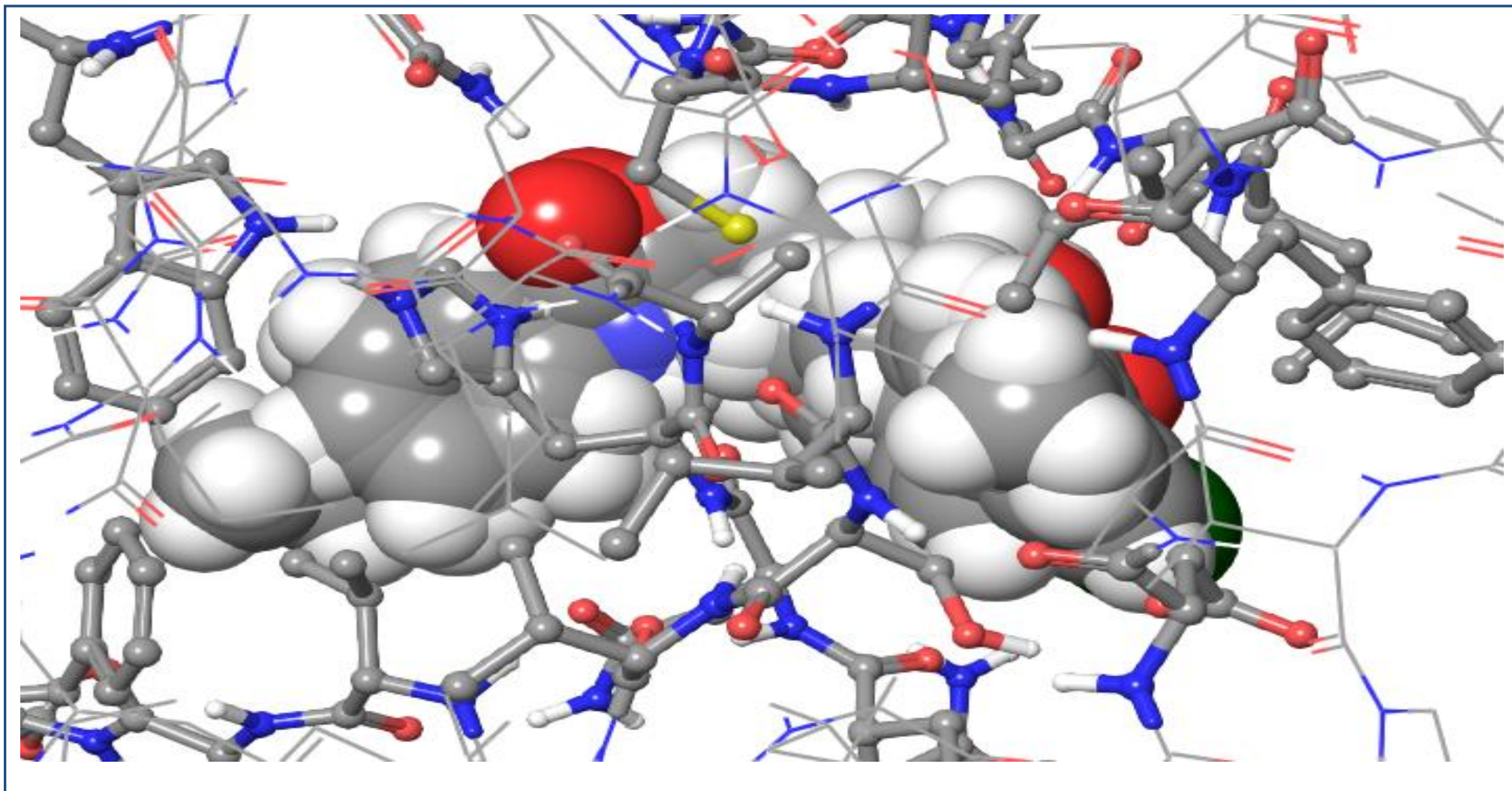
Figure 40 (G): The superimposed docking confirmation (space-filling model) of RMT-2; (2-(4-(4-methylbenzoyl)piperazin-1-yl)-*N*-phenylacetamide), RMT-20; (2-(4-(4-ethylbenzoyl)piperazin-1-yl)-*N*-phenylacetamide) and RMT-19; 2-(4-(2-chlorobenzoyl)piperazin-1-yl)-*N*-phenylacetamide in chain A of falcipain-2 protein (3BPF.pdb)

### 5.3.7. Biological activities/pharmacology for Series IV

The inhibitory activities of synthesized compounds were analyzed by their ability to block the *in vitro* protease activity of recombinant falcipain-2 **(Tables 13)**.

The basic scaffold has four different variable groups T_1, T_2, T_3 and T_3' correspond to R_1, R_2 and R_3 (T_3 and T_3'), substituents. T_3' terminal on the designed structure, occupying S1' subsite of the target was explored with different hydrophobic residues (phenyl substituents) and T_1 position, occupying S2 pocket (substrate specificity) was investigated with various hydrophobic substrate (i.e., Leu, Ile, Val, Phe and Phg; discussed in **Section 5.1.2.1**). The *N*-terminal amino acids to occupy S_3 pocket denoted by R_2 anchors were surveyed as heterocyclic residues (corresponding to the standard ligand K11017; discussed in literature review section **3**) to generate significant structure activity relationships **(Figure 41)**.

A total of twenty compounds were evaluated at 10 μM concentrations in the protease assay

targeting falcipain-2. Preliminary investigation of this series exhibited potent inhibition (> 75% to 80%) against falcipain-2 protease at 10 μM concentrations. Therefore, the whole series was evaluated at different concentrations to generate IC_{50} values.
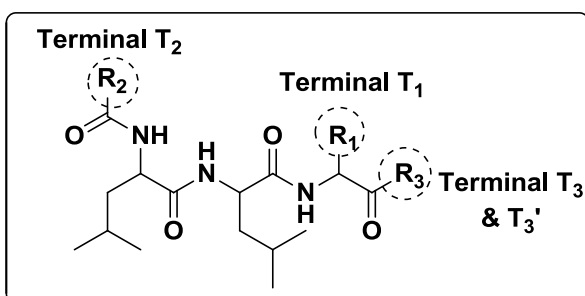
To understand the importance of the terminal-3 side chain in the designed target moiety, the precursors of final compounds **22-26 (RMQ 1 to 5)**, **30 (RMQ-6)**, and **31-35 (RMQ-7 to 11)** were initially screened. The preliminary screening of these intermediates did not show any significant activity against falcipain-2 enzyme.

Introduction of a terminal side chain in R_3 portion to examine its influence on enzymatic activity of compounds **36-37 (RMQ-12 and 13)**, resulted in broad difference in enzyme activity, compared to the preliminary hit, identified from *in silico* screen compound **(KM-1')**. Among these compounds, molecule **36** (**RMQ-12)**, exhibited the inhibitory activity with an IC_{50} value 11.6 ± 0.8 μM and compound **37 (RMQ-13)**, showed the promising inhibitory activity (IC_{50} = 3.0 ± 0.5 μM) against falcipain-2 enzyme.

In order to understand the importance of dihydroimidazole moiety in the target compound to the binding efficacy, it was decided to substitute it with a pyrrolidine ring without modifying the terminal side chain. Thus, dihydroimidazole group was replaced with a pyrrolidine moiety at T_3 position, affording compounds **38-41 (RMQ 14 to 17)**, showed potent activities with IC_{50} = 1.9 ± 0.8, 4.8 ± 1.1, 0.44 ± 0.04, and 0.41 ± 0.08 μM, respectively. Thus, compounds **40-**

41 (RMQ 16-17), containing the pyrrolidine moiety at terminal-3 and phenyl group at terminal-1, were observed to be more potent as compared to compounds **38-39 (RMQ 14-15)**, containing the pyrrolidine moiety at terminal-3 and benzyl group at terminal-1.

Later, it was decided to change the terminal 3 with urea substituent, such as hydrazine hydrate, keeping the benzyl group at terminal-1. The generated compounds **42-43 (RMQ 18-19)**, containing hydrazine at terminal-3 and benzyl group at terminal-1, showed comparable activity to the compounds **RMQ-14 (Table 13)**. Surprisingly, compound **44 (RMQ-20)**, did not show any activity against falcipain-2 enzyme.

All compounds that displayed falcipain-2 inhibition were subsequently analyzed for their anti-malarial activities in *P. falciparum* 3D7 culture. Further, the corresponding inhibitory concentrations (IC_{50}) were determined. Two compounds **(RMQ-13** and **RMQ-14)** inhibited *P. falciparum* 3D7 cultures with an IC_{50} value less than 10 μM. Compound **RMQ-14** was the most effective inhibitor of parasite growth, with an IC_{50} of 0.9 ± 0.1 μM, which correlated well with the inhibition of falcipain-2 (1.9 ± 0.8 μM). Interestingly, compounds **RMQ-15**, **RMQ-16**, **RMQ-17**, **RMQ-18** and **RMQ-19** which exhibited potent inhibition of falcipain-2 did not inhibit *P. falciparum* 3D7 at concentrations below 10 μM **(Table 16)**.

Overall, an initial hit, a tri-peptide, **KM-1'**, was identified by structure-based tools; further modifications to specific regions of the tripeptide paved way to examine the structure activity relationship of the synthesized compounds with falcipain-2 enzyme.
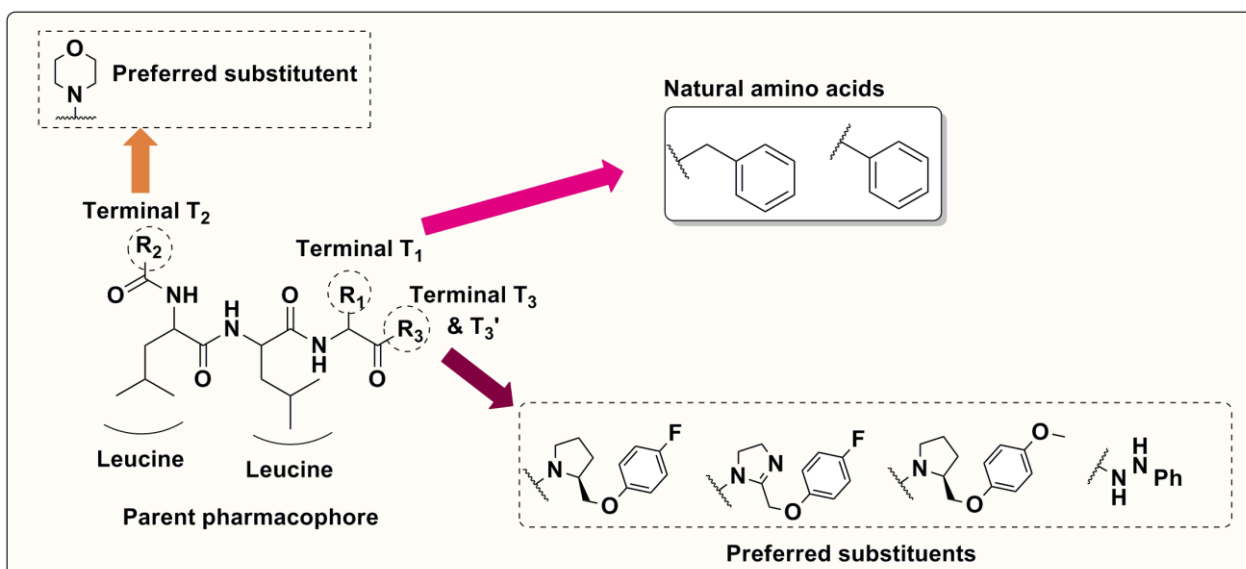
Figure 41: SAR of falcipain-2 inhibition of peptidomimetics (RMQ 1 to 20; Series IV)

5.3.8. Biological activities/pharmacology for Series V-VI

Based on the framework and affinity of the hit compound **KM-6** (IC_{50} = 26.0 ± 1.6 µM), fifteen novel molecules **(RMP 1 to 15)** were synthesized and screened against *Pf*ClpP at different concentrations to get IC_{50} value. The initial screening results showed that, IC_{50} value of these compounds were almost similar to the hit compound **(Table 14)**. The similar affinity in analogs **(RMP 1** to **15)** indicate that these compounds probably have no major substituent preference (competition) with respect to substrate at C2 position to the enzyme.
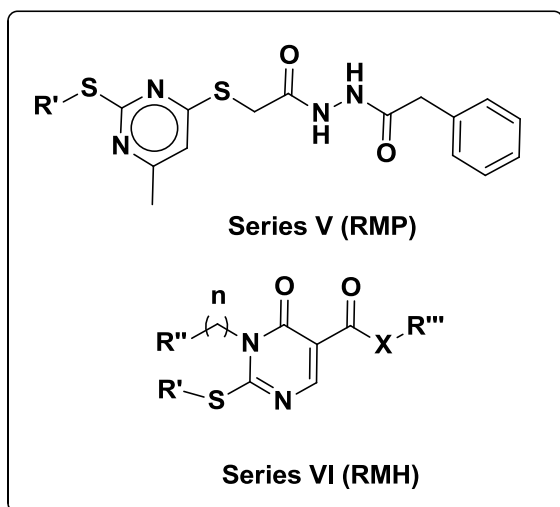
Series V (RMP)

Series VI (RMH)

Hence, chemical structure required additional modifications to improve the inhibition value. Keeping the common moiety of compounds **KM-11**, **KM-12** and **KM-13** (weak to moderate inhibitors; discussed in **Section 5.1.3.1.**) framework, three regions of these molecules were selected to generate a suitable pharmacophore model.

With a view to explore the effects of different substituents as shown by R', R'' and R''' on the pyrimidine moiety, a couple of analogs with electron withdrawing as well as electron donating groups were synthesized **(RMH-1 to 14)** and their ClpP inhibitory activity examined. In addition, the linker span (n) between the R'' substituents and the pyrimidine ring was changed to generate a significant SAR information (discussed in **Section 5.1.3.1.**) as shown in **Figure 42**.

Fortunately, one compound **RMH-1**, shown as a basic compound in **Figure 25B**; exhibited IC_{50} value 24.2 µM **(Table 15)**. Thus, various substitutions were introduced around the scaffold, specifically at sulphur atom at C2 position. The investigation of substitution with group **B** (2-bromo-1-(4-methoxyphenyl)ethanone), which possesses activating group: preferably methoxy group in *p*-position on the phenyl ring as in compound **RMH-2,** restored the inhibitory activity but was moderately active (IC_{50} value 44.6 µM).

However, investigation of a 2-chloro-*N*-(2-phenylacetyl)acetohydrazide group **(C)** at the 2nd position of the pyrimidine ring **(RMH-3)** showed lesser potency (IC_{50} value 72.6 µM) as compared to the hit compound **RMH-1**. Introduction of a basic moiety like 4-(2-

bromoethyl)morpholine group **(D)**, resulted compound **RMH 4**, showed the most potent activity among this series with IC$_{50}$ value 10.5 µM against *Pf*ClpP proteases.

Substituting pyrimidine 2nd position with ethyl 2-bromoacetate group **(E)** as in compound **RMH-5**, did not result in any improved potency and compound exhibited IC$_{50}$ values 58.2 µM. Compounds **RMH-6, RMH-7** and **RMH-8** were achieved by replacement of the group **B** to 2-bromo-1-(4-(diethylamino)phenyl)ethanone **(F)**, 2-bromo-1-(4-hydroxyphenyl)ethanone **(G)** and 4-(2-bromoacetyl)benzonitrile **(H)** groups and leads to markedly loss in potency **(Table 15)**. Interestingly, replacement of the group **B** to 2-bromo-1-morpholinoetanone **(I)** group, leads to generation of compound **RMH-9**, with an IC$_{50}$= 46.0 µM, close to compound **RMH-2**.

In order to assess the substitution at R''' position (replacement of amide group with ester moiety), compounds **(RMH 10, RMH 11 and RMH 12)** were synthesized and screened for their inhibition of ClpP enzyme. Compound **RMH 10** (linker span, n=0) and **RMH 12** (linker span, n=1) displayed moderate inhibitory activity (IC$_{50s}$= 42.4 & 39.7 µM, respectively), whereas **RMH-11** (linker span, n=0), showed weak inhibition as compared to **RMH-1**.

However, incorporation of the amide group at R''' position while keeping R' and R'' anchors same as in the compound **RMH 11**, leads to generation of compound **RMH 13**, with IC$_{50}$= 44.1 µM, close to compound **RMH-2**. Interestingly, **RMH-14** screening results showed poor inhibition value as compared to **RMH-1**.

All compounds that exhibited *Pf*ClpP inhibition were further investigated in the parasite cultures as anti-malarial agents. Two compounds **(RMH-2** and **RMH-4)** inhibited *P. falciparum* 3D7 cultures with an IC$_{50}$ less than 10 µM. Among them, **RMH-4** correlated well with the inhibition of ClpP enzyme value **(Table 17-18)**.

Overall, in this study a new scaffold of ClpP inhibitors by modification in hit compounds using ligand based drug design approach was investigated.
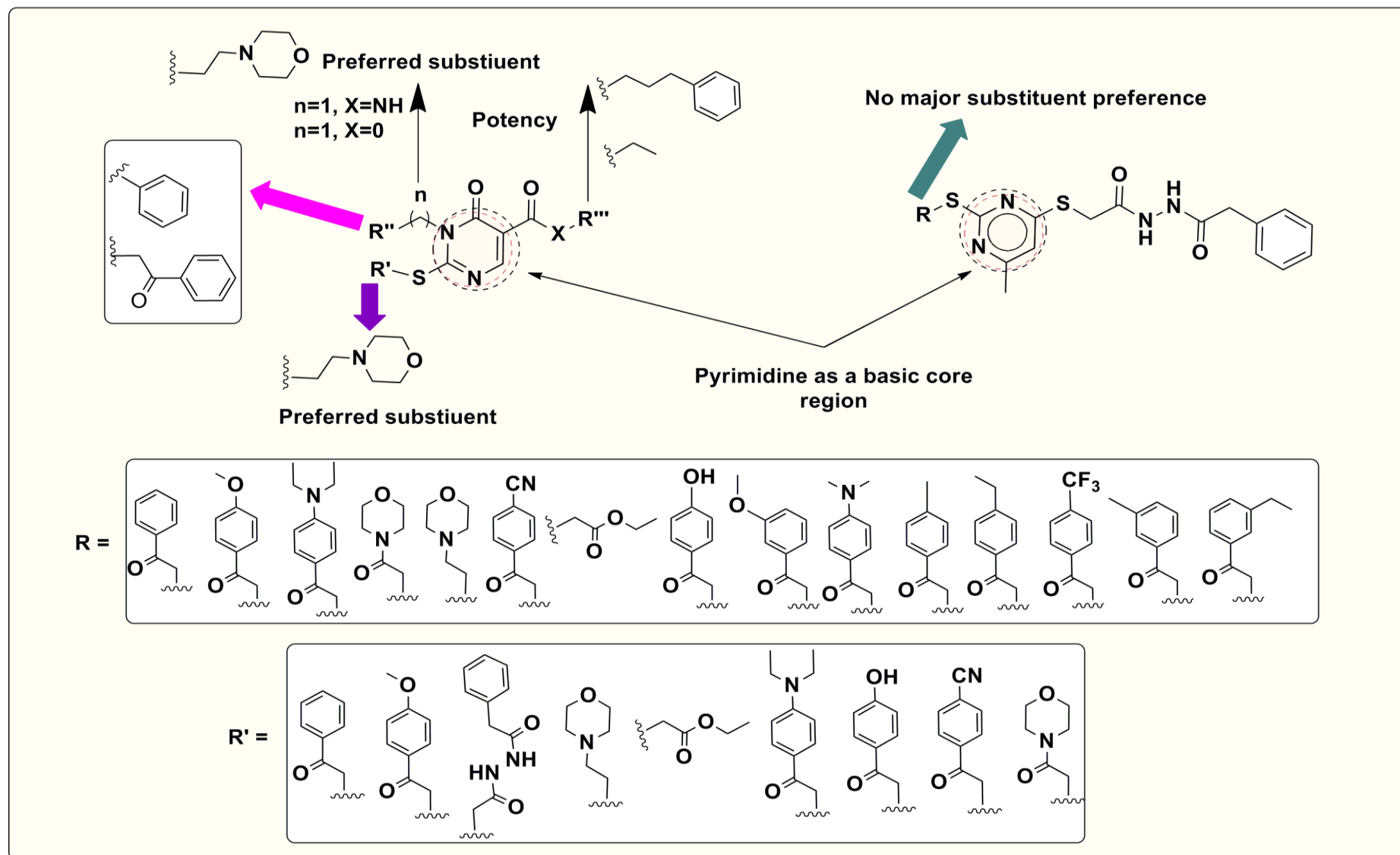
Figure 42: SAR of falcipain-2 inhibition of 2-(substituted)pyrimidin-4-ylthio)-*N*'-(2-phenylacetyl)-acetohydrazide derivatives (RMP 1 to 15; Series V) and 1,6-dihydropyrimidine-5-carboxamides derivatives (RMH 1 to14; Series VI)

6. SUMMARY AND CONCLUSIONS

The increasing ratio of morbidity and mortality due to malaria in humans, makes it a major public health problem in the world. Despite, more than a century of significant efforts to control malaria, the disease remains a major threat to public health. The National Malaria Control and Eradication Programmes have been hampered by technical, operational and social-economical difficulties, and spread of drug resistance in parasite and insecticide resistance in mosquito vectors is making malaria a formidable challenge. World Health Organization (WHO) Malaria report 2014, indicates that in the year 2013, there were 198 million malaria cases, leading to approximately 584,000 deaths, mostly among African children. While a number of medicines are present in market to treat malaria, however drug resistance, toxicity, and high-cost make the treatment complicated. Drug resistance against Artemisinin, the key compound in Artemisinin combination therapies (ACTs) is also emerging, and there is a need for safe and cost effective novel chemical classes of anti-malarial agents to treat malaria.

A multidisciplinary approach of developing novel chemical classes of drugs to address the persisting challenges of malaria were taken, offering a potential solution for the markets in the developing and developed world. This current work is based upon two targets, namely falcipain-2 and ClpP and six novel series **(I-VI)** of molecules were designed, synthesized and evaluated for priliminary anti-malarial activities.

Three series of derivatives, *viz.*, 2-(4-(substituted benzoyl)-1,4-diazepan-1-yl)-*N*-phenylacetamide derivatives, 1-(4-(Substituted)piperazin-1-yl)-2-(phenylamino)ethanone derivatives and 2-(4-(substituted benzoyl)piperazin-1-yl)-*N*-phenylacetamide derivatives as non-peptidic small molecules, were designed according to the pharmacophoric requirements of falcipain-2 inhibitors using ligand-based approach. Structural features of final compounds for **Series I** to **III**, were characterized by spectral data (IR, ^{1}H NMR, and mass) and elemental analyses. The purity of the final compounds was preliminary assured by TLC, in a minimum of two solvent systems and detected by UV/I_2 chamber and ninhydrin reagents.

The target compounds 2-(4-(substituted benzoyl)-1,4-diazepan-1-yl)-*N*-phenylacetamides **(Series I)**, were synthesized from the starting material aniline, in a sequence of reactions. All molecules were evaluated for their *in vitro* falcipain-2 inhibitor activity on recombinant falcipain-2 enzyme. Five compounds **RM-2, RM-7**, **RM-8, RM-10 and RM-11**, showed good inhibitory activity (> 60%), against falcipain-2 at 10 μM concentrations, while fifteen compounds **(RM 1** to **6, RM-9, RM 12** to **20)** showed weak to moderate inhibitor activity.

Compound **RM-7**, was the most potent compound from the series, exhibiting 72% inhibition at 10 μM concentrations.

SAR of 2-(4-(substituted benzoyl)-1,4-diazepan-1-yl)-*N*-phenylacetamides series clearly indicate that strong electron withdrawing group (trifluoromethyl) at 3rd, 4th positions and a strong electron releasing group (methoxy) at 2nd, 3rd positions, produced compounds that displayed marked inhibition as evidenced by compounds **RM-7, RM-8, RM-10** and **RM-11**. Higher homologation, i.e., replacing methyl with ethyl **(RM-19** and **RM-20)** and methoxy to ethoxy **(RM-13** and **RM-15)**, enhanced the lipophilicity of the generated compounds, but with decreased the inhibition value.
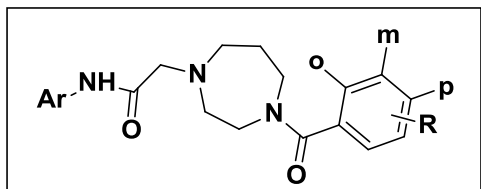
The 1-(4-(substituted)piperazin-1-yl)-2-(phenylamino)ethanone derivatives **(Series II)**, were synthesized by coupling of key intermediate 2-(phenylamino)-1-(piperazin-1-yl) ethanone with appropriate acids, using carbodiimide chemistry. The molecules were tested for their *in vitro* falcipain-2 inhibitor activity on recombinant falcipain-2 enzyme. Among the twenty novel derivatives tested, four compounds **(RMS-6, RMS-8, RMS-14** and **RMS-15)**, showed good inhibitory activity and eleven compounds **(RMS-1, RMS-2, RMS-7, RMS-9** to**13, RMS-16** and **RMS-17)** showed weak to moderate inhibitor activity.

The preliminary SAR of 1-(4-(substituted)piperazin-1-yl)-2-(phenylamino)ethanone series indicate that compound **RMS-8** containing methyl group as electron releasing substituent on phenyl nucleus at 4th position, was found to be most potent compound (50% of inhibition at 10 μM concentrations). Moreover, results of anti-malarial screening for this series of derivatives, against falcipain-2 enzyme demonstrated that compounds containing electron releasing substituents on phenyl nucleus showed reasonable anti-malarial activity **(RMS-14, RMS-15** and **RMS-6)** as compared to the electron withdrawing groups generated compounds.
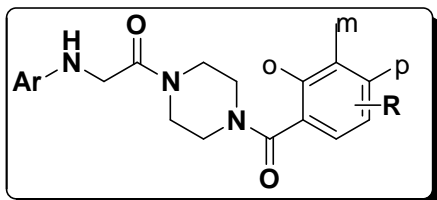
The new chemical entities for 2-(4-(substituted benzoyl)piperazin-1-yl)-*N*-phenylacetamide **(Series III)**, were synthesized from the key intermediate, *N*-phenyl-2-(piperazin-1-yl)acetamide, by coupling it with various substituted acids in the presence of HOBt and EDC·HCl. All the synthesized derivatives were evaluated at 10 μM concentrations for their *in vitro* falcipain-2 inhibitory activity. However, due to poor or no inhibition at 10 μM concentrations, all the compounds were subjected to assessment at
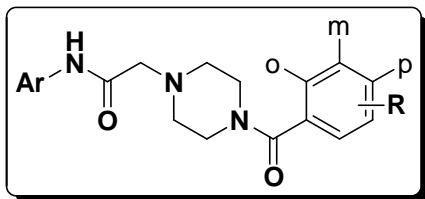
25 µM concentrations. The screening results of these synthesized compounds indicate that two compounds **RMT-2** and **RMT-20** displayed moderate inhibitory activity and rest of the tested compounds, exhibited poor or no inhibition.

Overall, SARs studies **(Figure 43)**, of the three series of analogs synthesized, indicate that linker plays a major role with the substitution on this phenyl group (hydrophobic residue) in the designed pharmacophore. It has been found that, increase in the ring size of the linker from piperazine **(Series II** and **III, Basic Structure II & III)** to homo-piperazine core nucleus with electron withdrawing substituent group (trifluoromethyl) present on the phenyl ring generated the potent compound **(RM-7, Series I, Basic Structure I)**, than that of compound with no substituent on the phenyl ring. Whereas, series II **(Basic Structure II)**, containing electron releasing substituent group (methyl) on phenyl nucleus produced significant active compound **(RMS-8)**, than that of compound with no substituent on the phenyl ring, as compared to series III **(Basic Structure III)**. On the other hand, results from series III suggest that, the introduction of either electron releasing or withdrawing substituent on the phenyl group negatively affected the potential of the formed carboxamides.

Based on the above, it is observed that that compounds from **Series I**, containing homo-piperazine ring (as a modification of the linker), led to identification of a new potential scaffold with moderate activity against FP-2 protease. In order to further enhance the inhibitory activity, it is thought worthwhile to optimize this scaffold with emphasis on modification of the linker size and flexibility.

Apart from the above factors, other molecular parameters such as electrostatic potential, electronic factors (ionization constant, polarisability and dipole moments), molecular shape, molecular volume, plausible geometries (flexible or rigid), and lipophilicity (aqueous solubility, partition coefficient, distribution constant) may also affect overall pharmacological action of the tested compounds. It is important to mention that the development of many potential drugs has been discontinued because of their poor pharmacokinetic properties, mainly absorption. For our study, further testing ought to be done to investigate the actual profiles of these compounds, as an extension of this work.

Various research groups have investigated the FP-2 inhibitors, which are mainly derived from peptide analogs having nanomolar IC_{50} values, due to the formation of covalent bond with thiol active site of 'Cys42', that behaves as a Michael acceptor. The poor selectivity for parasitic cysteine proteases over the human cysteine proteases remains a noteworthy concern. Therefore, as a part of continuing search for potential anti-malarial agents, it is

virtuous to explore new chemically diverse, structurally unique, analogs as peptidomimetic FP-2 inhibitors.

A pseudotripeptide **scaffold I** was designed using *in silico* screening tools and the three dimensional structures of falcipain-2. This scaffold was investigated at four positions, T_1, T_2, T_3, and T_3', with various targeted substitutions to understand the structure–activity relationships **(Series IV)**.

Multiple synthetic routes **(Scheme 4, 5, 6 and 7)**, were followed to synthesize the target compounds **(RMQ-1 to 20)**. Structural assignments for final derivatives **RMQ-1** to **20** were based on spectral data, (^{1}H NMR and mass spectroscopy). The purity of the some potent final compounds were confirmed by HPLC as representative samples .

The inhibitory activities of synthesized compounds **(RMQ-1 to 20)**, were analyzed by their ability to block *in vitro* protease activity of recombinant falcipain-2. In total twenty compounds were evaluated in falcipain-2 protease assay. Eight compounds **RMQ-12** to **19** showed significant activity against falcipain-2 enzyme. **RMQ-16** and **RMQ-17** were the most potent compounds from the series, having IC_{50} values in nano-molar range.
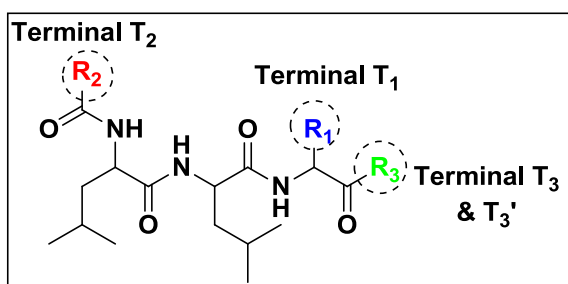
To study SAR, groups in terminal-2 position (R_2 groups) were replaced followed by replacement of terminal-3 side chains (R_3 groups) and also motifs (R_1 groups) within the basic scaffold, to assess its effects, on the enzyme inhibitory activity.

The preliminary screening of compounds **RMQ-1** to **RMQ-11** (different heterocyclic groups in R_2 position) did not show any significant activity against falcipain-2 enzyme. Introduction of a terminal side chain in R_3 portion to examine its influence on enzymatic activity yielded compounds **36-37 (RMQ-12** and **13)** which were screened. Investigation at R_3 position with 2-((4-fluorophenoxy)methyl)-4,5-dihydro-1H-imidazole **(Group I, Scheme 5)** and terminal-1 position with phenyl group **(Group B)**, yielded compounds **RMQ-12** and **13**, showed IC_{50s} value 11.6 ± 0.8 μM, 3.0 ± 0.5 μM, respectively as compared to preliminary hit compound **(KM-1')**.

Further, a side chain 2-((4-fluorophenoxy)methyl)pyrrolidine **(Group m)** and 2-((4-methoxyphenoxy)methyl)pyrrolidine **(Group n)** were added to assess the effect of R_3 position. This modification resulted in compounds **38-41 (RMQ 14-17)**, exhibiting potent activities with IC_{50} = 1.9 ± 0.8, 4.8 ± 1.1, 0.44 ± 0.04, and 0.41 ± 0.08 μM, respectively. Thus,

compounds **40-41 (RMQ 16-17)**, containing the pyrrolidine moiety at terminal-3 and benzyl group at terminal-1, were observed to be more potent as compared with compounds **38-39 (RMQ 14-15)**, containing the pyrrolidine moiety at terminal-3 and phenyl group at terminal-1.

It was then decided to change the terminal-3 with urea substituent (as in standard ligand E-64), such as hydrazine hydrate, keeping the benzyl group at terminal-1 and study its effects. The generated compounds **42-43 (RMQ 18-19)**, containing hydrazine at terminal-2 and benzyl group at terminal-1, showed comparable activity to the compounds **RMQ-14 (Table 13)**. Surprisingly, compound **44 (RMQ-20)**, did not show any activity against falcipain-2 enzyme. All compounds that displayed falcipain-2 inhibition were subsequently analyzed for their efficacy to inhibit *P. falciparum* parasite growth in vitro. Two compounds **(RMQ-13** and **RMQ-14)** inhibited *P. falciparum* 3D7 cultures with an IC_{50} value less than 10 µM.

The **Series V** and **VI** were designed based on compounds **(KM-1 to 13)**. *In vitro* data indicate that **KM-6** and **KM-11** were the most potent compounds from the series. Initially, various derivatives **(Series V)** of **KM-6** were generated to generate SAR. Synthesis of these derivatives was accomplished by synthesizing and reacting the appropriate key precursors **(5)** and **8 (A-O)** as shown in **Scheme-8**.

The initial screening results showed that IC_{50} value of **RMP 1 to 15**, compounds were almost
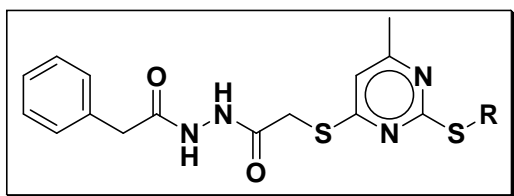
equipotent to the hit compound **(KM-6)**. Complex synthetic route for the synthesis of **KM-11**, prompted the design of a novel pharmacophore model and hence **KM-11** along with **KM-10** and **KM-12** were used to get some complementary features for the generation of a novel pharmacophore **(Figure 25A)**. Based on this pharmacophore, a series of derivatives were synthesized from starting material benzyl thiourea in a sequence of reactions as depicted in **Scheme 9**. Structural features of final compounds for **series V** and **VI** were characterized by spectral data ^{1}H NMR, ^{13}C NMR and mass data. The purity of the final compounds were assured by HPLC, in a minimum of two solvent systems.

The preliminary SAR indicate that compound **RMH-1,** shown as a basic compound in **Figure 25B**; exhibited IC_{50} value 24.2 µM. The investigation of substitution with group **B** (2-bromo-1-(4-methoxyphenyl)ethanone), possessing strong activating group; preferably methoxy group in *p*-

position on the phenyl ring as in compound **RMH-2,** restored the inhibitory activity but was moderately active (IC_{50} value 44.6 µM). However, investigation of a 2-chloro-*N'*-(2-phenylacetyl)acetohydrazide group **(C)** at the 2nd position of the pyrimidine ring **(RMH-3)** showed lesser potency (IC_{50} value 72.6 µM) as compared to the hit compound **RMH-1**. Introduction of basic moiety like 4-(2-bromoethyl)morpholine group **(D)**, resulted compound **RMH 4,** showed the most potent among this series with IC_{50} value 10.5 µM against *Pf*ClpP proteases. Substituting pyrimidine 2nd position with ethyl 2-bromoacetate group **(E)** as in compound **RMH-5** did not result in any improved potency, and compound exhibited IC_{50} values 58.2 µM. Compounds **RMH-6, RMH-7** and **RMH-8** were achieved by replacement of the group **B,** to **(F)**, **(G)** and **(H)** groups and leads to markedly lost in potency. Interestingly, replacement of the group **B** to 2-bromo-1-morpholinoetanone **(I)** group, leads to generation of compound **RMH-9**, with IC_{50}= 46.0 µM, close to compound **RMH-2**.
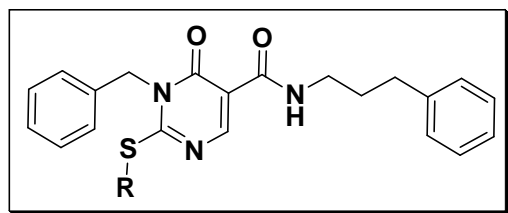
In order to assess the effect of ester group at 5th position (without substitution at N^3), compounds **RMH-10** and **RMH-11**, were screened. Interestingly, compound **RMH-10** displayed moderate inhibitory activity (IC_{50} = 42.4 µM), whereas **RMH 11** showed very weak inhibition. Further, screening of **RMH-12** & **RMH-13** in the homologous series, lead the generation of compounds with IC_{50} values of 39.7 & 44.1 µM, respectively as compared to **RMH-1**. Moreover, **RMH-14** showed weaker inhibition value as compared to **RMH-1**. All compounds that exhibited *Pf*ClpP inhibition were further investigated in the parasite cultures as anti-malarial agents. Two compounds **(RMH-2** and **RMH-4)** inhibited *P. falciparum* 3D7 cultures with an IC_{50} less than 10 µM.

Overall, SARs **(Figure 44)** of the series V and VI, demonstrated that, molecules generated from the novel pharmacophore displayed prominent inhibition for *Pf*ClpP protease as compared with derivatives generated from hit compound **KM-6**. The substitution at N^3 position (corresponding to R'' position) played a major role for the difference in the activity among the series V and VI. The substitution at three different positions as shown by R', R'' and R''' indicated that a bulkier and better lipophilic group, especially ethyl morpholine at R', benzyl group (hydrophobic) at R'' and amide group at R''' position as evident in compound **RMH-4** was predominantly tolerated and displayed potent inhibitory activity. The presence of a C=O dipole and, to a lesser extent a N-C dipole, allowed amides to act as H-bond acceptors. Whereas, the presence of N-H dipoles, allowed amides to function as H-bond donors as well. It is to be noted that, amides participate in hydrogen bonding with water and other protic solvents; the oxygen and nitrogen atoms accept hydrogen bonds from water and the N-H hydrogen atoms donate H-bonds. As a result of possible interactions such as these, the polarity of amides is greater than that of corresponding ester precursors.
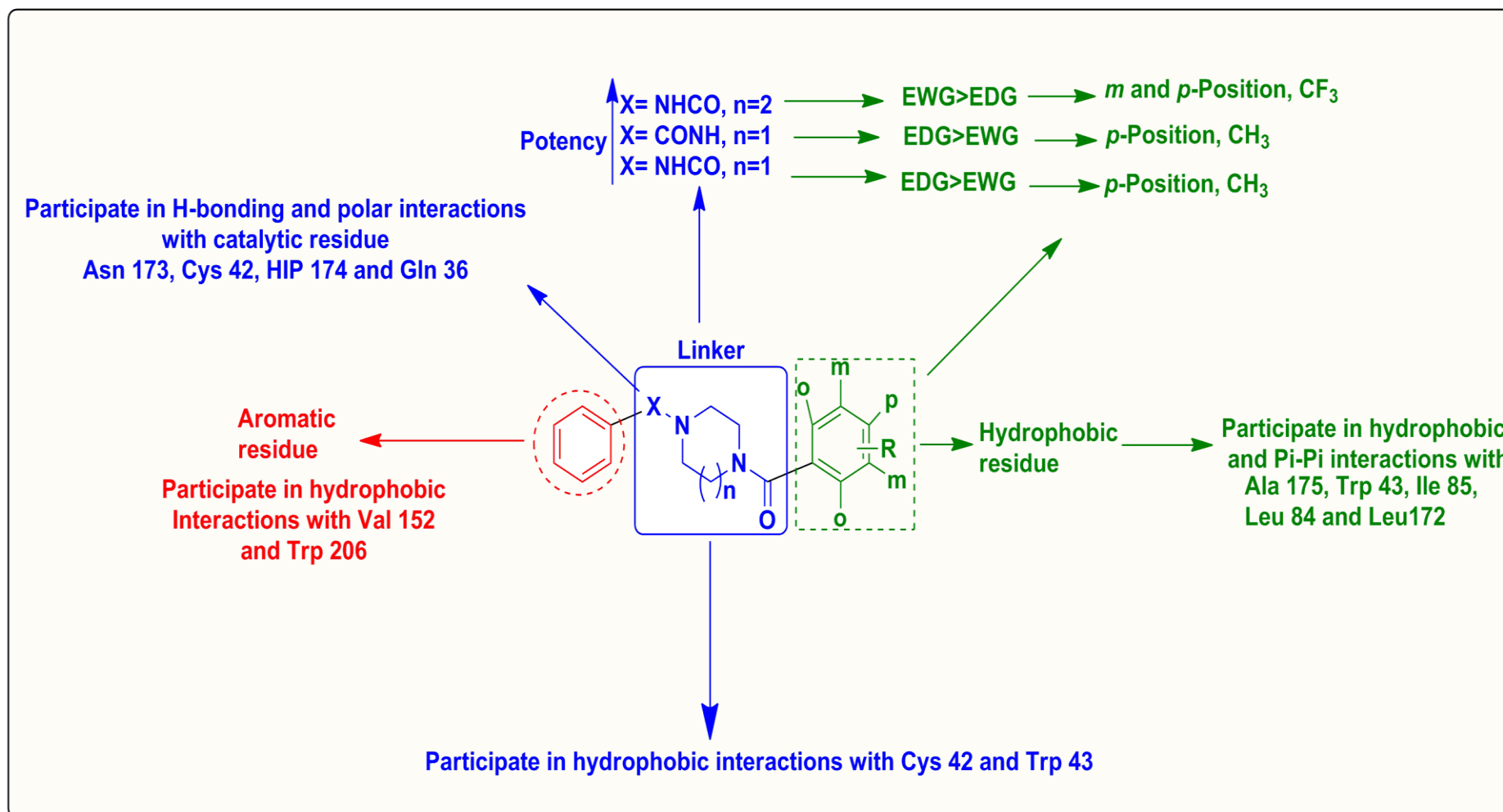
Figure 43: Combined structural activity relationship of Series I-III

Figure 44: Combined structural activity relationship of Series V-VI

In summation, the following conclusions were drawn:

❖ Among the three series **(I**, **II & III)** of derivatives, homo-piperazine core nucleus with electron withdrawing substituents present on the phenyl ring **(RM-7, Series I, Basic Structure I)**, showed potent inhibition indicating that linker played a major role in the designed pharmacophore for the difference in the activity.

❖ Molecules of series **IV**, derived from the novel pharmacophore, displayed potent inhibition of FP-2 protease. The substitution at three different positions (R_1, R_2 & R_3) played a key role for difference in the activity among the series of compounds.

❖ Among the peptidomimetics, **RMQ-16** and **RMQ-17 (Series IV)**, were the most potent compounds from the series, having IC_{50} values in nano-molar range against FP-2 enzyme. These compounds could be considered as leads, and an appropriate modification may possibly enhance inhibitory activity.

❖ Compound **RMQ-14** was the most effective inhibitor of parasite growth, with an IC_{50} of 0.9 ± 0.1 μM, which correlated well with the inhibition of falcipain-2.

❖ Overall, among the synthesized moieties against falcipain-2 enzyme **(Series I-IV)**, peptidomimetics **(Series IV)** showed better affinity and potent inhibitory activity as compared to non-peptidic molecules **Series I-III**.

❖ In **Series V**, compounds were almost equipotent to the hit compound **(KM-6)** for ClpP inhibition.

❖ Molecules of **Series VI**, generated from the novel pharmacophore, displayed prominent inhibition of ClpP protease as compared to the derivatives generated from hit compound **KM-6**. The substitution at N^3 position played a major role for the difference in the activity among the **Series V** and **VI**.

❖ Among the **Series VI, RMH 4**, was the most potent compound, having IC_{50} values in single digit micro-molar range and it can also be utilized as a potential lead compound in the designing of new candidates to optimize the inhibitory potencies of this class of compounds, with potent anti-malarial activity.

Among all series of compounds (109) synthesized, the following compounds were found to be most promising which could be used for further investigations.

SI No	Code (Series)	Significant FP-2 inhibition	Significant ClpP inhibition	Significant antiplasmodial activities
1	RM-7 (Series I)	√		--
2	RMQ-13 (Series IV)	√		√
3	RMQ-14 (Series IV)	√		√
4	RMQ-15 (Series IV)	√		--
5	RMQ-16 (Series IV)	√		--
6	RMQ-17 (Series IV)	√		--
7	RMQ-18 (Series IV)	√		--
8	RMQ-19 (Series IV)	√		--
9	RMH-4 (Series VI)		√	√

-- Indicates no significant antiplasmodial activity

√- Indicates significant enzymes (FP-2 or ClpP) and antiplasmodial activity

7. FUTURE SCOPE OF WORK

➢ A variety of amino acids (natural/unnatural) could be envisioned at R_1 position **(Terminal T$_1$)** on the hit compound **RMQ-14** and thus a number of lead analogs can be produced from this derivatives targeting falcipain-2. In the similar way, bidentate inhibitors similar to **RMQ-14** can be envisioned where R_2 and R_3 could be similar or different anchors.

➢ Recent studies have indicated that, the **1,6-dihydropyrimidine-5-carboxamides** would be an appropriate core scaffold for the design of ClpP protease inhibitors. Therefore, compounds similar to **RMH 4** can be explored with varying R', R'' and R''' groups.

➢ Development of a new selectively modelled series of compounds (hybrid pharmacophore) as dual inhibitors, based on optimized potent structures **RMQ-13, RMQ-14 and RMH-4**, targeting FP-2 and ClpP, respectively could be further explored.

➢ Based on the affirmative results of the work, it would be fruitful to investigate the effect of selected falcipain-2 and ClpP inhibitors on the morphology and development of *P. falciparum* parasite at asexual stage.

➢ Advancing the novel compounds targeting falcipain-2 and ClpP proteins, could include pharmacokinetics studies and comprehensive toxicology (*in vitro* and *in vivo*) on rodents.

➢ Drug combination studies using lead ClpP and falcipain-2 inhibitors, along with known anti-malarials could be carried out to develop a path for single-dose combination therapy for malaria.

➢ In order to combat the drug-resistant malaria, the hit compounds targeting two different targets, falcipain-2 and ClpP proteases can be investigated for superior drug resistance profile.

➢ Homology modelling for *Plasmodium falciparum* ClpP protease could be investigated as an extension of the work on most promising ClpP inhibitors.

8. REFERENCES

A research agenda for malaria eradication: drugs. (2011). *PLoS Med, 8*(1), e1000402.

Alam, A. (2014). Serine Proteases of Malaria Parasite Plasmodium falciparum: Potential as Antimalarial Drug Targets. *Interdiscip Perspect Infect Dis, 453186*(10), 1-7.

American Public Health Association (2008). Malaria. In DL Heymann, ed., Control of Communicable Diseases Manual, 9th ed., pp. 373–393. Washington, DC.

Ashok, P., Ganguly, S., & Murugesan, S. (2013). Review on in-vitro anti-malarial activity of natural beta-carboline alkaloids. *Mini Rev Med Chem, 13*(12), 1778-1791.

Banerjee, R., Liu, J., Beatty, W., Pelosof, L., Klemba, M., & Goldberg, D. E. (2002). Four plasmepsins are active in the Plasmodium falciparum food vacuole, including a protease with an active-site histidine. *Proc Natl Acad Sci U S A, 99*(2), 990-995.

Barradell, L. B., & Fitton, A. (1995). Artesunate. A review of its pharmacology and therapeutic efficacy in the treatment of malaria. *Drugs, 50*(4), 714-741.

Bartoloni, A., & Zammarchi, L. (2012). Clinical aspects of uncomplicated and severe malaria. *Mediterr J Hematol Infect Dis, 4*(1), e2012026.

Ben-Shahar, S., Cassouto, B., Novak, L., Porgador, A., & Reiss, Y. (1997). Production of a specific major histocompatibility complex class I-restricted epitope by ubiquitin-dependent degradation of modified ovalbumin in lymphocyte lysate. *J Biol Chem, 272*(34), 21060-21066.

Bota, D. A., Ngo, J. K., & Davies, K. J. (2005). Downregulation of the human Lon protease impairs mitochondrial structure and function and causes cell death. *Free Radic Biol Med, 38*(5), 665-677.

Bottcher, T., & Sieber, S. A. (2008). Beta-lactones as privileged structures for the active-site labeling of versatile bacterial enzyme classes. *Angew Chem Int Ed Engl, 47*(24), 4600-4603.

Brotz-Oesterhelt, H., Beyer, D., Kroll, H. P., Endermann, R., Ladel, C., Schroeder, W., Hinzen, B., Raddatz, S., Paulsen, H., Henninger, K., Bandow, J. E., Sahl, H., & Labischinski, H. (2005). Dysregulation of bacterial proteolytic machinery by a new class of antibiotics. *Nat Med, 11*(10), 1082-1087.

Cassera, M. B., Zhang, Y., Hazleton, K. Z., & Schramm, V. L. (2011). Purine and pyrimidine pathways as targets in Plasmodium falciparum. *Curr Top Med Chem, 11*(16), 2103-2115.

Cerami, C., Frevert, U., Sinnis, P., Takacs, B., Clavijo, P., Santos, M. J., & Nussenzweig, V. (1992). The basolateral domain of the hepatocyte plasma membrane bears receptors for the circumsporozoite protein of Plasmodium falciparum sporozoites. *Cell, 70*(6), 1021-1033.

Chaiyaroj, S. C., Coppel, R. L., Novakovic, S., & Brown, G. V. (1994). Multiple ligands for cytoadherence can be present simultaneously on the surface of Plasmodium falciparum-infected erythrocytes. *Proc Natl Acad Sci U S A, 91*(23), 10805-10808.

Chakka, S. K., Kalamuddin, M., Mundra, S., Mahesh, R., Malhotra, P., Mohmmed, A., & Kotra, L. P. (2015). Identification of novel class of falcipain-2 inhibitors as potential antimalarial agents. *Bioorg Med Chem, 23*(9), 2221-2240.

Chawira, A. N., Warhurst, D. C., Robinson, B. L., & Peters, W. (1987). The effect of combinations of qinghaosu (artemisinin) with standard antimalarial drugs in the suppressive treatment of malaria in mice. *Trans R Soc Trop Med Hyg, 81*(4), 554-558.

Chiyanzu, I., Hansell, E., Gut, J., Rosenthal, P. J., McKerrow, J. H., & Chibale, K. (2003). Synthesis and evaluation of isatins and thiosemicarbazone derivatives against cruzain, falcipain-2 and rhodesain. *Bioorg Med Chem Lett, 13*(20), 3527-3530.

Choi, H. J., Cui, M., Li, D. Y., Song, H. O., Kim, H. S., & Park, H. (2013). Anti-malarial activity of new N-acetyl-L-leucyl-L-leucyl-L-norleucinal (ALLN) derivatives against Plasmodium falciparum. *Bioorg Med Chem Lett, 23*(5), 1293-1296.

Clough, B. & Wilson, R. J. M. (2001). Antibiotics and the plasmodial plastid organelle. In *Antimalarial Chemotherapy: Mechanisms of Action, Resistance, and New Directions in Drug Discovery* (ed. P. J. Rosenthal), pp.265-286. Totawa, NJ: Humana Press.

Coatney, G. R. (1963). Pitfalls in a discovery: the chronicle of chloroquine. *Am J Trop Med Hyg, 12*(2), 121-128.

Coombs, G. H., Goldberg, D. E., Klemba, M., Berry, C., Kay, J., & Mottram, J. C. (2001). Aspartic proteases of Plasmodium falciparum and other parasitic protozoa as drug targets. *Trends Parasitol, 17*(11), 532-537.

Croft, A. (2000). Extracts from "Clinical Evidence". Malaria: prevention in travellers. *BRIT MED J, 321*(7254), 154-160.

Dahl, E. L., & Rosenthal, P. J. (2008). Apicoplast translation, transcription and genome replication: targets for antimalarial antibiotics. *Trends Parasitol, 24*(6), 279-284.

Dalal, S., & Klemba, M. (2007). Roles for two aminopeptidases in vacuolar hemoglobin catabolism in Plasmodium falciparum. *J Biol Chem, 282*(49), 35978-35987.

Dasaradhi, P. V., Mohmmed, A., Kumar, A., Hossain, M. J., Bhatnagar, R. K., Chauhan, V. S., & Malhotra, P. (2005). A role of falcipain-2, principal cysteine proteases of Plasmodium falciparum in merozoite egression. *Biochem Biophys Res Commun, 336*(4), 1062-1068.

Deck, L. M., Royer, R. E., Chamblee, B. B., Hernandez, V. M., Malone, R. R., Torres, J. E., Hunsaker, L. A., Piper, R. C., Makler, M. T., & Vander Jagt, D. L. (1998). Selective inhibitors of human lactate dehydrogenases and lactate dehydrogenase from the malarial parasite *Plasmodium falciparum*. *J Med Chem, 41*(20), 3879-3887.

Desai, P. V., Patny, A., Gut, J., Rosenthal, P. J., Tekwani, B., Srivastava, A., & Avery, M. (2006). Identification of novel parasitic cysteine protease inhibitors by use of virtual screening. 2. The available chemical directory. *J Med Chem, 49*(5), 1576-1584.

Desai, P.V., Pantny, A., Sabnis, Y., Tekwani, B., Gut, J., Rosenthal, P., Srivastava, A., & Avery, M., (2004). Identification of novel parasitic cysteine protease inhibitors using virtual screening. 1. The ChemBridge database. *J Med Chem, 47*(26), 6609–6615.

Deupi, X., Olivella, M., Govaerts, C., Ballesteros, J. A., Campillo, M., & Pardo, L. (2004). Ser and Thr residues modulate the conformation of pro-kinked transmembrane alpha-helices. *Biophys J, 86*(1 Pt 1), 105-115.

DiFiglia, M., Sapp, E., Chase, K. O., Davies, S. W., Bates, G. P., Vonsattel, J. P., & Aronin, N. (1997). Aggregation of huntingtin in neuronal intranuclear inclusions and dystrophic neurites in brain. *Science, 277*(5334), 1990-1993.

Dominguez, J. N., Leon, C., Rodrigues, J., Gamboa de Dominguez, N., Gut, J., & Rosenthal, P. J. (2005). Synthesis and evaluation of new antimalarial phenylurenyl chalcone derivatives. *J Med Chem, 48*(10), 3654-3658.

Dominguez, J. N., Lopez, S., Charris, J., Iarruso, L., Lobo, G., Semenov, A., Olson, J. E., & Rosenthal, P. J. (1997). Synthesis and antimalarial effects of phenothiazine inhibitors of a Plasmodium falciparum cysteine protease. *J Med Chem, 40*(17), 2726-2732.

Dunn, C. R., Banfield, M. J., Barker, J. J., Higham, C. W., Moreton, K. M., Turgut-Balik, D., Brady, R. L. & Holbrook, J. J. (1996). The structure of lactate dehydrogenase from *Plasmodium falciparum* reveals a new target for anti-malarial design. *Nat. Struct. Biol. 3*(11), 912-915.

Dvorak, J. A., Miller, L. H., Whitehouse, W. C., & Shiroishi, T. (1975). Invasion of erythrocytes by malaria merozoites. *Science, 187*(4178), 748-750.

El Bakkouri, M., Pow, A., Mulichak, A., Cheung, K. L., Artz, J. D., Amani, M., Fell, S., de Koning-Ward, T. F., Goodman, C. D., McFadden, G. I., Ortega, J., Hui, R., & Houry, W. A. (2010). The Clp chaperones and proteases of the human malaria parasite Plasmodium falciparum. *J Mol Biol, 404*(3), 456-477.

El Bakkouri, M., Rathore, S., Calmettes, C., Wernimont, A. K., Liu, K., Sinha, D., Asad, M., Jung, P., Hui, R., Mohmmed, A., & Houry, W. A. (2013). Structural insights into the inactive subunit of the apicoplast-localized caseinolytic protease complex of Plasmodium falciparum. *J Biol Chem, 288*(2), 1022-1031.

Ettari, R., Bova, F., Zappala, M., Grasso, S., & Micale, N. (2010). Falcipain-2 inhibitors. *Med Res Rev, 30*(1), 136-167.

Ettari, R., Micale, N., Schirmeister, T., Gelhaus, C., Leippe, M., Nizi, E., Di Francesco, M. E., Grasso, S., & Zappala, M. (2009). Novel peptidomimetics containing a vinyl ester moiety as highly potent and selective falcipain-2 inhibitors. *J Med Chem, 52*(7), 2157-2160.

Ettari, R., Nizi, E., Di Francesco, M. E., Dude, M. A., Pradel, G., Vicik, R., Schirmeister, T., Micale, N., Grasso, S., & Zappala, M. (2008). Development of peptidomimetics with a vinyl sulfone warhead as irreversible falcipain-2 inhibitors. *J Med Chem, 51*(4), 988-996.

Foth, B. J., Ralph, S. A., Tonkin, C. J., Struck, N. S., Fraunholz, M., Roos, D. S., Cowman, A. F. and McFadden, G. I. (2003). Dissecting apicoplast targeting in the malaria parasite *Plasmodium falciparum*. *Science* 299(5607), 705-708.

Friesner, R. A., Banks, J.L., Murphy, R. B., Halgren, T. A., Klicic, J. J., Mainz, D. T., Repasky, M. P., Knoll, E. H., Shelley, M., Perry, J. K., Shaw, D. E., Francis, P., & Shenkin, P.S. (2004). Glide: a new approach for rapid, accurate docking and scoring. 1. Method and assessment of docking accuracy. *J Med Chem, 47*(7), 1739–1749.

Gerald, N., Mahajan, B., & Kumar, S. (2011). Mitosis in the Human Malaria Parasite Plasmodium falciparum . *Eukaryotic Cell*, *10*(4), 474–482.

Gersch, M., Gut, F., Korotkov, V. S., Lehmann, J., Bottcher, T., Rusch, M., Hedberg, C., Waldmann, H., Klebe, G., & Sieber, S. A. (2013). The mechanism of caseinolytic protease (ClpP) inhibition. *Angew Chem Int Ed Engl, 52*(10), 3009-3014.

Gersch, M., Kolb, R., Alte, F., Groll, M., & Sieber, S. A. (2014). Disruption of oligomerization and dehydroalanine formation as mechanisms for ClpP protease inhibition. *J Am Chem Soc, 136*(4), 1360-1366.

Ghosh, A., Edwards, M. J., & Jacobs-Lorena, M. (2000). The journey of the malaria parasite in the mosquito: hopes for the new century. *Parasitol Today, 16*(5), 196-201.

Ginsburg, H. (1994). Transport pathways in the malaria-infected erythrocyte: characterization and their use as potential targets for chemotherapy. *Mem Inst Oswaldo Cruz, 2*, 99-109.

Glickman, M. H., & Ciechanover, A. (2002). The ubiquitin-proteasome proteolytic pathway: destruction for the sake of construction. *Physiol Rev, 82*(2), 373-428.

Gluzman, I. Y., Francis, S. E., Oksman, A., Smith, C. E., Duffin, K. L., & Goldberg, D. E. (1994). Order and specificity of the Plasmodium falciparum hemoglobin degradation pathway. *J Clin Invest, 93*(4), 1602-1608.

Go, M. L. (2003). Novel antiplasmodial agents. *Med Res Rev, 23*(4), 456-487.

Goldberg, D. E., Slater, A. F., Beavis, R., Chait, B., Cerami, A., & Henderson, G. B. (1991). Hemoglobin degradation in the human malaria pathogen Plasmodium falciparum: a catabolic pathway initiated by a specific aspartic protease. *J Exp Med, 173*(4), 961-969.

Goodman, C. D., Su, V., & McFadden, G. I. (2007). The effects of anti-bacterials on the malaria parasite Plasmodium falciparum. *Mol Biochem Parasitol, 152*(2), 181-191.

Gottesman, S. (2003). "Proteolysis in bacterial regulatory circuits." *Annu. Rev. Cell Dev. Biol. 19*: 565-587.

Halgren, T. A., Murphy, R. B., Friesner, R. A., Beard, H. S., Frye, L. L., Pollard, W. T., & Banks, J. L. (2004). Glide: a new approach for rapid, accurate docking and scoring. 2. Enrichment factors in database screening. *J Med Chem, 47*(7), 1750–1759.

Hanada, K., Tamai, M., Yamagishi, S., Ohmura, S., Sawada, J., & Tanaka, I. (1978). Studies on thiol protease inhibitors. Part II. Structure and synthesis of E-64, a new thiol protease inhibitor. *Agric Biol Chem, 42*(3), 529–536.

Hartwell, L. H., & Kastan, M. B. (1994). Cell cycle control and cancer. *Science, 266*(5192), 1821-1828.

Herm-Gotz, A., Agop-Nersesian, C., Munter, S., Grimley, J. S., Wandless, T. J., Frischknecht, F., & Meissner, M. (2007). Rapid control of protein level in the apicomplexan Toxoplasma gondii. *Nat Methods, 4*(12), 1003-1005.

Hinzen, B., Raddatz, S., Paulsen, H., Lampe, T., Schumacher, A., Habich, D., Hellwig, V., Benet-Buchholz, J., Endermann, R., Labischinski, H., & Brotz-Oesterhelt, H. (2006). Medicinal chemistry optimization of acyldepsipeptides of the enopeptin class antibiotics. *ChemMedChem, 1*(7), 689-693.

Hochstrasser, M. (1996). Ubiquitin-dependent protein degradation. *Annu Rev Genet, 30*, 405-439.

Hogg, T., Nagarajan, K., Herzberg, S., Chen, L., Shen, X., Jiang, H., Wecke, M., Blohmke, C., Hilgenfeld, R., Schmidt, C. L. (2006). Structural and functional characterization of Falcipain-2, a hemoglobinase from the malarial parasite Plasmodium falciparum. *J Biol Chem, 281*(35), 25425-25437.

http://www.cdc.gov/dpdx/, CDC; 2014.

Huang, L., Lee, A., & Ellman, J. A. (2002). Identification of potent and selective mechanism-based inhibitors of the cysteine protease cruzain using solid-phase parallel synthesis. *J Med Chem, 45*(3), 676-684.

Hwang, B. J., Park, W. J., Chung, C. H., & Goldberg, A. L. (1987). Escherichia coli contains a soluble ATP-dependent protease (Ti) distinct from protease La. *Proc Natl Acad Sci U S A, 84*(16), 5550-5554.

J.m. Moulder, in "Biochemistry and physiology of protozoa" (A. Lowoff, ed.), Vol 2, Acedemic press, Newyork, 1951

Jenal, U., & Hengge-Aronis, R. (2003). Regulation by proteolysis in bacterial cells. *Curr Opin Microbiol, 6*(2), 163-172.

Jeong, J. J., Kumar, A., Hanada, T., Seo, P. S., Li, X., Hanspal, M., & Chishti, A. H. (2006). Cloning and characterization of Plasmodium falciparum cysteine protease, falcipain-2B. *Blood Cells Mol Dis, 36*(3), 429-435.

Jorgensen, W. L., Maxwell, D. S., & Tirado, R. J. (1996). Development and testing of the OPLS all-atom force field on conformational energetics of organic liquids. *J Am Chem Soc, 118*(45), 11225–11236.

Kamchonwongpaisan, S., Samoff, E., & Meshnick, S. R. (1997). Identification of hemoglobin degradation products in Plasmodium falciparum. *Mol Biochem Parasitol, 86*(2), 179-186.

Kang, S. G., Dimitrova, M. N., Ortega, J., Ginsburg, A., & Maurizi, M. R. (2005). Human mitochondrial ClpP is a stable heptamer that assembles into a tetradecamer in the presence of ClpX. *J Biol Chem, 280*(42), 35424-35432.

Katayama-Fujimura, Y., Gottesman, S., & Maurizi, M. R. (1987). A multiple-component, ATP-dependent protease from Escherichia coli. *J Biol Chem, 262*(10), 4477-4485.

Kenniston, J. A., Baker, T. A., Fernandez, J. M., & Sauer, R. T. (2003). Linkage between ATP consumption and mechanical unfolding during the protein processing reactions of an AAA+ degradation machine. *Cell, 114*(4), 511-520.

Keough, D. T., Ng, A. L., Winzor, D. J., Emmerson, B. T., & de Jersey, J. (1999). Purification and characterization of Plasmodium falciparum hypoxanthine-guanine-xanthine phosphoribosyltransferase and comparison with the human enzyme. *Mol Biochem Parasitol, 98*(1), 29-41.

Kerr, I. D., Lee, J. H., Pandey, K. C., Harrison, A., Sajid, M., Rosenthal, P. J., & Brinen, L. S. (2009). Structures of falcipain-2 and falcipain-3 bound to small molecule inhibitors: implications for substrate specificity. *J Med Chem, 52*(3), 852-857.

Kiatfuengfoo, R., Suthiphongchai, T., Prapunwattana, P., & Yuthavong, Y. (1989). Mitochondria as the site of action of tetracycline on Plasmodium falciparum. *Mol Biochem Parasitol, 34*(2), 109-115.

Kim, D. H., Park, J. I., Chung, S. J., Park, J. D., Park, N. K., & Han, J. H. (2002). Cleavage of beta-lactone ring by serine protease. Mechanistic implications. *Bioorg Med Chem, 10*(8), 2553-2560.

Kirstein, J., Zuhlke, D., Gerth, U., Turgay, K., & Hecker, M. (2005). A tyrosine kinase and its activator control the activity of the CtsR heat shock repressor in B. subtilis. *EMBO J, 24*(19), 3435-3445.

Klayman, D. L., Bartosevich, J. F., Griffin, T. S., Mason, C. J., & Scovill, J. P. (1979). 2-Acetylpyridine thiosemicarbazones. 1. A new class of potential antimalarial agents. *J Med Chem, 22*(7), 855-862.

Kohler, S., Delwiche, C. F., Denny, P. W., Tilney, L. G., Webster, P., Wilson, R. J., Palmer, J. D. & Roos, D. S. (1997). A plastid of probablegreen algal origin in apicomplexan parasites. *Science,* 275(5305), 1485-1489.

Korde, R., Bhardwaj, A., Singh, R., Srivastava, A., Chauhan, V. S., Bhatnagar, R. K., & Malhotra, P. (2008). A prodomain peptide of Plasmodium falciparum cysteine protease (falcipain-2) inhibits malaria parasite development. *J Med Chem, 51*(11), 3116-3123.

Krungkrai, J. (1995). Purification, characterization and localization of mitochondrial dihydroorotate dehydrogenase in Plasmodium falciparum, human malaria parasite. *Biochim Biophys Acta, 1243*(3), 351-360.

Kumar, A., Dasaradhi, P. V., Chauhan, V. S., & Malhotra, P. (2004). Exploring the role of putative active site amino acids and pro-region motif of recombinant falcipain-2: a principal hemoglobinase of Plasmodium falciparum. *Biochem Biophys Res Commun, 317*(1), 38-45.

Kuo, P. C., Shi, L. S., Damu, A. G., Su, C. R., Huang, C. H., Ke, C. H., Wu, J. B., Lin, A. J., Bastow, K. F., Lee, K. H. & Wu, T. S. (2003). Cytotoxic and antimalarial beta-carboline alkaloids from the roots of Eurycoma longifolia. *J Nat Prod, 66*(10), 1324-1327.

Lambros, C., & Vanderberg, J. P. (1979). Synchronization of Plasmodium falciparum erythrocytic stages in culture. *J Parasitol, 65*(3), 418-420.

Lee, B. J., Singh, A., Chiang, P., Kemp, S. J., Goldman, E. A., Weinhouse, M. I., Vlasuk, G. P., & Rosenthal, P. J. (2003). Antimalarial activities of novel synthetic cysteine protease inhibitors. *Antimicrob Agents Chemother, 47*(12), 3810-3814.

Lee, I. S., & Hufford, C. D. (1990). Metabolism of antimalarial sesquiterpene lactones. *Pharmacol Ther, 48*(3), 345-355.

Leung, E., Datti, A., Cossette, M., Goodreid, J., McCaw, S. E., Mah, M., Nakhamchik, A., Ogata, K., El Bakkouri, M., Cheng, Y. Q., Wodak, S. J., Eger, B. T., Pai, E. F., Liu, J., Gray-Owen, S., Batey, R. A., & Houry, W. A. (2011). Activators of cylindrical proteases as antimicrobials: identification and development of small molecule activators of ClpP protease. *Chem Biol, 18*(9), 1167-1178.

Li, H., Huang, J., Chen, L., Liu, X., Chen, T., Zhu, J., Lu, W., Shen, X., Li, J., Hilgenfeld, R., & Jiang, H. (2009). Identification of novel falcipain-2 inhibitors as potential antimalarial agents through structure-based virtual screening. *J Med Chem, 52(*15), 4936–4940.

Li, R., Kenyon, G. L., Cohen, F. E., Chen, X., Gong, B., Dominguez, J. N., Davidson, E., Kurzban, G., Miller, R. E., Nuzum, E. O., Rosenthal, P. J., & McKerrow, J. H. (1995). In vitro antimalarial activity of chalcones and their derivatives. *J Med Chem, 38*(26), 5031-5037.

Lin, A. J., & Miller, R. E. (1995). Antimalarial activity of new dihydroartemisinin derivatives. 6. alpha-Alkylbenzylic ethers. *J Med Chem, 38*(5), 764-770.

Lindner, J., Meissner, K. A., Schettert, I., & Wrenger, C. (2013). Trafficked Proteins-Druggable in Plasmodium falciparum? *Int J Cell Biol, 435981*(10), 1-28.

Lindsey, D. F., Amerik, A., Deery, W. J., Bishop, J. D., Hochstrasser, M., & Gomer, R. H. (1998). A deubiquitinating enzyme that disassembles free polyubiquitin chains is required for development but not growth in Dictyostelium. *J Biol Chem, 273*(44), 29178-29187.

Lipinski, C. A., Lombardo, F., Dominy, B. W., & Feeney, P. J. (1997). Experimental and computational approaches to estimate solubility and permeability in drug discovery and development settings. *Adv Drug Deliv Rev, 23*(1-3), 3-25.

Liu, J., Istvan, E. S., Gluzman, I. Y., Gross, J., & Goldberg, D. E. (2006). Plasmodium falciparum ensures its amino acid supply with multiple acquisition pathways and redundant proteolytic enzyme systems. *Proc Natl Acad Sci U S A, 103*(23), 8840-8845.

Looareesuwan, S., Chulay, J. D., Canfield, C. J., & Hutchinson, D. B. (1999). Malarone (atovaquone and proguanil hydrochloride): a review of its clinical development for treatment of malaria. Malarone Clinical Trials Study Group. *Am J Trop Med Hyg, 60*(4), 533-541.

Lupas, A., Flanagan, J. M., Tamura, T., & Baumeister, W. (1997). Self-compartmentalizing proteases. *Trends Biochem Sci, 22*(10), 399-404.

Mahesh, R. & Mundra, S. (2015). Evaluation of novel 1-(4-(substituted)piperazin-1-yl)-2-(phenylamino)ethanone derivatives as Falcipain-2 inhibitors. *J Young Pharm. 7*(2), 96-105.

Mahesh, R., Mundra, S., Devadoss, T., & Kotra, L. P. (2014). Design, synthesis and evaluation of 2-(4-(substituted benzoyl)-1,4-diazepan-1-yl)-N phenylacetamide derivatives as a new class of falcipain-2 inhibitors. *Arab* J *Chem*, http://dx.doi.org/10.1016/j.arabjc.2014.11.008.

Mane, U. R., Li, H., Huang, J., Gupta, R. C., Nadkarni, S. S., Giridhar, R., Naik, P. P., & Yadav, M. R. (2012). Pyrido[1,2-a]pyrimidin-4-ones as antiplasmodial falcipain-2 inhibitors. *Bioorg Med Chem, 20*(21), 6296-6304.

Maurizi, M. R., Singh, S. K., Thompson, M. W., Kessel, M., & Ginsburg, A. (1998). Molecular properties of ClpAP protease of Escherichia coli: ATP-dependent association of ClpA and clpP. *Biochemistry, 37*(21), 7778-7786.

Maurya, R., Soni, A., Anand, D., Ravi, M., Raju, K. S., Taneja, I., Naikade, N. K., Puri, S. K., Wahajuddin., Kanojiya, S., & Yadav, P. P. (2012). Synthesis and antimalarial activity of 3,3-spiroanellated 5,6-disubstituted 1,2,4-trioxanes. *ACS Med Chem Lett, 4*(2), 165-169.

Meanwell, N. A. (2011). Synopsis of some recent tactical application of bioisosteres in drug design. *J Med Chem, 54*(8), 2529-2591.

Meissner, M., Schluter, D., & Soldati, D. (2002). Role of Toxoplasma gondii myosin A in powering parasite gliding and host cell invasion. *Science, 298*(5594), 837-840.

Micale, N., Kozikowski, A. P., Ettari, R., Grasso, S., Zappala, M., Jeong, J. J., Kumar, A., Hanspal, M., Chishti, A. H. (2006). Novel peptidomimetic cysteine protease inhibitors as potential antimalarial agents. *J Med Chem, 49*(11), 3064-3067.

Michel, K. H., & Kastner, R. E. (1985). A54556 Antibiotics and Process for Production Thereof. US Patent 4492650.

Montalbetti C., A., G., N., & Falque, V. (2005). Amide bond formation and peptide coupling. *Tetrahedron*, *61*(2005), 10827-10852.

Moura, P. A., Dame, J. B., & Fidock, D. A. (2009). Role of Plasmodium falciparum digestive vacuole plasmepsins in the specificity and antimalarial mode of action of cysteine and aspartic protease inhibitors. *Antimicrob Agents Chemother, 53*(12), 4968-4978.

Mundra, S., & Mahesh, R. (2016). Pyridine-based microwave assisted one-pot synthetic protocol for the synthesis of ethyl 3-substituted-4-oxo-2-thioxo-1,2,3,4-tetrahydropyrimidine-5-carboxylates. *Res Chem Intermediat*, *42*(5), 4207-4219.

Neuwald, A. F., Aravind, L., Spouge, J. L., & Koonin, E. V. (1999). AAA+: A class of chaperone-like ATPases associated with the assembly, operation, and disassembly of protein complexes. *Genome Res, 9*(1), 27-43.

Nixon, G. L., Pidathala, C., Shone, A. E., Antoine, T., Fisher, N., O'Neill, P. M., Ward S. A., & Biagini, G. A. (2013). Targeting the mitochondrial electron transport chain of Plasmodium falciparum: new strategies towards the development of improved antimalarials for the elimination era. *Future Med Chem, 5*(13), 1573-1591.

Nussenzweig, R. S., & Long, C. A. (1994). Malaria vaccines: multiple targets. *Science, 265*(5177), 1381-1383.

Olliaro, P. L., & Yuthavong, Y. (1999). An overview of chemotherapeutic targets for antimalarial drug discovery. *Pharmacol Ther, 81*(2), 91-110.

Pandey, K. C., & Dixit, R. (2012). Structure-function of falcipains: malarial cysteine proteases. *J Trop Med, 345195* (10), 1-19.

Pandey, K. C., Wang, S. X., Sijwali, P. S., Lau, A. L., McKerrow, J. H., & Rosenthal, P. J. (2005). The Plasmodium falciparum cysteine protease falcipain-2 captures its substrate, hemoglobin, via a unique motif. *Proc Natl Acad Sci U S A, 102*(26), 9138-9143.

Ploypradith, P. (2004). Development of artemisinin and its structurally simplified trioxane derivatives as antimalarial drugs. *Acta Trop, 89*(3), 329-342.

Polgar, L. (2005). The catalytic triad of serine peptidases. *Cell Mol Life Sci, 62*(19-20), 2161-2172.

Power, J. C., Asgian, J. L., Ekici, O. D., & James, K. E. (2002). Irreversible inhibitors of serine, cysteine, and threonine proteases. *Chem Rev, 102*(12), 4639-4750.

Price, R. N., Cassar, C., Brockman, A., Duraisingh, M., van Vugt, M., White, N. J., Nosten, F., & Krishna, S. (1999). The pfmdr1 gene is associated with a multidrug-resistant phenotype in Plasmodium falciparum from the western border of Thailand. *Antimicrob Agents Chemother, 43*(12), 2943-2949.

Price, R. N., Tjitra, E., Guerra, C. A., Yeung, S., White, N. J., & Anstey, N. M. (2007). Vivax malaria: neglected and not benign. *Am J Trop Med Hyg, 77*(6), 79-87.

Prusiner, S. B. (1997). Prion diseases and the BSE crisis. *Science, 278*(5336), 245-251.

Ralph, S. A., Van Dooren, G. G., Waller, R. F., Crawford, M. J., Fraunholz, M. J., Foth, B. J., Tonkin, C. J., Roos, D. S., & McFadden, G. I. (2004). Tropical infectious diseases: metabolic maps and functions of the Plasmodium falciparum apicoplast. *Nat Rev Microbiol, 2*(3), 203-216.

Ramya, T. N., Karmodiya, K., Surolia, A., & Surolia, N. (2007). 15-deoxyspergualin primarily targets the trafficking of apicoplast proteins in Plasmodium falciparum. *J Biol Chem, 282*(9), 6388-6397.

Rathore, S., Sinha, D., Asad, M., Böttcher, T., Afreen, F., Chauhan, V. S., Gupta, D., Sieber, S., & Mohmmed A. (2010). A cyanobacterial serine protease of Plasmodium falciparum is targeted to the apicoplast and plays important role in its growth and development. *Mol. Microbiol. 77*(4), 873–890.

Reid, B. G., Fenton, W. A., Horwich, A. L., & Weber-Ban, E. U. (2001). ClpA mediates directional translocation of substrate proteins into the ClpP protease. *Proc Natl Acad Sci U S A, 98*(7), 3768-3772.

Rizzi, L., Sundararaman, S., Cendic, K., Vaiana, N., Korde, R., Sinha, D., Mohmmed, A., Malhotra, P., & Romeo, S. (2011). Design and synthesis of protein-protein interaction mimics as Plasmodium falciparum cysteine protease, falcipain-2 inhibitors. *Eur J Med Chem, 46*(6), 2083-2090.

Roos, D. S., Crawford, M. J., Donald, R. G., Fraunholz, M., Harb, O. S., He, C. Y., Kissinger, J. C., Shaw, M. K. & Striepen, B. (2002). Mining the Plasmodium genome database to define organellar function: what does the apicoplast do? *Philos. Trans. R. Soc. Lond. B. Biol. Sci.* 357(1417), 35-46.

Rosenthal, P. J. (2003). Antimalarial drug discovery: old and new approaches. *J Exp Biol, 206*(Pt 21), 3735-3744.

Rosenthal, P. J. (2004). Cysteine proteases of malaria parasites. *Int J Parasitol, 34*(13-14), 1489-1499.

Rosenthal, P. J. (2011). Falcipains and other cysteine proteases of malaria parasites. *Adv Exp Med Biol, 712*, 30-48.

Rosenthal, P. J., Lee, G. K., & Smith, R. E. (1993). Inhibition of a Plasmodium vinckei cysteine proteinase cures murine malaria. *J Clin Invest, 91*(3), 1052-1056.

Rosenthal, P. J., McKerrow, J. H., Aikawa, M., Nagasawa, H., & Leech, J. H. (1988). A malarial cysteine proteinase is necessary for hemoglobin degradation by Plasmodium falciparum. *J Clin Invest, 82*(5), 1560-1566.

Rosenthal, P. J., Olson, J. E., Lee, G. K., Palmer, J. T., Klaus, J. L., & Rasnick, D. (1996). Antimalarial effects of vinyl sulfone cysteine proteinase inhibitors. *Antimicrob Agents Chemother, 40*(7), 1600-1603.

Rosenthal, P. J., Sijwali, P. S., Singh, A., & Shenai, B. R. (2002). Cysteine proteases of malaria parasites: targets for chemotherapy. *Curr Pharm Des, 8*(18), 1659-1672.

Sabnis, Y. A., Desai, P. V., Rosenthal, P. J., & Avery, M. A. (2003). Probing the structure of falcipain-3, a cysteine protease from Plasmodium falciparum: comparative protein modeling and docking studies. *Protein Sci, 12*(3), 501-509.

Sabnis, Y., Rosenthal, P. J., Desai, P., & Avery, M. A. (2002). Homology modeling of falcipain-2: validation, de novo ligand design and synthesis of novel inhibitors. *J Biomol Struct Dyn, 19*(5), 765-774.

Sajid, M., & McKerrow, J. H. (2002). Cysteine proteases of parasitic organisms. *Mol Biochem Parasitol, 120*(1), 1-21.

Sandvoss, L. M., & Carlson, H. A. (2003). Conformational behavior of beta-proline oligomers. *J Am Chem Soc, 125*(51), 15855-15862.

Schirmeister, T., & Kaeppler, U. (2003). Non-peptidic inhibitors of cysteine proteases. *Mini Rev Med Chem, 3*(4), 361-373.

Schlitzer, M. (2007). Malaria chemotherapeutics part I: History of antimalarial drug development, currently used therapeutics, and drugs in clinical development. *ChemMedChem, 2*(7), 944-986.

Schulz, F., Gelhaus, C., Degel, B., Vicik, R., Heppner, S., Breuning, A., Leippe, M., Gut, J., Rosenthal, P. J., & Schirmeister, T. (2007). Screening of protease inhibitors as antiplasmodial agents. Part I: Aziridines and epoxides. *ChemMedChem, 2*(8), 1214-1224.

Seok, J. W., Lee, Y. S., Moon, E. K., Lee, J. Y., Jha, B. K., Kong, H. H., Chung,D. I., & Hong, Y. (2011). Expressed sequence tag analysis of the erythrocytic stage of Plasmodium berghei. *Korean J Parasitol, 49*(3), 221-228.

Shenai, B. R., & Rosenthal, P. J. (2002). Reducing requirements for hemoglobin hydrolysis by Plasmodium falciparum cysteine proteases. *Mol Biochem Parasitol, 122*(1), 99-104.

Shenai, B. R., Lee, B. J., Alvarez-Hernandez, A., Chong, P. Y., Emal, C. D., Neitz, R. J., Roush, W. R., & Rosenthal, P. J. (2003). Structure-activity relationships for inhibition of cysteine protease activity and development of Plasmodium falciparum by peptidyl vinyl sulfones. *Antimicrob Agents Chemother, 47*(1), 154-160.

Shenai, B. R., Lee, B. J., Alvarez-Hernandez, A., Chong, P. Y., Emal, C. D., Neitz, R. J., Roush, W.R., & Rosenthal, P. J. (2003). Structure-activity relationships for inhibition of cysteine protease activity and development of Plasmodium falciparum by peptidyl vinyl sulfones. *Antimicrob Agents Chemother, 47*(1), 154-160.

Shenai, B. R., Sijwali, P. S., Singh, A., & Rosenthal, P. J. (2000). Characterization of native and recombinant falcipain-2, a principal trophozoite cysteine protease and essential hemoglobinase of Plasmodium falciparum. *J Biol Chem, 275*(37), 29000-29010.

Sherman, I. W. (1979). Biochemistry of Plasmodium (malarial parasites). *Microbiol Rev, 43*(4), 453-495.

Shi, W., Ting, L. M., Kicska, G. A., Lewandowicz, A., Tyler, P. C., Evans, G. B., Furneaux, R. H., Kim, K., Almo, S. C., & Schramm, V. L. (2004). Plasmodium falciparum purine nucleoside phosphorylase: crystal structures, immucillin inhibitors, and dual catalytic function. *J Biol Chem, 279*(18), 18103-18106.

Sijwali, P. S., Koo, J., Singh, N., & Rosenthal, P. J. (2006). Gene disruptions demonstrate independent roles for the four falcipain cysteine proteases of Plasmodium falciparum. *Mol Biochem Parasitol, 150*(1), 96-106.

Sijwali, P. S., Shenai, B. R., & Rosenthal, P. J. (2002). Folding of the Plasmodium falciparum cysteine protease falcipain-2 is mediated by a chaperone-like peptide and not the prodomain. *J Biol Chem, 277*(17), 14910-14915.

Singh, S. K., Guo, F., & Maurizi, M. R. (1999). ClpA and ClpP remain associated during multiple rounds of ATP-dependent protein degradation by ClpAP protease. *Biochemistry, 38*(45), 14906-14915.

Slater, A. F. (1993). Chloroquine: mechanism of drug action and resistance in Plasmodium falciparum. *Pharmacol Ther, 57*(2-3), 203-235.

Smilkstein, M., Sriwilaijaroen, N., Kelly, J. X., Wilairat, P., & Riscoe, M. (2004). Simple & inexpensive fluorescence-based technique for high-throughput antimalarial drug screening. *Antimicrob Agents Chemother, 48*(5), 1803-1806.

Socha, A. M., Tan, N. Y., LaPlante, K. L., & Sello, J. K. (2010). Diversity-oriented synthesis of cyclic acyldepsipeptides leads to the discovery of a potent antibacterial agent. *Bioorg Med Chem, 18*(20), 7193-7202.

Sturm, A., Amino, R., van de Sand, C., Regen, T., Retzlaff, S., Rennenberg, A., Krueger, A., Pollok, J. M., Menard, R., Heussler, V. T. (2006). Manipulation of host hepatocytes by the malaria parasite for delivery into liver sinusoids. *Science, 313*(5791), 1287-1290.

Thompson, M. W., Singh, S. K., & Maurizi, M. R. (1994). Processive degradation of proteins by the ATP-dependent Clp protease from Escherichia coli. Requirement for the multiple array of active sites in ClpP but not ATP hydrolysis. *J Biol Chem, 269*(27), 18209-18215.

Tomoda, H., Kumagai, H., Ogawa, Y., Sunazuka, T., Hashizume, H., Nagashima, H., & Omura, S. (1997). Synthesis of Four Chiral Isomers of beta-Lactone DU-6622 and Inhibition of HMG-CoA Synthase by the Specific (2R,3R)-Isomer. *J Org Chem, 62*(7), 2161-2165.

Trager, W., & Jensen, J. B. (1976). Human malaria parasites in continuous culture. *Science, 193*(4254), 673–675.

Turgay, K., Hahn, J., Burghoorn, J., & Dubnau, D. (1998). Competence in Bacillus subtilis is controlled by regulated proteolysis of a transcription factor. *EMBO J, 17*(22), 6730-6738.

Turgay, K., Hamoen, L. W., Venema, G., & Dubnau, D. (1997). Biochemical characterization of a molecular switch involving the heat shock protein ClpC, which controls the activity of ComK, the competence transcription factor of Bacillus subtilis. *Genes Dev, 11*(1), 119-128.

Umezawa, H., Aoyagi, T., Morishima, H., Matsuzaki, M., & Hamada, M. (1970). Pepstatin, a new pepsin inhibitor produced by Actinomycetes. *J Antibiot, 23*(5), 259-262.

Vedadi, M., Lew, J., Artz, J., Amani, M., Zhao, Y., Dong, A., Wasney, G. A., Gao, M., Hills, T., Brokx, S., Qiu, W., Sharma, S., Diassiti, A., Alam, Z., Melone, M., Mulichak, A., Wernimont, A., Bray, J., Loppnau, P., Plotnikova, O., Newberry, K., Sundararajan, E., Houston, S., Walker, J., Tempel, W., Bochkarev, A., Kozieradzki, I., Edwards, A., Arrowsmith, C., Roos, D., Kain, K., & Hui, R. (2007). Genome-scale protein expression and structural biology of Plasmodium falciparum and related Apicomplexan organisms. *Mol Biochem Parasitol, 151*(1), 100-110.

Verissimo, E., Berry, N., Gibbons, P., Cristiano, M. L., Rosenthal, P. J., Gut, J., Ward, S. A., & O'Neill, P. M. (2008). Design and synthesis of novel 2-pyridone peptidomimetic falcipain 2/3 inhibitors. *Bioorg Med Chem Lett, 18*(14), 4210-4214.

Vial, H. J., & Ancelin, M. L. (1992). Malarial lipids. An overview. *Subcell Biochem, 18*, 259-306.

Waller, R. F., & McFadden, G. I. (2005). The apicoplast: a review of the derived plastid of apicomplexan parasites. *Curr Issues Mol Biol, 7*(1), 57-79.

Waller, R. F., Reed, M. B., Cowman, A. F., & McFadden, G. I. (2000). Protein trafficking to the plastid of Plasmodium falciparum is via the secretory pathway. *EMBO J, 19*(8), 1794-1802.

Walsh, C. T., & Wencewicz, T. A. (2014). Prospects for new antibiotics: a molecule-centered perspective. *J Antibiot, 67*(1), 7-22.

Wang, L., Zhang, S., Zhu, J., Zhu, L., Liu, X., Shan, L., Huang, J., Zhang, W., & Li, H. (2014). Identification of diverse natural products as falcipain-2 inhibitors through structure-based virtual screening. *Bioorg Med Chem Lett, 24*(5), 1261–1264.

Wang, R., Gao, Y., & Lai, L. (2000). Lig Builder: A multi-purpose program for structure-based drug design. *J Mol Model*, *6*(7), 498–516.

Wang, S. X., Pandey, K. C., Scharfstein, J., Whisstock, J., Huang, R. K., Jacobelli, J., Fletterick, R. J., Rosenthal, P. J., Abrahamson, M., Brinen, L. S., Rossi, A., Sali, A., & McKerrow, J. H. (2007). The structure of chagasin in complex with a cysteine protease clarifies the binding mode and evolution of an inhibitor family. *Structure, 15*(5), 535-543.

Wang, S. X., Pandey, K. C., Somoza, J. R., Sijwali, P. S., Kortemme, T., Brinen, L. S., Fletterick, R. J., Rosenthal, P. J., & McKerrow, J. H. (2006). Structural basis for unique mechanisms of folding and hemoglobin binding by a malarial protease. *Proc Natl Acad Sci U S A, 103*(31), 11503-11508.

Wang, W. M., Ge, G., Lim, N. H., Nagase, H., & Greenspan, D. S. (2006). TIMP-3 inhibits the procollagen N-proteinase ADAMTS-2. *Biochem J, 398*(3), 515-519.

Warhurst, D. C. (1986). Antimalarial drugs: mode of action and resistance. *J Antimicrob Chemother, 18 Suppl B*, 51-59.

Weldon, D. J., Shah, F., Chittiboyina, A. G., Sheri, A., Chada, R. R., Gut, J., Rosenthal, P. J., Shivakumar, D., Sherman, W., Desai, P., Jung, J-C., & Avery, M. A. (2014). Synthesis, biological evaluation, hydration site thermodynamics, and chemical reactivity analysis of alpha-keto substituted peptidomimetics for the inhibition of Plasmodium falciparum. *Bioorg Med Chem Lett, 24*(5), 1274-1279.

Wickner, S., M. R. Maurizi and S. Gottesman (1999). "Posttranslational quality control: folding, refolding, and degrading proteins." *Science 286*(5446), 1888-1893.

Wickner, S., Maurizi, M. R., & Gottesman, S. (1999). Posttranslational quality control: folding, refolding, and degrading proteins. *Science, 286*(5446), 1888-1893.

Wilson, C. M., Volkman, S. K., Thaithong, S., Martin, R. K., Kyle, D. E., Milhous, W. K., & Wirth, D. F. (1993). Amplification of pfmdr 1 associated with mefloquine and halofantrine resistance in Plasmodium falciparum from Thailand. *Mol Biochem Parasitol, 57*(1), 151-160.

Wisniewski, T., Ghiso, J., & Frangione, B. (1997). Biology of A beta amyloid in Alzheimer's disease. *Neurobiol Dis, 4*(5), 313-328.

World Health Organization. World Malaria Report (2012), WHO Press: Geneva.

World Health Organization. World Malaria Report 2014, WHO Press: Geneva.

Wu, Y., Wang, X., Liu, X., & Wang, Y. (2003). Data-mining approaches reveal hidden families of proteases in the genome of malaria parasite. *Genome Res, 13*(4), 601-616.

Yu, A. Y., & Houry, W. A. (2007). ClpP: a distinctive family of cylindrical energy-dependent serine proteases. *FEBS Lett, 581*(19), 3749-3757.

Zhang, K., & Schweizer, F. (2009). Design and synthesis of glucose-templated proline-lysine chimera: polyfunctional amino acid chimera with high prolyl cis amide rotamer population. *Carbohydr Res, 344*(5), 576-585.

Zimmer, C. (2000). *Parasite Rex: inside the bizarre world of nature's most dangerous creatures.* New York: The Free Press.

Zucca, M., Scutera, S., & Savoia, D. (2013). New chemotherapeutic strategies against malaria, leishmaniasis and trypanosomiases. *Curr Med Chem, 20*(4), 502-526.

Publications from thesis

Mundra S, Mahesh R. Pyridine-based microwave assisted one-pot synthetic protocol for the synthesis of ethyl 3-substituted-4-oxo-2-thioxo-1,2,3,4-tetrahydropyrimidine-5-carboxylates. Research on Chemical Intermediates. 2016; 42, 4207-4219

Mahesh R, Mundra S. Evaluation of novel 1-(4-(substituted)piperazin-1-yl)-2-(phenylamino)ethanone derivatives as Falcipain-2 inhibitors. Journal of young Pharmacist. 2015; 2, 96-105

Chakka S K, Kalamuddin M, Mundra S, Mahesh R, Malhotra P, Mohmmed A, Kotra LP. Identification of novel class of falcipain-2 inhibitors as potential antimalarial agents. Biorganic and Medicinal Chemistry 2015; 23, 2212-2240

Mahesh R, Mundra S, Devadoss T, Kotra LP. Design, synthesis and evaluation of 2-(4-(substituted benzoyl)-1,4-diazepan-1-yl)-N phenylacetamide derivatives as a new class of falcipain-2 inhibitors. Arabian Journal of Chemistry, 2014; http://dx.doi.org/10.1016/j.arabjc.2014.11.008.

Mundra S, Thakur V, Bello M, Rathore S, Asad M, Wei L, Yang J, Chakka S K, Mahesh R, Malhotra P, Mohmmed A, Kotra LP. Structure-activity relationships of ClpP protease inhibitors as potential antimalarial agents (under communication)

Other Publications

Mahesh R, Devadoss T, Dhar AK, Venkatesh SM, Mundra S, Pandey DK, Bhatt S, Jindal AK. Ligand-based design, synthesis, and pharmacological evaluation of 3-Methoxyquinoxalin-2-carboxamides as structurally novel serotonin type-3 receptor antagonists. Archiv der Pharmazie 2012; 9, 687-694

Conference Presentations

Mundra S, Mahesh R. Design, synthesis and screening of falcipain-2 Inhibitors as potential anti-malarial Agents. International Conference organized by Indian Pharmacological Society (IPSCON-2016), October 21-23, 2016, PGIMER, Chandigarh. India.

Mundra S, Mahesh R. Identification of novel class of falcipain-2 inhibitors as potential anti-malarial agents. Organic chemistry in sustainable development: Recent advantages and future challenges (OCSD-2016), August 29-30, 2016, BITS Pilani, Pilani Campus, Pilani, India.

Mundra S, Mahesh R. Evaluation of novel class of falcipain-2 inhibitors as potential anti-malarial agents. New Frontiers In Chemistry-From Fundamentals To Applications (NFCFA 2015), December 18-19, 2015, BITS Pilani, Goa Campus, Goa, India.

Mundra S, Mahesh R. Design, synthesis and screening of falcapin-2 inhibitors as novel anti-malarial agents. 2nd Nirma Institute of Pharmacy International Conference, NIPICON January 23–25, 2014, Ahmadabad–India.

Mahesh R, Mundra S. Fluorimetric assay for estimation of falcipain-2 inhibitor activity using Victor multi-label counter. Biomedical Engineering & Science Technology (BEST) Symposium at St. Michael's Hospital, June 13, 2013, Toronto-Canada.

Mahesh R, Mundra S. Design and synthesis of novel anti-malarial agents. Biological Therapeutics Symposium, May 2-3, 2013, University of Toronto, Toronto-Canada

Mahesh R, Mundra S. Design and synthesis of falcipain-2 Inhibitor's as a potential anti-malarial Agents. Chemical Biophysics Symposium, April 21-23, 2013, Toronto-Canada.

Other Presentations

Mahesh R, Dhar AK, Jindal A, Muthu VS, Mundra S. Design, synthesis and pharmacological evaluation of Novel 2-(4-substituted piperazine 1-yl)-1,8-naphthyridine 3-carboxylic acids as 5-HT3 receptor antagonists for the management of depression. Indian Pharmaceutical Association (IPA) Convention, March 17-18, 2012, Manipal, Karnataka, India

Mahesh R, Sudali MV, Murugesan S, Dhar AK, Mundra S, Jindal A. Design and docking study of 4-benzyl-3-oxo-3,4-dihydroquinoxaline-2-carboxamide analogs as phosphodiestrase-IV (PDE-IV) inhibitors. Indian Pharmaceutical Association (IPA) Convention, March 17-18, 2012, Manipal, Karnataka, India

Biography of Prof. R. Mahesh

Prof. R. Mahesh is currently Professor, Pharmacy Department & Dean, Faculty Affairs Division, BITS, Pilani. He received his Ph.D. degree in 1997 from BITS, Pilani. He has been involved in teaching and research for the past two decades. His areas of interest include, Medicinal chemistry, Neuropharmacology, Clinical Pharmacy and Therapeutics. He has published several research and review articles in peer reviewed national and international journals. He has successfully completed several funded research projects and is currently the Principal Investigator of several projects funded by UGC, ICMR, DST and DBT, New Delhi. He has guided several Ph.D and M. Pharm students. He has received awards for best papers presented in National/International conferences and paper published in well reputed journals. He is the life member of Association of Pharmacy Teachers of India, Society of Neurochemistry of India and Indian Pharmacological Society.

Biography of Mr. Sourabh Mundra

Mr. Sourabh Mundra completed his B. Pharm. in 2006 from Guru Jambheshwar University, Hissar (Haryana) and M. Pharm. in 2008 from Annamalai University, Chidambaram (Tamil Nadu). He has worked as a Research Associate in Jubilant Life Science, Noida, U.P (India). His areas of interests include drug design for various therapeutic targets and method development for organic compound synthesis. He is the recipient of DBT-SRF fellowship during doctoral program. He has received various awards (as author and co-author). He has presented papers in national and international conferences and published research articles in peer reviewed international and national journals.